NONLINEAR ANALYSIS AND CONTROL OF CHEMICAL REACTORS

by

Nikola Samardzija

Submitted in accordance with the requirements for the degree of Doctor of Philosophy

at

The University of Leeds
Department of Chemical Engineering

under supervision of

Professor C. McGreavy

and

Professor W. H. Ray
(The University of Wisconsin, Madison, Wisconsin, USA)

November, 1997

The candidate confirms that the work submitted is his own and that appropriate credit has been given where reference has been made to the work of others.

ABSTRACT

This thesis carries out a detailed study of a nonlinear spectral theory that is useful for modeling and controlling chemical reactors. The motivation for this work originates from a few reports which have demonstrated in the past that the nonlinear spectral method offers a useful mathematical framework for classifying and quantifying nonlinear complexities of large degrees of freedom, as well as for qualifying a general nonlinear dynamic behavior. We present and discuss this new theory and show that it extends the familiar linear systems notion of characteristic modes (eigenmodes), as well as the notions of mathematical quantities known as the eigenvectors and eigenvalues, into a multi-dimensional nonlinear domain, *i.e.*, applies to model dimensions one, two, three and higher. This approach offers a new insight into nonlinear phenomena, and as such has a significant theoretical and practical value. In the theory of nonlinear systems the spectral framework provides some useful answers regarding the issues of multivariate process complexity, stability and control. Similarly, in applications it often leads to a simple relation between a desired process behavior and control parameters. We demonstrate this by showing how a process operating point, its behavior, and its domain of attraction are determined by nonlinear structures which characterize both a process and its control realization. In addition, we show that by a correctly modeling and regulating process nonlinearities one can obtain a nonlinear control solution that often outperforms the conventional first-order realizations. That is, there exist important nonlinear structural and dynamic process relations which determine a feasibility of a control realization. This is demonstrated by studying control behaviors of several highly exothermic continuously stirred tank reactor processes.

TABLE OF CONTENTS

LIST OF FIGURES

CHAPTER 7

LIST OF TABLES

CHAPTER 7

APPENDIX A.IV

APPENDIX A.V

GLOSSARY OF CONVENTIONS USED

x	The plain small case letter signifies a scalar quantity.
x	The bold small case letter signifies a column vector $\mathbf{x}=[x_1, x_2,.., x_i,.., x_m]^t$, in which $x_1, x_2,.., x_i,.., x_m$ are scalar quantities.
$\mathbf{e}_i$	Denotes the usual standard basis vector with 1 for the i-th vector component and 0 for all the other components.
$\mathbb{R}^m$	The standard m-dimensional vector (Euclidean) space.
process state and state variables	The state of a system or of a mathematical process is a minimum set of numbers (called state variables) which contain sufficient information about the history of the process to allow computation of future behavior.
state vector	The vector $\mathbf{x}=[x_1, x_2,...., x_m]^t$ defined by state variables $x_1, x_2,...., x_m$.
state-space	Each state **x** of a system may be conventionally viewed as a point in the m-dimensional Euclidean space. The coordinates of this space are the state variables $x_1, x_2,...., x_m$.
Euclidean or L_2-norm	$\|\mathbf{x}\|_2 = \sqrt{\sum_{i=1}^{m} x_i^2}$
$\overleftrightarrow{x}$	Translated state variable.
$\overleftrightarrow{\mathbf{x}}$	Translated state vector.
trivial point	The null state defined by $x_i=0$ for all i=1,..,m.
invariant set	The invariant set $\mathbb{M} \subset \mathbb{R}^m$ of a dynamic process is the set of all state-space points with the property that if at $t=t_o$ the state $\mathbf{x}(t_o)$ is in $\mathbb{M}$, then for any time $-\infty \le t \le \infty$, **x**(t) also belongs to $\mathbb{M}$..
invariant	The state-space structure defined by an invariant set.
periodic solution	A solution that satisfies $\mathbf{x}(t)=\mathbf{x}(t+T)$ for some positive $T<\infty$.
periodic orbit	The state-space invariant structure defined by periodic solutions.
differential equation	The equation $\dot{\mathbf{x}} = \mathbf{F}[\mathbf{x}]$ is called the differential equation corresponding to the vector field defined by **F**[**x**]: a dot over a letter denotes differentiation with respect to t: $\dot{\mathbf{x}} = \frac{d\mathbf{x}}{dt}$.

equilibrium, steady-state or singular point	The trivial invariant set which contains only one point for all t. Also, the point which satisfies the solution $\dot{\mathbf{x}} = \mathbf{F}[\mathbf{x}] = 0$.
asymptotic stability	The steady-state, $\mathbf{x}_s$, of a process described by $\dot{\mathbf{x}} = \mathbf{F}[\mathbf{x}]$ is asymptotically stable, with respect to a set $U \subset \mathbb{R}^m$, if every process trajectory starting in U converges to $\mathbf{x}_s$ as $t \to \infty$.
global asymptotic stability[1]	The asymptotically stable steady-state $\mathbf{x}_s$ is globally asymptotically stable if $U = \mathbb{R}^m$.
$\mathbf{v}$	used to designate an eigenvector.
$\lambda,\ \theta$	are used to designate eigenvalues.
$f_k(\mathbf{x})$	a homogeneous scalar function in $\mathbf{x} \in \mathbb{R}^m$, or a k-form.
$\mathbf{F}_k[\mathbf{x}]$	an m-dimensional k-form function.
$\Lambda_k\{\ \mathbb{K}^m\ \}$	k-form geometric spectra, where $\mathbb{K}^m$ can be either a $\mathbb{R}^m$ (real) or $\mathbb{C}^m$ (complex) space.
$\Lambda_k\{\ \mathbb{K}^m\ \}$	k-form algebraic spectra, where $\mathbb{K}$ can be either a $\mathbb{R}$ (real) or $\mathbb{C}$ (complex) number.
$s_{k,m}$	a characteristic or eigen-number for an m-dimensional k-form.
$p_{k,m}$	degrees of freedom, or a number of algebraically independent vectors which characterize an m-dimensional k-form.
$\mathbf{u}(t)$	control vector function.
$d\mathbf{u}/dt$	control speed.

[1] The term asymptotic stability in the large is also used.

ACKNOWLEDGMENTS

Although only one author is listed on the thesis, this work could not have been accomplished without the collaboration and support of several key individuals. The two persons who particularly deserve recognition and credit are my advisors Professor Colin McGreavy and Professor Harmon Ray. Working with them was truly a fortunate and quite educational experience. I have enjoyed very much sharing the technical knowledge and ideas with them, as well as experiencing their unique but different guiding styles. In particular, Professor McGreavy's keen pragmatic sense has influenced me to focus the ideas presented in this thesis on practical problems. In contrast, Professor Ray provided necessary motivation and suggestions for crossing the gap between theory and reality. I am indebted to both of them for their invaluable guidance and support.

I am also grateful to the DUPONT Company for generously providing time and resources needed for this research. Special recognition goes to Dr. Dave Smith at DUPONT's Central Research and Development Department who was integral in forming this research effort, and who also has patiently supported it. Recognition also goes to my colleagues Dr. Tunde Ogunnaike and Dr. Ron Pearson who have during the early phases of this work shared ideas and helped me with the related literature.

Finally I want to thank my parents and my family for their support and encouragement. I am very grateful for their belief in my work and ideas.

CHAPTER 1 - INTRODUCTION

In this chapter we introduce the justification for studying the topic of nonlinear dynamics and control. We show its importance by examining several elementary chemical reaction schemes, and at the end the scope of the thesis is outlined.

1.1. ISOTHERMAL CHEMICAL REACTIONS

Let us begin by considering a reactive mixture of m constituents $X_1,..,X_m$ with the following properties:

i) The reaction is isothermal (T=constant)

ii) The reaction volume V may be open or closed to the outside world.

iii) The reaction is irreversible and diffusion fluxes are negligible.

iv) The reaction is in mechanical equilibrium and is not subject to external fields.

Then by applying the principle of mass conservation to such a reaction mixture one obtains the following rate equations

$$\begin{aligned} \frac{dx_1}{dt} &\equiv \dot{x}_1 = f_1(x_1,\cdots, x_m) \\ &\vdots \\ \frac{dx_m}{dt} &\equiv \dot{x}_m = f_m(x_1,\cdots, x_m) \end{aligned} \quad , \tag{1.1.1}$$

where the small case letters $x_1,..,x_m$ respectively denote concentrations of the species $X_1,..,X_m$. This is a rather general set of equations which determine the system of ordinary differential equations (ODE), and is such that can also be used to model population dynamics in biological systems. The left-most terms in Equation (1.1.1) are the concentration time derivatives, while the right-most terms are generally nonlinear functions of the polynomial type which describe production rates. For convenience derivatives from now on are denoted by the "dot" mark above the concentration symbols.

An example of the process just described is given by the first-order irreversible homogeneous unimolecular batch type reaction scheme,

$$X_1 \xrightarrow{k_1} X_2$$

$$X_2 \xrightarrow{k_2} A$$

in which k_1 and k_2 are the reaction rate constants. The concentration dynamics for this reaction mixture are described by the rate equations

$$\begin{aligned} \dot{x}_1 &= -k_1 x_1 \\ \dot{x}_2 &= k_1 x_1 - k_2 x_2 \end{aligned} \quad , \tag{1.1.2}$$

which form a linear ODE system. Similarly, if bimolecular reaction steps are considered rate equations with second-order or quadratic terms are obtained. For example, the batch process with bimolecular reaction steps

$$2X_1 \xrightarrow{k_1} X_2$$

$$2X_2 \xrightarrow{k_2} A$$

is described by the rate equations

$$\begin{aligned} \dot{x}_1 &= -2k_1x_1^2 \\ \dot{x}_2 &= k_1x_1^2 - 2k_2x_2^2 \end{aligned} \quad , \tag{1.1.3}$$

which form a nonlinear ODE system.

It is also possible to combine unimolecular and bimolecular reaction steps to obtain more complex reactions. In this instance both the linear and quadratic terms are present in the rate equations. A system of this form is given by the autocatalitic Lotka-Volterra scheme

$$\begin{aligned} A + X_1 &\xrightarrow{k_1} 2X_1 \\ X_1 + X_2 &\xrightarrow{k_2} 2X_2 \\ X_2 + B &\xrightarrow{k_3} E + B \end{aligned}$$

for which the rate equations are

$$\begin{aligned} \dot{x}_1 &= Ak_1x_1 - k_2x_1x_2 \\ \dot{x}_2 &= k_2x_1x_2 - Bk_3x_2 \end{aligned} \quad , \tag{1.1.4}$$

and which again form a nonlinear ODE system.

Needless to say that the process models considered are rather idealistic, however, it has been demonstarted that they represent essential features of chemical reactions. Consequently, the value of such descriptions is not so much in the accuracy of the models derived, but in their ability to educate us about the general dynamic behavior of chemical reactions. For example, if we consider the process in Equation (1.1.2) and treat the process variables x_1 and x_2 as points in the positive two-dimensional Euclidean space, then as the time progresses the points form trajectories which describe reaction dynamics. This is illustrated in Figure 1.1.1 where the concentration behavior of two species indicates that X_1 is consumed by the intermediate X_2 prior to being converted into the final product A. As a result, the reaction dynamics forms parabolic type trajectories that asymptotically approach the x_2-axis which subsequently takes the solutions into the origin. Similarly the nonlinear process in Equation (1.1.3) has the reaction dynamics illustrated in Figure 1.1.2.

Here, however, the parabolic trajectories approach the asymptote L rather than the x_2-axis. This implies that X_1 is never fully consumed by X_2, and that the final product A is reached through a composition of X_1 and X_2 which is defined by the asymptote L. Therefore, the two reaction mixtures exhibit significant dynamic differences which are vividly captured in the x_1-x_2 concentration space.

These differences are even more pronounced when Equation (1.1.4.) is considered. In this case the reaction dynamics exhibits a periodic behavior depicted in Figure 1.1.3. With the exception of trajectories along the x_1 and x_2-axes, all other trajectories in the positive Euclidean space form closed orbits. Along these orbits concentrations of species cycle, implying that the reaction continuously absorbs and regenerates its constituents in an autocatalytic manner. By comparing the last figure with the previous ones it is evident that the Lotka-Volterra dynamics are more complex. The present scheme exhibits the parabolic type orbits in presence of the two equilibrium points, O and S, and the two asymptotes defined by the Euclidean coordinates. Furthermore, in comparison to the first two reactions the Lotka-Volterra scheme can be broken down into the two subprocesses that are formally related to the linear and quadratic terms present in the rate equations. Thus, the first subprocess is created by considering the linear term in Equation (1.1.4), or

$$\begin{aligned} \dot{x}_1 &= Ak_1x_1 \\ \dot{x}_2 &= -Bk_3x_2 \quad , \end{aligned} \tag{1.1.5}$$

while the second is

$$\begin{aligned} \dot{x}_1 &= -k_2x_1x_2 \\ \dot{x}_2 &= k_2x_1x_2 \quad , \end{aligned} \tag{1.1.6}$$

and is derived by using the nonlinear quadratic term. Figure 1.1.4 illustrates the behavior of these subprocesses and indicates the manner in which they blend in order to achieve the more complex periodic structure.

From the present discussion it is evident that the illustrations are signatures of the reaction schemes considered. It is also intuitively quite apparent that the reaction complexity and dynamics present in these signatures can be analyzed by examining the subprocesses derived from the rate equations. In the next section we will demonstrate that this type of argument can be applied to any chemical reaction scheme for which the ODE model exists. For now, however, we need to introduce and define mathematical terms and qualitative features that are used in the study of dynamic systems.

In this thesis we will use the conventional Euclidean *state-space* representation to capture process behavior. For instance, in the examples presented trajectories were used to record the behavior of process variables, concentrations, in this space. Therefore, such variables will also be referred to as the *process states*, or simply the *states*. We further adopt the notation $\Re^m$ to represent the real m-dimensional state-space, where the superscript m also designates the number of process variables. Moreover, for the chemical and biological processes modeled by rate equations only the positive state-space coordinates are of interest. This is because the negative concentrations are not possible. However, when modeling a general physical process or developing a general theory the entire state-space must be considered.

By embedding a reaction dynamics into the abstract state-space setting we are now in position to identify and study different nonlinear features and behaviors. For instance, in the three reaction schemes that were presented we find the following common features:

a) **Within the state-space region of interest the reaction dynamics are *bounded*, *i.e.*, no trajectories escape to infinity.**

b) **There are states at which a reaction is in equilibrium. These are referred to as the *steady-states*[2] .**

c) **There exist asymptotic or spectral lines which guide reaction dynamics. They are referred to as the *invariant rays*, or simply the *invariants*.**

---

[2] For the closed systems these states are more often referred to as the equilibrium points.

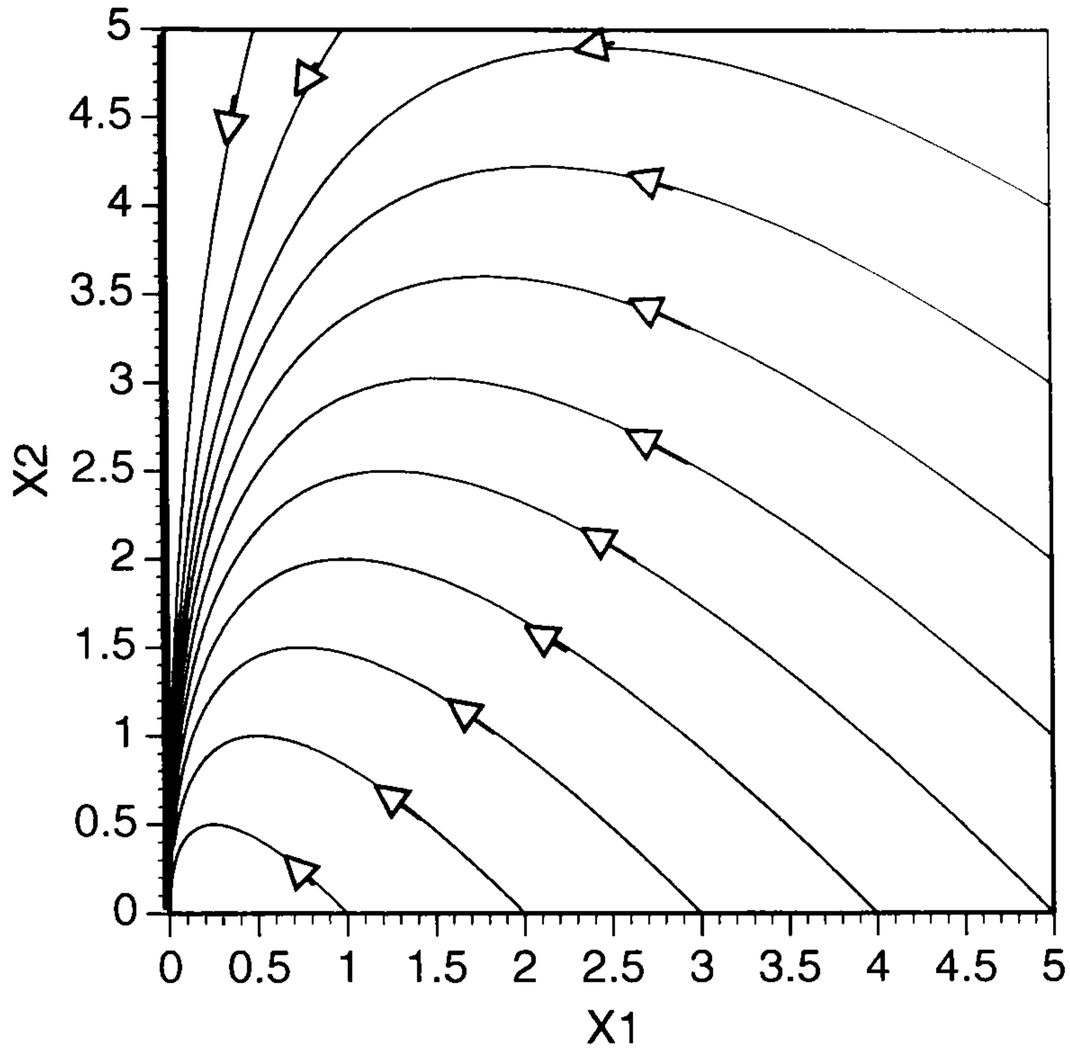

Behavior of concentrations in the rate expression defined by Equation (1.1.2) for the parameter values k_1=1.0 and k_2=0.5.

FIGURE 1.1.1.

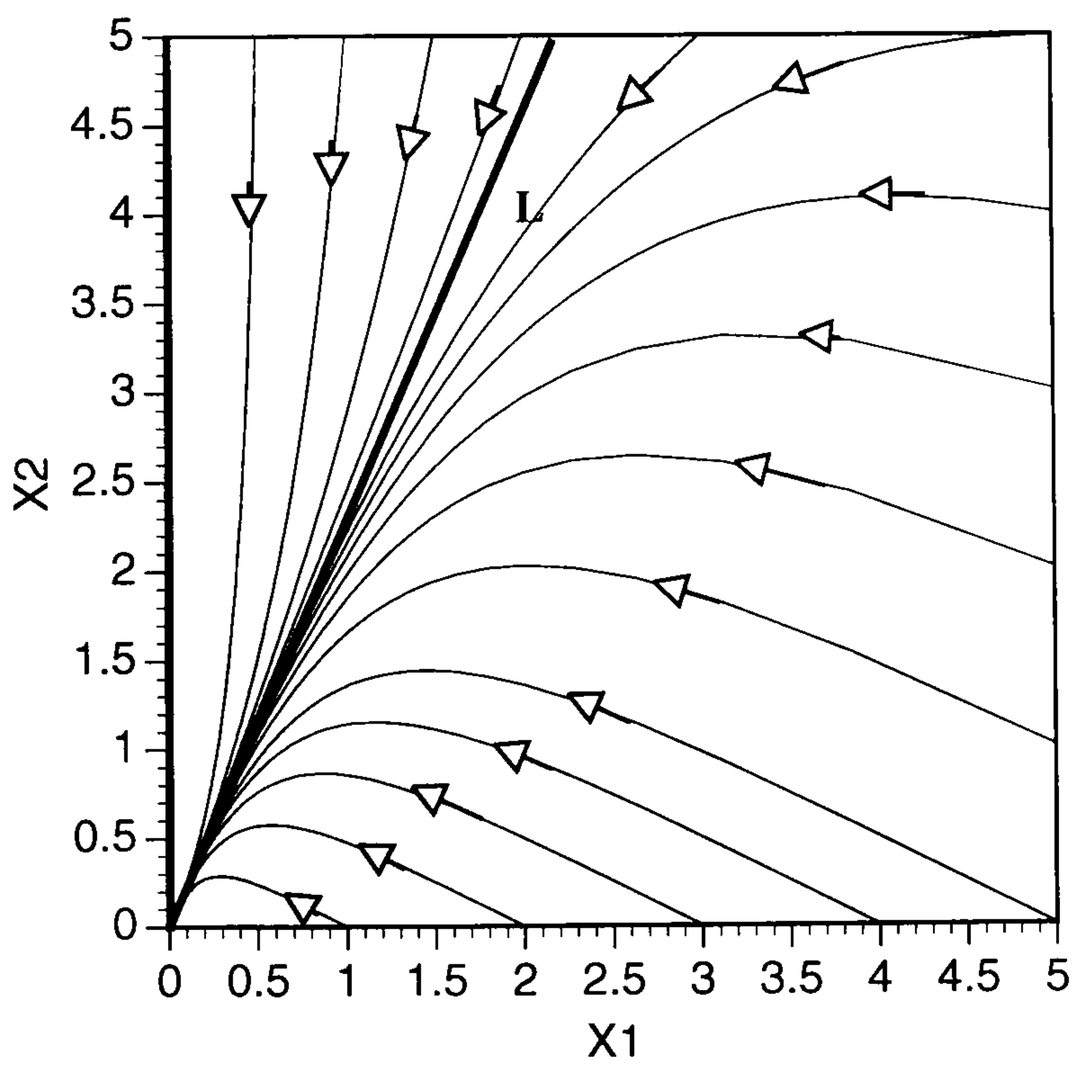

Behavior of concentrations in the rate expression defined by Equation (1.1.3) for the parameter values k_1=1.0 and k_2=0.5.

FIGURE 1.1.2.

d) The trajectories exhibit parabolic curvatures which determine the system excitability or *reactivity*.

These four features are so common in reaction processes that understanding of the reaction properties is practically impossible without identifying them. For example it is well known that the parabolic behavior is necessary in chemical and biological systems because it provides a condition known as the *positive feedback*, and without which useful reaction behaviors such as growth and aggregation could not be possible. In fact, a desire to control these behaviors in a laboratory or industrial setting is what often makes chemical and biological processes interesting and challenging.

1.2. TEMPERATURE CONSIDERATIONS

By examining the rate equations with only the linear and quadratic terms are only present, one rapidly concludes that a dynamics of such reaction scheme is rather uneventful. This is best described by the following well known result (Tyson and Light 1973, Nicholis and Prigogine 1977):

Theorem 1.2.1: ***It is impossible to have a limit cycle surrounding an unstable node or focus in reaction sequences involving two variable intermediates if the reaction steps are only uni- and/or bimolecular.***

The dull dynamic behavior persists even when the number of variable intermediates is greater than two (Smale 1976), although the limit cycle behavior may occur for dimensions greater than three (Dancsó and Farkas 1989). In any event, dynamic responses of chemical systems with unimolecular and bimolecular reaction steps will generally fit one of the signatures presented in Figures 1.1.1-4. Hence, the question is what can be done to make reaction models more interesting and more realistic.

The first obvious choice is to increase reaction molecularity by considering trimolecular or higher-order molecular interaction. For example, this is demonstrated by the trimolecular two variable limit cycle models (Nicholis and Prigogine 1977; Gray and Scott 1994; Scott 1994), and by the trimolecular, three variable, oscillatory models

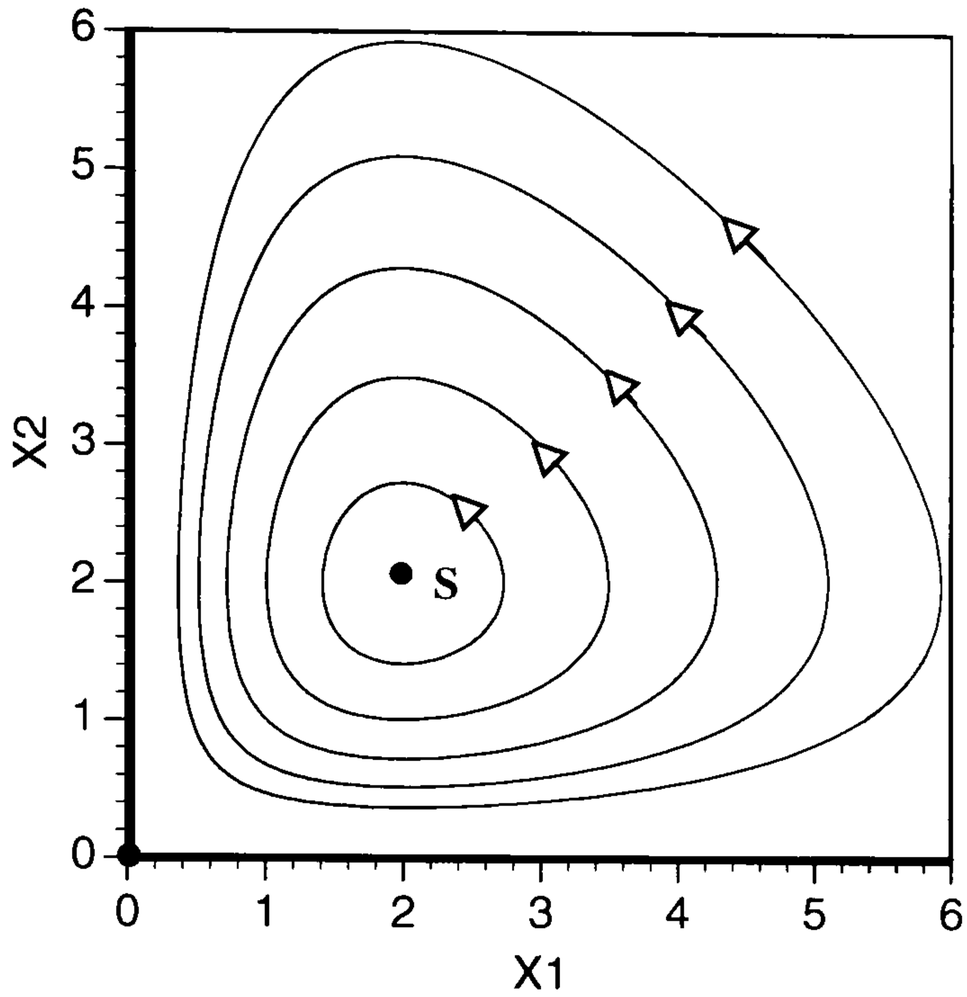

Reaction dynamics for the rate expression in Equation (1.1.4) with the parameter values A=B=2 and $k_1=k_2=k_3=1$.

FIGURE 1.1.3.

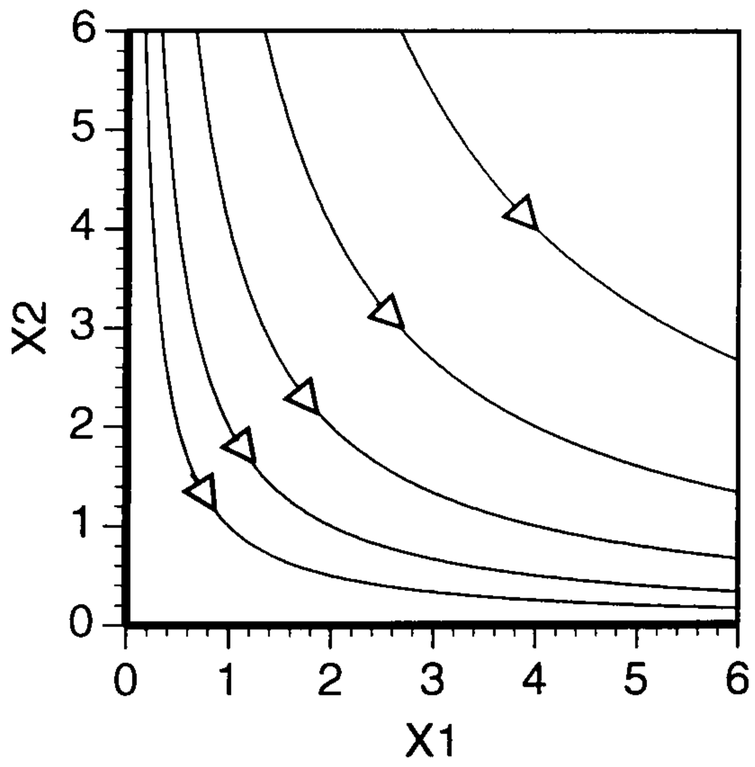

a) hyperbolic dynamics of the linear term, Equation (1.1.5).

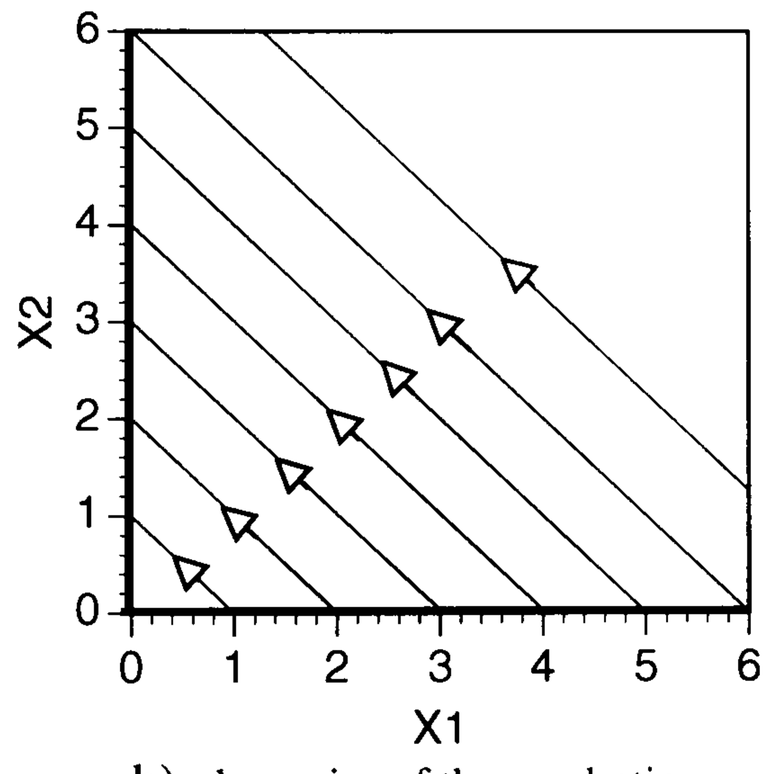

b) dynamics of the quadratic term, Equation (1.1.6).

Asymptotic or spectral lines in the Lotka-Volterra subprocesses.

FIGURE 1.1.4.

(Samardzija and Greller 1988, 1992; Samardzija, Greller and Wasserman 1989; Gray and Scott 1994; Scott 1994; Samardzija 1995). Unfortunately, such enrichments of reaction sequence are rather unrealistic since the probabilities of higher-order molecular interactions are quite low. Therefore, we are forced to look for some other alternative.

The next possibility is given by relaxing one of the chemical reaction constraints. The obvious choice is that the temperature is not constant, implying that reactions are now temperature dependent. This is accomplished by slightly modifying Equation (1.1.1) so that the equation for the energy conservation is included. In general this equation has the form

$$c\frac{dT}{dt} = \text{div } h\nabla T + \sum_x \left(-\Delta H_x\right) w_x(T, x_1, \cdots, x_m) \qquad (1.2.1)$$

where c is the specific heat of the mixture, the first term on the right corresponds to the total rate of heat flow across the surface $\sum$ that surrounds the mixture, h is the heat transfer coefficient, ΔH_x the heat of reaction x, and w_x depends on temperature in a highly nonlinear, usually exponential, fashion through the rate constants, k_i. An important example of such a reaction model is given by the first-order, exothermic, irreversible reaction A->B carried out in a Continuously Stirred Tank Reactor (CSTR). The initial analysis of this reaction was reported in the landmark papers by Aris and Amundson (1958), and later was refined by Uppal, Ray and Poore (1974). We now examine a refined model.

The CSTR process which allows a fresh feed of pure A to be mixed with a perfect undelayed recycle stream with recycle flow rate $(1-\lambda)F$ is illustrated in Figure 1.2.1, and is described by the mass and energy balance equations

$$\begin{aligned} V\frac{dc_A}{dt'} &= \lambda F c_{Af} + F(1-\lambda)c_A - Fc_A - Vk_0 Exp\left\{-\frac{E}{RT}\right\} c_A \\ V\rho C_P\frac{dT}{dt'} &= \rho C_P F\left(\lambda T_f + (1-\lambda)T - T\right) + V(-\nabla H)\, k_0 Exp\left\{-\frac{E}{RT}\right\} c_A - hA(T-T_c) \end{aligned} \qquad (1.2.2)$$

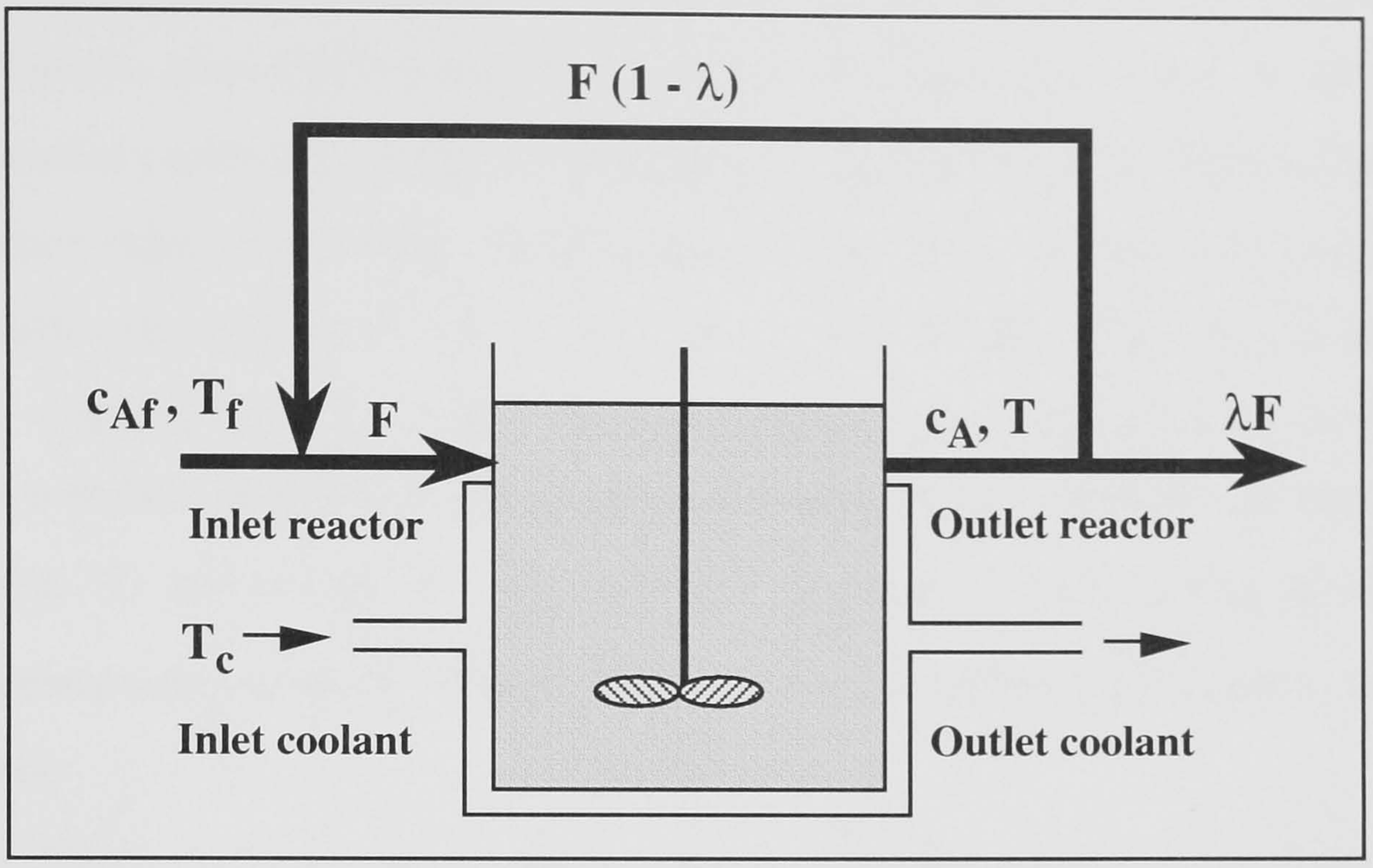

FIGURE 1.2.1.: A CSTR schematic in which pure A is mixed with a recycle stream with recycle flow rate F(1- λ).

in which the parameters are defined in Table 1.2.1. By defining the dimensionless variables as presented in Table 1.2.2, Uppal *et al* (1974) have shown that the above model reduces into the more manageable dimensionless formulation

$$\frac{dx_1}{dt} = -x_1 + Da\,(1-x_1)\,Exp\left\{\frac{x_2}{1+x_2/\gamma}\right\}$$

$$\frac{dx_2}{dt} = -x_2 + BDa\,(1-x_1)\,Exp\left\{\frac{x_2}{1+x_2/\gamma}\right\} - \beta(x_2-x_{2c}) \quad . \tag{1.2.3}$$

In this form the CSTR process dynamics can be analyzed in terms of the four dimensionless parameters B, Da, β and γ. For example, if the dimensionless activation energy γ>40 then Equation (1.2.3) can further be simplified to the form

$$\frac{dx_1}{dt} = -x_1 + Da\,(1-x_1)\,Exp\{x_2\}$$

$$\frac{dx_2}{dt} = -x_2 + BDa\,(1-x_1)\,Exp\{x_2\} - \beta(x_2-x_{2c}) \quad , \tag{1.2.4}$$

in which the Arrhenius' or exponential type nonlinearity depends only on the dimensionless temperature x_2 (Uppal *et al* 1974).

Unfortunately, from these model descriptions it is not at all obvious how one can treat dynamics of the CSTR process as was done in the Lotka-Volterra case. In fact, the mathematical expressions in the last three equations do not reveal the presence of any quadratic or higher-order terms. To obtain these terms, however, one needs to evaluate the Taylor series expansion about the state-space point of interest. If this point is defined by the coordinates $\{x_{1s},x_{2s}\}$, then for convenience sake we represent it by using the vector notation $\mathbf{x}_s=\begin{bmatrix}x_{1s}\\x_{2s}\end{bmatrix}=[x_{1s},x_{2s}]^t$ in which the superscript t signifies the transpose operation. We also use the notation $\mathbf{x}_s\in R^2$ to indicate that this point belongs to the real two-dimensional state-space. With this the Taylor series expansion of Equation (1.2.4) becomes

$$\dot{\mathbf{x}} = \mathbf{F}[\mathbf{x}] = \mathbf{F}_0[\mathbf{x}_s] + \sum_{k=1}^{\infty} \mathbf{F}_k[\mathbf{x}-\mathbf{x}_s] \qquad (1.2.5.a)$$

where

$$\dot{\mathbf{x}} = \left[\frac{dx_1}{dt}, \frac{dx_2}{dt}\right]^t ,$$

$$\mathbf{F}[\mathbf{x}] = \begin{bmatrix} -x_1 + Da\,(1-x_1)\,Exp\{x_2\} \\ -x_2 + BDa\,(1-x_1)\,Exp\{x_2\} - \beta(x_2-x_{2c}) \end{bmatrix},$$

$$\mathbf{F}_0[\mathbf{x}_s] = \mathbf{F}[\mathbf{x}_s], \quad \text{and}$$

$$\mathbf{F}_k[\mathbf{x}-\mathbf{x}_s] = \frac{1}{k!}\left.\frac{\partial^k \mathbf{F}[\mathbf{x}]}{\partial \mathbf{x}^k}\right|_{\mathbf{x}=\mathbf{x}_s} [\mathbf{x} - \mathbf{x}_s] \circ (k) =$$

$$= \begin{cases} \begin{bmatrix} -1 - Da\,Exp\{x_{2s}\} & Da\,(1-x_{1s})\,Exp\{x_{2s}\} \\ -B\,Da\,Exp\{x_{2s}\} & \left(BDa\,(1-x_{1s})\,Exp\{x_{2s}\} - 1 - \beta\right) \end{bmatrix} \begin{bmatrix} x_1 - x_{1s} \\ \\ x_2 - x_{2s} \end{bmatrix} & ; \quad \text{for } k=1 \\ \dfrac{Da\,(1-x_{1s})\,Exp\{x_{2s}\}}{k!}\left(\dfrac{-k}{(1-x_{1s})}(x_1-x_{1s})(x_2-x_{2s})^{k-1} + (x_2-x_{2s})^k\right)\begin{bmatrix} 1 \\ B \end{bmatrix} & ; \quad \text{for } k>1 \end{cases}$$

Table 1.2.1: CSTR parameters.

A	heat transfer area	;	c	concentration
C_p	specific heat	;	E	activation energy
F	volumetric feed rate	;	h	heat transfer coefficient
ΔH	heat of reaction	;	k_0	reaction rate constant for 1st-order reaction A->B
R	universal gas constant	;	t'	time
V	reaction volume	;	λ	coefficient of recirculation
ρ	density			
	Subscripts			
A	species A	;	c	cooling medium
f	feed state			

Table 1.2.2: Dimensionless CSTR parameters.

$x_1 = \frac{c_{Af} - c_A}{c_{Af}}$	conversion	;	$x_2 = \frac{T - T_f}{T_f}\left(\frac{E}{RT_f}\right)$	dimensionless temperature
$\tau = \frac{V}{F\lambda}$	residence time	;	$t = \frac{t'F\lambda}{V} = \frac{t'}{\tau}$	dimensionless time
$\gamma = \frac{E}{RT_f}$	dimensionless activation energy	;	$Da = \frac{k_0 V e^{-\gamma}}{F\lambda} = k_0 \tau e^{-\gamma}$	Damköhler number
$x_{2c} = \frac{T_c - f}{T_f}\gamma$	dimensionless cooling temperature	;	$B = \frac{(-\Delta H)c_{Af}}{\rho C_p T_f}\gamma$	dimensionless adiabatic temperature rise
$\beta = \frac{hA}{F\lambda\rho C_p} = \frac{hA\tau}{V\rho C_p}$	dimensionless heat transfer coefficient			

and where the operation $[\mathbf{x}\text{-}\mathbf{x}_s]o(k)$ stands for the power expansion up to and including. the degree k of all vector elements within the brackets. Therefore, terms such as $(x_1 - x_{1s})(x_2 - x_{2s})^{k-1}$ and $(x_2 - x_{2s})^k$ must be present throughout the expansion, implying that the derived Taylor series has not clearly unfolded the linear, quadratic or any higher-order terms. This is because the bias created by the point $\mathbf{x}_s$ will in general unfold all the terms of the k-th order polynomial, which implies that each $\mathbf{F}_k[\mathbf{x}\text{-}\mathbf{x}_s]$ will contain the constant, first, second, including up to the k-order terms. However, this can be corrected by introducing the coordinate translation $\overleftrightarrow{\mathbf{x}}=\mathbf{x} - \mathbf{x}_s$. In the new coordinates the Taylor series becomes the power series

$$\dot{\overleftrightarrow{\mathbf{x}}} = \mathbf{F}[\overleftrightarrow{\mathbf{x}}+\mathbf{x}_s] = \mathbf{F}_0[\mathbf{x}_s] + \sum_{k=1}^{\infty} \mathbf{F}_k[\overleftrightarrow{\mathbf{x}}] \qquad (1.2.5.b)$$

where $\mathbf{F}_0[\mathbf{x}_s] = \mathbf{F}[\mathbf{x}_s]$ as before, while $\mathbf{F}_k[\overleftrightarrow{\mathbf{x}}] = \frac{1}{k!} \frac{\partial^k \mathbf{F}[\mathbf{x}]}{\partial \mathbf{x}^k}\Big|_{\mathbf{x}=\mathbf{x}_s} \overleftrightarrow{\mathbf{x}}\, o\,(k)$. Hence, by translating coordinates to $\mathbf{x}_s$ we have unfolded exactly all k-th order terms and the power series derived, can be viewed as a chemical reaction scheme with higher-order interaction sequences. Furthermore, observe that the new coordinates are translated dimensionless conversion and temperature and therefore do now allow appearance of both positive and negative values of conversion. As a result, the entire state space becomes important. In addition, when $\mathbf{x}_s$ is a steady-state then the requirement $\mathbf{F}_0[\mathbf{x}_s]=0$ must be satisfied and the last equation reduces to

$$\dot{\overleftrightarrow{\mathbf{x}}} = \mathbf{F}[\overleftrightarrow{\mathbf{x}}+\mathbf{x}_s] = \sum_{k=1}^{\infty} \mathbf{F}_k[\overleftrightarrow{\mathbf{x}}] \qquad (1.2.6)$$

in which each

$$\mathbf{F}_k[\overleftrightarrow{\mathbf{x}}] = \frac{1}{k!} \frac{\partial^k \mathbf{F}[\mathbf{x}]}{\partial \mathbf{x}^k}\Big|_{\mathbf{x}=\mathbf{x}_s} \overleftrightarrow{\mathbf{x}}\, o\,(k) = \begin{bmatrix} f_{1,k}(\overleftrightarrow{\mathbf{x}}) \\ f_{2,k}(\overleftrightarrow{\mathbf{x}}) \end{bmatrix}, \text{ or}$$

$$\mathbf{F}_k[\overleftrightarrow{\mathbf{x}}] = \begin{cases} \begin{bmatrix} \dfrac{-1}{1-x_{1s}} & x_{1s} \\ \dfrac{-Bx_{1s}}{1-x_{1s}} & \left(Bx_{1s}-1-\beta\right) \end{bmatrix} \begin{bmatrix} \overleftrightarrow{x}_1 \\ \overleftrightarrow{x}_2 \end{bmatrix} & ; \quad \text{for } k=1 \\ \left(\dfrac{-x_{1s}}{(k-1)!\,(1-x_{1s})} \overleftrightarrow{x}_1 \overleftrightarrow{x}_2^{\,k-1} + \dfrac{x_{1s}}{k!} \overleftrightarrow{x}_2^{\,k} \right) \begin{bmatrix} 1 \\ B \end{bmatrix} & ; \quad \text{for } k>1 \ . \end{cases}$$

Observe that for all $k>1$ we have that $f_{2,k}(\overleftrightarrow{\mathbf{x}}) = B\, f_{1,k}(\overleftrightarrow{\mathbf{x}})$. Furthermore, note that to evaluate the power series terms in the form presented the equilibrium condition $\mathbf{F}_0[\mathbf{x}_s]=0$, or

$$\begin{aligned} x_{1s} &= Da(1-x_{1s})\,Exp\{x_{2s}\} \\ (1-\beta)x_{2s} &= BDa(1-x_{1s})\,Exp\{x_{2s}\} + \beta x_{2c} \ , \end{aligned} \tag{1.2.7}$$

must be applied.

We demonstrate this unfolding procedure by considering the following CSTR process parameters; $B=7.06$, $Da=0.1322$, $\beta=0.74$, and $x_{2c}=0$. The simulation of Equation (1.2.4) is illustrated in Figure 1.2.2, which, as discussed by Uppal *et al* (1974), depicts a stable limit cycle surrounding an unstable focus given by the steady-state solution $x_1=0.632312$ and $x_2=2.565591$. Now, by defining the translated coordinates

$$\overleftrightarrow{x}_1 = x_1 - 0.632312 \text{ and } \overleftrightarrow{x}_2 = x_2 - 2.565591$$

one can evaluate the power series representation at the steady-state, or Equation (1.2.6), for which

$$\mathbf{F}_k[\overleftrightarrow{\mathbf{x}}] = \frac{1}{k!} \left. \frac{\partial^k \mathbf{F}[\mathbf{x}]}{\partial \mathbf{x}^k} \right|_{\mathbf{x}=\mathbf{x}_s} \overleftrightarrow{\mathbf{x}} \circ (k)$$

$$= \begin{cases} \begin{bmatrix} -2.719697 & 0.632312 \\ -12.14106 & 2.724122 \end{bmatrix} \begin{bmatrix} \overleftrightarrow{x}_1 \\ \overleftrightarrow{x}_2 \end{bmatrix} & ; \quad \text{for } k=1 \\ \left(\dfrac{-0.632312}{(k-1)!\,(1-0.632312)} \overleftrightarrow{x}_1 \overleftrightarrow{x}_2^{\,k-1} + \dfrac{0.632312}{k!} \overleftrightarrow{x}_2^{\,k} \right) \begin{bmatrix} 1 \\ 7.06 \end{bmatrix} & ; \quad \text{for } k>1 \ . \end{cases}$$

If we now consider only the first-order ($k=1$) approximation of the original CSTR model, then it is easy to show that the state-space trajectories of the linearized system form an unstable focus. As a result, the linearized system captures quite accurately the true process

dynamics inside the limit cycle region. However, the dynamics outside the limit cycle region in Figure 1.2.1 are not well described. To increase the accuracy of the approximating system we add the quadratic (k=2) term. By doing so we have created a structure similar to the uni- and bimolecular reaction scheme. Consequently. Theorem 1.2.1 indicates that the new approximation is still insufficient to capture the true CSTR dynamics accurately. Therefore, we are forced to include an analog of the trimolecular step, or the k=3 term. For the new process approximation a stable limit cycle is formed, as illustrated in Figure 1.2.3. In fact, one can say that the 3-order approximation captures all essential dynamic features found in the original CSTR model. This is clearly illustrated in Figures 1.2.4. a) and b), where again the parabolic nature of the trajectories is observed.

We conclude this section by remarking that there exist other series type representations of nonlinear systems. In particular of significant importance is the Volterra series (Isidori 1989), and needs to be mentioned since it is not going to be treated in the thesis.

1.3. SCOPE OF THESIS

The order unfolding example clearly demonstrates that each $\mathbf{F}_k[\overleftrightarrow{\mathbf{x}}]$ term contains properties which influence the CSTR dynamics. Therefore, it is reasonable to expect that the properties of all $\mathbf{F}_k[\overleftrightarrow{\mathbf{x}}]$ terms for $0 \leq k < \infty$ must reveal the entire CSTR behavior and complexity. This is not only true for the CSTR model considered but also for any ODE model, independent of the fact whether it models a physical, chemical or biological reality. Consequently, a theory which examines the general properties of $\mathbf{F}_k[\overleftrightarrow{\mathbf{x}}]$ terms, from now on referred to as the *homogenous* or *k-form* theory, is important and is presented in the next three chapters.

Chapter 2 begins by examining the general algebraic structure and properties of the homogeneous forms. Well known linear system concepts such as the characteristic equation, eigenvalues and eigenvectors are thgen extended into a nonlinear homogeneous domain. The nonlinear eigenmodes and the homogeneous eigenspectra are also defined.

These results are used in Chapter 3 to examine the stability of the homogenous systems. Here, we analyze and relate different forms of stability to properties of the homogeneous spectra. Chapter 4 applies algebraic and qualitative results to study control of the homogeneous systems. It is demonstrated that a homogeneous process is state controllable as long as control addresses all process eigenmodes. The study of homogeneous systems is concluded by showing that the state controllable homogeneous process is stabilizable in the same fashion as is a controllable linear process.

In Chapter 5 the proposed homogeneous or k-form theory is extended to study properties of heterogeneous systems. It is demonstrated how homogeneous eigenspectra blend into manifolds of the polynomial processes. This is illustrated by examining the exothermic CSTR manifold topology and dynamics. We also confirm that the complexity and behavior of such dynamics is globally and locally determined by the properties of homogeneous spectra. These results are further verified for the spectra of three industrial CSTR processes.

The theory and results derived are used in Chapter 6 to analyze the two-dimensional heterogeneous process controllability and stabilization. In particular we present a detailed study of an exothermic CSTR control problem. Several nonlinear and linear control strategies which regulate an unstable CSTR operating point are proposed and examined. In addition, the feasibility of each control strategy is evaluated and the results obtained compared. Based on this analysis, we show that the control speed is an important design parameter which is directly related to the process nonlinear structure, and as such significantly influences the practicality of a control strategy. Chapter 7 shows how the two-dimensional control analysis can be extended into the multivariable domain and is illustrated by reference to the regulation of a three-dimensional homogeneous vinyl polymerization model.

The important conclusions in this thesis and a discussion on future directions of the presented research are given in Chapter 8. Moreover, to make the new results and contributions to the theory of nonlinear analysis and control clear most chapters are concluded by a table which summarizes the topics covered.

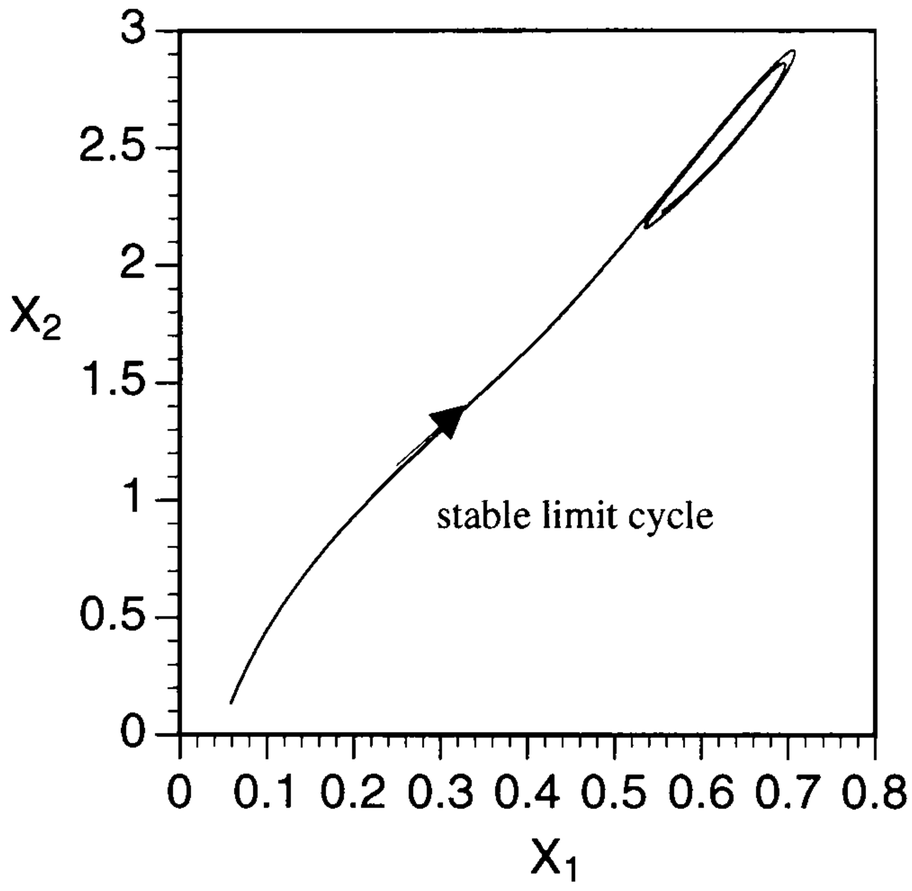

The dimensionless CSTR behavior for the process parameters B=7.06, Da=0.1322, β=0.7 and x_{2c}=0.0.

FIGURE 1.2.2.

The process variables are the translated dimensionless conversion and temperatue respectively defined as

$$\overleftrightarrow{X}_1 = X_1 - 0.632312 \;;\; \overleftrightarrow{X}_2 = X_2 - 2.565591$$

where X_1=0.632312 and X_2=2.565591 define the steady-state point of the original system. The dotted box outlines an approximate region that has been translated.

The CSTR behavior approximated by the 3-order power series representation.

FIGURE 1.2.3.

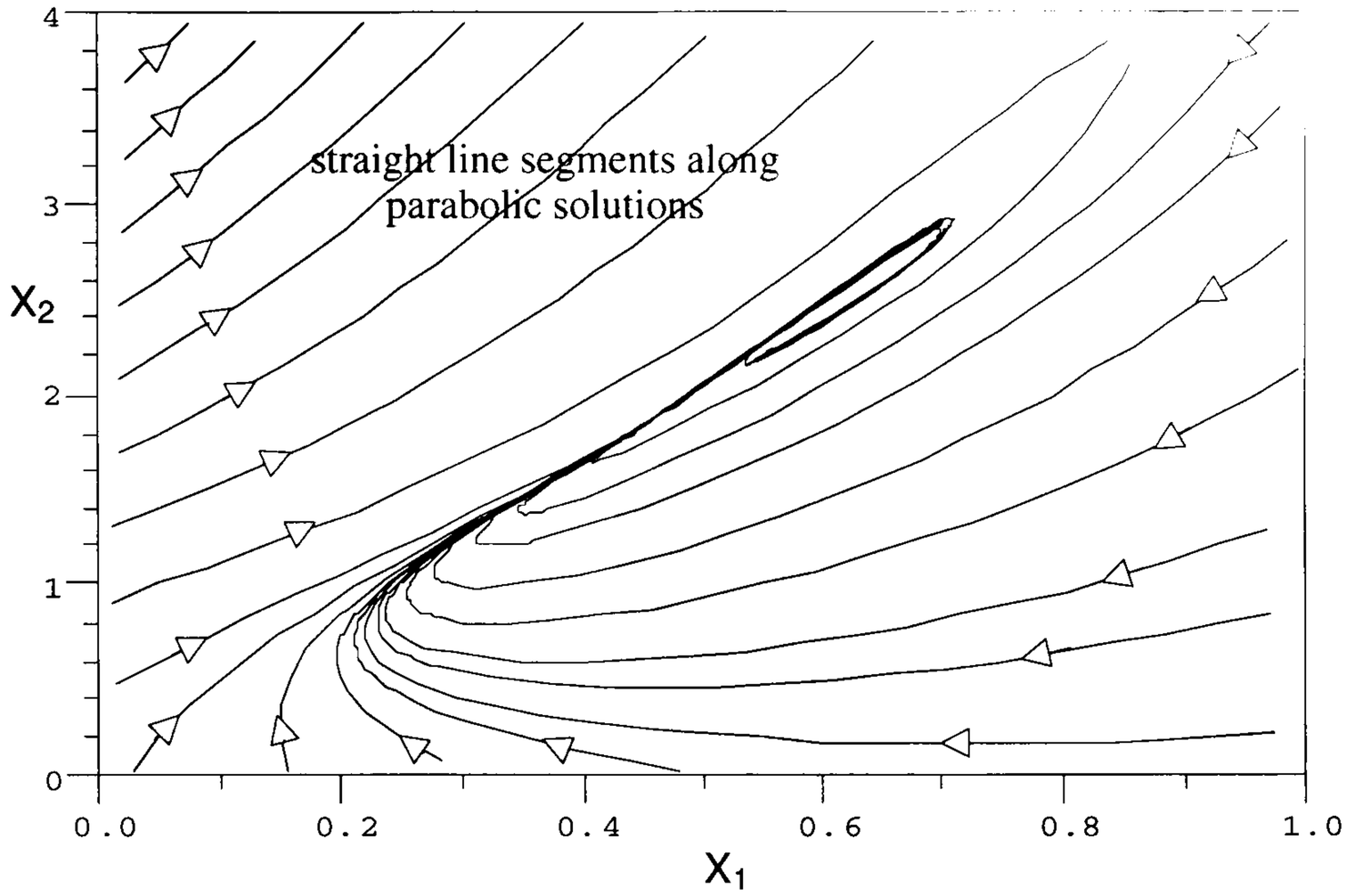

a) The exact model.

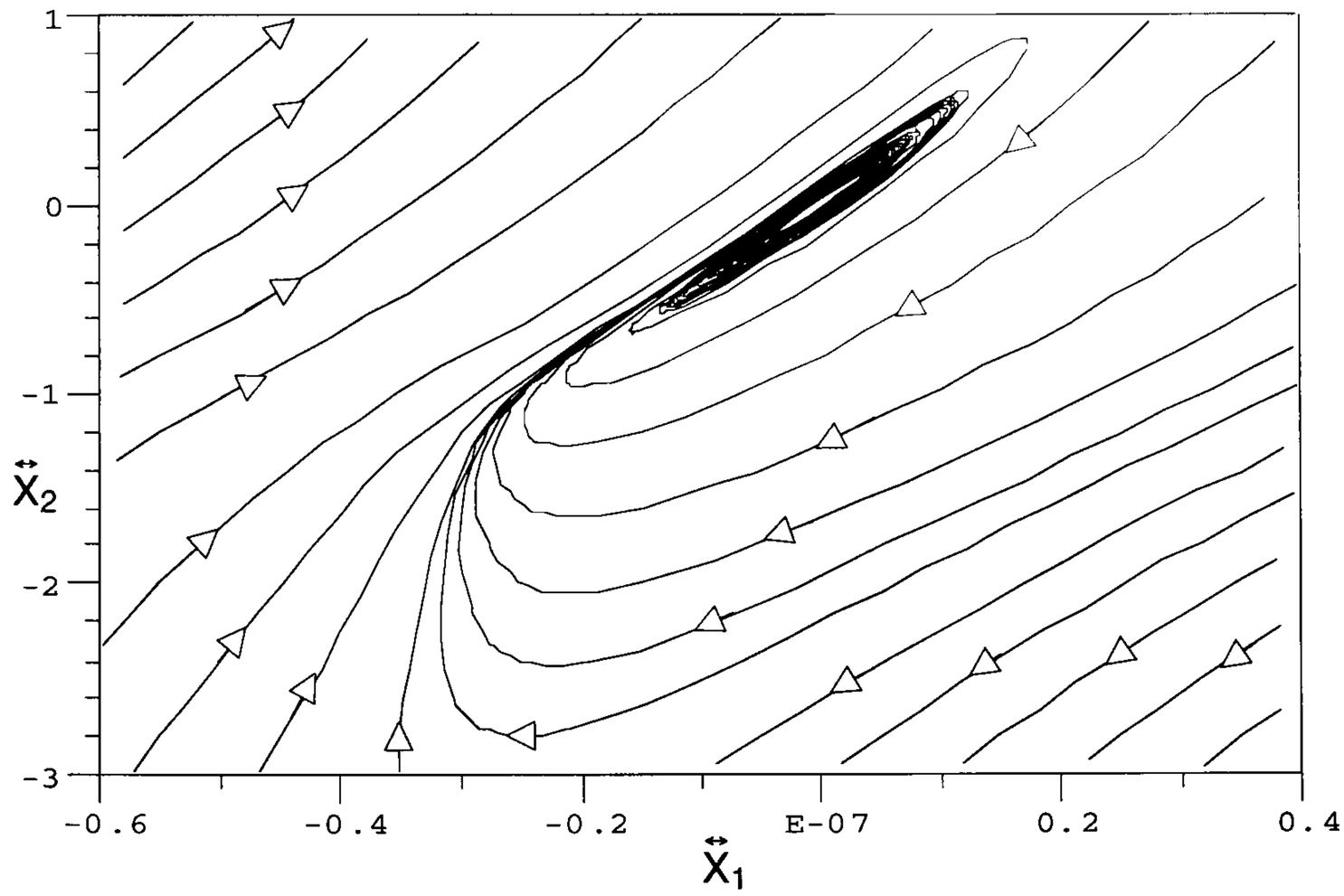

b) The 3-order power series approximation.

The global CSTR dynamics for the process parameters B=7.06, Da=0.1322, β=0.74 and x_{2c}=0.0.

FIGURE 1.2.4.

CHAPTER 2 - K-FORM SYSTEMS AND THEIR SPECTRA

Before we begin it is noted that all algebraic solutions of various nonlinear equations reported in the thesis are computed by using *Mathematica*®. Similarly, all dynamic state-space and time simulations were achieved by using either the CONSYD simulation program developed at the University of Wisconsin - Madison and the California Institute of Technology, or by implementing a conventional FORTRAN ODE solver. There was no need to develop any customized software programs for computational purposes discussed in this thesis.

2.1. K-FORMS

Let $\mathbf{x}=[x_1, x_2,..., x_m]^t \in \Re^m$, be a m-dimensional vector. A polynomial of the form $cx_1^{p_1}x_2^{p_2}...x_m^{p_m}$ is called a monomial in $x_1, x_2,..., x_m$, where each p_i is an integer and c is a coefficient. A monomial is said to be of degree k, where $k=\sum_{i=1}^{m} p_i$, and is real when $c \in \Re$. Furthermore, a scalar polynomial which is a sum of monomials each of degree k, is homogeneous of degree k. It is also referred to as the k-form in m variables, and is abbreviated by $f_k(\mathbf{x})$. For example, the standard linear, quadratic and cubic forms

are respectively homogeneous polynomials of degree 1, 2 and 3. It can be shown that any scalar k-form contains up to $p_{k,m}=(k+m-1)!/[k!(m-1)!]$ monomial terms, which represents the combinatorial number of m-states taken k at a time.

Now let

$$\mathbf{z}_k(\mathbf{x}) = \left[x_1^k,\ x_1^{k-1}x_2,\ldots,\ x_1x_m^{k-1},\ x_2^k,\ldots,\ x_m^k\right]^t,$$

(where entries are ordered lexicographically) be the $p_{k,m}$-dimensional vector given by all possible monomial terms of degree k, and let $\mathbf{c}_{coef}=[c_1,\ c_2,\ \ldots,\ c_{p_{k,m}}]^t$ be the vector defined by the corresponding monomial coefficients. Then any k-form can be represented as

$$f_k(\mathbf{x}) = \mathbf{c}_{coef}{}^t\,\mathbf{z}_k(\mathbf{x}) = \mathbf{z}_k(\mathbf{x})^t\,\mathbf{c}_{coef}\ . \qquad (2.1.1)$$

$f_k(\mathbf{x})$ is real when $\mathbf{c}_{coef}\in \mathbb{R}^{p_{k,m}}$. As defined $\mathbf{z}_k(\mathbf{x})$ represents the k-form vector representation of $\mathbf{x}$, and is such that $\mathbf{z}_1(\mathbf{x})=\mathbf{x}$.

The following are fundamental k-form properties:

homogeneous property $$f_k(r\mathbf{x}) = r^k f_k(\mathbf{x}), \qquad (2.1.2)$$

where r is an arbitrary scalar multiplier, and

Euler's theorem $$\frac{\partial f_k(\mathbf{x})}{\partial \mathbf{x}}\,\mathbf{x} = k f_k(\mathbf{x}) \qquad (2.1.3)$$

.

These results are now generalized to define the real k-form vector operator $\mathbf{F}_k[\mathbf{x}]$: $\mathbb{R}^m \to \mathbb{R}^m$, where

$$\mathbf{F}_k[\mathbf{x}] = [f_{k,1}(\mathbf{x}),\ f_{k,2}(\mathbf{x}),\ \ldots,\ f_{k,m}(\mathbf{x})]^t = \begin{bmatrix} \mathbf{c}_{1\ coef}^t \\ \vdots \\ \mathbf{c}_{m\ coef}^t \end{bmatrix}_{m\times p_{k,m}} \mathbf{z}_k(\mathbf{x})\ , \qquad (2.1.4)$$

$$\mathbf{F}_k[r\mathbf{x}] = r^k\mathbf{F}_k[\mathbf{x}]\ , \qquad (2.1.5)$$

and

$$\frac{\partial \mathbf{F}_k(\mathbf{x})}{\partial \mathbf{x}}\,\mathbf{x} = k\mathbf{F}_k(\mathbf{x})\,. \tag{2.1.6}$$

For example, $\mathbf{F}_1[\mathbf{x}]$ is a real form of degree one written as $\mathbf{A}\mathbf{x}$, where $\mathbf{A}$ is a mxm real matrix. Any vector k-form can have up to $(m)x(p_{k,m})$ coefficients. In addition, every $\mathbf{F}_k[\mathbf{x}]$ form given in the power series expansion defined in Equation (1.2.6) is expressed as

$$\mathbf{F}_k[\mathbf{x}] = \frac{1}{k!}\left.\frac{\partial^k \mathbf{F}[\mathbf{x}]}{\partial \mathbf{x}^k}\right|_{\mathbf{x}=\mathbf{x}_s} \mathbf{x}\circ(k) = \frac{1}{k!}\,\mathbf{C}_{mxp_{k,m}}\,\mathbf{z}_k(\mathbf{x})\,, \quad \text{with} \tag{2.1.7}$$

$$\mathbf{C}_{mxp_{k,m}} = \left.\begin{bmatrix} \frac{d^k f_1(\mathbf{x})}{dx_1^k} & \frac{d^k f_1(\mathbf{x})}{dx_1^{k-1}dx_2} & \cdots & \frac{d^k f_1(\mathbf{x})}{dx_m^k} \\ \frac{d^k f_2(\mathbf{x})}{dx_1^k} & \frac{d^k f_2(\mathbf{x})}{dx_1^{k-1}dx_2} & \cdots & \frac{d^k f_2(\mathbf{x})}{dx_m^k} \\ \vdots & \vdots & \cdots & \vdots \\ \frac{d^k f_m(\mathbf{x})}{dx_1^k} & \frac{d^k f_m(\mathbf{x})}{dx_1^{k-1}dx_2} & \cdots & \frac{d^k f_m(\mathbf{x})}{dx_m^k} \end{bmatrix}\right|_{\mathbf{x}=\mathbf{x}_s} x \begin{bmatrix} 1 & 0 & 0 & \cdots & 0 \\ 0 & k & 0 & \cdots & 0 \\ 0 & 0 & \frac{k(k-1)}{2} & \cdots & 0 \\ \vdots & \vdots & \vdots & \ddots & \vdots \\ 0 & 0 & 0 & \cdots & 1 \end{bmatrix}$$

where $\mathbf{F}[\mathbf{x}]=[f_1(\mathbf{x}), f_2(\mathbf{x}),..., f_m(\mathbf{x})]^t$ is a differentiable vector function with differentiation ordered lexicographically, and the left-most $(p_{k,m}xp_{k,m})$ square matrix accounts for coefficients given by the binomial theorem. For k=1 this matrix is the usual Jacobian matrix.

Finally when a process of interest can be described by the following ODE,

$$\dot{\mathbf{x}} = \mathbf{F}_k[\mathbf{x}]\,, \tag{2.1.8}$$

we will refer to the process as a real autonomous, continuous in time and homogeneous of degree k. Here the notation $\dot{\mathbf{x}} \equiv \frac{d\mathbf{x}}{dt}$ represents the time derivative of process variables or states defined by $\mathbf{x}$, and $\mathbf{F}_k[\mathbf{x}]$ is a real k-form. A homogeneous process is forced or controlled if it is of the form

$$\dot{\mathbf{x}} = \mathbf{F}_k[\mathbf{x}] + \mathbf{B}[[\mathbf{x}]]\mathbf{u}\,, \tag{2.1.9}$$

where $\mathbf{u}\in \Re^n$ is a piecewise continuous control or forcing function and

$$\mathbf{B}[[\mathbf{x}]] = \sum_{j=0}^{q} \mathbf{B}_j[[\mathbf{x}]] \text{ for } 0 \leq q \leq k \,, \tag{2.1.10}$$

is a mxn control matrix in which the entries are real polynomial functions of maximal degree q. Observe that $\mathbf{B}[[\mathbf{x}]]$ can be expressed as the sum of the mxn real k-form matrices $\mathbf{B}_j[[\mathbf{x}]] = [\mathbf{B}_{j,1}[\mathbf{x}], \cdots, \mathbf{B}_{j,n}[\mathbf{x}]]$, j=1,...,q. When q=0, $\mathbf{B}[[\mathbf{x}]]$ is the usual real constant coefficient mxn matrix **B**. Hereafter, all k-form systems considered will be real.

2.2. K-FORM SPECTRA

There are a number of studies addressing the qualitative behavior of homogeneous processes. Coleman (1963, 1970, 1984) has used a technique based on the type number concept to study the autonomous or zero-input case. He shows that these systems have the trivial steady-state point which, depending on the sign of the type numbers, may be globally stable or unstable. Coleman has proved that the trivial steady-state is asymptotically stable when type numbers, which are analogs of eigenvalues, are all negative. This is an important result since for homogeneous processes it implies global asymptotic stability, or asymptotic stability in the large. The theory of homogeneous processes has also benefited from algebraic interpretations. Markus (1960) applied non-associative algebras to evaluate invariants present in a quadratic homogeneous system. He has classified these invariants as idempotents and nilpotents. Markus also shows that these invariants determine principal qualitative features of a quadratic process. Furthermore, by applying non-associative algebras Röhrl (1977) has proved an important theorem that in essence determines the invariant structure of homogeneous systems. Other important contributions in the theory of homogeneous processes are given by Liaghina (1951), Vulpe and Sibirskii (1977), Newton (1978), Kaplan and Yorke (1979), Date (1979), and Oka (1980, 1981), and more recently by Koditschek and Nerendra (1982), Dayawansa *et al.* (1990) and Dayawansa (1992).

By examining the literature cited it becomes quite evident that the global behavior of homogeneous processes is related to the properties of certain invariant state-space trajectories. It will be demonstrated that these trajectories are algebraically related to the

quantities known from the linear systems theory as the eigenvalues and eigenvectors. Hence, for any homogeneous process there exists a natural extension of the linear eigenspectra which defines the k-form or homogeneous eigenspectra. As a result, the following question emerges: *Is it possible to address the stability and control properties of an autonomous homogeneous process in the same fashion as for the autonomous linear systems?* To find the answer it is first necessary to define the homogenous or k-form eigenspectrum, and to evaluate its properties.

A way to define the homogeneous spectrum is through algebraic geometry interpretations of the *projection equation* (Samardzija 1983, 1995). This is accomplished as follows: For any nonzero component x_i in $\mathbf{x}$, henceforth referred to as the *projection state* or *variable*, we derive the *projection vector* $\mathbf{v}=(1/x_i)\mathbf{x}$. Thus, $\mathbf{x}=x_i\mathbf{v}$ which implies that the autonomous process in Equation (2.1.8) can be written in the projected form as

$$\dot{\mathbf{v}} = [\mathbf{F}_k[\mathbf{v}] - f_{k,i}(\mathbf{v})\mathbf{v}]\, x_i^{k-1}, \tag{2.2.1}$$

where $\mathbf{v}=[v_1, v_2,.., v_{i-1}, 1, v_{i+1},.., v_m]^t$, with each $v_j=x_j/x_i$, $j=1,..,m$. This is the projection equation. An important property of this equation is that all singular solutions, including the complex ones, are given by the characteristic equation

$$\mathbf{F}_k[\mathbf{v}] - \lambda\mathbf{v} = 0\ , \tag{2.2.2}$$

where

$$\lambda = f_{k,i}(\mathbf{v})\ . \tag{2.2.3}$$

These solutions form the *homogeneous spectra.*

The solutions of the characteristic equation are quantities λ and $\mathbf{v}$ respectively known as the eigenvalues and eigenvectors. All eigenvector solutions determine the *eigenvector set*

$$\chi_k\{\mathbb{K}^m\} = \{\text{all } \mathbf{v}\in\mathbb{K}^m, \text{s.t. } \mathbf{F}_k[\mathbf{v}] - f_{k,i}(\mathbf{v})\mathbf{v} = 0;\ \forall\, i\in\{1,..,m\}\},$$

where $\mathbb{K}$ can be either $\mathbb{R}$ or $\mathbb{C}$. This set defines the *geometric eigenspectrum.* Similarly, the *eigenvalue set*

$$\Lambda_k\{\mathbb{K}\} = \{\text{ all } \lambda \in \mathbb{K}\text{, s.t. } \lambda = f_{k,i}(\mathbf{v}) \text{ for each } \mathbf{v} \in \mathbb{X}_k\{\mathbb{K}^m\}\},$$

defines the *algebraic eigenspectrum*. The eigenvalues in $\Lambda_k\{\mathbb{K}\}$ are listed in the order which corresponds to the order of associated eigenvectors in $\mathbb{X}_k\{\mathbb{K}^m\}$. If for a particular projection state the resulting characteristic equation exhibits roots at infinity then these solutions will not explicitly appear. The roots at infinity imply that the selected projection state is zero, which violates the starting requirement used in deriving the projection equation. However, one can still evaluate such solutions by rederiving the characteristic equation for a different projection state. This formulation is implied in spectral definitions.

Any eigenvector $\mathbf{v} \in \mathbb{X}_k\{\mathbb{K}^m\}$ satisfies the characteristic equation with a *multiplicity* σ. From the relation in Equation (2.2.3) it is clear that the eigenvector multiplicity implies the identical multiplicity of the corresponding eigenvalue. The notation $\mathbf{v}_{(\sigma)}$ is used when $\mathbf{v}$ has a multiplicity $\sigma>1$. Also, the corresponding eigenvalue is written as $\lambda_{(\sigma)}$. The subscript is omitted when $\sigma=1$, and the corresponding eigen-pair is referred to as being *simple*. In addition, for lack of a better terminology we shall refer to $\mathbf{v} \in \mathbb{X}_k\{\mathbb{K}^m\}$ as either *nilpotent* or *idempotent* (Markus 1960). It is nilpotent when the corresponding $\lambda=0$. Otherwise, it is idempotent. When $\mathbb{X}_k\{\mathbb{K}^m\}$ contains nilpotent eigenvectors the homogeneous process is also said to be *singular*. Otherwise it is *nonsingular*. Observe that a nilpotent eigenvector in general may be complex. However, for k=1 it can only be real. All of these properties are easily verified for the linear case.

Example 2.2.1 To demonstrate the above ideas we consider the CSTR power series expansion given in Equation (1.2.6). For simplicity, and whenever there is no ambiguity, we write $\mathbf{x}$ for the translation variable $\overleftrightarrow{\mathbf{x}}$. Therefore, for k=1 the eigenspectra are given by the characteristic solutions of the Jacobian matrix defined in Equation (1.2.6). For k>1, however, we first arbitrarily select x_2 to be the projection state. With this choice a projection vector $\mathbf{v}=[v_1, 1]^t$ is derived, and for each $\mathbf{F}_k[\mathbf{x}]$ we evaluate the characteristic equation

$$f_{1,k}(\mathbf{v}) - v_1 f_{2,k}(\mathbf{v}) = 0\,,$$

or

$$f_{1,k}(\mathbf{v}) - v_1 B f_{1,k}(\mathbf{v}) = 0\,,$$

implying

$$f_{1,k}(\mathbf{v})\,(1 - v_1\,B) = \lambda\left(\frac{1}{B} - v_1\right) = 0\,,$$

with

$$\lambda = f_{2,k}(\mathbf{v}) = B\,f_{1,k}(\mathbf{v}) = B\left(\frac{-x_{1s}}{(k-1)!(1-x_{1s})}\,v_1 + \frac{x_{1s}}{k!}\right).$$

One can easily verify that the solutions are $v_1=1/B$ and $v_1=(1-x_{1s})/k$. If the projection state x_1 is selected the projection vector $\mathbf{v}=[1,v_2]^t$ is obtained and the resulting characteristic equation is

$$f_{2,k}(\mathbf{v}) - v_2\,f_{1,k}(\mathbf{v}) = 0$$

or

$$\lambda(B-v_2) = 0$$

with

$$\lambda = v_2^{k-1}\left(\frac{-x_{1s}}{(k-1)!(1-x_{1s})} + \frac{x_{1s}}{k!}\,v_2\right).$$

The new solutions are $v_2=B$, $v_2=k/(1-x_{1s})$, and $v_2=0$ with multiplicity k-1. Thus, the first two solutions are inverses of the solutions for v_1, while the third seemingly appears from nowhere. The reason for this is that the inverse of $v_2=0$ does not exist, which is interpreted as the projection at infinity. Consequently, by using the derived results the following eigenspectra are found:

$$\mathbb{X}_k\{\mathbb{R}^2\} = \left\{ \begin{bmatrix} 1 \\ B \end{bmatrix} \;;\; \begin{bmatrix} 1 \\ k/(1-x_{1s}) \end{bmatrix} \;;\; \begin{bmatrix} 1 \\ 0 \end{bmatrix}_{(k-1)} : k\geq 2 \right\} \quad \text{and}$$

$$\Lambda_k\{\mathbb{R}\} = \left\{ \frac{B^{k-1}x_{1s}}{k!}\left(B - \frac{k}{(1-x_{1s})}\right); \quad 0 \quad ; \; 0_{(k-1)} : k\geq 2 \right\}.$$

The last two eigenvectors are nilpotent, while the first is idempotent and is responsible for the rich nonlinear CSTR behavior. Incidentally, this eigenvector determines a state-space direction that depends on the dimensionless adiabatic temperature rise B. In Figures 1.2.3.a) and b) this direction is indicated by the straight line segments along the parabolic solutions above the limit cycle. The slopes of these parabolic straight line segments are defined by the value of B. We shall continue to explore properties of the CSTR dynamics in terms of the higher-order spectra in Chapter 5.

The cardinality of spectral sets, $|\mathbb{X}_k\{\mathbb{K}^m\}|$ and $|\Lambda_k\{\mathbb{K}\}|$, is also an important issue. Obviously, the number of eigenvalues in an algebraic eigenspectrum must be the

same as the number of eigenvectors in the corresponding geometric eigenspectrum. As a result the spectral cardinality is determined by the cardinality of the geometric eigenspectrum. This number, however, does not take into account multiplicities of the spectral elements. For this reason, when $|\mathbb{X}_k\{\mathbb{K}^m\}|$ is finite we introduce the number $s_{k,m}$ which accounts for all solutions that satisfy Equation (2.2.2), including multiplicities, and call it the *characteristic number* or *eigen-number*.

Theorem 2.2.1 *(Fundamental Spectral Theorem):* An autonomous homogeneous process has a cardinality $|\mathbb{X}_k\{\mathbb{K}^m\}|$ which is either finite or infinite. When it is finite $|\mathbb{X}_k\{\mathbb{K}^m\}| \le s_{k,m}$ where

$$s_{k,m} = \sum_{i=0}^{m-1} k^i = \begin{cases} m \text{ when } k=1 \\ \dfrac{k^m-1}{k-1} \text{ when } k>1 \end{cases}. \qquad (2.2.4)$$

When $|\mathbb{X}_k\{\mathbb{K}^m\}|$ exceeds the eigen-number value, $|\mathbb{X}_k\{\mathbb{K}^m\}|$ must be infinite.

Proof: First consider the case k=1. The characteristic equation, Equation (2.2.2), is now reduced to the well known expression $[\mathbf{A} - \lambda\mathbf{I}]\mathbf{v}=0$, where $\mathbf{A}$ is as defined earlier and $\mathbf{I}$ is the corresponding identity matrix. The result therefore follows from well known linear algebra arguments.

The case of interest is when k>1. We prove this case by substituting the original process variables back into Equation (2.2.2). That is, use the relation $\mathbf{v}=(1/x_i)\mathbf{x}$, so that the characteristic equation now becomes

$$\mathbf{F}_k[\mathbf{x}] - \theta\,\mathbf{x} = 0, \qquad (2.2.5)$$

with $\theta=\lambda x_i^{k-1}$. Since $\mathbf{x}$ is assumed to be of dimension m then, for any given θ, the characteristic equation has m polynomial equations in m process variables, where each equation is of degree k. Therefore this algebraic structure implies that there are k^m common solutions, including multiplicities, or there exists an invariant subspace in which infinitely many solutions are present. Clearly when infinitely many solutions exist $|\mathbb{X}_k\{\mathbb{K}^m\}|$ must also be infinite.

To prove the finite result we first observe that the solution $\mathbf{x}=0$ is always present. This is the trivial solution which is not included in the eigenspectra and as such must be subtracted from the total number, implying the term $k^m - 1$. However, this has been derived for the homogeneous process variables rather than the projection variables which determine the eigen solutions in $\mathbb{X}_k\{\mathbb{K}^m\}$. Hence, to obtain the number of characteristic solutions in terms of the projection variables, one needs once again to make the substitution $\mathbf{x}=x_i\mathbf{v}$ in Equation (2.2.5) giving

$$x_i^{k-1}\mathbf{F}_k[\mathbf{v}] - \theta\,\mathbf{v} = 0. \tag{2.2.6}$$

Now, since $v_i=1$ the i-th equation in this expression is

$$x_i^{k-1}f_{k,i}(\mathbf{v}) - \theta = 0. \tag{2.2.7}$$

Thus, for $k>1$ and $\theta\neq 0$, each eigenvector $\mathbf{v}$ determines k-1 nonzero solutions of x_i. Consequently for each $\mathbf{v}$ there must be precisely k-1 equivalent solutions in terms of the homogeneous process coordinate $\mathbf{x}$.

When $\theta=0$, Equation (2.2.7) becomes

$$x_i^{k-1}f_{k,i}(\mathbf{v}) - \theta = x_i^{k-1}f_{k,i}(\mathbf{v}) - 0 = x_i^{k-1}f_{k,i}(\mathbf{v}) - r\,0 = 0 \tag{2.2.8}$$

and one solution is $x_i=0$, which is not permissible. To find solutions which are admissible the following argument is needed: Since $\theta=0$ the eigenvector $\mathbf{v}$ is nilpotent, and $f_{k,i}(\mathbf{v})=0$. This implies that Equation (2.2.8) becomes $(x_i^{k-1} - r)\,0=0$. Now, without loss of generality let $r=1$ and the solutions for x_i are then the k-1 roots of unity. Thus, by eliminating all equivalent solutions the eigen-number in all instances becomes $(k^m-1)/(k-1)$. Therefore, a homogeneous spectrum with finite spectral cardinality must satisfy the condition $|\mathbb{X}_k\{\mathbb{K}^m\}|\leq s_{k,m}$. ♦

Röhrl (1977) originally observed this result for nonsingular homogeneous systems with finite spectral cardinality for which all eigen solutions are simple. Hence, he deserves much of the credit for an early insight into the spectral structure.

Corollary 2.2.1 $p_{k,m} \leq s_{k,m}$. The k-form vector dimension is equal to the characteristic number only when $m \leq 2$ or $k=1$.

Proof: For $k=1$, $p_{1,m} = s_{1,m} = m$. When $m=1$, $p_{k,1} = s_{k,1} = 1$. Similarly, for $m=2$, $p_{2,m} = s_{2,m} = m+1$. However, when $m>2$, $s_{k,m}$ grows by geometric progression as m increases. Hence, $s_{k,m}$ is always an upper bound for the growth of $p_{k,m}$. ♦

For linear processes Corollary 2.2.1 implies that $\mathbb{X}_1\{\mathbb{K}^m\}$ contains, at most, m eigenvectors when $|\mathbb{X}_1\{\mathbb{K}^m\}|$ is finite. It has exactly m eigenvectors when each is simple, or $|\mathbb{X}_1\{\mathbb{K}^m\}|=m$. Furthermore, it is also known that in this instance eigenvectors are linearly independent and span the entire vector space. Consequently, they form a complete m-dimensional linear basis. However, when the cardinality is finite and all eigenvectors are not simple, then $|\mathbb{X}_1\{\mathbb{K}^m\}|<m$. This implies that there are less than m linearly independent eigenvectors and they no longer form a complete m-dimensional linear basis. In this case, one often completes such basis by computing generalized eigenvectors. In any event, when the spectral cardinality is finite all eigenvectors are linearly independent. Conversely, when $|\mathbb{X}_1\{\mathbb{K}^m\}|$ is infinite, at most m eigenvectors are linearly independent and the remaining are linearly related. This occurs when the linear system has an invariant subspace in which all points satisfy the characteristic equation. In this event it can be shown that eigenvectors which span such a subspace must all have identical eigenvalues. As a result, the invariant subspace is called *trivial*. Therefore, when the linear process contains a trivial subspace it must have non-distinct eigenvalues.

Analogous geometric spectrum properties and explanations exist for $k>1$. To see this, we start again with the case in which the spectral cardinality is finite and all eigenvectors are simple. Each eigenvector $\mathbf{v} \in \mathbb{X}_k\{\mathbb{K}^m\}$ can be expressed as the $p_{k,m}$-dimensional, k-form vector $\mathbf{z}_k(\mathbf{v})$. Then, since $|\mathbb{X}_k\{\mathbb{K}^m\}|=s_{k,m}$, one has exactly $s_{k,m}$ vectors $\mathbf{z}_k(\mathbf{v})$. Moreover, from Corollary 2.2.1 it follows that $p_{k,m}$ of them, *i.e.*, $\mathbf{z}_k(\mathbf{v}_1), \mathbf{z}_k(\mathbf{v}_2), \ldots, \mathbf{z}_k(\mathbf{v}_{p_{k,m}})$, can always be selected.

Definition 2.2.1 $\mathbf{z}_k(\mathbf{v}_1), \mathbf{z}_k(\mathbf{v}_2), \ldots, \mathbf{z}_k(\mathbf{v}_{p_{k,m}})$ form a *k-form basis* if all are linearly independent. In this case $\mathbf{v}_1, \mathbf{v}_2, \ldots, \mathbf{v}_{p_{k,m}}$ are said to be *algebraically independent* and to form the *algebraic basis* $\mathbb{B}_k\{\mathbb{K}^m\}=\{\mathbf{v}_1, \mathbf{v}_2, \ldots \mathbf{v}_{p_{k,m}}\}$.

As a result, the quantity $p_{k,m}$ is also be referred to as the *algebraic degree* which similarly implies the *degrees of freedom*. Observe that for k=1, a linear basis is the algebraic basis, as well as the 1-form basis. All three bases are equivalent in meaning and presentation. This no longer holds when k>1, and the following result exists.

Corollary 2.2.2 A homogeneous system with the finite spectral cardinality can allow at most $(s_{k,m}-p_{k,m})$ algebraically dependent eigenvectors. If the number of algebraically dependent eigenvectors exceeds this value a trivial subspace exists, and $|\chi_k\{\xi^m\}|$ is infinite.

Proof: Recall that the spectral set of finite size has $|\chi_k\{\xi^m\}| \leq s_{k,m}$, and an algebraic degree $p_{k,m}$. Then for k=1, Corollary 2.2.1 implies that a linear process cannot have algebraically (linearly) dependent eigenvectors. If one such eigenvector exists, the spectral cardinality must be infinite due to presence of the trivial subspace. The same is true for homogeneous processes with k>1 and dimension m≤2. For k>1 and m>2, however, the algebraically dependent eigenvectors appear in spectral sets with finite cardinalities. According to Theorem 2.2.1 and Corollary 2.2.1 at most $(s_{k,m}-p_{k,m})$ algebraically dependent eigenvectors are allowed. When this number is exceeded a trivial subspace must appear.

Finally, in the case when the geometric spectra has less than $p_{k,m}$ algebraically independent eigenvectors, the algebraic basis is incomplete and no algebraically dependent eigenvectors are present. Moreover, eigenvectors with multiplicities two or higher must be present in order to satisfy the characteristic number, and the algebraic basis is completed by computing generalized eigenvectors. This is discussed in a greater detail in the next section. ♦

Remark: Note, Corollaries 2.2.1 and 2.2.2 extend the notions of linear independence and dependence, and linear basis into the non-associative k-form algebras.

It is quite important to make the distinction between algebraically dependent eigenvectors occurring in trivial subspaces and the ones occurring as a consequence of the eigen-number. The former ones are said to be *trivial*, while the latter are *generic*. Hence,

depending on the spectral multiplicities, a real homogeneous process of degree k>1 and dimension m>2 may allow generic algebraically dependent eigenvectors. These can be real or complex. However, the trivial algebraically dependent eigenvectors of a real homogeneous process can only be real (Samardzija 1983).

2.3. Linear Transformations and Canonical Forms

Linear transformations of the k-form structures provide an important algebraic technique which is useful for studying stability and control properties. By applying this technique we are able to perform scaling and rotation of the process trajectories in a manner which most clearly reveals a spectral structure. Basically, this is an extension of the linear transformation methods used in linear systems theory.

Let $\mathbf{T}$ be a mxm nonsingular matrix. Then for any $\mathbf{x},\mathbf{y}\in\mathbb{R}^m$, the linear transformation

$$\mathbf{x} = \mathbf{T}\mathbf{y} \tag{2.3.1}$$

transforms the original system in Equation (2.1.12) into

$$\dot{\mathbf{y}} = \mathbf{T}^{-1}\,\mathbf{F}_k[\mathbf{T}\mathbf{y}] \tag{2.3.2}$$

where $\mathbf{T}^{-1}$ is the inverse of $\mathbf{T}$. It is easy to verify that any linear transformation leaves the degree k of a homogeneous process invariant. The transformation, however, has the following effects on process spectra.

Theorem 2.3.1 Let $\{\mathbb{X}_k\{\mathbb{K}^m\},\ \Lambda_k\{\mathbb{K}\}\}$ and $\{\mathbb{Y}_k\{\mathbb{K}^m\},\ \Theta_k\{\mathbb{K}\}\}$ be the respective spectral sets of the processes in Equations (2.1.12) and (2.3.2). Then, $\mathbb{Y}_k\{\mathbb{K}^m\}\equiv \mathbf{T}^{-1}\,\mathbb{X}_k\{\mathbb{K}^m\}$, and $\Theta_k\{\mathbb{K}\}\equiv \Lambda_k\{\mathbb{K}\}$.

Proof: Let $\mathbf{w}\in \mathbb{Y}_k\{\mathbb{K}^m\}$ and $\theta\in\Theta_k\{\mathbb{K}\}$ be the eigen solutions for the system in Equation (2.3.2). Then the characteristic equation implies

$$\mathbf{T}^{-1}\mathbf{F}_k[\mathbf{T}\mathbf{w}] - \theta\ \mathbf{w} = 0\ , \tag{2.3.3}$$

or that

$$\mathbf{F}_k[\mathbf{T}\mathbf{w}] - \theta\ \mathbf{T}\mathbf{w} = 0\ . \tag{2.3.4}$$

Furthermore, since $\mathbf{v}=\mathbf{T}\mathbf{w}$ then

$$\mathbf{F}_k[\mathbf{v}] - \theta\ \mathbf{v} = 0\ . \tag{2.3.5}$$

This is the characteristic solution for the original system, which implies that $\mathbf{v}\in X_k\{\mathbb{K}^m\}$ and $\theta=\lambda$. ♦

This result shows that any linear transformation of a k-form system leaves the eigenvalue set invariant while the eigenvectors are multiplied by the transformation inverse. For certain linear transformations, the state-space location of eigenvectors is of particular interest.

Corollary 2.3.1 Let $\mathbf{v}_1,\ldots,\ \mathbf{v}_m\in X_k\{\mathbb{K}^m\}$ be linearly independent with respective eigenvalues $\lambda_1,\ldots,\ \lambda_m\in \Lambda_k\{\mathbb{K}\}$. Then the linear transformation $\mathbf{T}=[\mathbf{v}_1,\cdots,\mathbf{v}_m]$, takes the original system into the form

$$\dot{\mathbf{y}} = \mathbf{T}^{-1}\,\mathbf{F}_k[\mathbf{T}\mathbf{y}] = \mathbf{D}\ \mathbf{y}^k + \mathbf{H}_k[\mathbf{y}]\ , \tag{2.3.6}$$

where $\mathbf{y}^k=[y_1^k,\cdots,y_m^k]^t$, $\mathbf{H}_k[\mathbf{y}]$ is a m-dimensional k-form composed only of the cross-coupled terms, and

$$\mathbf{D} = \begin{bmatrix} \lambda_1 & \cdots & 0 \\ \vdots & \ddots & \vdots \\ 0 & \cdots & \lambda_m \end{bmatrix}_{m\times m}\ .$$

Proof: From Theorem 2.3.1 it follows that each $\mathbf{w}\in Y_k\{\mathbb{K}^m\}$ is given by the relation $\mathbf{T}^{-1}\mathbf{v}$, where $\mathbf{v}\in X_k\{\mathbb{K}^m\}$. This implies that the standard basis vectors $\mathbf{e}_i=\mathbf{T}^{-1}\mathbf{v}_i$, $i=1,\ldots,m$, must belong to $Y_k\{\mathbb{K}^m\}$. Furthermore, the eigenvalues corresponding to these vectors are $\lambda_1,\ldots,\ \lambda_m\in \Lambda_k\{\mathbb{K}\}$. The rest of the proof follows from recognizing that for each $\mathbf{e}_i$ the cross-coupling term $\mathbf{H}_k[\mathbf{e}_i]$ is zero and $\mathbf{e}_i^k=\mathbf{e}_i$. ♦

The transformation presented will henceforth be referred to as the *canonical transformation* . Clearly every homogeneous process which has m linearly independent

eigenvectors can be transformed into the canonical form. However, what if a geometric eigenspectrum has less than m linearly dependent eigenvectors? Then, according to Theorem 2.2.1, to satisfy the eigen-number requirement eigenvectors of multiplicity greater than one must be present. Such eigenvectors are then used to compute the generalized eigenvectors which complete the m-dimensional linear basis. This is accomplished as follows. Let $\sigma>1$ be the multiplicity of $\mathbf{v}\in \mathbb{X}_k\{\mathbb{K}^m\}$, then we form the recursive relations

$$\begin{aligned} &\mathbf{F}_k[\mathbf{v}] - \lambda\mathbf{v} = 0 \\ &\mathbf{F}_k[\mathbf{v}_{g,1}] - \lambda\mathbf{v}_{g,1} = \mathbf{v} \\ &\quad\vdots \\ &\mathbf{F}_k[\mathbf{v}_{g,\sigma-1}] - \lambda\mathbf{v}_{g,\sigma-1} = \mathbf{v}_{g,\sigma-2} \end{aligned} \tag{2.3.7}$$

where $\mathbf{v}_{g,1},\ldots,\ \mathbf{v}_{g,\sigma-1}$ are generalized eigenvectors of $\mathbf{v}$. Observe that in the case when $\mathbb{B}_k\{\mathbb{K}^m\}$ is incomplete, the same generalized eigenvectors are used to complete the algebraic basis, *i.e.*, see the proof of Corollary 2.2.2.

Corollary 2.3.2 Let $\mathbf{v}_1,\ldots,\mathbf{v}_q\in \mathbb{X}_k\{\mathbb{K}^m\}$, with $q<m$, be linearly independent such that the sum of eigenvector multiplicities is $\geq$ m. Then there exists a linear transformation **T** such that the transformed system has **D** in the Jordan canonical form.

Proof: This follows from arguments in Corollary 2.3.1, together with Equation (2.3.7). Alternatively, for a more rigorous proof, let $\mathbf{v}_q$ be of multiplicity $\sigma\geq(m-q)$. Then by using Equation (2.1.4) one can write the characteristic equation as

$$\begin{bmatrix} \mathbf{c}^t_{1\ \text{coef}} \\ \vdots \\ \mathbf{c}^t_{m\ \text{coef}} \end{bmatrix}_{m\times p_{k,m}} \mathbf{z}_k(\mathbf{v}_i) = \lambda_i\mathbf{v}_i \ , \ \text{for}\ \ i=1,\cdots,q \tag{2.3.8}$$

and Equation (2.3.7) as

$$\begin{bmatrix} \mathbf{c}^t_{1\ \text{coef}} \\ \vdots \\ \mathbf{c}^t_{m\ \text{coef}} \end{bmatrix}_{m\times p_{k,m}} \mathbf{z}_k(\mathbf{v}_{g,j}) = \lambda_q\mathbf{v}_{g,j} + \mathbf{v}_{g,j-1},\ \text{for}\ j=q+1,\cdots,\ m\ \ \text{with}\ \ \mathbf{v}_{g,q}=\mathbf{v}_q\ , \tag{2.3.9}$$

where $\mathbf{v}_{g,q+1},\ldots,\mathbf{v}_{g,m}$ are the generalized eigenvectors which complete a linear basis. In matrix form, these expressions reduce to

$$\begin{bmatrix} \mathbf{c}_{1\ \mathrm{coef}}^{t} \\ \vdots \\ \mathbf{c}_{m\ \mathrm{coef}}^{t} \end{bmatrix}_{m x p_{k,m}} \left[\mathbf{z}_k(\mathbf{v}_1),\cdots,\mathbf{z}_k(\mathbf{v}_q),\mathbf{z}_k(\mathbf{v}_{g,q+1}),\cdots,\mathbf{z}_k(\mathbf{v}_{g,m})\right] = \mathbf{T}\,\mathbf{J} \quad , \qquad (2.3.10)$$

where $\mathbf{J}$ is the Jordan matrix defined as

$$\mathbf{J} = \begin{bmatrix} \lambda_1 & \cdots & 0 & 0 & 0 & \cdots & 0 \\ \vdots & \ddots & \vdots & \vdots & \vdots & \ddots & \vdots \\ 0 & \cdots & \lambda_q & 1 & 0 & \cdots & 0 \\ 0 & \cdots & 0 & \lambda_q & 1 & \cdots & 0 \\ \vdots & \ddots & \vdots & \vdots & \vdots & \ddots & \vdots \\ 0 & \cdots & 0 & 0 & 0 & \cdots & \lambda_q \end{bmatrix}$$

and $\mathbf{T} = \left[\mathbf{v}_1,\cdots,\mathbf{v}_q,\mathbf{v}_{g,q+1},\cdots,\mathbf{v}_{g,m}\right]$. This implies that

$$\mathbf{J} = \mathbf{T}^{-1}\begin{bmatrix} \mathbf{c}_{1\ \mathrm{coef}}^{t} \\ \vdots \\ \mathbf{c}_{m\ \mathrm{coef}}^{t} \end{bmatrix}_{m x p_{k,m}} \left[\mathbf{z}_k(\mathbf{v}_1),\cdots,\mathbf{z}_k(\mathbf{v}_q),\mathbf{z}_k(\mathbf{v}_{g,q+1}),\cdots,\mathbf{z}_k(\mathbf{v}_{g,m})\right] \quad , \qquad (2.3.11)$$

which is the same as

$$\mathbf{J} = \mathbf{T}^{-1}\ \left[\mathbf{F}_k[\mathbf{v}_1],\cdots,\mathbf{F}_k[\mathbf{v}_q],\mathbf{F}_k[\mathbf{v}_{g,q+1}],\cdots,\mathbf{F}_k[\mathbf{v}_{q,m}]\right] \quad , \qquad (2.3.12)$$

or after using Theorem 2.3.1

$$\mathbf{J} = \mathbf{T}^{-1}\ \left[\mathbf{F}_k[\mathbf{T}\mathbf{e}_1],\cdots,\mathbf{F}_k[\mathbf{T}\mathbf{e}_q],\mathbf{F}_k[\mathbf{T}\mathbf{e}_{q+1}],\cdots,\mathbf{F}_k[\mathbf{T}\mathbf{e}_m]\right] \ . \qquad (2.3.13)$$

By bringing the inverse inside the matrix, we have

$$\mathbf{J} = \left[\mathbf{T}^{-1}\mathbf{F}_k[\mathbf{T}\mathbf{e}_1],\cdots,\mathbf{T}^{-1}\mathbf{F}_k[\mathbf{T}\mathbf{e}_q],\mathbf{T}^{-1}\mathbf{F}_k[\mathbf{T}\mathbf{e}_{q+1}],\cdots,\mathbf{T}^{-1}\mathbf{F}_k[\mathbf{T}\mathbf{e}_m]\right] \quad , \qquad (2.3.14)$$

or from Equation (2.3.6)

$$\mathbf{J} = \left[\mathbf{D}\mathbf{e}_1^k+\mathbf{H}_k[\mathbf{e}_1],\cdots,\mathbf{D}\mathbf{e}_q^k+\mathbf{H}_k[\mathbf{e}_q],\mathbf{D}\mathbf{e}_{q+1}^k+\mathbf{H}_k[\mathbf{e}_{q+1}],\cdots,\mathbf{D}\mathbf{e}_m^k+\mathbf{H}_k[\mathbf{e}_m]\right]. \qquad (2.3.15)$$

Finally, by observing that $\mathbf{H}_k[\mathbf{e}_i] = 0$ and $\mathbf{e}_i^k = \mathbf{e}_i$ for all i=1,...,m, the last expression reduces to

$$\mathbf{J} = [\mathbf{D}\mathbf{e}_1, \cdots, \mathbf{D}\mathbf{e}_q, \mathbf{D}\mathbf{e}_{q+1}, \cdots, \mathbf{D}\mathbf{e}_m] = \mathbf{D}[\mathbf{e}_1, \cdots, \mathbf{e}_m] = \mathbf{D}. \blacklozenge \qquad (2.3.16)$$

For k=1, Equation (2.3.10) reduces to the well known transformation used in the linear systems theory, **AT=TJ**. However, for k>1 the expression on the left is modified by the k-form vector representation, while the expression on the right remains the same. We now demonstrate Corollary 2.3.1.

Example 2.3.1 Consider the 3-dimensional cubic process

$$\begin{bmatrix} \dot{x}_1 \\ \dot{x}_2 \\ \dot{x}_3 \end{bmatrix} = \begin{bmatrix} -4x_1^3 - x_2^3 + x_1x_3^2 \\ x_1^3 + 6x_1x_2^2 + 4x_2^3 + x_2x_3^2 \\ x_1^3 + 3x_1x_3^2 + 2x_3^3 \end{bmatrix} \qquad (2.3.17)$$

which has the following spectra

$$\chi_3\{R^3\} = \left\{ \begin{bmatrix} 0 \\ 0 \\ 1 \end{bmatrix}, \begin{bmatrix} 1 \\ -1 \\ -1 \end{bmatrix}_{(12)} \right\} \text{ and } \Lambda_3\{R\} = \{2, -2_{(12)}\}.$$

Thus, there are two eigen components where one is of multiplicity 12. This implies that the eigen-number requirement is satisfied since $s_{3,3}=13$. Hence, the only canonical form possible is that of the Jordan type. This is accomplished by considering the transformation

$$\mathbf{T} = \begin{bmatrix} 0 & 1 & -0.8864058 \\ 0 & -1 & -0.1135941 \\ 1 & -1 & -0.1279188 \end{bmatrix}$$

where the third column is the generalized eigenvector computed by using Equation (2.3.7). Now by applying the transformation **x=Ty**, we obtain the Jordan canonical form

$$\begin{bmatrix} \dot{y}_1 \\ \dot{y}_2 \\ \dot{y}_3 \end{bmatrix} = \begin{bmatrix} 2 & 0 & 0 \\ 0 & -2 & 1 \\ 0 & 0 & -2 \end{bmatrix} \begin{bmatrix} y_1^3 \\ y_2^3 \\ y_3^3 \end{bmatrix} + \begin{bmatrix} -2y_1^2y_2 - 2y_1y_2^2 - 3.2988116y_1^2y_3 + 5.5742725y_1y_2y_3 + \\ 3y_2^2y_3 + 0.7457809y_1y_3^2 + 0.7245391y_2y_3^2 \\ y_1^2y_2 - 2y_1y_2^2 - 0.2558376y_1y_2y_3 + 8.5742725y_2^2y_3 - 2y_2y_3^2 \\ y_1^2y_3 - 2y_1y_2y_3 - 2y_2^2y_3 - 0.2558376y_1y_3^2 + 8.574272y_2y_3^2 \end{bmatrix}$$

which has the eigenspectra

$$Y_3\{R^3\} = \left\{ \begin{bmatrix} 1 \\ 0 \\ 0 \end{bmatrix}, \begin{bmatrix} 0 \\ 1 \\ 0 \end{bmatrix}_{(12)} \right\} \text{ and } \Lambda_3\{R\} = \{ 2, -2_{(12)} \}.$$

2.4. HOMOGENEOUS INVARIANTS, NILPOTENTS AND HOMOGENIZATION

Spectral solutions produce other useful results. By applying the homogeneous property (see Equations (2.1.2) and (2.1.5)), one creates an equivalence relation which generates the spectral extension (Samardzija 1993) that has already been identified as the collinear equivalence in the proof of Theorem 3.1. Under this extension, all solutions of the characteristic equation create spectral lines or rays in R^m, *i.e.*, $x=x_i v$ is the equation of line parametrized by the projection state x_i. Furthermore, the homogeneous property in Equation (2.1.2) implies that along any such line, eigenvalues scale according to the scaling relationship

$$\lambda(x_i) = f_{k,i}(x_i \mathbf{v}) = f_{k,i}(\mathbf{v}) x_i^{k-1} = \lambda x_i^{k-1}. \tag{2.4.1}$$

As a result, one can show that any real eigenvector $\mathbf{v} \in R^m$ creates a real ray which supports the characteristic solution

$$\mathbf{x}(t) = \begin{cases} x_{io} \mathrm{Exp}\{\lambda(t-t_o)\}\mathbf{v}; & \text{for } k=1 \\ \dfrac{x_{io}}{\left[1 - (k-1)(t-t_o)\lambda(x_{io})\right]^{1/(k-1)}} \mathbf{v}; & \text{for } k>1 \end{cases}, \tag{2.4.2}$$

where x_{io} is the projection state at $t=t_o$. Note, that for $k>1$ the denominator expression accounts for the spectral scaling of an eigenvalue corresponding to $\mathbf{v}$. Consequently, these solutions determine invariant rays identical to the invariants studied by Markus. He calls such invariants nilpotent when $\lambda=0$, otherwise they are idempotents. Moreover, this formulation allows eigenvalues to be identified as the type numbers studied by Coleman.

We also say that the real ray solutions define real *eigenmodes*. For instance, the

spectral sets for the rate equations defined in Equations (1.1.2) and (1.1.3) are, using Equation (1.1.2)

$$\chi_1\{R^2\} = \left\{ \begin{bmatrix} 1 \\ k_1/(k_2-k_1) \end{bmatrix} ; \begin{bmatrix} 0 \\ 1 \end{bmatrix} \right\} ;$$

$$\Lambda_1\{R\} = \{-k_1 ; -k_2\}$$

and Equation (1.1.3)

$$\chi_2\{R^2\} = \left\{ L = \begin{bmatrix} 1 \\ \frac{k_1}{2k_2}\left(1+\sqrt{1+2\frac{k_2}{k_1}}\right) \end{bmatrix}; L' = \begin{bmatrix} 1 \\ \frac{k_1}{2k_2}\left(1-\sqrt{1+\frac{2k_2}{k_1}}\right) \end{bmatrix} ; \begin{bmatrix} 0 \\ 1 \end{bmatrix} \right\} ;$$

$$\Lambda_2\{R\} = \{-2k_1 ; -2k_1 ; -2k_2\} .$$

All eigen solutions define real eigenmodes which determine the invariant lines depicted in Figures 1.1.1 and 1.1.2. Note that the invariants corresponding to the negative coordinate values have been ignored. This is because the concentration dynamics must be positive at all times. As a result in Figure 1.1.1, where $k_1>k_2$, the first component of the linear eigenspectra is not shown. Similarly, the second component L' in the quadratic eigenspectra is not present in Figure 1.1.2 because

$$\left(1-\sqrt{1+\frac{2k_2}{k_1}}\right)<0 \quad \text{for all } k_1,k_2>0.$$

By using the same arguments, one concludes that complex eigenvectors determine rays in C^m which support the complex characteristic solutions, or complex eigenmodes. However, for k>1 the general explicit form of these solutions is presently not known and we can only infer of invariance by studying vector field flows in R^m. In certain instances, which are discussed in the section on stability, the complex spectra are clearly identified as being responsible for formation of the invariant structures such as periodic orbits and stable or unstable foci. Consequently the invariant structures obtained from homogeneous spectra are qualitatively similar to the invariants present in the linear systems.

An important property of all invariant sets derived from the spectral solutions is that the points must satisfy the homogeneous property given by Equation (2.1.5). For this reason, we refer to such invariants as being *homogeneous*. These, however, are not the

only invariants that are possible in a homogeneous system. For example, there exist homogeneous processes which have limit cycles or chaotic behaviors. However, the points on these invariant structures do not satisfy Equation (2.1.5) and so are not accounted for in the homogeneous eigenspectra. To demonstrate how these cases occur, we consider the following general expression

$$\begin{bmatrix} \dot{x}_1 \\ \vdots \\ \dot{x}_r \\ \dot{x}_{r+1} \\ \vdots \\ \dot{x}_m \end{bmatrix} = \mathbf{F}_k[\mathbf{x}] = \begin{bmatrix} f_{k,1}(\mathbf{x}) \\ \vdots \\ f_{k,r}(\mathbf{x}) \\ \\ 0 \\ \vdots \\ 0 \end{bmatrix}, \tag{2.4.3}$$

where variables $x_{r+1},\ldots, x_m$ (referred to as the *homogenization variables*) have constant solutions for all times. Thus, by assigning desired solutions to these variables, a homogenized process can further be reduced to its *minimal realization* in variables $x_1,\ldots, x_r$, or

$$\begin{bmatrix} \dot{x}_1 \\ \vdots \\ \dot{x}_r \end{bmatrix} = \widetilde{\mathbf{F}}[\widetilde{\mathbf{x}}] = \begin{bmatrix} f_{k,1}(\widetilde{\mathbf{x}}) \\ \vdots \\ f_{k,r}(\widetilde{\mathbf{x}}) \end{bmatrix}, \tag{2.4.4}$$

where $\widetilde{\mathbf{x}} = [x_1,\cdots, x_r, c_{r+1},\cdots, c_m]^t$ with c_i representing a constant solution for x_i, i=r+1, ..,m, and $\widetilde{\mathbf{F}}[\widetilde{\mathbf{x}}]$ is the corresponding minimal realization of $\mathbf{F}_k[\mathbf{x}]$. Therefore, $\mathbf{F}_k[\mathbf{x}]$ is the *homogenized* version of $\widetilde{\mathbf{F}}[\widetilde{\mathbf{x}}]$, which is either the homogeneous or heterogeneous polynomial with degree of at most k. In an event when the minimal realization is of the heterogeneous type, homogeneous invariants are no longer the only possible invariant structures in the homogenized formulation. In other words, when the minimal realization describes a polynomial process containing a limit cycle, the homogenized version must also contain the same limit cycle. By contrast, when the minimal realization is of the homogeneous type, no invariants other than the homogeneous are possible.

Theorem 2.4.1 A homogenized realization is singular .

Proof: Let $\mathbf{x}=\widetilde{\mathbf{x}} = [x_1,\cdots, x_r, c_{r+1},\cdots, c_m]^t$ be an eigenvector, with c_i as defined earlier. Then if there exists $c_i\neq 0$, the relationship $\mathbf{F}_k[\widetilde{\mathbf{x}}]-\lambda\widetilde{\mathbf{x}}=0$ holds if, and only if, $\lambda=0$. Consequently, the eigenvector solution is nilpotent. Alternatively when all $c_i=0$,

the nonzero eigenvector solutions must be in the $\mathbb{K}^r$ subspace of $\mathbb{K}^m$, *i.e.*, recall that $\mathbb{K}$ can be either $\mathbb{C}$ or $\mathbb{R}$. This subspace has the eigen-number $s_{k,r}<s_{k,m}$, and as such must contain non-simple eigenvectors because the process is by definition m-dimensional. Moreover, the algebraic basis $B_k\{\mathbb{K}^m\}$ must also be incomplete since there are no eigenvector solutions in the subspace $\mathbb{K}^m$-$\mathbb{K}^r$. Thus, to complete the basis one needs to compute generalized eigenvectors.

Let the generalized eigenvector solution $\mathbf{x}_g=[x_{g1},..., x_{gm}]^t\in \mathbb{K}^m$ correspond to the non-simple eigen-pair λ and $\tilde{\mathbf{x}}$ of muliplicity σ. From Equation (2.3.7) it follows that

$$\mathbf{F}_k[\mathbf{x}_g] - \lambda\mathbf{x}_g= \begin{bmatrix} f_{k,1}(\mathbf{x}_g) \\ \vdots \\ f_{k,r}(\mathbf{x}_g) \\ 0 \\ \vdots \\ 0 \end{bmatrix} - \lambda \begin{bmatrix} x_{g,1} \\ \vdots \\ x_{g,r} \\ x_{g,r+1} \\ \vdots \\ x_{g,m} \end{bmatrix} = \begin{bmatrix} x_1 \\ \vdots \\ x_r \\ 0 \\ \vdots \\ 0 \end{bmatrix}_{(\sigma)} = \tilde{\mathbf{x}}, \qquad (2.4.5)$$

which again for nonzero solutions of $x_{g,r+1},..., x_{g,m}$ holds if, and only if, $\lambda=0$. Therefore, the process must be singular since a complete m-dimensional algebraic basis cannot have all vector components with $x_{g,r+1},..., x_{g,m}$ equal to zero. ♦

From the arguments presented it is evident that the invariant structure of singular homogeneous processes can be more intricate than the invariant structure found in nonsingular homogeneous systems. As a result the singular homogeneous processes in general require more careful considerations. The following example illustrates this point.

Example 2.4.1 The three-dimensional cubic process,

$$\begin{bmatrix} \dot{x}_1 \\ \dot{x}_2 \\ \dot{x}_3 \end{bmatrix} = \begin{bmatrix} x_2x_3^2 \\ -x_1^2x_2 - x_1x_3^2 + x_2x_3^2 \\ 0 \end{bmatrix}, \qquad (2.4.6)$$

has the singular eigenspectra

$$X_3\{R^3\} = \left\{ \begin{bmatrix} 1 \\ 0 \\ 0 \end{bmatrix}_{(5)}, \begin{bmatrix} 0 \\ 1 \\ 0 \end{bmatrix}_{(7)}, \begin{bmatrix} 0 \\ 0 \\ 1 \end{bmatrix} \right\}$$

$$\Lambda_3\{R\} = \{ 0_{(5)}, 0_{(7)}, 0 \} \ .$$

The homogenizing variable in this case is x_3 and when selected as the projection state it produces the simple eigenvector. The other two eigenvectors have multiplicities which add up to the process eigen-number $s_{3,3}=13$. Next, by allowing solution $x_3=c$, one derives the minimal realization

$$\begin{bmatrix} \dot{x}_1 \\ \dot{x}_2 \end{bmatrix} = \begin{bmatrix} x_2 c^2 \\ - x_1^2 x_2 - x_1 c^2 + x_2 c^2 \end{bmatrix}, \qquad (2.4.7)$$

which is of the heterogeneous type. Now, if we change variables such that $y = x_1$ and $\dot{y} = c^2 x_2$, the minimal realization becomes $\ddot{y} - (c^2 - y^2)\dot{y} + c^4 y = 0$, which for $c=1$ is the equation of the van der Pol's oscillator. This implies that the homogenized realization, Equation (2.2.6), must have limit cycle solutions and are illustrated in Figure 2.4.1. Observe that the x_3-axis is the nilpotent invariant along which limit cycles are stacked.

By contrast, if we allow a slight perturbation in the equation for $\dot{x}_3$, for example $\dot{x}_3 = -.02\ x_3^3$, then the nilpotent invariant becomes idempotent. This new invariant will annihilate limit cycle solutions by sweeping through the stack in an attempt to reach the steady-state solution. This is illustrated in Figure 2.4.2. For the perturbations with opposite signs the invariant would annihilate limit cycle solutions by forcing the process to become unbounded.

2.5. CHAPTER II SUMMARY

Table 2.5.1 summarizes topics of significance covered in Chapter II. The topics in bold letters identify ideas that are conceived during the preparation of this thesis.

Table 2.5.1: Topics covered in Chapter II.

k-form algebras
• projection equation • characteristic equation - eigenvectors and eigenvalues - simple and multiplicative eigen solutions - nilpotent (singular) and idempotent eigen solutions • homogeneous spectra - eigenvector set or geometric spectrum - eigenvalue set or algebraic spectrum - **characteristic number or eigen-number** - **Fundamental Spectral Theorem** • k-form basis - **algebraic dependence and independence** - **algebraic degree and degrees of freedom** - generalized eigenvectors - **algebraically dependent trivial and generic eigenvectors** • linear transformations and canonical forms • invariant structures - **homogeneous invariants and nonlinear eigenmodes** - **homogenized systems and non-homogeneous invariants**

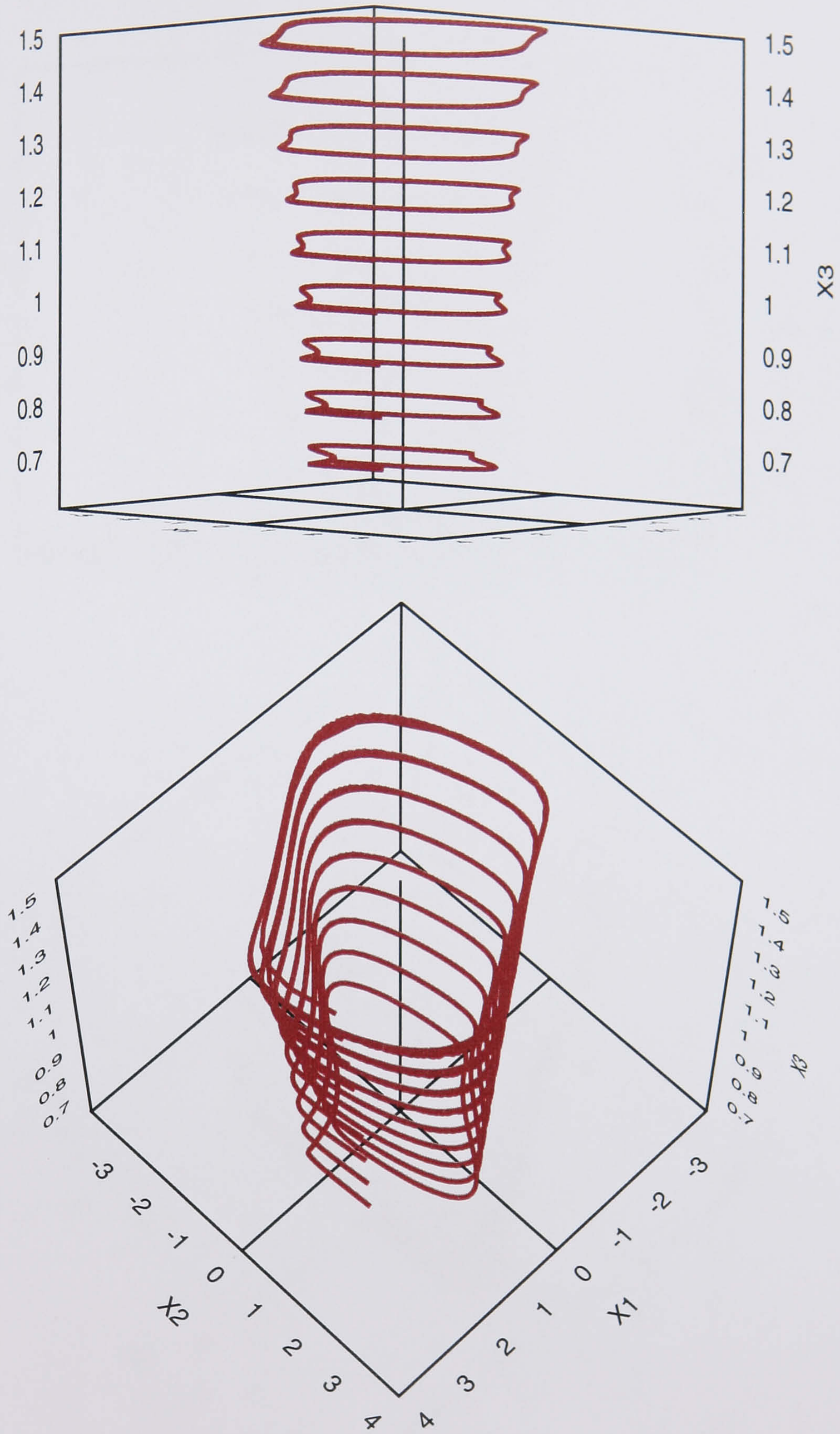

Three-dimensional state-space trajectories portray a stack of the van der Pol's limit cycles along the homogenization variable x_3.

FIGURE 2.4.1.

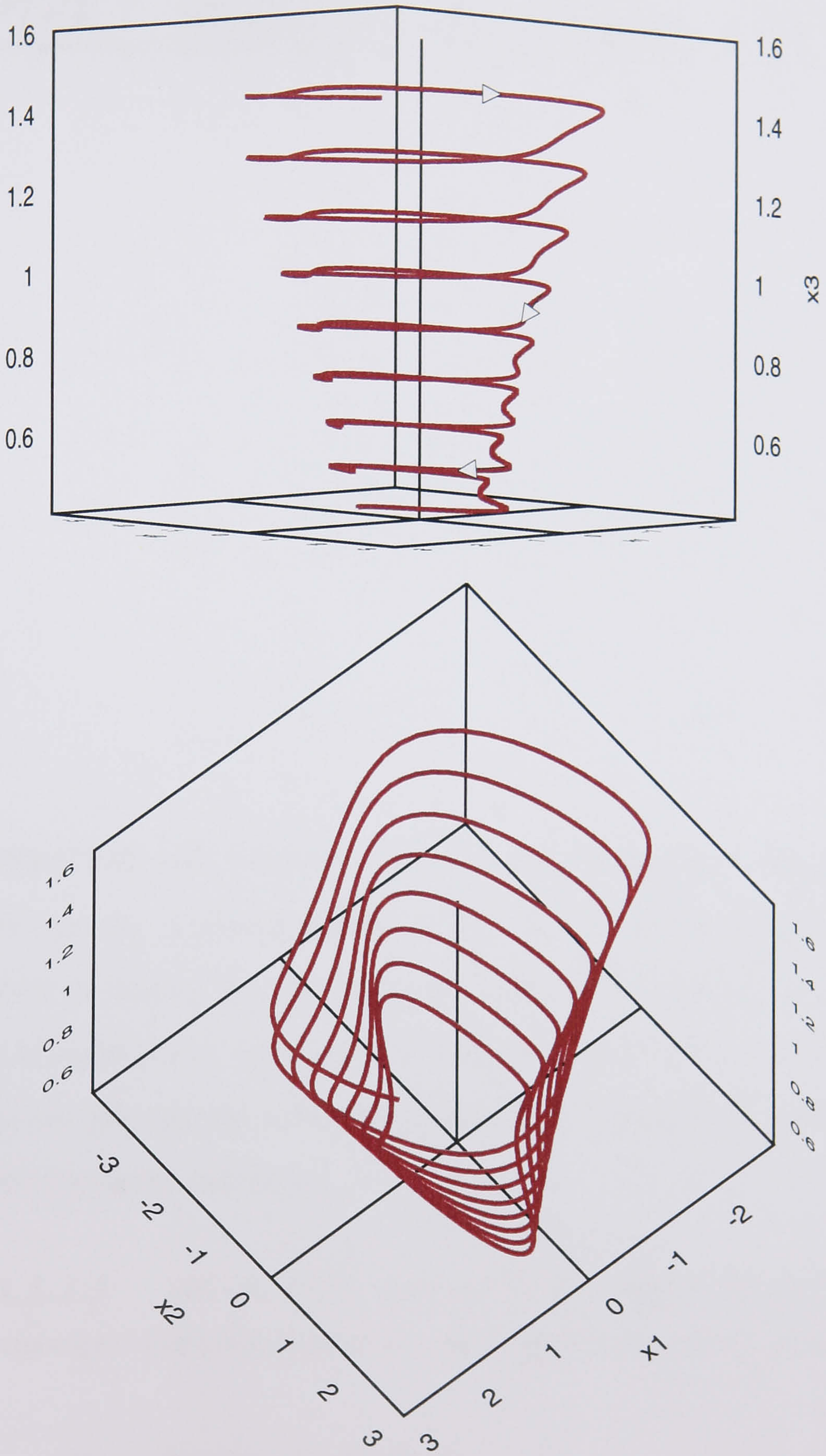

Annihilation of the van der Pol's limit cycles due to a loss of the homogenization property in variable x_3.

FIGURE 2.4.2.

CHAPTER 3 - STABILITY OF K-FORM SYSTEMS

3.1. OVERVIEW OF TWO-DIMENSIONAL STABILITY RESULTS

We start by reviewing stability results for the two-dimensional autonomous homogeneous processes. For these systems, stability is completely determined by the properties of eigenspectra, and the results have been reported in the early and mid 80's. Therefore, we only state the two-dimensional stability theorems while the proofs can be found in the appropriate references.

Theorem 3.1.1 Let $\mathbb{X}_k\{\mathbb{C}^2\}$ and $\Lambda_k\{\mathbb{C}\}$ be respectively the geometric and algebraic eigenspectra of a two-dimensional even degree homogeneous process. Then this process;

a) Is never periodic in $\mathbb{R}^2$.

b) Is never globally asymptotically stable.

c) Satisfies the necessary condition for marginal stability when all real eigenvectors in $\mathbb{X}_k\{\mathbb{C}^2\}$ are nilpotent.

For example, the implication of this theorem is that any bimolecular reaction scheme such as the one given in Equation (1.1.3) is never globally asymptotically stable.

It, however, may still exhibit an asymptotic stability in the region of interest, *i.e.*, the positive state space.

Theorem 3.1.2 When k is odd and $\mathcal{X}_k\{\mathbb{C}^2\}$ is purely complex, define the orientated Frommer's integral

$$I_{v_2} = \int_{\mathbb{R}} \frac{f_{k,1}(\mathbf{v})}{f_{k,2}(\mathbf{v}) - f_{k,1}(\mathbf{v})v_2}\, dv_2 , \quad \text{for} \quad \mathbf{v} = \begin{bmatrix} 1 \\ v_2 \end{bmatrix},$$

where integration is taken in direction of the v_2 flow. Then the process is;

a) Periodic if, and only if, $I_{v_2}=0$.

b) Has a stable focus if, and only if, $I_{v_2}<0$.

c) Has an unstable focus if, and only if, $I_{v_2}>0$.

Theorem 3.1.3 When k is odd and eigenvectors in $\mathcal{X}_k\{\mathbb{C}^2\}$ are mixed or purely real, the process;

a) Is globally asymptotically stable if, and only if, all eigenvalues associated with real eigenvectors are negative.

b) Satisfies the necessary condition for marginal stability when all eigenvalues associated with real eigenvectors are ≤ 0.

Remark The condition b) is also sufficient when at least one eigensolution is idempotent.

For proofs of these theorems see Samardzija (1983 and 1984). In addition, these results are also reported without using the spectral approach by Koditschek and Narendra (1982) for the quadratic processes, and more recently by Dayawansa *et al.* (1990) for processes of an arbitrary degree k.

3.2. MULTI-DIMENSIONAL CONSIDERATIONS

When m>2 it is no longer obvious how process stability is related to the properties of eigenspectra. This is because process complexity increases for the following three reasons.

The most apparent one is implied by Corollary 2.2.1 which states that now there are more eigenmodes than there are algebraic degrees of freedom. Thus, when m>2 we

need to evaluate qualitative behavior of the algebraically independent as well as dependent eigenmodes.

The second reason is implied by the possibility that nilpotent eigenvectors may be present. As was demonstrated in the van der Pol's example, such spectral components may support non-homogeneous invariants which exhibit more complex invariant structures. Even in two-dimensional cases this occurs.

Example 3.2.1 The two-dimensional homogeneous system

$$\begin{bmatrix} \dot{x}_1 \\ \dot{x}_2 \end{bmatrix} = \begin{bmatrix} A & 1 \\ 0 & A \end{bmatrix} \begin{bmatrix} x_1^k \\ x_2^k \end{bmatrix}, \tag{3.2.1}$$

has the characteristic equation

$$v\,(v^k - Av^{k-1} + A) = 0 \tag{3.2.2}$$

where the eigenvector $\mathbf{v}=[1,\ v]^t$ has the associated eigenvalue $\lambda=A+v^k$. For k=1, the eigen spectra are

$$\Sigma_1\{R^2\} = \left\{ \mathbf{e}_1=\begin{bmatrix} 1 \\ 0 \end{bmatrix}_{(2)} \right\} \text{ and } \Lambda_1\{R\} = \{A_{(2)}\}\ ,$$

which implies that there is only one eigenmode of multiplicity 2. Consequently, for k=1 the process given by Equation (3.2.1) is in the Jordan canonical form. By contrast, for k>1 and A≠0, Equation (3.2.1) is no longer in the Jordan form. This is because the characteristic equation now has k+1 spectral solutions, of which the eigen-pair $\mathbf{e}_1$ and A are of multiplicity 1. Therefore, Equation (3.2.1) cannot be in the canonical form. However, for A=0 the characteristic equation implies that $\mathbf{e}_1$ is of multiplicity k+1 and, hence, Equation (3.2.1) is in the Jordan form for all k≥1. Moreover, the process is singular and x_2 is the homogenization variable that generates the minimal realization

$$\dot{x}_1 = c^k\ , \tag{3.2.3}$$

where c is the solution of x_2. Clearly the process state x_1 is now unstable for any real c≠0. For the case k=1 this observation is predicted by the classic linear stability theorem which

states that the linear system cannot be marginally stable if the pole defined by A=0 is not simple. This result carries over to k>1.

Remark This example shows why the necessary conditions for marginal stability stated in Theorems 3.1.3 is not always sufficient.

The third reason for increase in complexity is attributed to the fact that in general both real and complex eigen solutions are possible. The real solutions determine the vector field flows which are guided by the ray type invariants, while the complex ones are responsible for the vector field curvature. Moreover, for m=2, it is easy to show that the global behavior is determined by the behavior of real eigenmodes while the complex ones can be ignored. This is stated in Theorems 3.1.1 and 3.1.3, and is further illustrated by the following example:

Example 3.2.2 The two-dimensional cubic system

$$\begin{aligned} \dot{x}_1 &= A(2x_1+Ax_2)x_1^2 - x_2^3 \\ \dot{x}_2 &= 2Ax_1^2x_2 + (2+A^2)x_1x_2^2 - 2x_2^3 \end{aligned} \tag{3.2.4}$$

has the characteristic equation

$$\begin{aligned} \lambda &= A(2+Av) - v^3 \\ v^2(v^2 - 2v + 2) &= 0 \end{aligned} \tag{3.2.5}$$

defined with respect to the projection state x_1. The spectral solutions are

$$\Sigma_3\{C^2\} = \left\{ \mathbf{e}_1=\begin{bmatrix} 1 \\ 0 \end{bmatrix}_{(2)}, \ \mathbf{v}_1 = \begin{bmatrix} 1 \\ 1+i \end{bmatrix}, \ \mathbf{v}_2 = \begin{bmatrix} 1 \\ 1-i \end{bmatrix} \right\} \text{ and}$$

$$\Lambda_3\{C\} = \{2A_{(2)}, \alpha+i\beta, \alpha-i\beta ; \text{with } \alpha= A^2 + 2A - 2 \text{ and } \beta= 2+A^2\},$$

where the real eigenmode is of multiplicity two, and the remaining two are complex. Note that the eigenvalues are dependent on A, while the eigenvectors are not. Furthermore, the eigenvalue parameters α and β are related to A as illustrated in Figure 3.2.1. The figure also depicts various stability regions. As indicated, the global behavior is not influenced by the behavior of complex eigenmodes. For example, when A>0 the real eigenmode is

always unstable. Consequently, for A>0 the process is globally unstable independent of how the complex eigenmodes behave.

This, however, does not imply that the complex eigenmodes have no significant effect on the process dynamics. To see this we first consider the case A=0, or the case of the nilpotent real invariant. In this instance the complex eigenmodes have the eigenvalue components α=-2 and β=2. The sign of α indicates that these modes are stabilizing while β is responsible for the curvature illustrated in Figure 3.2.2. Observe that all process trajectories begin and end along the nilpotent invariant indicated by the thick line. As such, the process is marginally stable.

Next, let A<0. For all negative A values the invariant is a stable idempotent. Thus, according to Theorem 3.1.3 the process is now globally asymptotically stable. Moreover, for -1.7< A<0, the changes in both α and β are relatively small while the change in the real eigenvalue, 2A, is significant. As a result this spectral arrangement promotes the spiral formation illustrated in Figure 3.2.3. Basically the stable idempotent now sweeps the points along the nilpotent invariant in Figure 3.2.2 into the origin. At A=2, however, the eigenvalue parameters are α=-2 and β=6. The significant increase in β now promotes the parabolic type curvature illustrated in Figure 3.2.4. This sets off a bubble formation within the state-space, which further implies that the process now exhibits a small degree of stiffness. By reducing A to -2.2 one increases β even more, and this in turn expands the bubble illustrated in Figure 3.2.5. Finally, for A=-2.8 the eigenvalue parameters are α=0.24 and β=9.84. Thus, the complex eigenmodes are now unstable since α>0, while β increases even further. As a result the bubble becomes more inflated, Figure 3.2.6, and forces the process to be quite stiff.

When m>2, the stability characterization of processes with the mixed spectra may not be as easy to accomplish as in the two-dimensional case. The primary reason being that now there may exist subspaces in which only complex eigenmodes are present. In such instances the periodic or focal type solutions must also be considered, as well as the solutions generated by the ray type invariants. Therefore, to make the analysis of multidimensional stability less confusing we will initially examine a behavior of

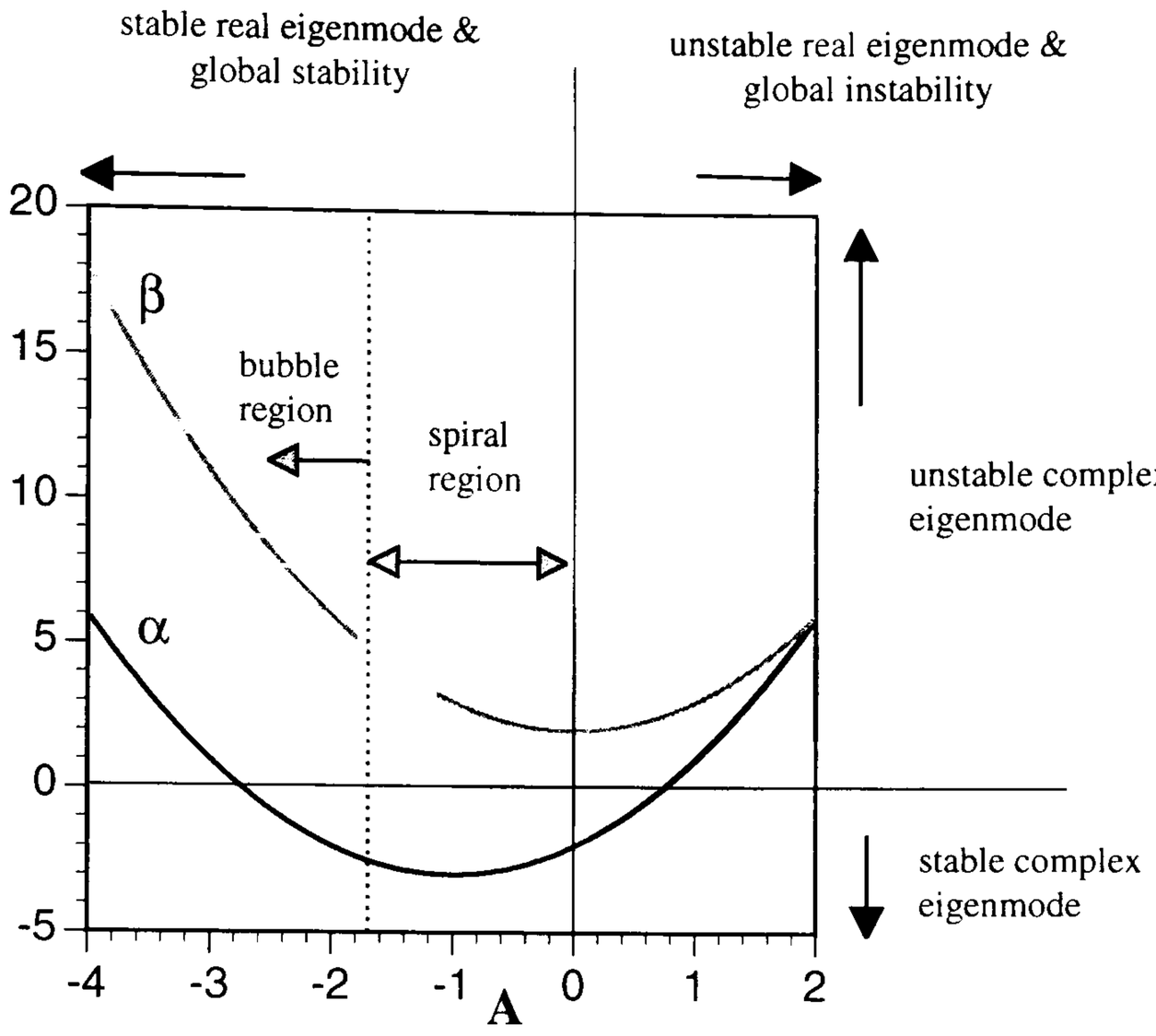

Regions in the parameter space which characterize the global process and eigenmode behaviors.

FIGURE 3.2.1.

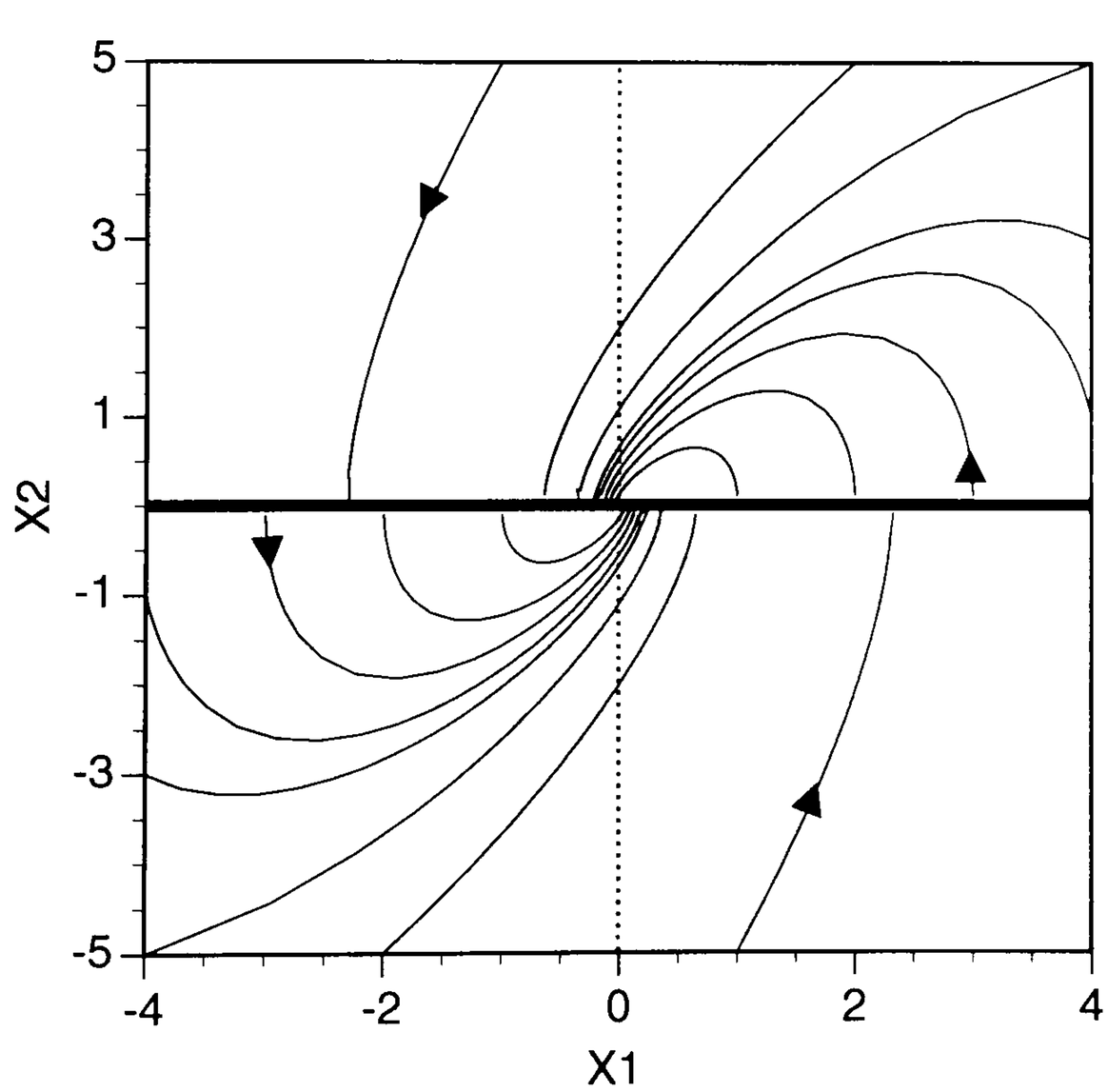

For the parameter value A=0.0, a presence of the complex eigenmode is indicated by the curved trajectories surrounding the nilpotent invariant.

FIGURE 3.2.2.

multivariate homogeneous processes for which the eigenspectra are purely real. The mixed case is considered subsequently.

3.3. MULTI-DIMENSIONAL STABILITY RESULTS FOR PROCESSES WITH PURELY REAL EIGENSPECTRA

Theorem 3.3.1 When the geometric eigenspectrum of a nonsingular autonomous homogeneous process is purely real, $\mathbb{X}_k\{\mathbb{R}^m\}$, then:

a) for k odd, the process is globally asymptotically stable if and only if eigenvalues are all negative.

b) for k even, the process is never stable.

Proof: The result applies to all nonsingular processes for which invariants are determined strictly by real eigenvectors. Thus, all invariants are homogeneous and define the ray type trajectories through the origin of $\mathbb{R}^m$. Consequently the if statement in a) is implied by the fact that the trivial solution has a local vector field entirely determined by the invariant rays which support stable characteristic solutions, Equation (2.4.2). Therefore, the trivial point is asymptotically stable, while the homogeneous property implies that the local stability is global. The alternate direction follows from the observation that the global asymptotic stability implies the local asymptotic stability, which is only possible if the eigenvalues are all negative. This was also verified by Samardzija (1983) and Coleman (1984). The statement b) is implied by the spectral scaling property which forces characteristic solutions to change qualitatively as the sign of an initial condition changes. ♦

Theorem 3.3.2 When the geometric eigenspectrum of a singular autonomous homogeneous process is purely real, $\mathbb{X}_k\{\mathbb{R}^m\}$, then;

a) For k odd, the process is marginally stable if all idempotents have negative eigenvalues and no nilpotents support non-homogeneous invariants.

b) For k even, any non-homogenized process is never marginally stable.

Proof: The proof follows from the observation that such a process contains only homogeneous invariants, none of which are unstable. Thus, no state-space trajectories have a direction along which they can become unbounded. They either approach the origin

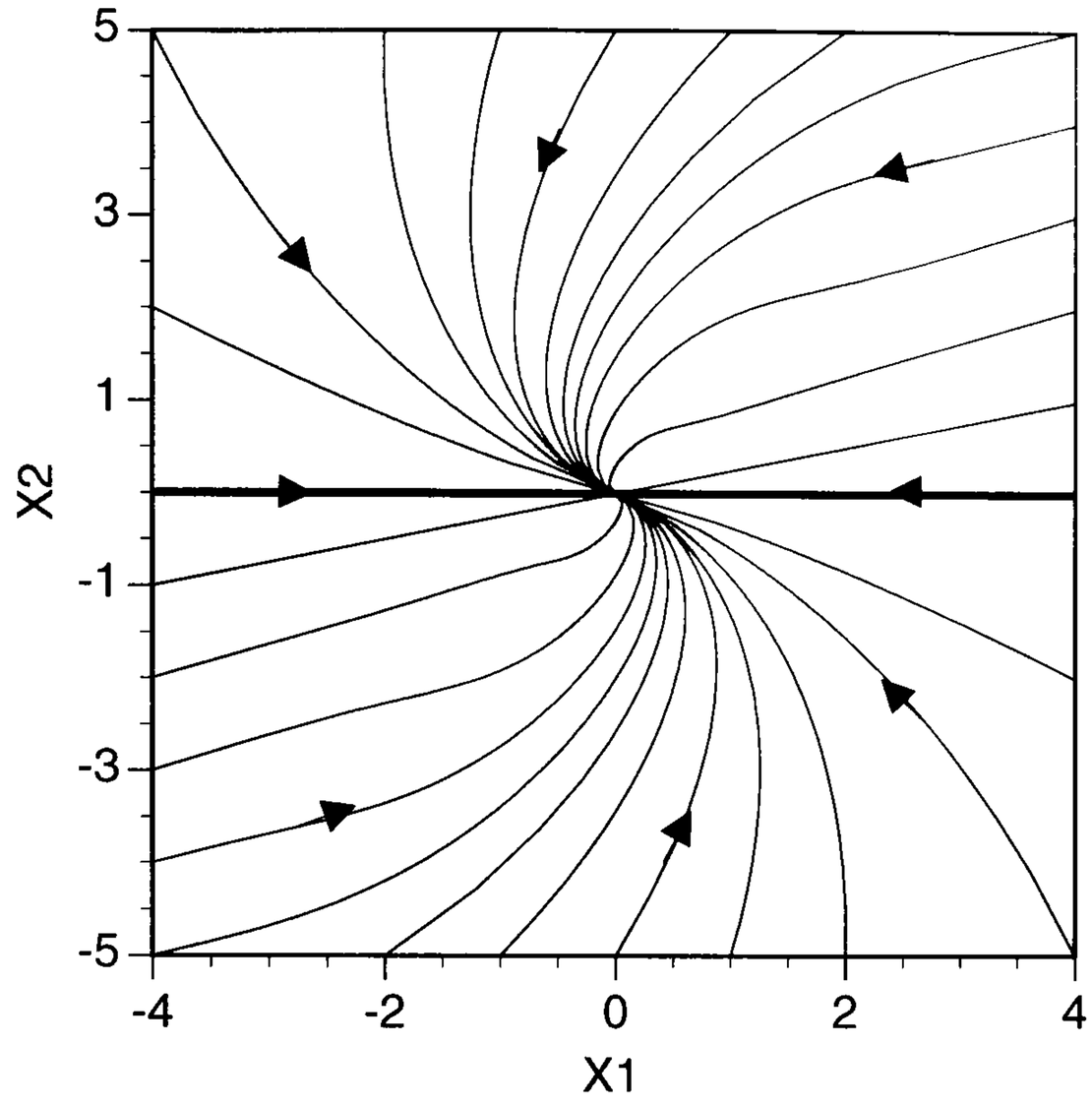

For the parameter value A=-1.7, a spiral vector field flow is promoted by the complex eigenmode.

FIGURE 3.2.3.

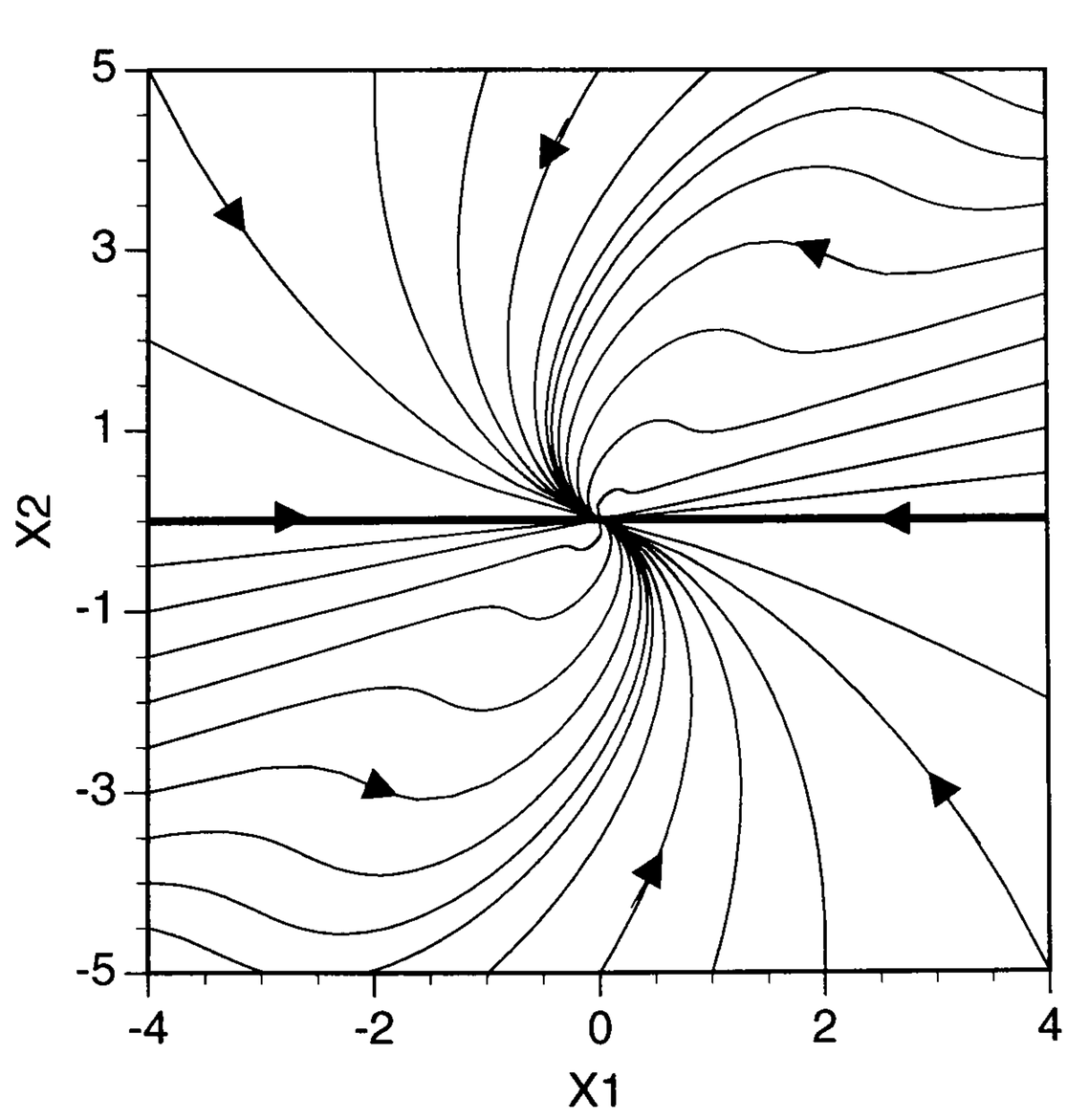

For the parameter value A=-2.0, a bubble formation is promoted by the increase in intensity of the complex eigenmode.

FIGURE 3.2.4.

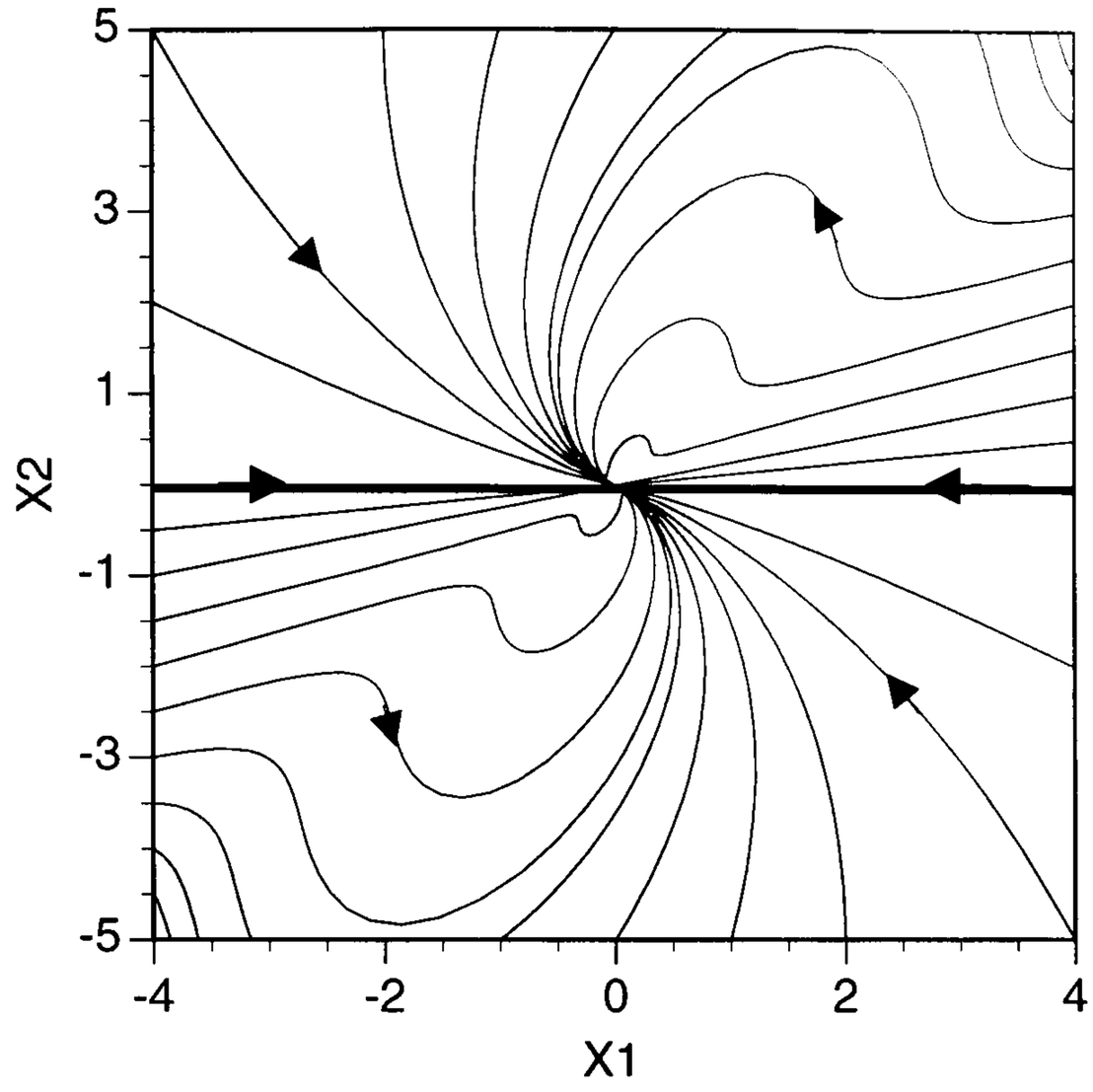

For the parameter value A=-2.2, the complex eigenmode is further intensified and a bubble expands.

FIGURE 3.2.6.

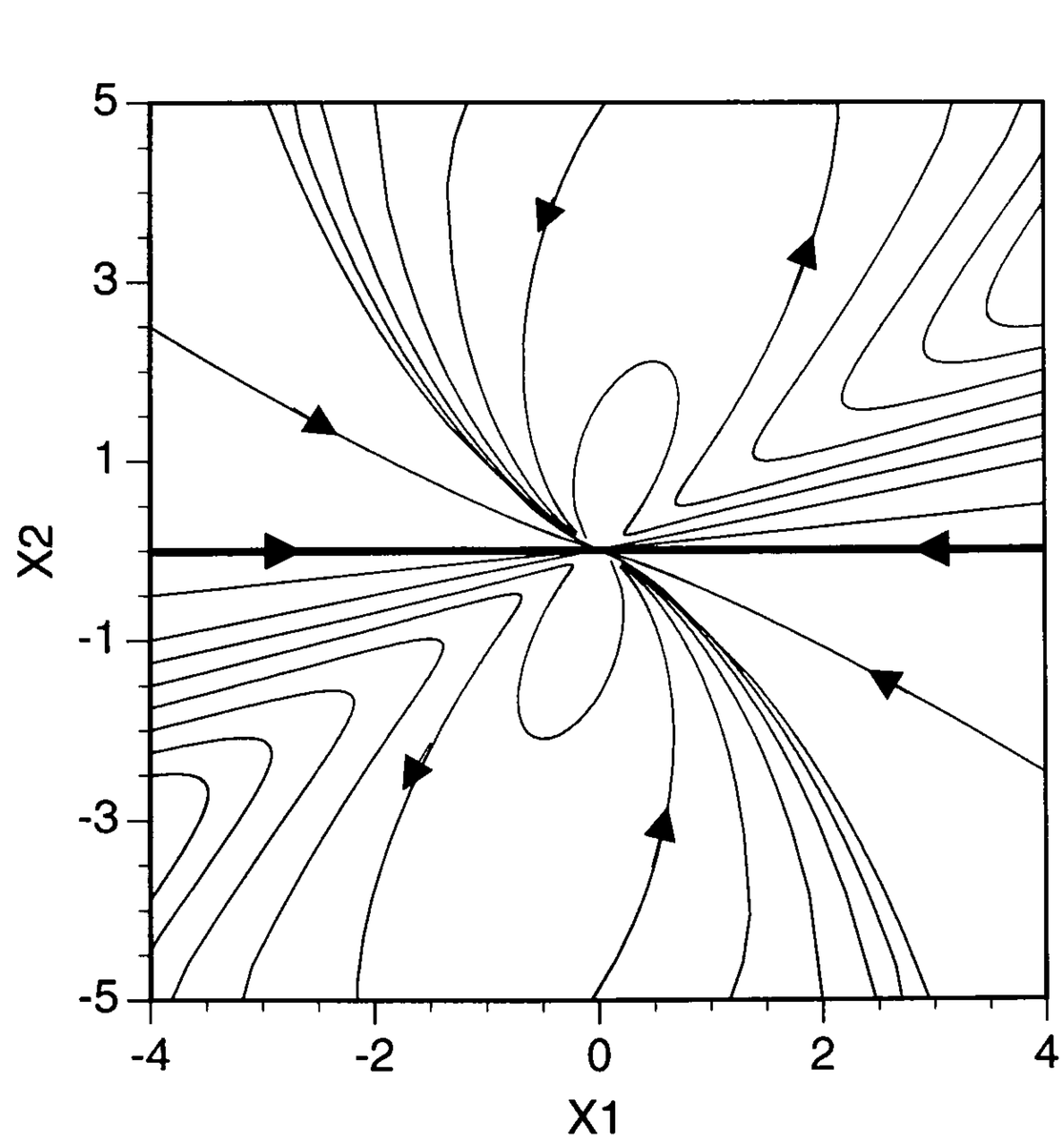

For the parameter value A=-2.8, the complex eigenmode inflates a bubble.

FIGURE 3.2.6.

or the points on one of the nilpotent invariants. However, if a nilpotent spectral component supports the non-homogeneous invariant the theorem in general does not hold. b) is implied by the fact that for k=even any existing idempotent is unstable.

The final question is, what if all spectral components are nilpotent? In this case we must have a homogenized structure and the theorem is invalid, see Example 3.2.1. ♦

Note that Theorem 3.3.1 provides a stronger result than Theorem 3.3.2. This is because homogenization is not an issue when processes are nonsingular.

3.4. MULTI-DIMENSIONAL STABILITY RESULTS FOR PROCESSES WITH MIXED AND PURELY COMPLEX EIGENSPECTRA

Let $X_k\{C^m\}$ be mixed, and let μ be the sum of the multiplicities associated with each complex eigenvector. For instance, $\mu=2$ in Example 3.2.2. Then the following result applies.

Theorem 3.4.1 A mixed geometric spectrum, $X_k\{C^m\}$, of an odd nonsingular autonomous homogeneous process is globally asymptotically stable if $\mu<k+1$, and all real eigenmodes are stable.

Proof: The requirement that all real eigenmodes are stable is implied by the earlier arguments. Moreover when $\mu<k+1$, then according to Theorem 3.1.2 the homogenous process does not have enough complex eigenmodes to support fully either periodic or focal type solutions. Consequently, the complex eigenmodes only create curvatures that in the final outcome are guided by the real spectral elements. This situation is qualitatively identical to the case in Example 3.2.2.♦

Remark Theorem 3.4.1. does not suggest that a process may not be globally asymptotically stable when $\mu\geq k+1$. The outcome, however, depends on algebraic relations between the spectral elements.

Finally, what can be said about processes which have purely complex eigenspectra? According to Theorem 2.2.1 these are only possible when k is odd and m is even. In such instances the eigen-number is even, implying that all spectral solutions can be complex. For two-dimensional systems, this is clearly demonstrated by Theorem 3.1.2 in which the Frommer's integral is used to classify the three types of oscillatory behavior. Similarly for m>2, these types of oscillatory behavior are also present. However, the classification cannot be formalized for higher dimensions, since in this case there does not exist an analog of the Frommer's integral. Exceptions do occur when oscillations can be decoupled into two-dimensional oscillating subsystems, in which case the Frommer's integral can be generalized. In all other cases, we can only use our intuitive reasoning to explain how oscillations are formed. For example, a process which contains purely complex spectra exhibits global asymptotic stability in form of a stable focus when all real eigenvalue parts are negative. In this case, all eigenmodes are stable, or *stabilizing*. By contrast, when all real eigenvalue parts are positive a process has an unstable focus and all the modes are unstable, or *destabilizing*. These claims are familiar for linear systems, in which case they can also be proved rigorously. For k>1, however, the rigorous proof is not presently known, but at the same time there are no known examples which contradict the above intuitive result.

This intuitive reasoning also leads to the notion of spectral balancing. Suppose that the purely complex eigenspectra has real eigenvalue parts which exhibit mixed signs. Some are positive, some negative, and some are zero. Then the question is: what can we qualitatively expect from such a process? The answer is determined from the algebraic balance of eigenmodes. That is, when all eigenmodes are algebraically balanced out, meaning that neither stabilizing nor destabilizing modes are prevalent, then one can expect a conservative or periodic behavior. However, if either stabilizing or destabilizing modes prevail a process is no longer in balance, and a formation of the focal stable or unstable solutions must appear. We now illustrate this reasoning.

Example 3.4.1 The skew-symmetric linear system

$$\begin{bmatrix} dx_1/dt \\ dx_2/dt \\ dx_3/dt \\ dx_4/dt \end{bmatrix} = \begin{bmatrix} 0 & -1 & 1 & -1 \\ 1 & 0 & -1 & 1 \\ -1 & 1 & 0 & -1 \\ 1 & -1 & 1 & 0 \end{bmatrix} \begin{bmatrix} x_1 \\ x_2 \\ x_3 \\ x_4 \end{bmatrix} \tag{3.4.1}$$

has the eigenspectra

$$X_1(C^4) = \left\{ \begin{bmatrix} 1 \\ -0.7071067811 + i\ 0.7071067811 \\ -i \\ 0.7071067811 - i\ 0.7071067811 \end{bmatrix}; \begin{bmatrix} 1 \\ -0.7071067811 - i\ 0.7071067811 \\ i \\ 0.7071067811 + i\ 0.7071067811 \end{bmatrix}; \begin{bmatrix} 1 \\ 0.7071067811 + i\ 0.7071067811 \\ i \\ -0.7071067811 + i\ 0.7071067811 \end{bmatrix}; \begin{bmatrix} 1 \\ 0.7071067811 - i\ 0.7071067811 \\ -i \\ -0.7071067811 - i\ 0.7071067811 \end{bmatrix} \right\}$$

$$\Lambda_1(C) = \begin{Bmatrix} -i\ 2.4142135623 ; i\ 2.4142135623 ; \\ -i\ 0.4142135623 ; i\ 0.4142135623 \end{Bmatrix} .$$

As is well known, this is a periodic conservative system because all spectral terms are balanced due to the zero real eigenvalue parts.

Now, consider the cubic skew-symmetric system

$$\begin{bmatrix} dx_1/dt \\ dx_2/dt \\ dx_3/dt \\ dx_4/dt \end{bmatrix} = \begin{bmatrix} 0 & -1 & 1 & -1 \\ 1 & 0 & -1 & 1 \\ -1 & 1 & 0 & -1 \\ 1 & -1 & 1 & 0 \end{bmatrix} \begin{bmatrix} x_1^3 \\ x_2^3 \\ x_3^3 \\ x_4^3 \end{bmatrix} \tag{3.4.1}$$

which has $s_{3,4}$=40 complex spectral components listed in Appendix I. By examining the eigenvalue set we see that in this case eigenvalues with zero, negative and positive real parts are present. However, they are all balanced out, since their total sum is zero. Therefore, the cubic system is also conservative as illustrated in Figure 3.4.1. Observe that in this case, an algebraic balancing is accomplished through the symmetric eigenvalue structure. However, in general it is possible to have a non-symmetric balance. See for example the conservative cubic system given by the equation known as the "shoemaker's last" (Davies 1962).

3.5. STRUCTURAL STABILITY AND ROBUSTNESS

The idea here is to observe changes in the qualitative behavior of a process for small perturbations in process parameters. When a perturbed system retains its original stability properties it is referred to as the structurally stable, otherwise it is structurally unstable. For homogeneous systems, structural stability is implied by the properties of the homogeneous spectra. The process in Equation (2.1.8) is structurally unstable when its geometric spectrum contains real nilpotents and/or has complex eigenvectors that support closed periodic orbits. Otherwise, it is structurally stable. Clearly, this is an extension of structural stability known for linear systems (Guckenheimer and Holmes 1983). As a result, the marginally stable and/or periodic homogeneous processes are structurally unstable. In the linear case these are implied by the requirement that the real eigenvalue parts are zero. For k>1 this condition still holds when eigenvectors are real. However, for periodic solutions the Frommer's integral is an analog of the linear case requirement. It can be shown that for k=1 the condition $I_{v_i}=0$, $v_i \in \mathbf{v}$, implies zero real eigenvalue parts. This no longer holds for k>1. In general, when $I_{v_i}=0$ the complex spectral elements are algebraically balanced out and the orbital stability is achieved. Thus, any small parameter perturbation disturbing the balance will result in an integral value that no longer is zero (*i.e.*, a stable or unstable focus).

Theorem 3.5.1 A stable even degree homogeneous process is never structurally stable.

Proof: Every even degree homogeneous process has an odd eigen-number. Thus, $\chi_{k=even}\{\mathbb{C}^m\}$ must have at least one real eigenvector. Consequently, since the stable property implies that no solutions can escape to infinity in finite or infinite times, this eigenvector must be nilpotent. ♦

The structural stability arising in homogenized processes is also an important issue. Observe that these processes are structurally unstable because the homogenization variables define nilpotent invariants. Thus, although a homogenized process is structurally unstable its minimal realization may be structurally quite stable. The van der Pol's oscillator

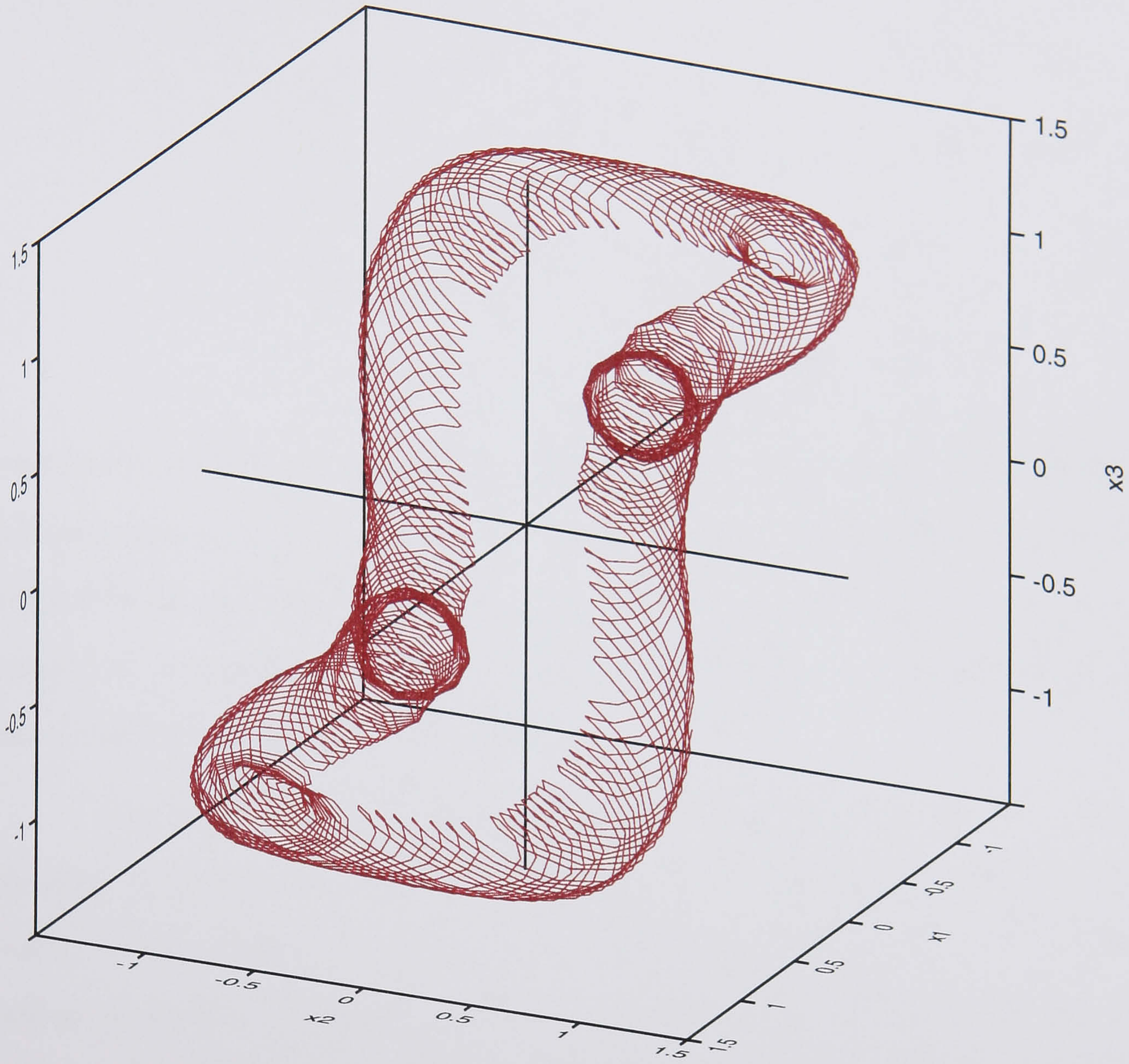

The 3-D view of the 4-dimensional skew-symmetric cubic periodic system for the initial conditions $x_1=x_2=x_3=x_4=1.0$.

FIGURE 3.4.1.

example illustrates this point. To demonstrate this further, consider Equation (2.4.3) written in the following way

$$\begin{bmatrix} \dot{x}_1 \\ \vdots \\ \dot{x}_r \\ \\ \dot{x}_{r+1} \\ \vdots \\ \dot{x}_m \end{bmatrix} = \mathbf{F}_k[\mathbf{x}] = \begin{bmatrix} f_{k,1}(\mathbf{x}) \\ \vdots \\ f_{k,r}(\mathbf{x}) \\ \\ \varepsilon f_{k,r+1}(\mathbf{x}) \\ \vdots \\ \varepsilon f_{k,m}(\mathbf{x}) \end{bmatrix}, \tag{3.5.1}$$

where now, each $\varepsilon f_{k,j}(\mathbf{x})$, j=r+1,..,m, is a perturbation term with error, ε multiplying an arbitrary k-form expression. Thus, when $\varepsilon=0$ the process is homogenized and invariants other than the homogeneous ones can appear. However, when $\varepsilon\neq0$, the process no longer can be considered as being homogenized. Therefore, invariants other than the homogeneous ones are now not possible.

We conclude this section by relating concepts of process robustness and structural stability. A dynamic process is said to be robust if it is stable, as well as structurally stable. In other words, the stable process behavior is not effected by the variations in process parameters. Moreover, a stable process X is said to have a greater degree of robustness than a stable process Y if a stable behavior of X tolerates a greater variation in process parameters than the process Y. As a result the k-form structures which are marginally stable or periodic are not robust in comparison with any odd k-form process for which the eigenvalues are set deep in the left complex plane.

3.6. CHAPTER III SUMMARY

Table 3.6.1 summarizes topics of significance covered in Chapter III. The topics in bold letters identify ideas that are conceived during the preparation of this thesis.

Table 3.6.1: Topics covered in Chapter III.

k-form stability
• two-dimensional stability - odd and even k-form systems - real, complex and mixed eigenspectra - global asymptotic, marginal and periodic stability • **multi-dimensional stability** - odd and even k-form systems - purely real eigenspectra - mixed and purely complex eigenspectra • **structural stability and robustness**

CHAPTER 4 - CONTROLLABILITY AND STABILIZABILITY

4.1. PROCESS CONTROLLABILITY WITH CONSTANT CONTROL MATRIX

To study control properties of the homogeneous processes we begin by considering the following process description

$$\dot{\mathbf{x}} = \mathbf{F}_k[\mathbf{x}] + \mathbf{B}\mathbf{u} \ , \tag{4.1.1}$$

where $\mathbf{B}=[\mathbf{b}_1, \mathbf{b}_2,..., \mathbf{b}_n]$ is a real mxn constant control matrix with column vectors $\mathbf{b}_i=[b_{i1}, b_{i2},..., b_{im}]^t$, $i=1,...,n$, and $\mathbf{u}\in \Re^n$ is a piecewise continuous control or forcing function. We shall soon demonstrate that this process description offers a natural extension of the state controllability concept defined for the linear systems. The more general case in which the control vector depends on the process states is treated subsequently.

The controllability properties of homogeneous systems were first addressed by Baillieul (1980, 1981). In his work a control criterion is accomplished through the use of Lie algebra. He recognized that under the Lie bracket operation the components in $\mathbf{F}_k[\mathbf{x}]$ and matrix $\mathbf{B}$ form the controllability set B whose elements may, or may not, span $\Re^m$.

When they do, the strong accessibility property is satisfied and a stabilizing state feedback may be achieved. Unfortunately, this framework does not include all algebraic relations, and as such provides only partial answers to the controllability issues. Therefore, the accessibility condition has been generalized by formulating the state controllability concept for homogeneous processes (Samardzija 1984, 1995). This approach shows that the accessibility condition does not account for coupling among the process states and therefore offers a limited number of stabilizing solutions. In contrast, the state controllability approach produces a broader class of state feedback realizations. This is now discussed.

When the state controllability for homogeneous processes is studied by using eigenspectra one needs to distinguish two cases. The first case involves all homogeneous processes for which $|\mathbb{X}_k\{\mathbb{K}^m\}|$ is finite, and the second case exists when $|\mathbb{X}_k\{\mathbb{K}^m\}|$ is infinite. This distinction is important since in the latter case the presence of a trivial subspace demands more detailed consideration. For example, it is well known that the linear system

$$\dot{\mathbf{x}} = \mathbf{D}\mathbf{x} + \mathbf{b}u \ , \tag{4.1.2}$$

where **D** is a mxm diagonal matrix, and **b** is a mx1 control vector, is state controllable as long as all eigenvalues on the **D**-diagonal are distinct and **b** has no zero rows. If two or more eigenvalues are identical the result no longer holds. This is because the eigenvectors with identical eigenvalues span the trivial subspace. As a result there exists a nonsingular linear transformation, **y=Tx**, that re-diagonalizes Equation (4.1.2) and produces a control vector $\mathbf{T}^{-1}\mathbf{b}$ with a zero row corresponding to one of the identical eigenvalues. Hence, the trivial subspace has a ray solution which cannot be addressed by a control u. Consequently, for infinite $|\mathbb{X}_1\{\mathbb{K}^m\}|$ the state controllability no longer holds in certain state-space directions. This situation is often remedied by allowing **b** to be a mxr matrix **B**, where r>1.

For k>1, a similar scenario exists. An interesting result on this subject is examined by Andreini *et al.* (1988). In the present study, however, we investigate the state controllability and stabilizability of those homogeneous processes for which the

spectral cardinality is finite. The theory presented can then be modified to accommodate cases for which the trivial subspace exists. Thus, from now on every geometric spectrum has a finite number of eigenvectors.

Let the homogeneous spectra be mixed, and let $|\mathbb{X}_k\{\mathbb{C}^m\}|=s\leq s_{k,m}$. Next, by using all process eigenvectors define the following matrix set,

$$\mathbb{T} = \left\{ \begin{array}{c} \mathbf{T}_\nu=[\mathbf{v}_\nu,..,\mathbf{v}_{m+\nu-1}]\ ;\ \text{with}\ \ \nu=1,..,s+1\text{-m},\quad s\leq s_{k,m}, \\ \text{and}\ \mathbf{v}_1,..,\mathbf{v}_s\in \mathbb{X}_k\{\mathbb{C}^m\} \\ \\ \text{or} \\ \\ \mathbf{T}=[\mathbf{v}_1,..,\mathbf{v}_s,\mathbf{v}_{s+1},..,\mathbf{v}_m]\ ;\ \ \text{when}\ \ s<\text{m},\ \text{and where} \\ \mathbf{v}_1,..,\mathbf{v}_s\in \mathbb{X}_k\{\mathbb{C}^m\}\ \text{and}\ \mathbf{v}_{s+1},..,\mathbf{v}_m\ \text{are generalized eigenvectors.} \end{array} \right\}.$$

Each $\mathbf{T}_\nu\in\mathbb{T}$ defines the linear transformation $\mathbf{x}=\mathbf{T}_\nu\mathbf{y}$ which transforms the original process Equation (4.1.1) into the canonical form

$$\dot{\mathbf{y}} = \mathbf{T}_\nu^{-1}\mathbf{F}_k[\mathbf{T}_\nu\mathbf{y}] + \mathbf{T}_\nu^{-1}\mathbf{B}\mathbf{u} = \mathbf{D}\mathbf{y}^k + \mathbf{H}_k[\mathbf{y}] + \mathbf{T}_\nu^{-1}\mathbf{B}\mathbf{u}\quad , \qquad (4.1.3)$$

where $\mathbf{y}^k=[y_1{}^k, y_2{}^k,.., y_m{}^k]^t$, **D** is mxm diagonal matrix with diagonal elements being the eigenvalues corresponding to the eigenvectors used in columns of $\mathbf{T}_\nu$, $\mathbf{H}_k[\mathbf{y}]$ is the residual vector containing only cross-coupled terms, and $\mathbf{T}_\nu{}^{-1}\mathbf{B}\mathbf{u}$ is the transformed control term. When s<m, **D** can be in the block diagonal Jordan form.

Theorem 4.1.1 The necessary state controllability conditions for the process defined in Equation (4.1.1) are;

a) For all canonical transformations $\mathbf{T}_\nu\in\mathbb{T}$ which generate diagonal matrices **D**, no row of $\mathbf{H}_k[\mathbf{y}]+\mathbf{T}_\nu{}^{-1}\mathbf{B}\mathbf{u}$ is zero.

b) For all canonical transformations $\mathbf{T}_\nu\in\mathbb{T}$ which generate **D** in the Jordan block form, no row of $\mathbf{H}_k[\mathbf{y}]+\mathbf{T}_\nu{}^{-1}\mathbf{B}\mathbf{u}$ that corresponds to the last row of each Jordan block is zero.

For the proof of the theorem see Samardzija (1984). Note that this formulation allows invariant rays, or eigenmodes, defined by both the algebraically independent and

the generically dependent eigenvectors to be tested. Thus, if any of the eigenmodes fail to satisfy the controllability criterion, the homogeneous process does not satisfy the necessary state controllability condition.

4.2. NECESSARY STATE CONTROLLABILITY CONDITION FOR PROCESSES WITH STATE DEPENDENT CONTROL MATRIX

To examine a more general case we consider the process

$$\dot{\mathbf{x}} = \mathbf{F}_k[\mathbf{x}] + \mathbf{B}_q[\,[\mathbf{x}]\,]\,\mathbf{u}\ , \tag{4.2.1}$$

for $0 \le q \le k$, where $\mathbf{B}_q[[\mathbf{x}]]=[\mathbf{B}_{q,1}[\mathbf{x}], \mathbf{B}_{q,2}[\mathbf{x}],..., \mathbf{B}_{q,n}[\mathbf{x}]]$ is a real q-form control matrix with each q-form column vector $\mathbf{B}_{q,i}[\mathbf{x}]=[b_{q,i1}(\mathbf{x}), b_{q,i2}(\mathbf{x}),...,b_{q,im}(\mathbf{x})]^t$ for $i=1,...,n$, and $\mathbf{u}$ as defined earlier. Clearly, for $q=0$ the controllability formulation is exactly the same as that addressed in the previous section. For $q>0$ the last theorem can be restated as follows:

Theorem 4.2.1 The necessary state controllability conditions for the process defined in Equation (4.2.1) are;

a) For all canonical transformations $\mathbf{T}_v \in \mathfrak{T}$ which generate diagonal matrices $\mathbf{D}$, no row of $\mathbf{H}_k[\mathbf{y}]+\mathbf{T}_v^{-1}\mathbf{B}_q[\,[\mathbf{y}]\,]\mathbf{u}$ is zero.

b) For all canonical transformations $\mathbf{T}_v \in \mathfrak{T}$ which generate $\mathbf{D}$ in the Jordan block form, no row of $\mathbf{H}_k[\mathbf{y}]+\mathbf{T}_v^{-1}\mathbf{B}_q[\,[\mathbf{y}]\,]\mathbf{u}$ that corresponds to the last row of each Jordan block is zero.

For $k=q=1$ this theorem implies the necessary state controllability conditions for a bilinear system.

4.3. STABILIZABILITY: *THREE-DIMENSIONAL EXAMPLE WITH CONSTANT CONTROL VECTOR*

It is known that any state controllable two-dimensional homogeneous system defined by Equation (4.2.1) can have all of its eigenvalues arbitrarily assigned (Samardzija 1984). Therefore, if the two-dimensional k-form process is unstable it can always be stabilized by a smooth homogeneous state feedback of degree equivalent to that of the

process. The same results, however, could not be claimed for dimensions greater than two. The reasons are implied by Theorem 2.2.1, and are further examined by studying the three-dimensional stabilization problems with constant control vector.

Example 4.3.1 Consider the three-dimensional cubic homogeneous polynomial system,

$$\dot{\mathbf{x}} = \mathbf{F}_3[\mathbf{x}] + \mathbf{bu} = \mathbf{D}\mathbf{x}^3 + \mathbf{H}_3[\mathbf{x}] + \mathbf{bu}\ , \tag{4.3.1}$$

where $\mathbf{x} \in R^3$, $\mathbf{D}=\mathbf{diag}[2, 1, -1]$, $\mathbf{b}=[1, 0, 0]^t$ and

$$\mathbf{H}_3[\mathbf{x}] = \begin{bmatrix} x_1^2(x_2 + x_3) - 2x_1(x_2^2 + x_3^2) \\ 2x_2^2(x_3 - 3x_1) + x_2(x_1^2 + x_3^2) \\ -2x_2^2x_3 - 2x_1x_3^2 + x_1x_2x_3 \end{bmatrix}.$$

The system is already in one of its canonical forms and the autonomous system has the characteristic equation which produces exactly $s_{3,3}=13$ simple spectral components:

$$\mathcal{X}_3\{C^3\} = \left\{ \begin{bmatrix} 1 \\ 0 \\ 0 \end{bmatrix}, \begin{bmatrix} 0 \\ 1 \\ 0 \end{bmatrix}, \begin{bmatrix} 0 \\ 0 \\ 1 \end{bmatrix}, \begin{bmatrix} 1 \\ -0.135041 \\ 0 \end{bmatrix}, \begin{bmatrix} 1 \\ 2.468374 \\ 0 \end{bmatrix}, \begin{bmatrix} 1 \\ 0 \\ 3.561552 \end{bmatrix}, \right.$$
$$\left. \begin{bmatrix} 1 \\ 0 \\ -0.561552 \end{bmatrix}, \begin{bmatrix} 0 \\ 1 \\ -0.5 + i\ 1.118033 \end{bmatrix}, \begin{bmatrix} 0 \\ 1 \\ -0.5 - i\ 1.118033 \end{bmatrix}, \begin{bmatrix} 1 \\ 0.0639982 \\ -0.561552 \end{bmatrix}, \right.$$
$$\left. \begin{bmatrix} 1 \\ -0.020517 + i\ 3.341215 \\ 3.561552 \end{bmatrix}, \begin{bmatrix} 1 \\ -0.020517 - i\ 3.341215 \\ 3.561552 \end{bmatrix}, \begin{bmatrix} 1 \\ 2.643703 \\ -0.561552 \end{bmatrix} \right\} \tag{4.3.1.g}$$

with the corresponding eigenvalues

$$\Lambda_3\{C\} = \begin{Bmatrix} 2.0\ ,\ 1.0\ ,\ -1.0\ ,\ 1.828485\ ,\ -7.717374\ ,\ -19.807764\ , \\ 0.807764\ ,\ -1.0 + i\ 1.118033\ ,\ -1.0 - i\ 1.118033\ ,\ 0.863570 \\ 2.498316 + i\ 3.615430\ ,\ 2.498316 - i\ 3.615430\ ,\ -10.526869 \end{Bmatrix}. \tag{4.3.1.a}$$

The system has mixed spectra with two pairs of complex, five positive real, and four negative real eigenvalues, and is unstable. Furthermore, any 10 eigenvectors in $\mathcal{X}_3\{C^3\}$ are algebraically independent and generate an algebraic basis. The remaining three eigenvectors are algebraically dependent.

To stabilize the system the two-dimensional state feedback procedure (Samardzija 1984) is adapted as follows. First, observe that in spite of $\mathbf{b} \in \mathcal{X}_3\{C^3\}$, the process still satisfies the necessary state controllability conditions because the requirement a) of Theorem 4.1.1 holds for all canonical realizations generated by transformations in $\mathcal{T}$. By contrast, the process does not satisfy the strong accessibility condition since elements of the Lie algebra generated by the homogeneous cubic polynomial and **b** do not span R^3 (Baillieul 1981). One can show that for this example the controllability rank is equal to one, which is also implied by the fact that $\mathbf{b} \in \mathcal{X}_3\{C^3\}$. Nevertheless, because the necessary state controllability condition is satisfied the state feedback which influences all eigenvalues can be designed. To realize such feedback we *à priori* assume the control form $u=g_3(\mathbf{x})$, where $g_3(\mathbf{x})$ is the scalar 3-form to be determined. Thus, from Equation (4.3.1) the process with state feedback becomes

$$\dot{\mathbf{x}} = \mathbf{F}_3[\mathbf{x}] + \mathbf{b}g_3(\mathbf{x}) \ . \tag{4.3.2}$$

This feedback formulation permits one to reassign process eigenvalues as follows: From Equation (4.3.2) the characteristic equation is

$$\mathbf{F}_3[\mathbf{x}] + \mathbf{b}g_3(\mathbf{x}) - \theta\mathbf{x} = 0 \ , \tag{4.3.3}$$

where the eigen-pairs **x** and θ are to be determined. Next, by selecting x_1 as the projection state one has that $\mathbf{x}=x_1\mathbf{v}$, where $\mathbf{v}=[1, v_2, v_3]^t$, implying

$$\mathbf{F}_3[\mathbf{v}] + \mathbf{b}g_3(\mathbf{v}) - \lambda\mathbf{v} = 0 \ , \tag{4.3.4}$$

where

$$\lambda = f_{3,1}[\mathbf{v}] + g_3(\mathbf{v}) = \frac{\theta}{x_1^2} \ . \tag{4.3.5}$$

Because of the equivalence relation one can now assign λ rather than θ. Thus, by combining the last two equations we derive

$$\mathbf{F}_3[\mathbf{v}] + \mathbf{b}f_{3,1}(\mathbf{v}) - \lambda(\mathbf{v} + \mathbf{b}) = 0 \ , \tag{4.3.6}$$

and the eigenvector satisfying any assigned λ can be evaluated. Observe that the last expression produces two cross-coupled algebraic equations of degree 3. Therefore, for each assigned λ one can have either 3^2 or infinitely many eigenvector solutions, including

multiplicities. For the general case this number is k^{m-1}, or infinitely many. Clearly, when k>1 each assigned λ generates a set of eigenvalues that qualify for a feedback design. Hence, to distinguish between the process eigenspectra and the set of all eigenvector solutions generated by any assigned λ, we refer to the latter set as being the *eigenvector pool*, and denote it by $P_k\{\Sigma^m|\lambda\}$.

After computing the desired eigenvector, the next step is to determine the state feedback $g_3(\mathbf{x})$ which compensates for the assigned eigenvalue. To accomplish this, recall that the algebraic degree $p_{3,3}=10$ is also the maximal degree of freedom which can be assigned for this control problem. Hence, the number of coefficients which determine $g_3(\mathbf{x})$ cannot exceed 10. Let the vector

$$\mathbf{c}_{coef}= [a_1, a_2, a_3, a_4, a_5, a_6, a_7, a_8, a_9, a_{10}]^t$$

define these coefficients, and let the corresponding 3-form vector presentation of $\mathbf{v}$ be

$$\mathbf{z}_3(\mathbf{v})= [1, v_2, v_3, v_2^2, v_2v_3, v_3^2, v_2^3, v_2^2v_3, v_2v_3^2, v_3^3]^t,$$

so that Equation (4.3.5) implies

$$g_3(\mathbf{v}) = \mathbf{z}_3(\mathbf{v})\, \mathbf{c}_{coef} = \lambda - f_{3,1}[\mathbf{v}]. \qquad (4.3.7)$$

Since this equation is linear in a_i, one assigned eigen-pair determines one coefficient while the remaining coefficients are linearly related. In order to determine 10 independent coefficients one needs 10 eigen-pairs such that 10 selected eigenvectors are algebraically independent. In this instance Equation (4.3.7) becomes

$$\mathbf{c}_{coef} = \Gamma^{-1}\left[\bar{\lambda} - \bar{\mathbf{f}}_{3,1}\right], \qquad (4.3.8)$$

where

$$\Gamma = \begin{bmatrix} \mathbf{z}_3(\mathbf{v}_1)^t \\ \bullet \\ \bullet \\ \mathbf{z}_3(\mathbf{v}_{10})^t \end{bmatrix}_{10x10} ; \quad \bar{\lambda} = \begin{bmatrix} \lambda_1 \\ \bullet \\ \bullet \\ \lambda_{10} \end{bmatrix}_{10x1} ; \quad \bar{\mathbf{f}}_{3,1} = \begin{bmatrix} f_{3,1}(\mathbf{v}_1) \\ \bullet \\ \bullet \\ f_{3,1}(\mathbf{v}_{10}) \end{bmatrix}_{10x1}.$$

The row vectors in Γ form the 10 dimensional 3-form basis while $\mathbf{v}_1, \mathbf{v}_2, \ldots, \mathbf{v}_{10}$ form the algebraic (cubic) basis. These pole placement relations are easily generalized for any state feedback assignment $g_k(\mathbf{x})$ where $\mathbf{x} \in \mathbb{R}^m$, and both k and m are arbitrary. In the general case, however, $p_{k,m}$ algebraically independent eigen-pairs are required to determine the full $g_k(\mathbf{x})$ structure.

To continue with the present example, rearrange the spectral structure by assigning eigenvalues $\lambda = -\phi_i$, $i = 1, \ldots, 10$, where for a convenience sake the ϕ_i's correspond to the first 10 numbers of the Fibonacci sequence. With such an assignment, the following spectral sets are odtained from Equation (4.3.6):

$$\Lambda_3\{\mathbb{R}\}^{\text{assigned}} = \{-1\ ,\ -2\ ,\ -3\ ,\ -5\ ,\ -8\ ,\ -13\ ,\ -21\ ,\ -34\ ,\ -55\ ,\ -89\ \},$$

with the one-to-one corresponding geometric spectrum

$$\mathcal{B}_3\{\mathbb{R}^3\}^{\text{selected}} = \left\langle \begin{bmatrix} 1 \\ 0.465694 \\ 0.425465 \end{bmatrix}, \begin{bmatrix} 1 \\ 0.824048 \\ 0.570330 \end{bmatrix}, \begin{bmatrix} 1 \\ 1.165662 \\ 0.564648 \end{bmatrix}, \begin{bmatrix} 1 \\ 1.267949 \\ 0 \end{bmatrix}, \begin{bmatrix} 1 \\ 3. \\ 0 \end{bmatrix}, \right.$$
$$\left. \begin{bmatrix} 1 \\ 2.907286 \\ -1.051560 \end{bmatrix}, \begin{bmatrix} 1 \\ 0 \\ -5.690415 \end{bmatrix}, \begin{bmatrix} 1 \\ 0 \\ 4.916079 \end{bmatrix}, \begin{bmatrix} 1 \\ 0 \\ -8.483314 \end{bmatrix}, \begin{bmatrix} 1 \\ 0 \\ 0 \end{bmatrix} \right\rangle,$$

where the eigenvectors are selected from the eigen pools listed in Appendix II. That is, out of each eigenvector pool, we arbitrarily select one real solution to form the desired eigenmode. However, in doing so we must make sure that the selected eigenvectors are algebraically independent and as such form the complete algebraic basis. When the selected eigenvectors are algebraically dependent, the algebraic basis is incomplete and less than 10 coefficients are uniquely determined. For our particular case, we select 10 algebraically independent real eigenvectors which form the above cubic basis $\mathcal{B}_3\{\mathbb{R}^3\}^{\text{selected}}$. They are already in the form $\mathbf{v} = [1, v_2, v_3]^t$ so that Γ, $\bar{\lambda}$ and $\bar{\mathbf{f}}_{3,1}$ can be readily obtained, and $\mathbf{c}_{\text{coef}}$ computed. Finally, from Equation (4.3.8) the state feedback realization is

$$
\begin{aligned}
g_3(\mathbf{x}) = {} & -91.0x_1^3 + 599.511300x_1^2x_2 - 587.869799x_1x_2^2 + \\
& 132.899788x_2^3 - 11.027659x_1^2x_3 - 740.182424x_1x_2x_3 + \\
& 404.675460x_2^2x_3 + 4.471860x_1x_3^2 + 426.526771x_2x_3^2 + \\
& 0.375026x_3^3 \ .
\end{aligned} \tag{4.3.9}
$$

The process in Equation (4.3.2) is now well defined with 10 assigned eigenvalues and 10 selected algebraically independent eigenvectors of multiplicity one. However, eigen-number indicates that in addition there must be at most three algebraically dependent generic eigenvectors. Consequently, the character of the algebraically related eigenmodes cannot be inferred from the procedure. This is verified by solving the characteristic equation for the compensated process, Equation (4.3.2). The eigen solutions produce the following complete spectral sets:

$$
\mathcal{X}_3\{\mathbb{R}^3\} = \left\{ \mathcal{B}_3\{\mathbb{R}^3\}^{\text{selected}} , \begin{bmatrix} 1 \\ 0.1780307 \\ 0 \end{bmatrix}, \begin{bmatrix} 1 \\ 0.333810 \\ 0.305697 \end{bmatrix}, \begin{bmatrix} 1 \\ 0.067798 \\ -0.658193 \end{bmatrix} \right\}
$$

and

$$
\Lambda_3\{\mathbb{R}\} = \left\{ \Lambda_3\{\mathbb{R}\}^{\text{assigned}} , -0.036489 , -0.593895 , 0.941774 \right\} .
$$

The homogeneous spectra of the compensated process is purely real and contains 13 eigen-pairs of multiplicity one. The three additional eigenvectors are generic. Furthermore, the first 12 eigenvectors have negative eigenvalues, while the last one has an associated positive eigenvalue. Hence, by Theorem 3.3.1 the compensated process is not stable.

Now let us reconsider the assigned eigenmodes. As stated earlier, each assigned eigenvalue produces the pool of 9 eigenvector solutions, of which one real is selected in $\mathcal{B}_3\{\mathbb{R}^3\}^{\text{selected}}$. Consequently, there is a freedom of choice in deciding which eigenmodes are selected. This is always true when k>1. Thus, by exercising this choice we produce the new spectra: $\Lambda_3\{\mathbb{R}\}^{\text{assigned}}$ as before and

$$\mathcal{B}_3\{\mathbb{R}^3\}^{\text{selected}}_{\text{new}} = \left\langle \begin{bmatrix} 1 \\ 0.734695 \\ -2.286523 \end{bmatrix}, \begin{bmatrix} 1 \\ 0.824048 \\ 0.570330 \end{bmatrix}, \begin{bmatrix} 1 \\ 1.165662 \\ 0.564648 \end{bmatrix}, \begin{bmatrix} 1 \\ 1.267949 \\ 0 \end{bmatrix}, \begin{bmatrix} 1 \\ 3. \\ 0 \end{bmatrix}, \right.$$
$$\left. \begin{bmatrix} 1 \\ 2.907286 \\ -1.051560 \end{bmatrix}, \begin{bmatrix} 1 \\ 0 \\ -5.690415 \end{bmatrix}, \begin{bmatrix} 1 \\ 0 \\ 4.916079 \end{bmatrix}, \begin{bmatrix} 1 \\ 0 \\ -8.483314 \end{bmatrix}, \begin{bmatrix} 1 \\ 0 \\ 0 \end{bmatrix}, \right\rangle ,$$

where the different real solution satisfying the eigenvalue -1 is entered as the first eigenvector. This forms the new cubic basis which determines the matrix Γ_{new}, and creates the state feedback

$$\begin{aligned} g_3(\mathbf{x}) = & -91.0x_1^3 + 215.229412x_1^2x_2 - 156.702266x_1x_2^2 + \\ & 31.875265x_2^3 - 11.027659x_1^2x_3 + 13.657987x_1x_2x_3 - \\ & 5.045884x_2^2x_3 + 4.471860x_1x_3^2 - 3.252171x_2x_3^2 + \\ & 0.375026x_3^3 \ . \end{aligned} \tag{4.3.10}$$

The spectra of the compensated process are now:

$$\mathcal{X}_3\{\mathbb{R}^3\}^{\text{updated}} = \left\langle \mathcal{B}_3\{\mathbb{R}^3\}^{\text{selected}}_{\text{new}}, \begin{bmatrix} 1 \\ 0.742276 \\ 0 \end{bmatrix}, \begin{bmatrix} 1 \\ 0.784382 \\ -2.347684 \end{bmatrix}, \begin{bmatrix} 1 \\ 3.055020 \\ -2.578550 \end{bmatrix} \right\rangle$$

and

$$\Lambda_3\{\mathbb{R}\}^{\text{updated}} = \left\{ \Lambda_3\{\mathbb{R}\}^{\text{assigned}}, -2.902683 , -1.262383 , -17.103097 \right\}.$$

The process has all negative eigenvalues, and according to Theorem 3.3.1 the last state feedback has stabilized it since the process is globally asymptotically stable.

4.4. STABILIZABILITY: *THREE-DIMENSIONAL EXAMPLE WITH STATE DEPENDENT CONTROL VECTOR*

Example 4.4.1 We now consider the same three-dimensional cubic homogeneous polynomial system with the following control vector,

$$\dot{\mathbf{x}} = \mathbf{F}_3[\mathbf{x}] + \mathbf{bu} = \mathbf{Dx}^3 + \mathbf{H}_3[\mathbf{x}] + \mathbf{B}_q[\mathbf{x}]\, u \ , \tag{4.4.1}$$

where, with the exception for $\mathbf{B}_q[\mathbf{x}]$, all symbols are as defined in Example 4.3.1. For the control vector we select q=1 such that

$$\mathbf{B}_1[\mathbf{x}] = \begin{bmatrix} b_{1,1}(\mathbf{x}) \\ b_{1,2}(\mathbf{x}) \\ b_{1,3}(\mathbf{x}) \end{bmatrix} = \begin{bmatrix} b_1x_1+b_2x_2+b_3x_3 \\ 0 \\ 0 \end{bmatrix} = \mathbf{Bx} = \begin{bmatrix} b_1 & b_2 & b_3 \\ 0 & 0 & 0 \\ 0 & 0 & 0 \end{bmatrix} \begin{bmatrix} x_1 \\ x_2 \\ x_2 \end{bmatrix}, \qquad (4.4.2)$$

and we look for the cubic state feedback solution $\mathbf{B}_1[\mathbf{x}]u$. Therefore, u must be the quadratic form $g_2(\mathbf{x})$, implying that the state feedback is the 3-form $\mathbf{B}_3[\mathbf{x}]=\mathbf{B}_1[\mathbf{x}]g_2(\mathbf{x})$. Thus, the question is how to obtain the quadratic form $g_2(\mathbf{x})$, and whether such feedback can stabilize the entire system. Observe that the present problem has fewer degrees of freedom than in Example 4.3.1. This is because the requirement for u has now been reduced by one degree, which implies that there are fewer coefficients to be determined. We now examine this in greater detail.

As before, one can verify that the process satisfies the necessary state controllability condition. That is there does not exist a linear transformation $\mathbf{T}_v \in \mathrm{I}'$ which violates the conditions in Theorem 4.2.1 Next, express the three-dimensional quadratic form to be determined as

$$g_2(\mathbf{x}) = \left[x_1^2, x_1x_2, x_1x_3, x_2^2, x_2x_3, x_3^2\right] \begin{bmatrix} a_1 \\ a_2 \\ a_3 \\ a_4 \\ a_5 \\ a_6 \end{bmatrix} = \mathbf{z}_2(\mathbf{x})^t\, \mathbf{c}_{coef.} \qquad (4.4.3)$$

Clearly, all vector dimensions are given by the quadratic degree of freedom $p_{2,3}=6$. The resulting process with feedback is now

$$\dot{\mathbf{x}} = \mathbf{D}\mathbf{x}^3 + \mathbf{H}_3[\mathbf{x}] + \mathbf{B}_3[\mathbf{x}] \qquad (4.4.4)$$

where,

$$\mathbf{B}_3[\mathbf{x}] = \mathbf{B}_1[\mathbf{x}]\, \mathbf{z}_2(\mathbf{x})^t\, \mathbf{c}_{coef} = \mathbf{Bx}\, \mathbf{z}_2(\mathbf{x})^t\, \mathbf{c}_{coef}$$

$$= \begin{bmatrix} b_1 & b_2 & b_3 \\ 0 & 0 & 0 \\ 0 & 0 & 0 \end{bmatrix} \begin{bmatrix} x_1 \\ x_2 \\ x_3 \end{bmatrix} \mathbf{z}_2(\mathbf{x})^t\, \mathbf{c}_{coef.}$$

Inspection of this equation reveals that although the process satisfies the necessary state controllability conditions, this is not enough to assure that a globally stabilizing cubic state

feedback exists. To see this, suppose that $b_2=0$. In this case the term x_2^3 will be missing from all cubic state feedback realizations and the vector $\mathbf{x}'=[0,\ 1,\ 0]^t$ implies $\mathbf{B}_3[\mathbf{x}']=0$. However, $\mathbf{x}'$ is also the eigenvector of the autonomous structure with the associated eigenvalue 1 (see the spectra (4.3.1.g)). Thus, when $b_2=0$ the process can never be stabilized under any kind of algebraic arrangement in u even when the necessary state controllability conditions are satisfied. The same observation holds for $b_1=0$. However, when $b_3=0$ the possibility for stabilization exists because $\mathbf{B}_3[\mathbf{x}]=0$ for $\mathbf{x}=[0,\ 0,\ 1]^t$ which is the eigenvector with eigenvalue -1. Hence, the inaccessible eigenmode is already stable. Therefore, if for any linear transformation $\mathbf{T}_v\in\Gamma$ the canonical realization produces $\mathbf{T}_v^{-1}\mathbf{B}\mathbf{T}_v$ with zero columns, it is necessary to find whether all unstable eigenmodes are accessible. By contrast, all eigenmodes are accessible when there are no zero columns in all $\mathbf{T}_v^{-1}\mathbf{B}\mathbf{T}_v$ realizations, and we say that the process is *fully cross-coupled*. Note that for $q=1$, the full cross-coupling condition is complementary to the necessary state controllability condition and as such it resembles that of the state observability requirement for a linear system. The case $q>1$ is more general and will be treated later.

To continue with the present state feedback design, we set $b_1=b_2=1$ and $b_3=0$. With this assignment the system is not fully cross-coupled, and the inaccessible eigenmode is stable. Nevertheless, by evaluating the characteristic equation for Equation (4.4.4), we derive the following relations: for any assigned λ compute $\mathbf{v}=[1,\ v_2,\ v_3]^t$ from the expressions

$$\begin{aligned} &b_{1,1}(\mathbf{v})f_{3,2}(\mathbf{v}) - b_{1,2}(\mathbf{v})f_{3,1}(\mathbf{v}) + \lambda\,(b_{1,2}(\mathbf{v}) - v_2 b_{1,1}(\mathbf{v})) = 0 \\ &b_{1,1}(\mathbf{v})f_{3,3}(\mathbf{v}) - b_{1,3}(\mathbf{v})f_{3,1}(\mathbf{v}) + \lambda\,(b_{1,3}(\mathbf{v}) - v_3 b_{1,1}(\mathbf{v})) = 0\ , \end{aligned} \tag{4.4.5}$$

and

$$g_2(\mathbf{v}) = \mathbf{z}_2(\mathbf{v})\,\mathbf{c}_{coef} = \frac{\lambda - f_{3,1}(\mathbf{v})}{b_{1,1}(\mathbf{v})}\ . \tag{4.4.6}$$

Note that in this example $b_{1,2}(\mathbf{x})=b_{1,3}(\mathbf{x})=0$, implying that the expressions in Equation (4.4.5) can be simplified further. Furthermore, since $\mathbf{c}_{coef}$ is of dimension $p_{2,3}=6$, at most 6 eigenvalues may be assigned arbitrarily. As a result, for any 6 assigned eigenvalues the following relation uniquely determines $\mathbf{c}_{coef}$:

$$\mathbf{c}_{coef} = \Gamma^{-1}\left[\bar{\lambda} - \bar{\mathbf{f}}_{3,1}\right] \tag{4.4.7}$$

where

$$\Gamma = \begin{bmatrix} \mathbf{z}_3(\mathbf{v}_1)^t \\ \bullet \\ \bullet \\ \mathbf{z}_3(\mathbf{v}_6)^t \end{bmatrix}_{6\mathbf{x}6} \quad ; \quad \bar{\lambda} = \begin{bmatrix} \dfrac{\lambda_1}{b_{1,1}(\mathbf{v}_1)} \\ \bullet \\ \bullet \\ \dfrac{\lambda_6}{b_{1,1}(\mathbf{v}_6)} \end{bmatrix}_{6x1} \quad ; \quad \bar{\mathbf{f}}_{3,1} = \begin{bmatrix} \dfrac{f_{3,1}(\mathbf{v}_1)}{b_{1,1}(\mathbf{v}_1)} \\ \bullet \\ \bullet \\ \dfrac{f_{3,1}(\mathbf{v}_6)}{b_{1,1}(\mathbf{v}_6)} \end{bmatrix}_{6\mathbf{x}1}.$$

Compared with the previous example, the present degrees of freedom is reduced by 4, and the 7 remaining eigenmodes must be algebraically related. This gives the impression that the number of algebraic combinations that qualify for the desired state feedback realization is also reduced. To some extent this is correct, but not completely. The reason is that now each assigned eigenvalue generates a larger eigen pool. For instance, each assigned eigenvalue in the present example creates two cross-coupled algebraic equations of degree k+q=4. This is determined by the $b_{1,i}(\mathbf{v})f_{3,j}(\mathbf{v})$ terms for i,j=1,2,3 in Equation (4.4.5). Hence, each assigned λ generates either $4^2=16$ eigen solutions, multiplicities included, or infinitely many. By contrast, in the preceding example the control vector was independent of the process states (q=0) and the generated eigenvector pools contain $3^2=9$ solutions. Consequently the pool size has now increased from 9 to 16, which further implies that in the present example the number of eigenvector choices within the assigned pool has also increased. In general, however, the eigenvector pool size for an assigned λ is given by $(k+q)^{m-1}$. Hence, as q increases the eigenvector pool size also increase, while the algebraic degrees of freedom decreases.

To stabilize the present problem we now assign the eigenvalues $\lambda_i=-\pi_i$, i=1,..,6. where again for a convenience sake the π_i's correspond to the first six prime numbers. For this choice, the assigned algebraic eigenspectrum is

$$\Lambda_3\{R\}^{assigned} = \{-1\ ,\ -2\ ,\ -3\ ,\ -5\ ,\ -7\ ,\ -11\ \},$$

and generates the eigenvector pools given in Appendix III. From these pools we select the following quadratic basis

$$B_2\{R^3\}^{\text{selected}} = \left\{ \begin{bmatrix} 1 \\ 0 \\ 0 \end{bmatrix} ; \begin{bmatrix} 1 \\ 0 \\ -2.7320508 \end{bmatrix} ; \begin{bmatrix} 1 \\ 0 \\ 1 \end{bmatrix} ; \begin{bmatrix} 1 \\ 4.7320508 \\ 0 \end{bmatrix} ; \begin{bmatrix} 1 \\ 1.6548929 \\ -3.0439060 \end{bmatrix} ; \begin{bmatrix} 1 \\ 2.6997951 \\ -0.6507048 \end{bmatrix} \right\}$$

which produces Γ given in Appendix III. Applying this basis, one derives the quadratic state feedback realization

$$g_2(\mathbf{x}) = -3x_1^2 + 2.84308649x_1x_2 - 2.3660254x_1x_3 - 0.2093289x_2^2 + 2.9408838x_2x_3 + 1.3660254x_3^2 \ . \tag{4.4.8}$$

The complete spectra for the process stabilized by this control are

$$X_3\{C^3\} = \left\{ B_2\{R^3\}^{\text{selected}} ; \begin{bmatrix} 1 \\ -6.7794740 \\ 0 \end{bmatrix} ; \begin{bmatrix} 1 \\ 0.2978209 \\ 0 \end{bmatrix} ; \begin{bmatrix} 1 \\ 0.4063007 \\ 0.3779844 \end{bmatrix} ; \begin{bmatrix} 1 \\ 0.4334373 \\ -1.8342671 \end{bmatrix} ; \begin{bmatrix} 1 \\ -0.3742231 + i\,0.1997560 \\ 0.0362118 + i\,1.3121911 \end{bmatrix} ; \begin{bmatrix} 1 \\ -0.3742231 - i\,0.1997560 \\ 0.0362118 - i\,1.3121911 \end{bmatrix} ; \begin{bmatrix} 0 \\ 0 \\ 1 \end{bmatrix} \right\}$$

and

$$\Lambda_3\{C\} = \left\{ \Lambda_3\{R\}^{\text{assigned}} ; 87.6381135 ; -0.6982282 ; -0.8227011 ; 0.3616997 ; 1.0736065 - i\,2.2206466 ; 1.0736065 + i\,2.2206466 ; -1 \right\} .$$

The presence of two positive eigenvalues associated with the real eigenvectors indicates that the feedback realization is not globally stabilizing.

Now let us select the new quadratic basis

$$B_3\{R^3\}^{\text{selected}}_{\text{new}} = \left\{ \begin{bmatrix} 1 \\ 0 \\ 0 \end{bmatrix} ; \begin{bmatrix} 1 \\ 0 \\ -2.7320508 \end{bmatrix} ; \begin{bmatrix} 1 \\ 0 \\ 1 \end{bmatrix} ; \begin{bmatrix} 1 \\ 4.7320508 \\ 0 \end{bmatrix} ; \begin{bmatrix} 1 \\ 2 \\ 0 \end{bmatrix} ; \begin{bmatrix} 1 \\ 2.1700006 \\ -3.1799530 \end{bmatrix} \right\}$$

which produces Γ_{new} given in Appendix III. The quadratic state feedback function is now

$$g_2(\mathbf{x}) = -3x_1^2 + 0.3759039x_1x_2 - 2.3660254x_1x_3 + 0.3120480x_2^2 + 2.1815682x_2x_3 + 1.3660254x_3^2 \ , \tag{4.4.9}$$

and the complete spectra for the process is given by

$$X_3\{C^3\}=\left\{ B_3\{R^3\}^{\text{selected}}_{\text{new}};\ \begin{bmatrix}1\\0.6772190\\0\end{bmatrix};\ \begin{bmatrix}1\\1.2039255\\0.5575269\end{bmatrix};\ \begin{bmatrix}1\\2.1370191\\0.0406867\end{bmatrix};\ \begin{bmatrix}1\\0.5507748\\-2.0299423\end{bmatrix};\ \begin{bmatrix}1\\-0.2660336+i\,0.1848018\\-0.0132568+i\,1.1262190\end{bmatrix};\ \begin{bmatrix}1\\-0.2660336-i\,0.1848018\\-0.0132568-i\,1.1262190\end{bmatrix};\ \begin{bmatrix}0\\0\\1\end{bmatrix} \right\}$$

and

$$\Lambda_3\{C\}=\left\{ \Lambda_3\{R\}^{\text{assigned}};\ -2.6046886\ ;\ -3.1208383\ ;\ -7.0797117\ ;\ -0.1167122\ ;\ 0.9554292-i\,1.8411221\ ;\ 0.95542925+i\,1.8411221\ ;\ -1 \right\}.$$

All eigenvalues which correspond to the real eigenvectors are now negative. Furthermore, since the sum of multiplicities associated with complex eigenvectors $\mu=2<k+1=4$, then Theorem 3.4.1 implies that the process is globally asymptotically stable. Thus, the new feedback realization globally stabilizes the process. However, observe that the complex eigenmode solutions are unstable. This is signified by the fact that the respective eigenvalues have positive real parts. As a result the state-space now contains a bubble similar to the one discussed in Example 3.2.2. The temporal and state-space behaviors of the process variables are illustrated in Figure 4.4.1.

In conclusion, the process can be globally stabilized even though the full cross-coupling criterion is not satisfied. Observe that the autonomous inaccessible stable eigenmode is still present in the spectra of the stabilized process. It is given by the last eigen elements in the stabilized spectra.

4.5. General Stabilizability Results

The results in the two examples are now generalized. We again consider the general control problem defined in Equation (4.2.1). Theorem 4.2.1 provides the necessary state controllability conditions which for $q=0$ are sufficient to imply that all eigenmodes are accessible. This, however, is no longer true when $1\leq q\leq k$, and the condition defined as full cross-coupling must also be considered. In the preceding example we have demonstrated that for $q=1$ this condition is similar to the state observability

criterion. However, for q>1 the full cross-coupling condition exhibits a more general structure. To show this we transform Equation (4.2.1) into the canonical form by considering the transformation $\mathbf{T}_v \in \Gamma$. This produces

$$\dot{\mathbf{x}} = \mathbf{D}\,\mathbf{x}^k + \mathbf{H}_k[\mathbf{x}] + \mathbf{B}_q[\,[\mathbf{x}]\,]\,\mathbf{u} \tag{4.5.1}$$

where the cross-coupling term $\mathbf{H}_k[\mathbf{x}]=[h_{k,1}(\mathbf{x}),...,h_{k,m}(\mathbf{x})]^t$, and the control matrix

$$\mathbf{B}_q[\,[\mathbf{x}]\,] = [\mathbf{B}_{q,1}[\mathbf{x}],\cdots,\mathbf{B}_{q,n}[\mathbf{x}]\,] = [\mathbf{B}_{coef,1}\,\mathbf{z}_q(\mathbf{x}),\cdots,\mathbf{B}_{coef,n}\,\mathbf{z}_q(\mathbf{x})] \tag{4.5.2}$$

where each $\mathbf{B}_{coef,i}$ is a $mxp_{q,m}$ coefficient matrix of $\mathbf{B}_{q,i}[\mathbf{x}]$. Thus, for $q\geq 1$ the full cross-coupling condition requires that all contributions of the form x_j^q, j=1,...,m, must be present in the state feedback realizations. This is now stated in a more concise form.

Theorem 4.5.1 The process in Equation (4.5.1) is fully cross-coupled if and only if the following conditions are satisfied:

a) For any canonical transformation $\mathbf{T}_v \in \Gamma$ which generates the diagonal matrix $\mathbf{D}$, not all column vectors in $\mathbf{B}_{coef,i}$, i=1,..,n, that correspond to the terms $x_j^q \in \mathbf{z}_q(\mathbf{x})$, j=1,...,m, are zero.

b) For any canonical transformation $\mathbf{T}_v \in \Gamma$ which generates $\mathbf{D}$ in the Jordan block form, not all column vectors of $\mathbf{B}_{coef,i}$, i=1,..,n, that correspond to the term associated with the first column of any Jordan block, are zero.

Proof: We prove case b first. Suppose that for some $\mathbf{T}_v \in \Gamma$ the resulting canonical realization generates Jordan blocks in $\mathbf{D}$. Then there must be a j, $1\leq j<m$, which defines a Jordan block of the size $\varphi+1$ ($\varphi\geq 1$) so that

$$\begin{aligned}
\dot{x}_j &= \lambda_j x_j^k + x_{j+1}^k + h_{k,j}(\mathbf{x}) + \sum_{i=1}^{n} \mathbf{r}_{i,j}\mathbf{z}_q(\mathbf{x})u_i \\
\dot{x}_{j+1} &= \lambda_j x_{j+1}^k + x_{j+2}^k + h_{k,j+1}(\mathbf{x}) + \sum_{i=1}^{n} \mathbf{r}_{i,j+1}\mathbf{z}_q(\mathbf{x})u_i \\
&\vdots \\
\dot{x}_{\varphi+j} &= \lambda_j x_{\varphi+j}^k + h_{k,\varphi+j}(\mathbf{x}) + \sum_{i=1}^{n} \mathbf{r}_{i,\varphi+j}\mathbf{z}_q(\mathbf{x})u_i
\end{aligned}, \tag{4.5.3}$$

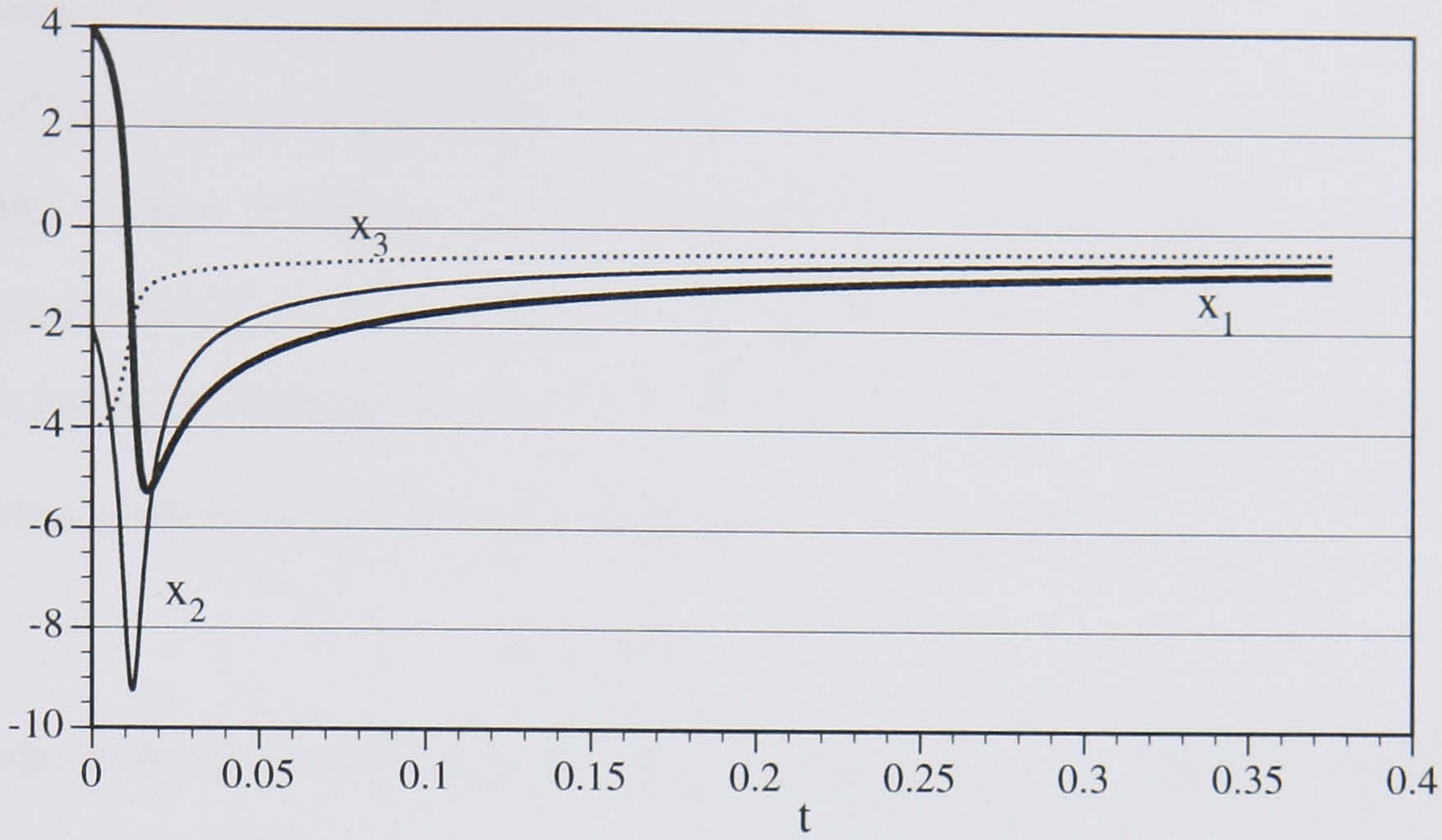

a) Temporal behavior shows transient spikes due to presence of unstable complex eigenmodes.

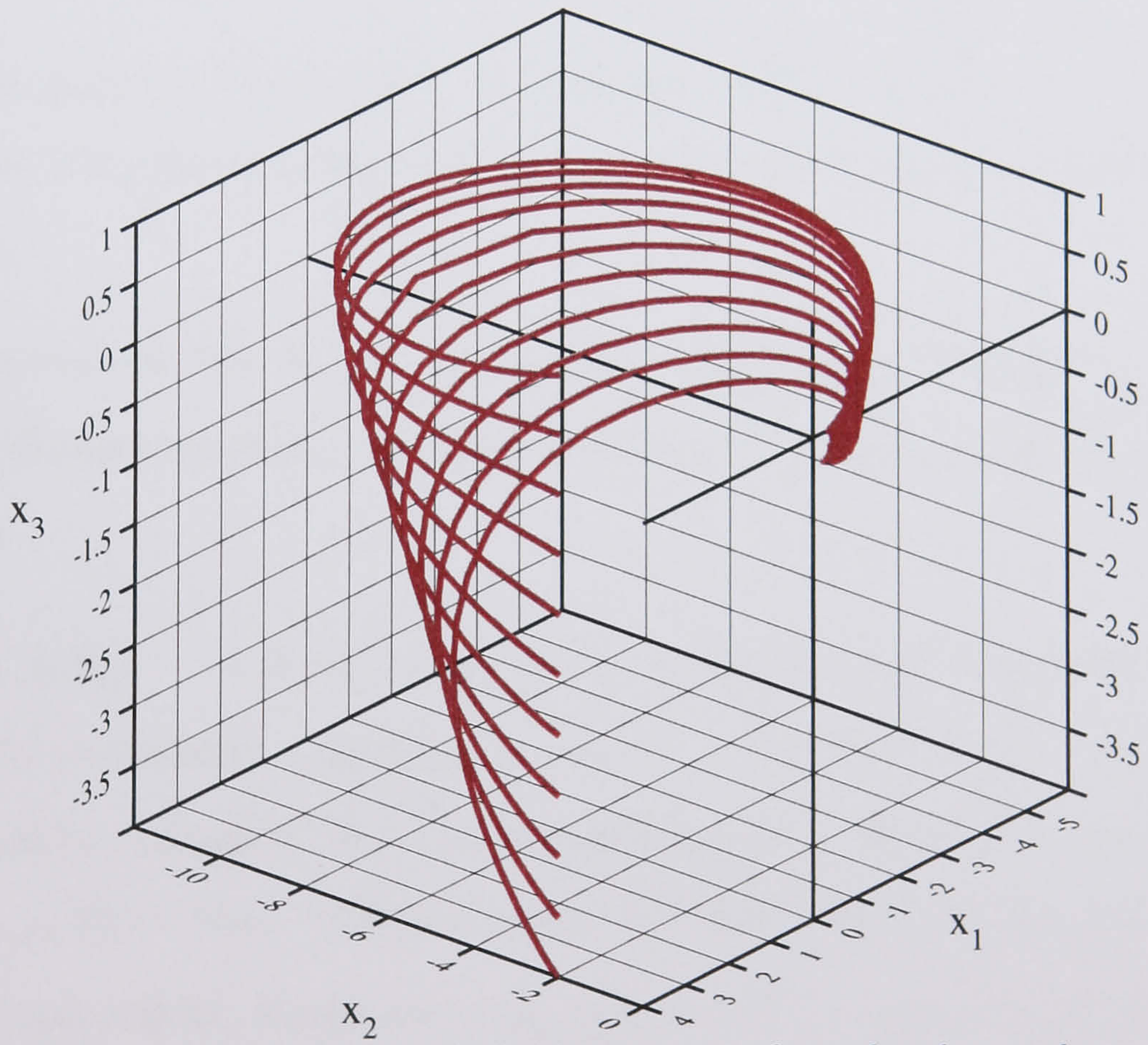

b) The state-space curvature indicating presence of complex eigenmodes.

Effects of the complex eigenmodes.

FIGURE 4.4.1.

and where $\mathbf{r}_{i,j}$, $\mathbf{r}_{i,j+1}$,.., $\mathbf{r}_{i,\varphi+j}$ are appropriate row vectors of $\mathbf{B}_{coef,i}$, i=1,..,n. Now, the "if" part follows from the fact that if for all i=1,..,n each $\mathbf{B}_{coef,i}$ has the column vector $\mathbf{b}_{i,\rho}=0$, where $1\leq\rho\leq p_{k,m}$ and corresponds to the term $x_j^q\in\mathbf{z}_q(\mathbf{x})$, then the ρ–th component in all row vectors of each $\mathbf{B}_{coef,i}$ must be zero. Consequently, by letting $\mathbf{x}=\mathbf{e}_j$, or the j-th standard basis vector in $\Re^m$, all right-hand terms in the canonical representation are 0 for all times except in the j-th equation, which becomes

$$\dot{x}_j = \lambda_j x_j^k \ . \tag{4.5.4}$$

Clearly, $\mathbf{e}_j$ defines an invariant which cannot be altered by a control $\mathbf{u}$, implying that the process is not fully cross-coupled. The "only if" part follows from the observation that if at least one $\mathbf{b}_{i,\rho}\neq 0$ then $\mathbf{u}$ can influence λ_j. Condition a) now follows by letting $\varphi=0$. ♦

Definition 4.5.1 The process in Equation (4.2.1) is said to be *algebraically controllable* if it satisfies both the full cross-coupling and the necessary state controllability conditions.

Observe that only for q=0, the algebraic controllability is implied by the necessary state controllability condition. The additional full cross-coupling requirement is necessary when q>0.

Theorem 4.5.2 Let the homogeneous process defined in Equation (4.2.1) be algebraically controllable. Then for q=0 and k=1, or q=0 and m≤2, the entire algebraic spectrum can be reassigned. For a process with any other choice of integers k, m and q, at most $p_{k-q,m}$ eigenvalues in $\Lambda_k\{C\}$ can be arbitrarily placed, while the remaining must be algebraically related. Furthermore, the state feedback is unique only for k=1.

Proof: Since $\mathbf{u}\in\Re^n$, then without loss of generality we can select a control function of the form $\mathbf{u}=\mathbf{w}g_{k-q}(\mathbf{x})$, where $\mathbf{w}=[w_1,...,w_n]^t\in\Re^n$ is the constant control term that is arbitrarily determined and $g_{k-q}(\mathbf{x})$ is a (k-q)-form which depends on assigned eigenvalues. This control selection produces the overall feedback term $\mathbf{B}_q[[\mathbf{x}]]\mathbf{w}g_{k-q}(\mathbf{x})$, which is homogeneous and of degree k. As such, it is compatible with the process model $\mathbf{F}_k[\mathbf{x}]$ and generates the overall characteristic equation

$$\mathbf{F}_k[\mathbf{v}] + \mathbf{B}_q[\,[\mathbf{v}]\,]\,\mathbf{w}\; g_{k-q}(\mathbf{v}) = \lambda\mathbf{v}\;, \tag{4.5.5}$$

or in component form

$$\begin{aligned} f_{k,1}(\mathbf{v}) + g_{k-q}(\mathbf{v})\sum_{i=1}^{n} w_i \mathbf{r}_{i,1}\mathbf{z}_q(\mathbf{v}) &= \lambda \\ f_{k,2}(\mathbf{v}) + g_{k-q}(\mathbf{v})\sum_{i=1}^{n} w_i \mathbf{r}_{i,2}\mathbf{z}_q(\mathbf{v}) &= \lambda v_2 \\ &\vdots \\ f_{k,m}(\mathbf{v}) + g_{k-q}(\mathbf{v})\sum_{i=1}^{n} w_i \mathbf{r}_{i,m}\mathbf{z}_q(\mathbf{v}) &= \lambda v_m \end{aligned} \tag{4.5.6}$$

where again, without loss of generality x_1 is selected as the projection state and as before $\mathbf{r}_{i,j}$, $\mathbf{r}_{i,j+1}$,.., $\mathbf{r}_{i,j+J}$ are appropriate row vectors of $\mathbf{B}_{coef,i}$, i=1,..,n. Now, for any assigned λ, the first equation implies that

$$g_{k-q}(\mathbf{v}) = \frac{\lambda - f_{k,1}(\mathbf{v})}{\sum_{i=1}^{n} w_i \mathbf{r}_{i,1}\mathbf{z}_q(\mathbf{v})} \tag{4.5.7}$$

and the remaining m-1 equations become

$$\begin{aligned} f_{k,2}(\mathbf{v})\sum_{i=1}^{n} w_i \mathbf{r}_{i,1}\mathbf{z}_q(\mathbf{v}) - f_{k,1}(\mathbf{v})\sum_{i=1}^{n} w_i \mathbf{r}_{i,2}\mathbf{z}_q(\mathbf{v}) &= \lambda\left[\sum_{i=1}^{n} w_i (v_2\mathbf{r}_{i,1} - \mathbf{r}_{i,2})\mathbf{z}_q(\mathbf{v})\right] \\ &\vdots \\ f_{k,m}(\mathbf{v})\sum_{i=1}^{n} w_i \mathbf{r}_{i,1}\mathbf{z}_q(\mathbf{v}) - f_{k,1}(\mathbf{v})\sum_{i=1}^{n} w_i \mathbf{r}_{i,m}\mathbf{z}_q(\mathbf{v}) &= \lambda\left[\sum_{i=1}^{n} w_i (v_m\mathbf{r}_{i,1} - \mathbf{r}_{i,m})\mathbf{z}_q(\mathbf{v})\right] \end{aligned} \tag{4.5.8}$$

which are used to evaluate eigenvector pools for assigned λ's. Moreover, since the highest degree terms in these expressions are of the power k+q, then the resulting algebraic system in variables $v_2,\ldots,v_m$ contains m-1 cross-coupled equations of the maximal degree k+q. As such, they produce eigenvector pools containing $(k+q)^{m-1}$ solutions, multiplicities included, or infinitely many eigenvectors. Furthermore, the control degrees of freedom is determined by the number of coefficients in $g_{k-q}(\mathbf{x})$, which is $p_{k-q,m}$. Consequently, at most, $p_{k-q,m}$ eigenvalues can be assigned to determine $g_{k-q}(\mathbf{x})$. The other claims follow from Corollaries 2.2.1 and 2.2.2. ♦

Note that in the proof of the theorem we have considered **u** to be of a particular form. This is irrelevant since the final outcome is always the same. For example,

suppose that n=m and that $\mathbf{B}_q[[\mathbf{x}]]$ is an mxm matrix which is nonsingular over some set $\mathbb{M} \subseteq \mathbb{R}^m$ or that $\mathbf{B}_q[[\mathbf{x}]]^{-1}$ exists for all $\mathbf{x} \in \mathbb{M}$. Then by substituting $\mathbf{u}=[g_{k-q,1}(\mathbf{x}),....g_{k-q,m}(\mathbf{x})]^t$ back into Equation (4.5.5) we obtain

$$\mathbf{u} = \mathbf{B}_q[[\mathbf{v}]]^{-1}\left[\lambda\mathbf{v} - \mathbf{F}_k[\mathbf{v}]\right], \tag{4.5.9}$$

where $\mathbf{v} \in \mathbb{M}$, and

$$\mathbf{u} = \begin{bmatrix} g_{k-q,1}(\mathbf{v}) \\ g_{k-q,2}(\mathbf{v}) \\ \vdots \\ g_{k-q,m}(\mathbf{v}) \end{bmatrix} =$$

$$= \begin{bmatrix} g_{11} & g_{12} & \cdots & g_{1p_{k-q,m}} \\ g_{21} & g_{22} & \cdots & g_{2p_{k-q,m}} \\ \vdots & \vdots & \cdots & \vdots \\ g_{m1} & g_{m2} & \cdots & g_{mp_{k-q,m}} \end{bmatrix}_{(mxp_{k-q,m})} \begin{bmatrix} 1 \\ v_2 \\ \vdots \\ v_m^{k-q} \end{bmatrix} = \mathbf{G}\ \mathbf{z}_{k-q}(\mathbf{v}). \tag{4.5.10}$$

Next, by arbitrary selecting $p_{k-q,m}$ eigenvalues and eigenvectors that belong to $\mathbb{M}$ such that the $p_{k-q,m}xp_{k-q,m}$ square matrix $\mathbf{V}=[\mathbf{z}_{k-q}(\mathbf{v}_1),.., \mathbf{z}_{k-q}(\mathbf{v}_{p_{k-q,m}})]$ is nonsingular, we obtain

$$\mathbf{G} = \left[\Psi_1, \cdots, \Psi_{p_{k-q,m}}\right]\mathbf{V}^{-1} \tag{4.5.11}$$

where each $\Psi_i = \mathbf{B}_q[[\mathbf{v}_i]]^{-1}\left[\lambda_i\mathbf{v}_i - \mathbf{F}_k[\mathbf{v}_i]\right]$. Thus, in this particular instance we can determine **u** by solving the system of linear algebraic equations. However, note that the algebraic degree of freedom can never exceed the value $p_{k-q,m}$.

Corollary 4.5.1 If a homogeneous process does not satisfy the algebraic controllability conditions, then only the algebraically accessible eigenmodes are controllable.

Proof: This is just a restriction of Theorem 4.5.1 to the algebraically controllable subspace.♦

Corollary 4.5.2 A compensated odd degree process with the real geometric eigenspectrum is globally asymptotically stable if and only if all eigenvalues are negative. In addition, a compensated odd degree process with the mixed geometric eigenspectrum

such that $\mu<k+1$, is globally asymptotically stable if all eigenvalues corresponding to the real eigenvectors are negative. In these instances a compensating state feedback is called stabilizing.

Proof: Apply Theorems 3.3.1 and 3.4.1.♦

For even degree processes the stabilizing state feedback satisfying conditions of Corollary 4.5.2 does not exist. However, for the two-dimensional processes we have the following.

Corollary 4.5.3 Any two-dimensional compensated process with a mixed geometric spectrum has stabilizing state feedback if and only if;

a) For k=odd, each real eigenvector in $X_3\{C^2\}$ has $\lambda\leq 0$.

b) For k=even, each real eigenvector in $X_3\{C^2\}$ is nilpotent.

The stabilized odd degree system is either asymptotically stable in the large, or marginally stable. The stabilized even degree system is always marginally stable.

Proof: Follows from Theorems 3.1.1, 3.1.3, 4.5.2 and Corollary 4.5.1. ♦

Corollary 4.5.4 Every unstable two-dimensional homogeneous process with q=0 which satisfies the necessary state controllability condition is stabilizable.

Proof: Apply Theorem 4.5.1 and Corollary 4.5.3.

Theorems 4.5.1 and 4.5.2, and Corollaries 4.5.1 and 4.5.2 are general results that are presented for the first time in this thesis. Corollaries 4.5.3 and 4.5.4 have been addressed earlier, Samardzija (1984). In addition, Dayawansa et al. (1990) show a related result for the singular two-dimensional homogeneous processes.

4.6. K-FORM STABILIZABILITY AND NONLINEAR COMPLEXITY

By now it is apparent that the methods based on the global algebraic stabilizability grow in computational complexity as the process integers k, m and q increase. For instance, for k=3, m=5, and q=0 the process eigen-number is $s_{3,5}=121$, while $p_{3,5}=35$.

Furthermore, each assigned eigenvector may produce a finite eigenvector pool with as many as $(k+q)^{m-1}=81$ choices. These computational requirements are further magnified by the fact that in general as many as $[(k+q)^{m-1}]^{p_{k-q,m}}$ eigenvector combinations may be possible for an acceptable homogeneous basis realization, which for the case considered is 81^{35}. Consequently as k, m and q increase the nonlinear complexity grows and the computation of process eigenspectra and state feedback realizations rapidly become unmanageable. Therefore, there is a need for a more practical approach. We illustrate such a method first and then generalize the procedure.

Example 4.6.1 Again, we consider Example 4.3.1 except that this time assumption is that the control matrix (or vector) has no particular form. We also place no restriction on the control dimension n. Furthermore, we assume that no spectral information is available and that the only option is to use the process model given by Equation (4.3.1) where **b** is now replaced by the initially unknown mxn matrix **B**. That is,

$$\dot{\mathbf{x}} = \mathbf{D}\mathbf{x}^3 + \mathbf{H}_3[\mathbf{x}] + \mathbf{B}\mathbf{u}\ , \tag{4.6.1}$$

where **D** and $\mathbf{H}_3[\mathbf{x}]$ are as defined earlier, and $\mathbf{u}\in \Re^n$ where n is to be determined. We therefore form the characteristic equation for the autonomous case, or

$$\mathbf{D}\mathbf{v}^3 + \mathbf{H}_3[\mathbf{v}] = \lambda\ \mathbf{v}\ . \tag{4.6.2}$$

This is the nonlinear algebraic system for which solutions are the elements of the spectra (4.3.1.g) and (4.3.1.a). In order to determine whether the process requires stabilization we first need to identify if the process has any real unstable eigenmodes. To accomplish this, assign any positive number to λ and find the zeros of Equation (4.6.2). Observe that the spectral scaling property allows us to assign any positive (negative or zero) value for λ as long as the invariant is unstable (stable or nilpotent), and k>1 is odd. Hence, for k=3, we guess λ=5 and use it to evaluate

$$\mathbf{D}\mathbf{v}^3 + \mathbf{H}_3[\mathbf{v}] - 5\ \mathbf{v} = 0\ . \tag{4.6.3}$$

The last is accomplished by applying the Newton's iterative method from initial point $v_1=v_2=v_3=1$. The solution obtained is $\mathbf{v}=[1.5811388, 0, 0]^t$ which, when normalized by

the first component, produces the eigenvector $\mathbf{e}_1=[1,\ 0,\ 0]^t$, and the eigenvalue $\lambda_{n1}=\lambda/v_1^2=5/1.5811388^2=2$. These solutions define the unstable eigenmode given by the first eigen components in the spectra (4.3.1.g) and (4.3.1.a) .

Now that the unstable direction has been identified we proceed to design the state feedback which compensates the process in this direction. Let $\mathbf{B}=\mathbf{e}_1$ so that

$$\dot{\mathbf{x}} = \mathbf{D}\mathbf{x}^3 + \mathbf{H}_3[\mathbf{x}] + \mathbf{e}_1 g_3(\mathbf{x}) \ , \tag{4.6.4}$$

where

$$u = g_3(\mathbf{x}) = \mathbf{z}_3(\mathbf{x})^t\,\mathbf{g}=\left[x_1^3, x_1^2x_2,\ x_1^2x_3, x_1x_2^2,\ x_1x_2x_3,\ x_1x_3^2,\ x_2^3,\ x_2^2x_3,\ x_2x_3^2,\ x_3^3\right]\begin{bmatrix} g_1 \\ g_2 \\ \vdots \\ g_9 \\ g_{10} \end{bmatrix}$$

is the state feedback which stabilizes the unstable eigenmode and is yet to be determined. The last is obtained by deriving the updated characteristic equation

$$\mathbf{D}\mathbf{v}^3 + \mathbf{H}_3[\mathbf{v}] + \mathbf{e}_1 g_3(\mathbf{v}) = \theta\ \mathbf{v} \ , \tag{4.6.5}$$

and assigning a new eigenvalue θ for the $\mathbf{e}_1$-direction. We can do this since for any θ selected $\mathbf{v}=\mathbf{e}_1$ is always the eigenvector solution for Equation (4.6.5), or

$$\mathbf{D}\mathbf{e}_1^3 + \mathbf{H}_3[\mathbf{e}_1] + \mathbf{e}_1 g_3(\mathbf{e}_1) = \theta\ \mathbf{e}_1 \ , \tag{4.6.6}$$

which, for the first component reduces to

$$\mathbf{e}_1 g_3(\mathbf{e}_1) = \left(\theta - \lambda_{n1}\right)\mathbf{e}_1 \ . \tag{4.6.7}$$

Moreover, since $g_3(\mathbf{e}_1)=\mathbf{z}_3(\mathbf{e}_1)^t\,\mathbf{g}=g_1$, the last expression simplifies to

$$g_1 = \left(\theta - \lambda_{n1}\right) . \tag{4.6.8}$$

Now, suppose that one is to assign the new eigenvalue $\theta=-1$ to stabilize the $\mathbf{e}_1$-direction, then the solution is $g_1=-3$, implying that $u=-3x_1^3$. The process in the stabilized $\mathbf{e}_1$-direction is now

$$\dot{\mathbf{x}} = \mathbf{D}\mathbf{x}^3 + \mathbf{H}_3[\mathbf{x}] - 3\ x_1^3\ \mathbf{e}_1 . \tag{4.6.9}$$

Next we repeat the entire procedure. We set λ=5, and initiate the search for an unstable eigenmode in the updated process, Equation (4.6.9), or

$$\mathbf{D}\mathbf{v}^3 + \mathbf{H}_3[\mathbf{v}] - 3\,\mathbf{e}_1 - 5\mathbf{v} = 0. \tag{4.6.10}$$

Using Newton's method with the initial point v_1=-1, and v_2=v_3=1, the solution is $\mathbf{v}$=[0, 2.2360679, 0]^t. The normalized solution produces the eigenvector $\mathbf{e}_2$=[0, 1, 0]^t with the associated eigenvalue λ_{n2}=5/2.2360679^2=1. These solutions give the second eigen components in the spectra (4.3.1.g) and (4.3.1.a). This unstable eigenmode needs to be compensated which is accomplished by letting $\mathbf{B}$=[$\mathbf{e}_1$, $\mathbf{e}_2$] and $\mathbf{u}$=[-3x_1^3, $g_3(\mathbf{x})$]^t, implying that the new updated process equations are

$$\dot{\mathbf{x}} = \mathbf{D}\mathbf{x}^3 + \mathbf{H}_3[\mathbf{x}] + [\mathbf{e}_1, \mathbf{e}_2]\begin{bmatrix} -3x_1^3 \\ g_3(\mathbf{x}) \end{bmatrix}, \tag{4.6.11}$$

where $g_3(\mathbf{x})$ is the new state feedback to be determined. As before, we derive the update characteristic equation

$$\mathbf{D}\mathbf{v}^3 + \mathbf{H}_3[\mathbf{v}] + [\mathbf{e}_1, \mathbf{e}_2]\begin{bmatrix} -3v_1^3 \\ g_3(\mathbf{v}) \end{bmatrix} = \theta\,\mathbf{v}, \tag{4.6.12}$$

in which the new eigenvalue θ is assigned for the $\mathbf{e}_2$-direction. Thus, for any θ selected, $\mathbf{v}$=$\mathbf{e}_2$ is always the eigenvector solution satisfying

$$\mathbf{D}\mathbf{e}_2^3 + \mathbf{H}_3[\mathbf{e}_2] + [\mathbf{e}_1, \mathbf{e}_2]\begin{bmatrix} 0 \\ g_3(\mathbf{e}_2) \end{bmatrix} = \theta\,\mathbf{e}_2, \tag{4.6.13}$$

or

$$\mathbf{e}_2 g_3(\mathbf{e}_2) = (\theta - \lambda_{n2})\,\mathbf{e}_2\,. \tag{4.6.14}$$

But from the definition u=$g_3(\mathbf{e}_2)$=$\mathbf{z}_3(\mathbf{e}_2)^t\,\mathbf{g}$=$g_7$, we have that

$$g_7 = (\theta - \lambda_{n2})\,. \tag{4.6.15}$$

By assigning θ=-4 the solution is g_7=-5, which implies that $\mathbf{u}$=[-3x_1^3, -5x_2^3]^t. The process with stabilized $\mathbf{e}_1$ and $\mathbf{e}_2$-directions is now

$$\dot{\mathbf{x}} = \mathbf{D}\mathbf{x}^3 + \mathbf{H}_3[\mathbf{x}] + [\mathbf{e}_1, \mathbf{e}_2]\begin{bmatrix} -3x_1^3 \\ -5x_2^3 \end{bmatrix}. \tag{4.6.16}$$

If we now attempt to identify an unstable real eigenmode from the latest update, Newton's method produces $\mathbf{v}=[0,\ 0,\ 0]^t$ for any initial condition selected. This implies that all real unstable process eigenmodes have been stabilized. To verify this, the entire spectra for Equation (4.6.16) has been evaluated, and they are:

$$X_3\{R^3\} = \left\{ \begin{bmatrix} 1 \\ 0 \\ 0 \end{bmatrix}, \begin{bmatrix} 0 \\ 1 \\ 0 \end{bmatrix}, \begin{bmatrix} 0 \\ 0 \\ 1 \end{bmatrix}, \begin{bmatrix} 1 \\ -3.7655644 \\ 0 \end{bmatrix}, \begin{bmatrix} 1 \\ 0.2655644 \\ 0 \end{bmatrix}, \right.$$
$$\begin{bmatrix} 1 \\ 0 \\ 0.3819660 \end{bmatrix}, \begin{bmatrix} 1 \\ 0.3006598 \\ 0.3819660 \end{bmatrix}, \begin{bmatrix} 1 \\ -3.4186938 \\ 0.3819660 \end{bmatrix}, \begin{bmatrix} 1 \\ 0 \\ 2.6180339 \end{bmatrix},$$
$$\left. \begin{bmatrix} 1 \\ 2.7475279 \\ 2.6180339 \end{bmatrix}, \begin{bmatrix} 1 \\ -3.6294939 \\ 2.6180339 \end{bmatrix}, \begin{bmatrix} 0 \\ 1 \\ 0.6180339 \end{bmatrix}, \begin{bmatrix} 0 \\ 1 \\ -1.6180339 \end{bmatrix} \right\}$$

with corresponding eigenvalues

$$\Lambda_3\{R\} = \begin{Bmatrix} -1.0\ ,\ -4.0\ ,\ -1.0\ ,\ -33.1245154\ ,\ -0.8754845\ , \\ -0.9098300\ ,\ -0.7899629\ ,\ -27.7034592\ ,\ -12.0901699 \\ -24.4404614\ ,\ -42.0661163\ ,\ -2.3819660\ ,\ -4.6180339 \end{Bmatrix}.$$

Therefore, the stabilized process has 13 real and simple spectral components, all of which have negative eigenvalues. Consequently, this recursive procedure has produced the globally stabilizing state feedback.

4.7. Recursive Pole Placement and Stabilizability as an Evolutionary Process

The preceding example has demonstrated a stabilization method based on a *recursive pole placement* approach. This is a useful computational algorithm which accommodates various adaptation strategies. For example, if the process model describes dynamics of m biological or chemical species in competition, then for all species to coexist the eigenmodes must display some structure. This does not necessarily imply that eigenmodes must all be stable or unstable. In general, for the odd eigenspectra the eigenvalues are required to have mixed signs so *aggressive* ($\lambda>0$), *passive* ($\lambda\approx0$) and *evasive* ($\lambda<0$) behaviors are possible among the competing species. In contrast, for even

spectra, aggressive and evasive behaviors are combined whenever $\lambda \neq 0$, while the passive behavior still demands a nilpotent eigen structure. Thus, for competing species to survive they need to adapt their aggressive-passive-evasive policy by adjusting their spectra according to the information and resources available. For the proposed recursive pole placement method, this is accomplished by a continuous adaptation or training of the control matrix **B** followed by tuning of **u**. As a result, this method offers a natural approach to the problem of adaptation and particularly is useful in instances when large degrees of freedom exist.

It is also interesting to note that this algorithm provides a unique simulation platform because it allows evolution to enter naturally into the process modeling scheme. This is because the recursive pole placement method starts with some initial model description $\mathbf{F}[\mathbf{x}]$, which subsequently *evolves* as **B** and **u** adapt. Thus, if we identify such a model midway through its evolution, it is impossible to know the initial description without knowing its spectral "history". This is because the continuous state feedback assignments have scrambled the initial model description $\mathbf{F}[\mathbf{x}]$. We now examine one scenario of this kind.

Consider the following process description

$$\dot{\mathbf{x}} = \mathbf{F}_k[\mathbf{x}] + \sum_{i=1}^{n} \mathbf{b}_i \, u_i \ , \tag{4.7.1}$$

in which $\mathbf{F}_k[\mathbf{x}]$ is the initial description, $\mathbf{b}_i$ is the control vector associated with the control law $u_i = g_{k,i}(\mathbf{x})$, and i=1,..,n signifies the evolution step. In addition, we also assume that the spectral information regarding $\mathbf{F}_k[\mathbf{x}]$ is unavailable, and that $\mathbf{b}_i$, $u_i = g_{k,i}(\mathbf{x})$ and the final evolution step n are all initially unknown. The question is then: how does the process adapt by reassigning eigenvalues?

To answer the question two computational steps must be considered. First, the eigenmode for which an eigenvalue needs to be reassigned is identified, and then the control law is evaluated. To identify the adapting eigenmode, we apply Newton's method, as discussed in Example 4.6.1. Basically, by determining the eigenmode type of

interest, *i.e.*, aggressive ($\lambda>0$), passive ($\lambda=0$) or evasive ($\lambda<0$), we form the algebraic problem

$$\mathbf{F}_k[\mathbf{v}] = \lambda_1 \mathbf{v}, \tag{4.7.2}$$

which, for a selected λ_1, is then solved for $\mathbf{v}$ by using Newton's method. The same can be obtained by using a dynamic artificial neural network algorithm proposed by Samardzija and Waterland (1991), and Samardzija (1993). In either case, a solution other than $\mathbf{v}\equiv 0$ produces the eigenvector which corresponds to λ_1. As a result, the process now adapts in the direction identified by reassigning λ_1. This is the second stage of the first adaptation and is expressed as

$$g_{k,1}(\mathbf{v}_1) = \mathbf{z}_3(\mathbf{v}_1)^t \begin{bmatrix} g_{11} \\ g_{12} \\ \vdots \\ g_{1p_{k,m}} \end{bmatrix} = \theta_1 - \lambda_1, \tag{4.7.3}$$

where $\mathbf{v}_1\neq 0$ is the solution of Equation (4.7.2) for predetermined λ_1, θ_1 is the new assigned eigenvalue, and $g_{k,1}(\mathbf{x})$ is the control law which regulates the $\mathbf{v}_1$-direction. The last expression allows the coefficients of $g_{k,1}(\mathbf{x})$ to be determined. With this, the first evolution step is completed and the initial eigenmode defined by $\mathbf{v}_1$ and λ_1 is regulated. Hence, the process equation takes the updated form,

$$\dot{\mathbf{x}} = \mathbf{F}_k[\mathbf{x}] + \mathbf{v}_1 g_{k,1}(\mathbf{x}). \tag{4.7.4}$$

At this point, the process may continue or stop adapting. If it stops, the updated geometric spectrum is such that it generally differs from the initial description. The exceptions are $\mathbf{v}_1$ which is present in both the initial and updated realizations, and all eigenvectors which annihilate $g_{k,1}(\mathbf{x})$. This is clearly illustrated in Example 4.6.1 where the eigenvector $\mathbf{e}_3=[0,\ 0,\ 1]^t$ annihilates the state feedback $\mathbf{u}=[-3x_1^3,\ -5x_2^3]^t$, and is present in both the initial and compensated process realizations. Consequently, if the new eigenmode structure is such that the compensated process performance is acceptable then no further adaptations are needed. But, when performance is not acceptable the process of adaptation continues. One can either go back to Equation (4.7.3) and reassign θ_1 until the performance falls within acceptable limits, or it can continue by evolving the last update.

In the first instance, emphasis on θ_1 may significantly increase a demand for control resources and performance, implying that the control law may become infeasible. This strategy has no effect on annihilating eigenmodes.

By contrast the new process update promotes evolution and in general, a more feasible process structure results. As before, the adapting eigenmode is identified by solving the characteristic problem

$$\mathbf{F}_k[\mathbf{v}] + \mathbf{v}_1\, g_{k,1}(\mathbf{v}) = \lambda_2 \mathbf{v}\ , \tag{4.7.5}$$

where λ_2 is predetermined. The results are then applied to evaluate the state feedback $g_{k,2}(\mathbf{x})$ which satisfies the following first-order algebraic system

$$\begin{bmatrix} g_{k,2}(\mathbf{v}_1) \\ g_{k,2}(\mathbf{v}_2) \end{bmatrix} = \begin{bmatrix} \mathbf{z}_3(\mathbf{v}_1)^t \\ \mathbf{z}_3(\mathbf{v}_2)^t \end{bmatrix} \begin{bmatrix} g_{21} \\ g_{22} \\ \vdots \\ g_{2p_{k,m}} \end{bmatrix} = \begin{bmatrix} 0 \\ \theta_2 - \lambda_2 \end{bmatrix}. \tag{4.7.6}$$

This system permits one to evaluate the coefficients of $g_{k,2}(\mathbf{x})$. Observe that the first equation is simply the condition which requires $\mathbf{v}_1$ to annihilate the state feedback $g_{k,2}(\mathbf{x})$, while the second equation assigns the new eigenvalue θ_2 to $\mathbf{v}_2$. The first equation is necessary to assure that the new state feedback has not altered the already established eigenmode described by $\mathbf{v}_1$ and θ_1. As a result, after the two evolution steps we have the update

$$\dot{\mathbf{x}} = \mathbf{F}_k[\mathbf{x}] + \mathbf{v}_1\, g_{k,1}(\mathbf{x}) + \mathbf{v}_2\, g_{k,2}(\mathbf{x}), \tag{4.7.7}$$

in which $\mathbf{v}_1$ and $\mathbf{v}_2$ are process eigenvectors with respective eignevalues θ_1 and θ_2. All other non-annihilating spectral components of the process in Equation (4.7.4) have again been altered, and the recursive procedure either terminates or continues to adapt.

After the j-th evolution step, the equations have the following form:

$$\mathbf{F}_k[\mathbf{v}] + \sum_{i=1}^{j-1} \mathbf{v}_i\, g_{k,i}(\mathbf{v}) = \lambda_j \mathbf{v}\ , \tag{4.7.8}$$

which identifies $\mathbf{v}_j$ by using either Newton's or the neural network method,

$$\begin{bmatrix} g_{k,j}(\mathbf{v}_1) \\ g_{k,j}(\mathbf{v}_2) \\ \vdots \\ g_{k,j}(\mathbf{v}_j) \end{bmatrix} = \begin{bmatrix} \mathbf{z}_3(\mathbf{v}_1)^t \\ \mathbf{z}_3(\mathbf{v}_2)^t \\ \vdots \\ \mathbf{z}_3(\mathbf{v}_j)^t \end{bmatrix} \begin{bmatrix} g_{j1} \\ g_{j2} \\ \vdots \\ g_{jp_{k,m}} \end{bmatrix} = \begin{bmatrix} 0 \\ 0 \\ \vdots \\ \theta_j - \lambda_j \end{bmatrix}, \tag{4.7.9}$$

which allows $g_{k,j}(\mathbf{x})$ to be determined for an assigned θ_j, and the j-th process update

$$\dot{\mathbf{x}} = \mathbf{F}_k[\mathbf{x}] + \sum_{i=1}^{j} \mathbf{v}_i \, g_{k,i}(\mathbf{x}) \, . \tag{4.7.10}$$

Note, that all eigenvectors $\mathbf{v}_i$, i=1,..,j-1, annihilate the state feedback $g_{k,j}(\mathbf{x})$, which implies that the j-th process update has j spectral components that are given by the eigenvectors $\mathbf{v}_1, \mathbf{v}_2, ...,\mathbf{v}_j$ with respective eigenvalues $\theta_1,\theta_2,...,\theta_j$.

Theorem 4.7.1 The j-th evolution step has exhausted j degrees of freedom if, and only if, $\mathbf{v}_1, \mathbf{v}_2, ..., \mathbf{v}_j$ are algebraically independent. The maximal number of algebraically independent evolution steps is $p_{k,m}$.

Proof: Observe that the algebraic independence of $\mathbf{v}_1, \mathbf{v}_2, ..., \mathbf{v}_j$ implies that the k-form vector representations $\mathbf{z}_k(\mathbf{v}_1), \mathbf{z}_k(\mathbf{v}_2), ..., \mathbf{z}_k(\mathbf{v}_j)$ must be linearly independent. Therefore, for j=1, it follows from Equation (4.7.3) that any arbitrary assigned coefficients $g_{11},..., g_{1p_{k,(m-1)}}$ will uniquely determine the final state feedback coefficient $g_{1p_{k,m}}$. Thus, one degree of freedom is exhausted. For j=2, Equation (4.7.6) implies that $g_{21},..., g_{2p_{k,(m-2)}}$ can be arbitrary assigned and the last two coefficients $g_{2p_{k,(m-1)}}$ and $g_{2p_{k,m}}$ are uniquely determined as long as $\mathbf{z}_k(\mathbf{v}_1)$ and $\mathbf{z}_k(\mathbf{v}_2)$ are not collinear. This implies that two degrees of freedom are used up. Similarly, for any $2<j\leq p_{k,m}$, the number of arbitrary assigned coefficients is equal to $p_{k,m}$-j when $\mathbf{z}_k(\mathbf{v}_1), \mathbf{z}_k(\mathbf{v}_2), ..., \mathbf{z}_k(\mathbf{v}_j)$ are linearly independent, and the remaining j coefficient are uniquely determined. Thus, the j degrees of freedom are manipulated by the j-th evolution step. This proves the "if" part of the theorem. The "only if" claim follows from the observation that if $\mathbf{z}_k(\mathbf{v}_1)$, $\mathbf{z}_k(\mathbf{v}_2), ..., \mathbf{z}_k(\mathbf{v}_j)$ are linearly dependent, or $\mathbf{v}_1, \mathbf{v}_2, ..., \mathbf{v}_j$ are algebraically related, more than $p_{k,m}$-j coefficients are arbitrary assigned. This is because the rank of matrix $[\mathbf{z}_k(\mathbf{v}_1),$

$\mathbf{z}_k(\mathbf{v}_2)$, ..., $\mathbf{z}_k(\mathbf{v}_j)$], which in turn is equal to the number of degrees of freedom used, determines the number of the unique coefficients. The final claim is now obvious. ♦

This theorem shows that a k-form process needs to accomplish its control objective in the $p_{k,m}$ algebraically independent evolution steps. If at that time this objective is not reached, the process needs to reassign the eigenvalues. For instance, in Example 4.6.1 no such strategy was required since the stabilization objective was accomplished in two evolution steps.

4.8. CHAPTER IV SUMMARY

Table 4.8.1 summarizes topics of significance covered in Chapter IV. The topics in bold letters identify ideas that are conceived during the preparation of this thesis.

Table 4.8.1 Topics covered in Chapter IV.

k-form controllability
• the necessary state controllability conditions • controllable and uncontrollable eigenmodes • **fully cross-coupled processes** • **algebraic controllability**
k-form stabilizability
• **multi-dimensional state feedback stabilizability** - **degree of state feedback = process degree** - **degree of state feedback < process degree** - **relations to nonlinear complexity** - **recurrent pole placement**

CHAPTER 5 - HETEROGENEOUS PROCESSES AND CSTR DYNAMICS

5.1. POLYNOMIAL EXTENSION

The multivariate k-form stability and control results can be applied to regulate a chemical process of interest. For instance, the results presented can be used to regulate dynamics of the idealized homogeneous reactor models described by Equations (1.1.2) and (1.1.3). But, when chemical processes are heterogeneous we have yet to show how to use the k-form theory. Thus, our next objective is to extend the k-form results to the class of heterogeneous dynamic structures described by the multivariable polynomial functions. This choice of nonlinear representation is general enough to cover a large class of natural phenomena modeled by the nonlinear differential equations. Even in the case when nonlinearities are not of the polynomial type one can often obtain the polynomial realizations by evaluating either the full or truncated power series expansion. This was demonstrated earlier for the exothermic CSTR process given in Equation (1.2.4).

We begin by considering the polynomial differential equation

$$\dot{\mathbf{x}} = \sum_{j=r}^{k} \mathbf{F}_j[\mathbf{x}] + \mathbf{B}\,[[\mathbf{x}]]\mathbf{u} \;\; ; \quad 0 \le r < k \,, \tag{5.1.1}$$

where the symbols are as defined previously. For the autonomous case one has

$$\dot{\mathbf{x}} = \mathbf{F}_r[\mathbf{x}] + \sum_{j=r+1}^{k-1} \mathbf{F}_j[\mathbf{x}] + \mathbf{F}_k[\mathbf{x}] \;\; ; \; 0 \le r < k \; . \tag{5.1.2}$$

By assigning the projection state x_i one can derive an analog of the projection equation, Equation (2.2.1), for the heterogeneous case. The generalized projection equation is

$$\dot{\mathbf{v}} = \sum_{j=r}^{k} [\mathbf{F}_j[\mathbf{v}] - f_{j,i}(\mathbf{v})\, \mathbf{v}] x_i^{j-1}, \tag{5.1.3}$$

and as before all singular solutions of are given by the relations

$$\mathbf{Ce}(\mathbf{v}, x_i) \equiv \sum_{j=r}^{k} [\mathbf{F}_j[\mathbf{v}] - f_{j,i}(\mathbf{v})\, \mathbf{v}] x_i^{j-1} = \sum_{j=r}^{k} \mathbf{F}_j[\mathbf{v}]\, x_i^{j-r} - \beta(x_i)\, \mathbf{v} = 0, \tag{5.1.4}$$

and

$$\beta(x_i) \equiv \sum_{j=r}^{k} f_{j,i}(\mathbf{v}) x_i^{j-r} = \sum_{j=r}^{k} \lambda_j(x_i). \tag{5.1.5}$$

The last two expressions define the characteristic value problem for a polynomial process. These equations are now algebraic in both $\mathbf{v}$ and x_i, which agrees with the fact that a process is heterogeneous. Solutions of $\mathbf{v}$ form an algebraic set, or *algebraic variety*, parametrized by x_i and denoted as $\mathbf{v}\{x_i\}$, while $\beta(x_i)$ is an eigenvalue at each variety point x_i. From now on we refer to $\mathbf{v}\{x_i\}$ as the *eigen-variety* and $\beta(x_i)$ as the *eigenfunction*.. Jointly, these quantities determine a polynomial eigenmode. It is easy to show that all solutions of Equations (5.1.4) and (5.1.5) respectively define geometric and algebraic eigenspectra.

Observe that in this formulation an eigen element $\mathbf{v}\{x_i\}$ is no longer a single eigenvector in the geometric spectrum. Instead it is a continuous collection of eigenvectors parametrized by the projection state x_i, and as such forms a smooth characteristic manifold. The vector field flow along any such manifold is determined by the eigenfunction sign. That is, a $\mathbf{v}\{x_i\}$-manifold at a projection point x_i is stable, unstable or singular (center) when the associated $\beta(x_i)$ is respectively negative, positive or zero.

As defined, these manifolds represent generalizations of homogeneous invariants. This is further illustrated by the following theorem:

Theorem 5.1.1 If the homogeneous processes $\dot{\mathbf{x}} = \mathbf{F}_r[\mathbf{x}]$ and $\dot{\mathbf{x}} = \mathbf{F}_k[\mathbf{x}]$ are globally asymptotically stable, then the heterogeneous process in Equation (5.1.2) has the asymptotically stable trivial steady-state and is bounded.

Proof: The following two limits

$$\lim_{x_i \to 0} \mathbf{Ce}(\mathbf{v},x_i) \to \mathbf{F}_r[\mathbf{v}] - f_{r,i}(\mathbf{v})\mathbf{v} \tag{5.1.6}$$

and

$$\lim_{|x_i| \to \infty} \mathbf{Ce}(\mathbf{v},x_i) \to \mathbf{F}_k[\mathbf{v}] - f_{k,i}(\mathbf{v})\mathbf{v} \tag{5.1.7}$$

determine the local homogeneous structure of the trivial point, and the global bounding structure in $\mathbb{R}^m$. Thus, in the heterogeneous case the local stability of the trivial point and the globally bounding behavior are determined by the structurally stable dynamics of the lowest and highest degree homogeneous terms. ♦

Example 5.1.1 *(Process dynamics and manifold anatomy)*

To illustrate the theorem we consider the following two-dimensional cubic polynomial process

$$\begin{aligned} \dot{x}_1 &= ax_1 - x_2^3 - 2x_1x_2^2 \\ \dot{x}_2 &= -2x_2 + x_1^3 - 2x_1x_2^2 - 2x_2^3 \end{aligned} \tag{5.1.8}$$

where $a \in \mathbb{R}$, and which can easily be analyzed by using any of the classical methods. However, for our present purpose we analyze it by separating it into two distinct homogeneous processes: the linear,

$$\begin{aligned} \dot{x}_1 &= ax_1 \\ \dot{x}_2 &= -2x_2 \end{aligned} \tag{5.1.9}$$

and the cubic

$$\begin{aligned} \dot{x}_1 &= - x_2^3 - 2x_1x_2^2 \\ \dot{x}_2 &= x_1^3 - 2x_1x_2^2 - 2x_2^3 . \end{aligned} \tag{5.1.10}$$

The spectra for the homogeneous realizations are accordingly

$$X_1\{R^2\} = \left\{\mathbf{e}_1=\begin{bmatrix}1\\0\end{bmatrix},\ \mathbf{e}_2=\begin{bmatrix}0\\1\end{bmatrix}\right\}$$
$$\Lambda_1\{R\} = \{a\ ,\ -2\}\ .$$

and

$$X_3\{R^2\} = \left\{\mathbf{s}_1=\begin{bmatrix}1\\1\end{bmatrix}_{(2)},\ \mathbf{s}_2=\begin{bmatrix}1\\-1\end{bmatrix}_{(2)}\right\}$$
$$\Lambda_3\{R\} = \{-3_{(2)}\ ,\ -1_{(2)}\}\ .$$

The k=1 spectra contain two simple eigenmodes which determine the behavior of Equation (5.1.9). For a>0 the linear system is hyperbolically unstable, for a=0 the system is marginally stable, and for a<0 it is globally asymptotically stable. By contrast, all eigen components in the cubic spectra have multiplicity 2, and therefore Equation (5.1.10) is globally asymptotically stable.

Next, by allowing x_1 to be the projection state, we derive the characteristic equation

$$\mathbf{Ce}(v,x_1) = (v^2 - 1)^2x_1^2 - (2 + a)\,v = 0, \qquad (5.1.11)$$

with the eigenfunction

$$\beta(x_1) = a - (v + 2)\,v^2x_1^2\ . \qquad (5.1.12)$$

Inspections of both $\mathbf{Ce}(v,x_1)$ and $\beta(x_1)$ now reveal that as $x_1\to 0$, the solutions of Equation (5.1.8) approaches those of the linear system in Equation (5.1.9). Similarly, when $|x_1|\to\infty$ the solutions approach the cubic system eigenspectra. Thus, for a=-20 both linear and cubic terms exhibit global asymptotic stability. Consequently, Theorem 5.1.1. implies that the polynomial process is globally bounded and the trivial point is asymptotically stable. This is illustrated in Figure 5.1.1.c), while Figures 5.1.1.a) and b) portray dynamics of the individual homogeneous terms. Observe that the structure of the local vector field surrounding the trivial steady-state in Figure 5.1.1.c) is essentially the same as that of the linear realization, while the bounding behavior resembles the cubic behavior. Furthermore the system is globally asymptotically stable since there are no additional steady-states present.

By contrast, when a=2 the phase portraits are displayed in Figure 5.1.2. The hyperbolically unstable linear system violates the conditions of Theorem 5.1.1, implying that the polynomial system no longer has the asymptotically stable trivial steady-state. This is depicted in Figure 5.1.2.c) together with the appearance of two nontrivial stable steady-states. As such the system is globally bounded, but not globally asymptotically stable. The two nontrivial steady-states can also be verified by examining the eigenfunctions. This is because at a steady-state point an eigenfunction must satisfy the condition $\beta(x_1)=0$. If this were not so, a point could not be in the equilibrium, implying that it would have to repel ($Re\{\beta(x_1)\}>0$) or be attracted ($Re\{\beta(x_1)\}<0$). Thus, to meet the steady-state requirement we must have the relation

$$a - (v + 2)\, v^2 x_1^2 = 0\,, \tag{5.1.13}$$

which implies that for any assigned nonzero value of x_1, a <u>real</u> solution of v that also satisfies Equation (5.1.11) determines the nontrivial steady-state point. Thus, a nontrivial steady-state in polynomial systems is determined by the *spectral blend* of the k-form spectra. Stated differently, the individual homogeneous eigenspectra are blended into the state-space manifolds which determine dynamic and steady-state features of the polynomial processes.

We now demonstrate the spectral blending for the case a=2. Inspection of Equation (5.1.11) shows that for any assigned projection state, one must have four manifold solutions. The two solutions are always real and two are complex conjugate, implying that two manifolds are real and two are complex. Furthermore, since complex manifolds cannot be graphically displayed in $\Re^2$, we introduce the convention by which the magnitude multiplied by the sign of the real part determines the manifold projection in the state-space. That is, if a complex manifold is represented as

$$x_i\, \mathbf{v}\{x_i\} = x_i \left\{ \begin{bmatrix} 1 \\ u\{x_i\} \end{bmatrix} \pm i \begin{bmatrix} 1 \\ w\{x_i\} \end{bmatrix} \right\}$$

where $\mathbf{v}\{x_i\}$ is an eigen-vaiety, then the state-space projection is given by

$$x_i \begin{bmatrix} 1 \\ CM \end{bmatrix}$$

system: *linear form* $\dot{x}_1 = -20x_1$, $\dot{x}_2 = -2x_2$

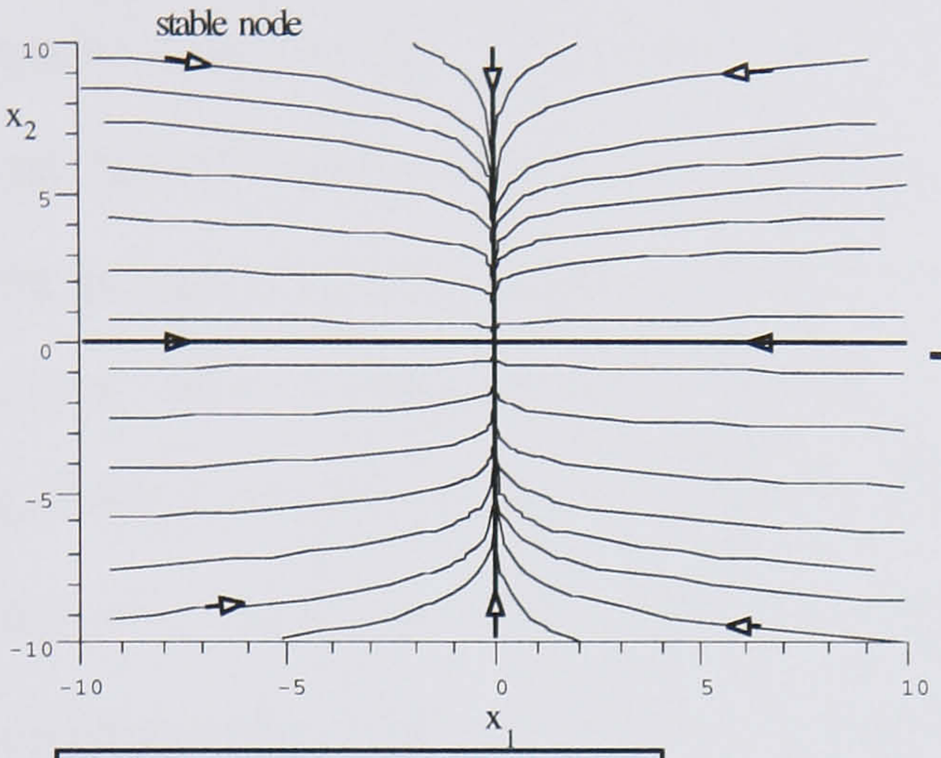

eigenspectra:

$$\mathbb{X}_1\{\mathbb{R}^2\} = \left\langle \mathbf{e}_1 = \begin{bmatrix} 1 \\ 0 \end{bmatrix}, \mathbf{e}_2 = \begin{bmatrix} 0 \\ 1 \end{bmatrix} \right\rangle$$

$$\mathbb{\Lambda}_1\{\mathbb{R}\} = \{ 2 , -2 \} .$$

a)

+

system: *cubic form* $\dot{x}_1 = -x_2^3 - 2x_1x_2^2$, $\dot{x}_2 = x_1^3 - 2x_1x_2^2 - 2x_2^3$

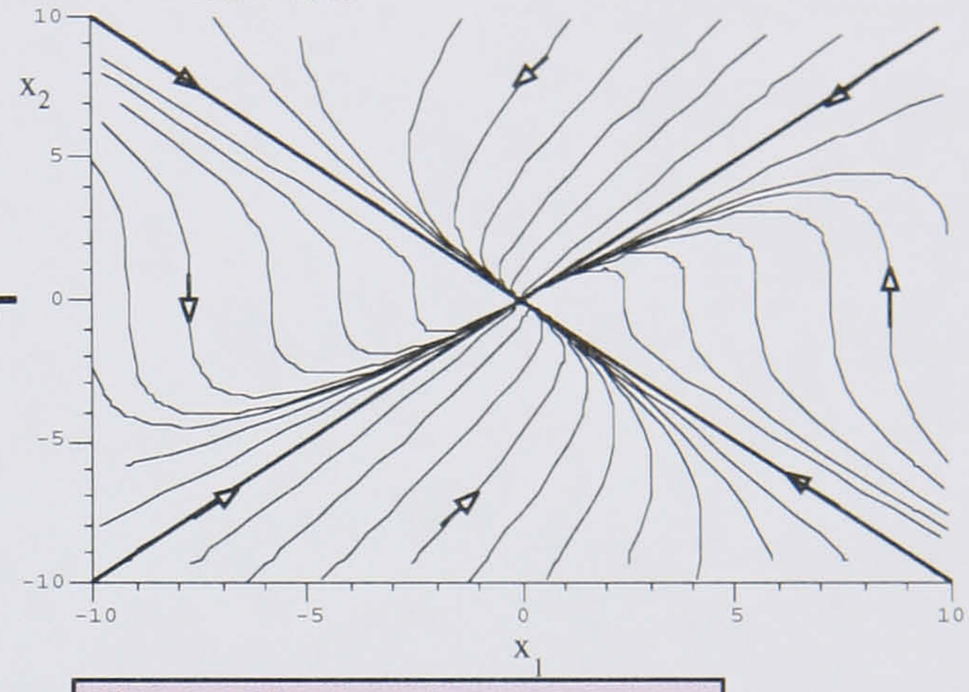

eigenspectra:

$$\mathbb{X}_3\{\mathbb{R}^2\} = \left\langle \mathbf{s}_1 = \begin{bmatrix} 1 \\ 1 \end{bmatrix}_{(2)}, \mathbf{s}_2 = \begin{bmatrix} 1 \\ -1 \end{bmatrix}_{(2)} \right\rangle$$

$$\mathbb{\Lambda}_3\{\mathbb{R}\} = \{ -3_{(2)} , -1_{(2)} \} .$$

b)

=

polynomial system: $\dot{x}_1 = -20x_1 - x_2^3 - 2x_1x_2^2$, $\dot{x}_2 = -2x_2 + x_1^3 - 2x_1x_2^2 - 2x_2^3$

and is globally bounded with stable trivial steady-state

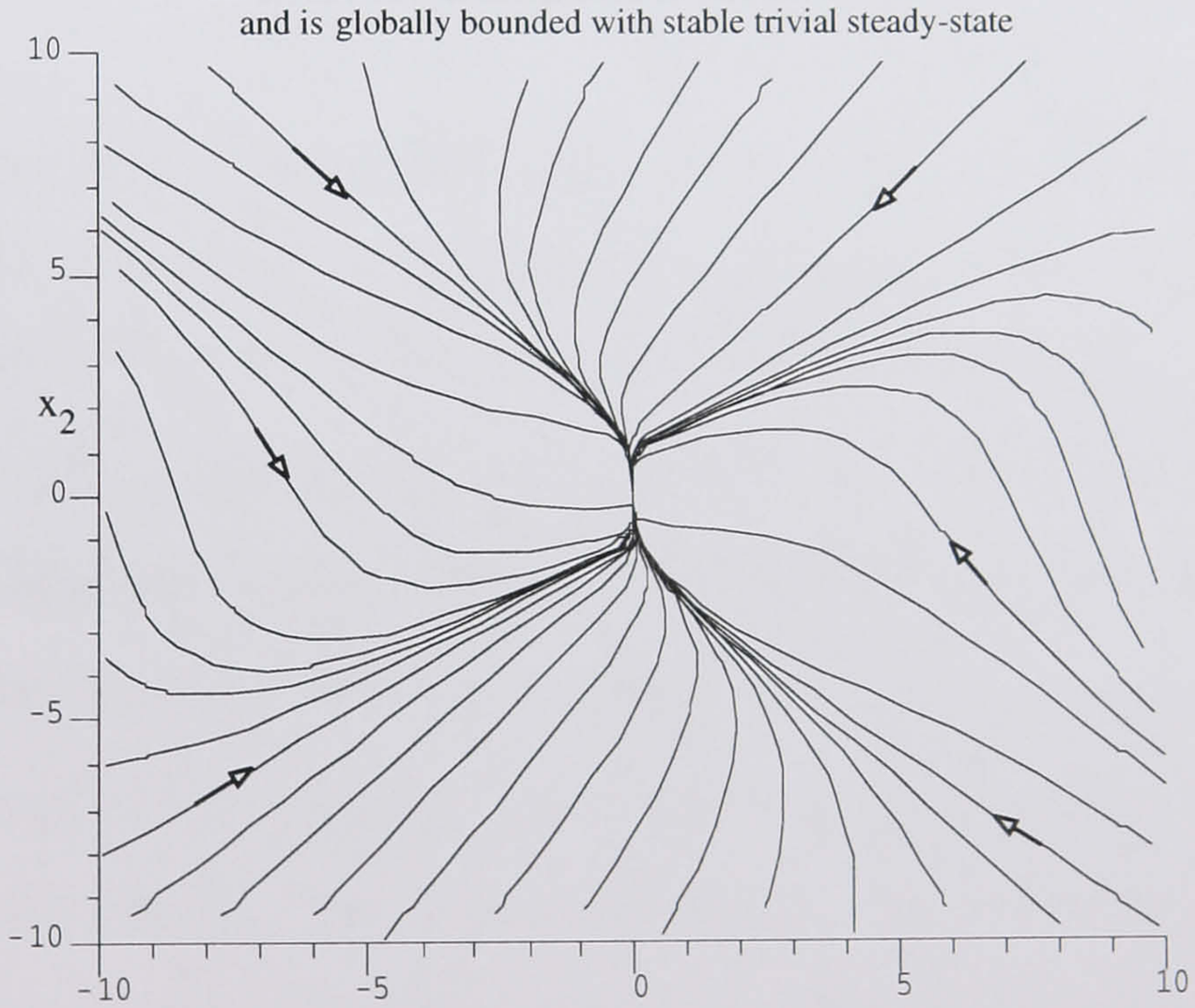

c)

Polynomial blending of homogeneous processes of different orders.

FIGURE 5.1.1.

with

$$CM= sgn[u(x_i)]\ [u^2(x_i) + w^2(x_i)]^{1/2}, \qquad (5.1.14)$$

where *sgn*[.] is the sign function. Thus, the four manifold solutions are represented by the three distinct lines where the line corresponding to the complex solutions accounts for the presence of the complex conjugate pair. This is depicted in Figure 5.1.3.a) where CSM, SM, LUM and GSM respectively stand for the Complex Stable, Stable (real), Locally Unstable (real) and Globally Stable (real) Manifolds. Note that as $x_1 \to 0$, or $|x_1| \to \infty$, these manifolds approach the invariants determined respectively by the linear or cubic geometric spectra. Moreover, the dynamics along the manifolds are determined by the eigenfunction signs which are also illustrated in Figure 5.1.3.a). Observe that the complex eigenfunction has the real projection

$$\begin{aligned} \beta_{CM} &= sgn[Re\{\beta(x_1)\}]\ |\beta(x_1)| \\ &= sgn[Re\{\beta(x_1)\}]\ [Re(\beta(x_1))^2 + Im(\beta(x_1))^2)]^{1/2}\,. \end{aligned} \qquad (5.1.15)$$

Also, note that the LUM and GSM structures determine the single real manifold solution which changes qualitatively at the steady-state point (**ss**). In addition, from Equation (5.1.12) it follows that $\beta_{LUM} \to 2$ as $x_1 \to 0$, which is the unstable eigenvalue in $\Lambda_1(\mathbb{R})$. Similarly, both β_{CSM} and β_{SM} approach the stable linear eigenvalue as $x_1 \to 0$. However, in this case a singularity exists at $x_1=0$, as is indicated by the small circle. The singularity disappears when x_2 is selected as the projection state.

The manifold organization also reflects the parallel structure of the two real manifolds GSM and SM. This is the consequence of the second order multiplicity in the cubic spectra, and can be interpreted as follows: when the linear form is not present in the process description, the two manifolds GSM and SM degenerate into the single invariant of multiplicity two, given by $\mathbf{s}_1 \in \Sigma_3(\mathbb{R}^2)$. Thus, the appearance of the linear form splits this invariant into the two parallel manifolds, each of the multiplicity one. In return, the split allows formation of LUM, which establishes the local hyperbolic topology.

system: *linear form* $\dot{x}_1 = 2x_1$, $\dot{x}_2 = -2x_2$

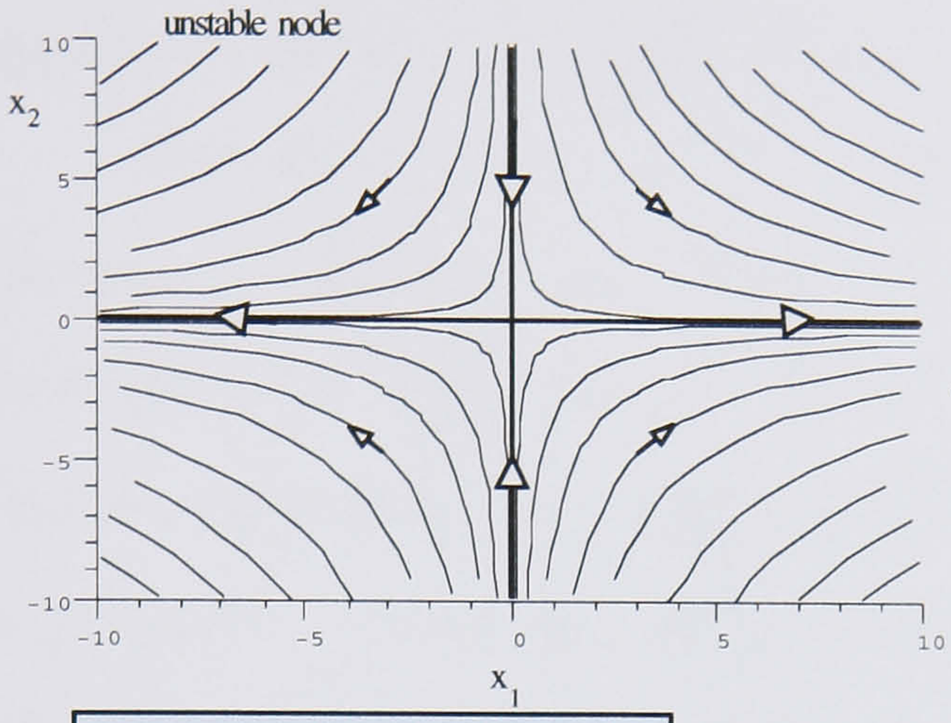

eigenspectra:

$$\mathbb{X}_1\{\mathbb{R}^2\} = \left\{ \mathbf{e}_1 = \begin{bmatrix} 1 \\ 0 \end{bmatrix}, \mathbf{e}_2 = \begin{bmatrix} 0 \\ 1 \end{bmatrix} \right\}$$

$$\mathbb{A}_1\{\mathbb{R}\} = \{ 2 , -2 \} .$$

a)

system: *cubic form* $\dot{x}_1 = -x_2^3 - 2x_1x_2^2$, $\dot{x}_2 = x_1^3 - 2x_1x_2^2 - 2x_2^3$

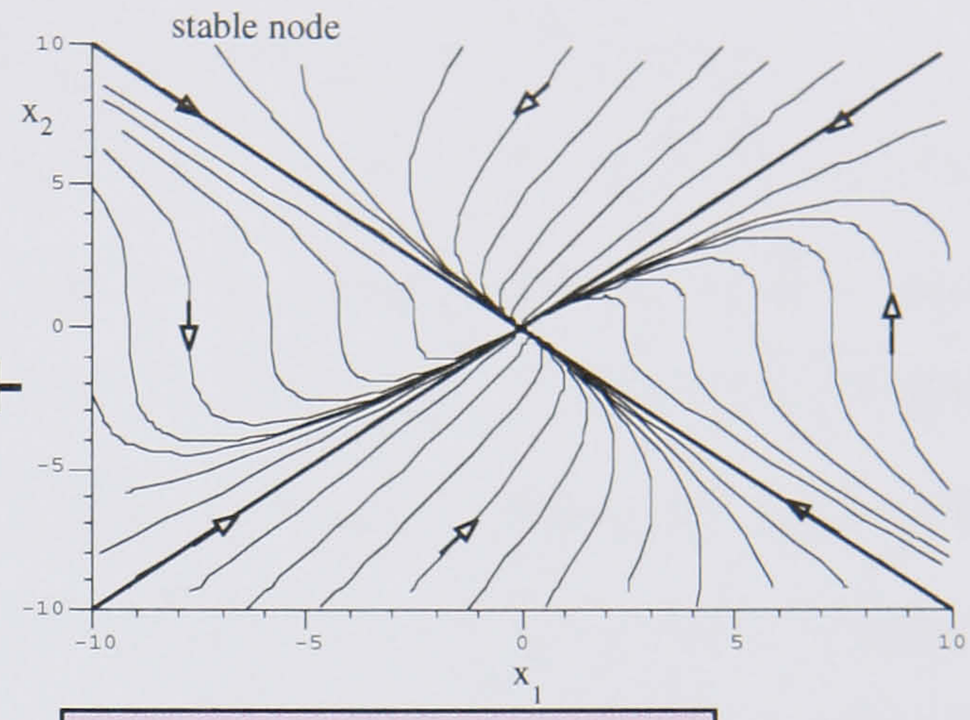

eigenspectra:

$$\mathbb{X}_3\{\mathbb{R}^2\} = \left\{ \mathbf{s}_1 = \begin{bmatrix} 1 \\ 1 \end{bmatrix}_{(2)}, \mathbf{s}_2 = \begin{bmatrix} 1 \\ -1 \end{bmatrix}_{(2)} \right\}$$

$$\mathbb{A}_3\{\mathbb{R}\} = \{ -3_{(2)} , -1_{(2)} \} .$$

b)

=

polynomial system: $\dot{x}_1 = 2x_1 - x_2^3 - 2x_1x_2^2$, $\dot{x}_2 = -2x_2 + x_1^3 - 2x_1x_2^2 - 2x_2^3$

and is globally bounded with unstable trivial steady-state

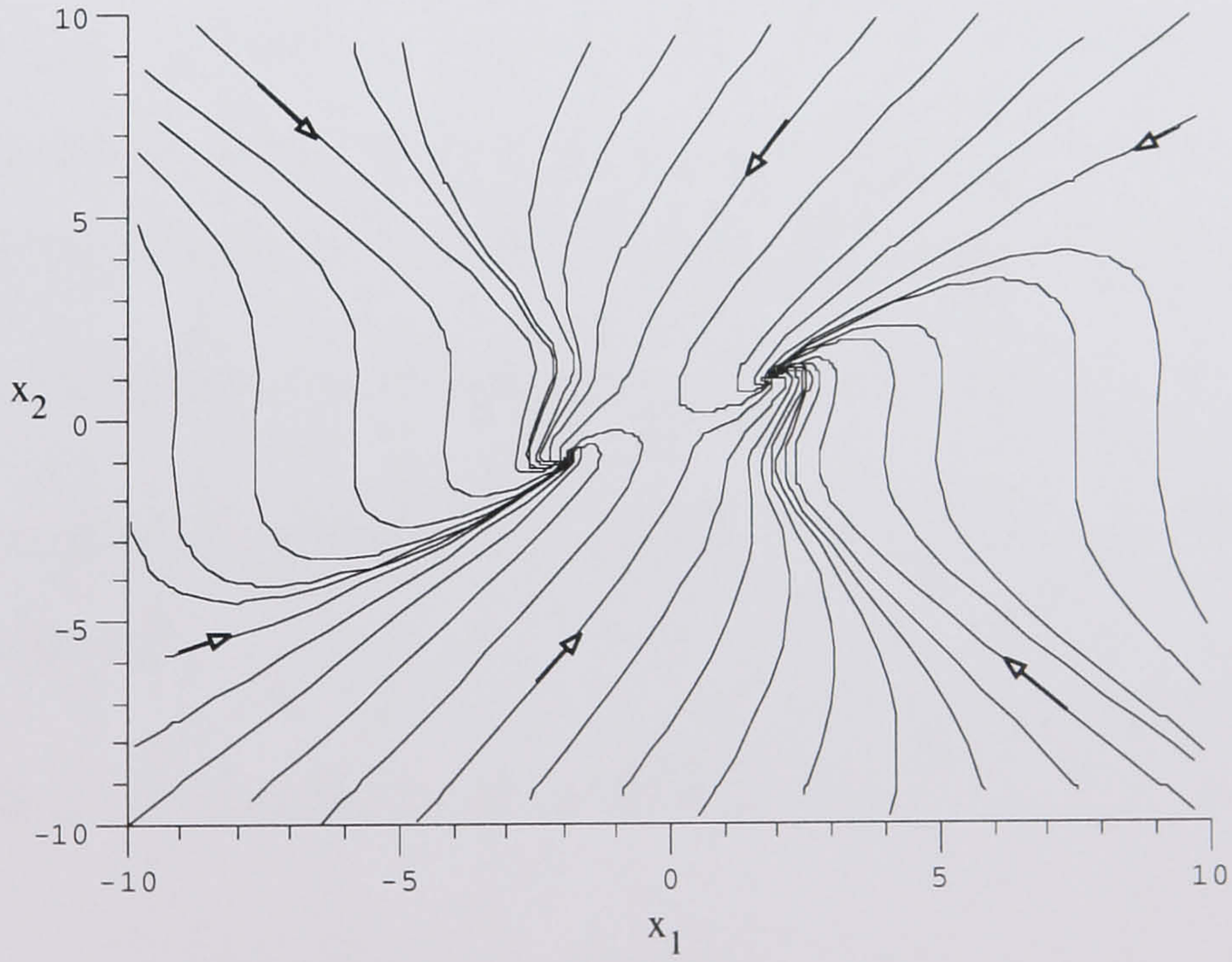

c)

The polynomial blend of the unstable linear and the stable cubic forms.

FIGURE 5.1.2.

We conclude this example by superimposing the computed manifolds over the phase portrait given in Figure 5.1.2.c). The result is shown in Figure 5.1.3.b), and it depicts how the manifold anatomy shapes the local and global process dynamics.

When $\mathbf{F}_r[\mathbf{x}]$ or $\mathbf{F}_k[\mathbf{x}]$ are structurally unstable, Theorem 5.1.1 is no longer true. This is because there exists a $\mathbf{v}$ in Equation (5.1.6), or Equation (5.1.7), which is real and nilpotent, or $\mathbf{F}_r[\mathbf{x}]$ and $\mathbf{F}_k[\mathbf{x}]$ contain complex eigenspectra that generate periodic solutions. In the first case the spectra of the intervening terms can influence the behavior in the $\mathbf{v}$ direction, while in the second instance, the orbital balance of the lowest or highest degree forms is perturbed by the intermediate k-forms. Furthermore, when r is even and geometric spectrum of $\mathbf{F}_r[\mathbf{x}]$ has no nilpotents, Theorem 3.3.1 implies that a heterogeneous process can never have the asymptotically stable trivial steady-state. Similarly, when $\mathbf{F}_k[\mathbf{x}]$ is even, with geometric eigenspectrum containing no nilpotents, a process is never bounded. This is also verified in Theorem 3' (Coleman 1984). These observations are now summarized:

Corollary 5.1.1 If $\mathbf{F}_r[\mathbf{x}]$ and $\mathbf{F}_k[\mathbf{x}]$ contain real nilpotent eigenvectors, nothing can be said about a stability of the trivial steady-state or whether a process is bounded or not. In this case homogeneous spectra of the intervening k-forms must be considered.

Proof: This follows from the proof of Theorem 5.1.1. ♦

This corollary is an extension of the center manifold theorem and is illustrated by the following example.

Example 5.5.2 The quadratic polynomial system

$$\begin{bmatrix} \dot{x}_1 \\ \dot{x}_2 \\ \dot{x}_3 \end{bmatrix} = \begin{bmatrix} -a_1x_1 + x_2^2 \\ -a_2x_2 + x_3^2 \\ -a_3x_3 \end{bmatrix} \quad ; \quad a_1,a_2,a_3>0 \tag{5.5.16}$$

has the linear spectra which are responsible for the asymptotically stable trivial steady-state. The quadratic term is homogenized and as such is singular with the nilpotent eigenvector $\mathbf{v}=[1,\ 0,\ 0]^t_{(7)}$. Since the multiplicity is equal to $s_{2,3}$, no other element exists in the

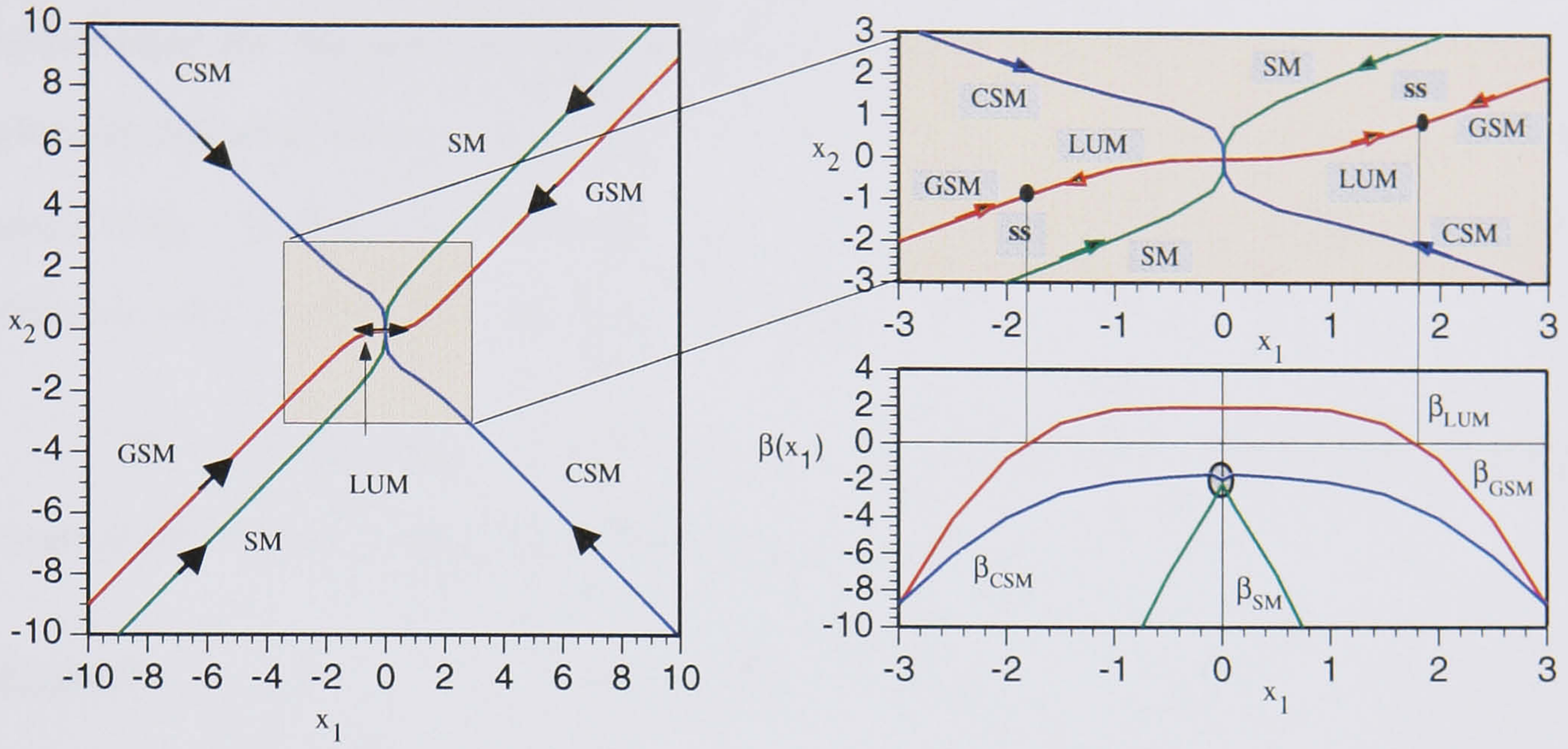

legend:

SM - stable manifold (real)
CSM - complex stable maniflod
GSM - globally stable manifold
LUM - locally unstable manifold
ss - steady-state

manifold solutions for the heterogeneous characteristic equation:

$$(v^2 - 1)^2 x_1^2 - 4v = 0$$

where the flow is determined by the eigenfunction

$$\beta(x_1) = 2 - (v + 2) v^2 x_1^2,$$

and $x_2 = v x_1$.

a)

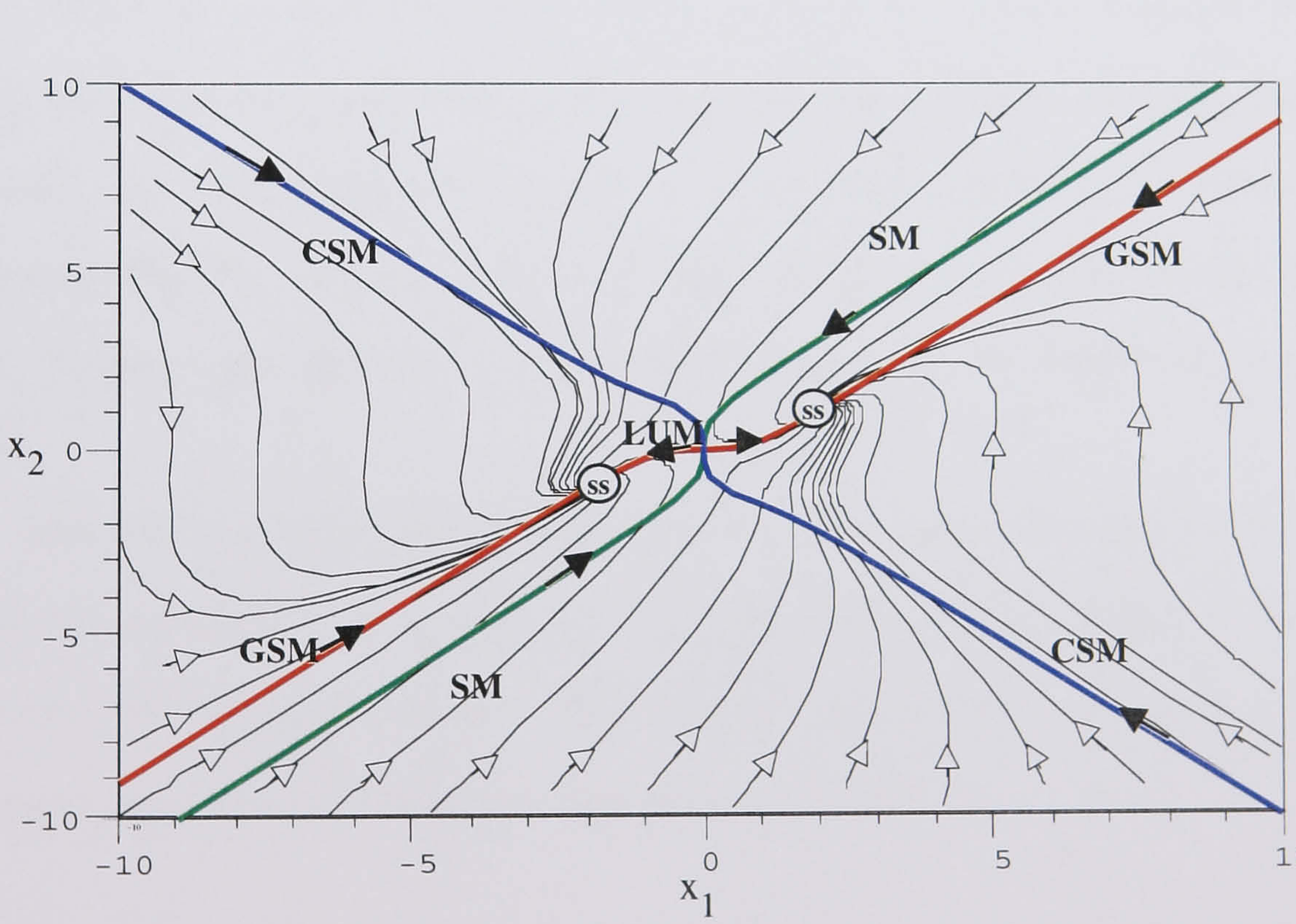

Stable and unstable manifolds superimposed over the phase diagram in Figure 5.1.2.c.

b)

Manifolds of the cubic polynomial process.

FIGURE 5.1.3.

quadratic spectrum. Therefore, the entire quadratic spectrum is nilpotent and is responsible for the process being structurally unstable. Nevertheless, the system is globally bounded because its behavior is entirely determined by the behavior of the first-order term. Hence, the first-order asymptotic stability induces boundedness, which in this case also implies global asymptotic stability.

In some instances, Corollary 5.1.1 can be applied to design a stabilizing state feedback for a structurally unstable homogeneous process.

Example 5.1.3 The rigid body rotation problem

$$\begin{bmatrix} \dot{x}_1 \\ \dot{x}_2 \\ \dot{x}_3 \end{bmatrix} = \begin{bmatrix} a_1 x_2 x_3 \\ a_2 x_1 x_3 \\ a_3 x_1 x_2 \end{bmatrix} + \mathbf{Bu}\ , \tag{5.1.17}$$

where $-1 \le a_i \le 1$ and $a_1+a_2+a_3+a_1a_2a_3=0$ is the quadratic homogeneous process that can be globally asymptotically stabilized by using the linear state feedback (Baillieul 1980). This is because the uncompensated process is structurally unstable with three nilpotent eigenvectors and four complex eigen pairs responsible for periodic solutions (Samardzija 1984). To prove the existence of the periodic orbits, one can apply Theorem 3.1.2 as follows.

From the constraints imposed on the coefficients, it is evident that one of a_i's must have an opposite sign from the other two. Suppose that a_1 is the coefficient and x_1 is the projection state which determines the projection vector $\mathbf{v}=[1,\ v_2,\ v_3]^t$. With this assignment, the following Frommer's integrals are derived

$$I_{v_i} = \int_{\mathbb{R}} \frac{f_{2,1}(\mathbf{v})}{f_{2,i}(\mathbf{v}) - f_{2,1}(\mathbf{v})v_i}\, dv_i = \int_{\mathbb{R}} \frac{a_1 v_i}{a_i - a_1 v_i^2}\, dv_i, \qquad i=2,3. \tag{5.1.18}$$

Because a_1 has the opposite sign from a_2 and a_3, both integrands have complex poles. All combinations of the pole solutions determine the four complex eigenvectors. Furthermore, since both integrands are odd symmetric functions, then $I_{v_2}=I_{v_3}=0$. Thus, the nilpotent

and the balanced spectral components of the quadratic term can now be perturbed by a stable linear structure.

One can also apply the k-form controllability and stabilizability results to any polynomial case. To accomplish this we need the following definitions.

Definition 5.1.1 The polynomial process in Equation (5.1.1) has j-order stabilizing homogeneous spectra if for some $\mathbf{F}_j[\mathbf{x}]$, the homogeneous process $\dot{\mathbf{x}}=\mathbf{F}_j[\mathbf{x}]$ is stable.

Definition 5.1.2 The polynomial process in Equation (5.1.1) satisfies the j-order necessary state controllability condition if for $\mathbf{F}_j[\mathbf{x}]$ there exists a q-form, $\mathbf{B}_q[[\mathbf{x}]]$, $0\leq q\leq j$, in $\mathbf{B}[[\mathbf{x}]]$ such that the process $\dot{\mathbf{x}}=\mathbf{F}_j[\mathbf{x}]+\mathbf{B}_q[[\mathbf{x}]]\mathbf{u}$ satisfies the same condition. When all forms in Equation (5.1.1) satisfy the necessary state controllability condition, the polynomial process fully satisfies the same condition.

Definition 5.1.3 The polynomial process in Equation (5.1.1) is j-order fully cross-coupled or algebraically controllable if for $\mathbf{F}_j[\mathbf{x}]$ there exists a q-form $\mathbf{B}_q[[\mathbf{x}]]$, $0\leq q\leq j$, in $\mathbf{B}[[\mathbf{x}]]$ such that the process $\dot{\mathbf{x}}=\mathbf{F}_j[\mathbf{x}]+\mathbf{B}_q[[\mathbf{x}]]\mathbf{u}$ satisfies the corresponding requirements. When all forms in Equation (5.1.1) are fully cross-coupled or algebraically controllable, then the polynomial process is entirely fully cross-coupled or algebraically controllable.

Corollary 5.1.2 If for odd k and r, Equation (5.1.1) admits a stabilizing state feedback such that the k-order and r-order stabilizing spectra as defined by Corollary 4.5.2 exist, then the trivial steady-state is asymptotically stable and the heterogeneous process is bounded.

Proof: Apply Theorem 5.1.1.♦

Based on the results one can think of a polynomial system as being an algebraic mix of homogeneous spectra, with the mix being determined by Equations (5.1.3) and (5.1.4). At the extreme limits of the projection state x_i, the mix simplifies to the spectra of the highest and lowest degree forms. However, in regions between these extremes the

spectral mix generates manifolds which create complex dynamic structures. These in turn produce behaviors that can often be counter intuitive even in simple two-dimensional cases.

Example 5.1.4 The polynomial system

$$\begin{bmatrix} \dot{x}_1 \\ \dot{x}_2 \end{bmatrix} = \begin{bmatrix} -10x_1 + 3x_1^3 + x_1^2x_2 \\ -x_2 - 11.7857x_1^3 + 5.91071x_1^2x_2 - 0.93631x_1x_2^2 + 0.0363095x_2^3 \end{bmatrix} + \begin{bmatrix} 1 \\ 0 \end{bmatrix} u \quad (5.1.19)$$

has the first-order spectra $\Sigma_1\{R^2\}=\{\mathbf{e}_1, \mathbf{e}_2\}$ and $\Lambda_1\{R\}=\{-10, -1\}$. Moreover, the process has first-order stabilizing spectra and the trivial solution is asymptotically stable. However, the control vector $\mathbf{b}=[1, 0]^t$ does not satisfy the necessary state controllability condition for the first-order term. But this is irrelevant if the existing local behavior is acceptable.

For the cubic term, the spectra are:

$$\Sigma_3\{C^2\} = \left\{ \begin{bmatrix} 1 \\ 0.711990\text{-i } 2.397235 \end{bmatrix}, \begin{bmatrix} 1 \\ 0.711990\text{+i } 2.397235 \end{bmatrix}, \begin{bmatrix} 1 \\ 51.903936 \end{bmatrix}, \begin{bmatrix} 0 \\ 1 \end{bmatrix} \right\}$$

and

$$\Lambda_3\{C\} = \{3.711990\text{-i } 2.397235\ ,\ 3.711990\text{+i } 2.397235\ ,\ 54.903936\ ,\ 0.036309\}\ .$$

The two eigenvectors are real and define unstable directions. Therefore, the process has 3-order destabilizing spectra. Furthermore, the process satisfies the 3-order necessary state controllability criteria and by Corollary 4.5.4 and Corollary 5.1.2 it can be globally stabilized. This is accomplished by assigning the new algebraic spectrum

$$\Lambda_3\{R\}^{\text{assigned}} = \{-1.0\ ,\ -0.2\ ,\ -0.75\ ,\ -0.5\}\ ,$$

to obtain the corresponding real geometric spectrum

$$\Sigma_3\{R^2\}^{\text{evaluated}} = \left\{ \begin{bmatrix} 1 \\ 10 \end{bmatrix}, \begin{bmatrix} 1 \\ 4 \end{bmatrix}, \begin{bmatrix} 1 \\ 15 \end{bmatrix}, \begin{bmatrix} 1 \\ 3 \end{bmatrix} \right\}\ .$$

With such an assignment compute the state feedback

$$u = g_3(\mathbf{x}) = -5.92857x_1^3 + 0.27024x_1^2x_2 - 0.173214x_1x_2^2 + 0.00654762x_2^3. \quad (5.1.20)$$

which produces the 3-order compensated process

$$\begin{bmatrix}\dot{x}_1\\ \dot{x}_2\end{bmatrix}=\begin{bmatrix}-10x_1 -2.92857x_1^3 +1.27024\, x_1^2x_2 -0.173214\, x_1\, x_2^2 +0.00654762\, x_2^3\\ -x_2 - 11.7857x_1^3 + 5.91071x_1^2x_2 - 0.93631x_1\, x_2^2 +0.0363095x_2^3\end{bmatrix}, \quad (5.1.21)$$

that is bounded and has the asymptotically stable trivial steady-state. In addition, one may intuitively expect that the process is globally asymptotically stable since each term individually generates a process that is. This, however, is not true because the spectral mix of the compensated process produces five steady-states

$$\left\{\mathbf{x}_{s1}=\begin{bmatrix}0\\0\end{bmatrix};\ \mathbf{x}_{s2}=\begin{bmatrix}-0.122896\\-6.84584\end{bmatrix};\ \mathbf{x}_{s3}=\begin{bmatrix}0.122896\\6.84584\end{bmatrix};\ \mathbf{x}_{s4}=\begin{bmatrix}-2.14378\\-38.8534\end{bmatrix};\ \mathbf{x}_{s5}=\begin{bmatrix}2.14378\\38.8534\end{bmatrix}\right\},$$

of which three are stable and two are unstable. They are illustrated in Figure 5.1.4. Thus, the stability here is in the sense of Lyapunov. On the other hand, if one redefines the state feedback as $u=g_3(\mathbf{x})^{new}=8x_1+g_3(\mathbf{x})$, the spectral character of individual terms remains the same. In this instance the compensated process has only the trivial steady-state, and is globally asymptotically stable.

5.2. EXOTHERMIC CSTR DYNAMICS

In Section 1.2. the nonlinear model describing dynamics of the first-order exothermic CSTR scheme was introduced. It was demonstrated how the model can be approximated by using a polynomial description, *i.e.*, Equation (1.2.6). The result was then applied to compare the phase portraits of the 3-order polynomial approximation to that of the original equations, Figures 1.2.3.a) and b). The conclusion reached was that the two process realizations had identical dynamic properties. Therefore, the question is what is the polynomial approximation that adequately captures a CSTR behavior? For the example discussed in Section 1.2, the 3-order approximation worked quite well. But, is this true for all process parameters B, Da, β and x_{2c}. This is examined next.

system: *linear form* $\dot{x}_1 = -10\,x_1$, $\dot{x}_2 = x_2$

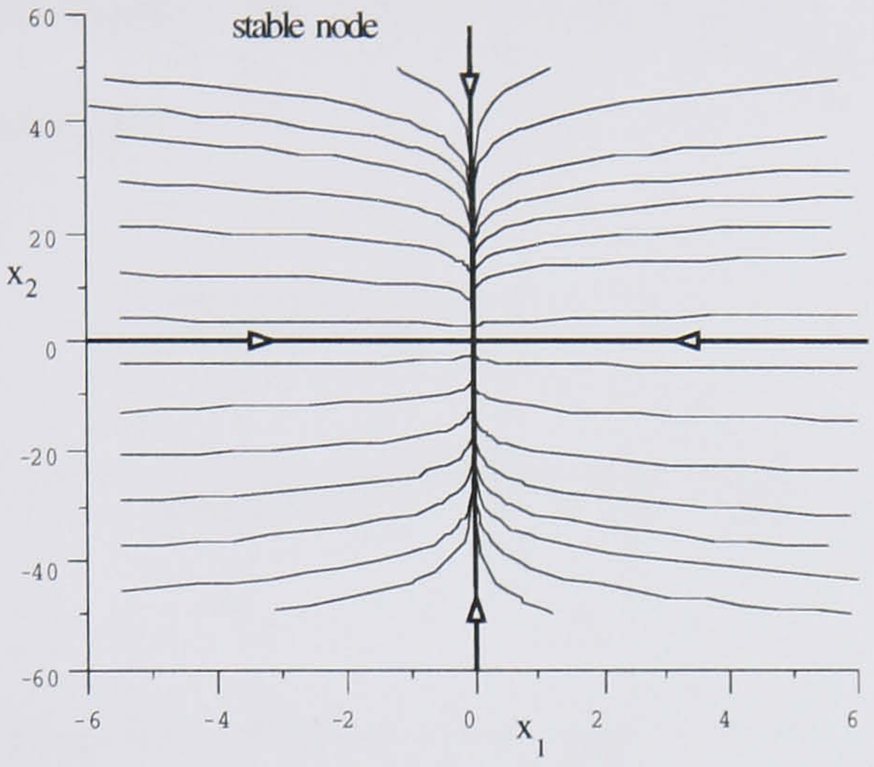

eigenspectra:

$$\mathbb{X}_1\{\mathbb{R}^2\} = \left\{ \mathbf{e}_1 = \begin{bmatrix} 1 \\ 0 \end{bmatrix},\ \mathbf{e}_2 = \begin{bmatrix} 0 \\ 1 \end{bmatrix} \right\}$$

$$\mathbb{\Lambda}_1\{\mathbb{R}\} = \{ -10\ ,\ -1 \}\ .$$

+

system: *cubic form*

$\dot{x}_1 = -2.92857x_1^3 + 1.27024x_1^2x_2 - 0.173214x_1x_2^2 + 0.006547x_2^3$

$\dot{x}_2 = -11.7857x_1^3 + 5.91071x_1^2x_2 - 0.93631x_1x_2^2 - 0.0363095x_2^3$

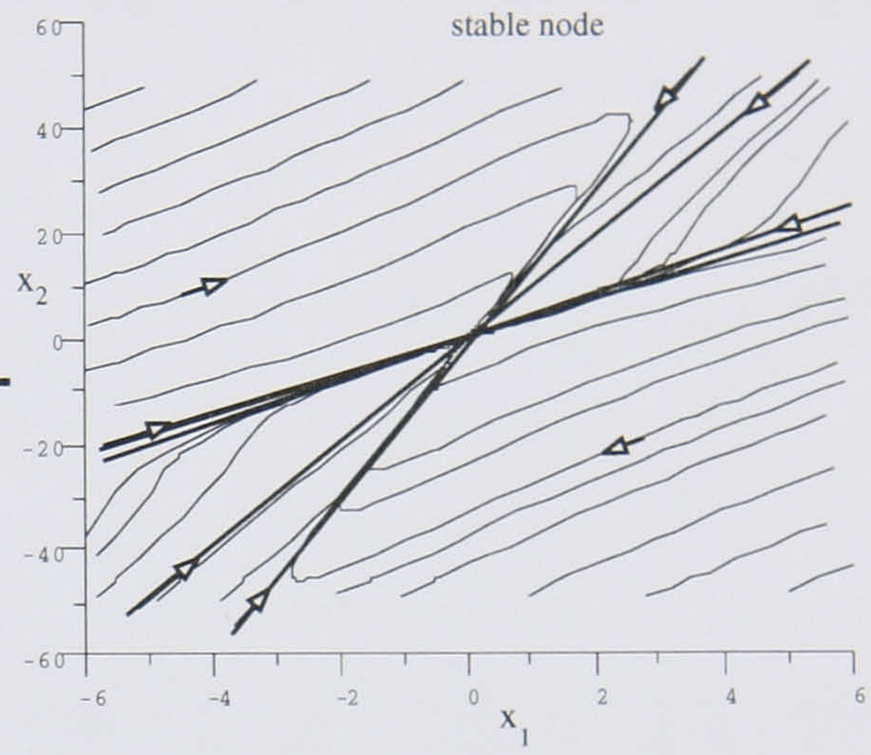

eigenspectra:

$$\mathbb{X}_3\{\mathbb{R}^2\} = \left\{ \begin{bmatrix} 1 \\ 10 \end{bmatrix},\ \begin{bmatrix} 1 \\ 4 \end{bmatrix},\ \begin{bmatrix} 1 \\ 15 \end{bmatrix},\ \begin{bmatrix} 1 \\ 3 \end{bmatrix} \right\}$$

$$\mathbb{\Lambda}_3\{\mathbb{R}\} = \{ -1.0\ ,\ -0.2\ ,\ -0.75\ ,\ -0.5 \}\ .$$

=

polynomial system:

$\dot{x}_1 = -10x_1 - 2.92857x_1^3 + 1.27024x_1^2x_2 - 0.173214x_1x_2^2 + 0.006547x_2^3$

$\dot{x}_2 = -x_2 - 11.7857x_1^3 + 5.91071x_1^2x_2 - 0.93631x_1x_2^2 - 0.0363095x_2^3$

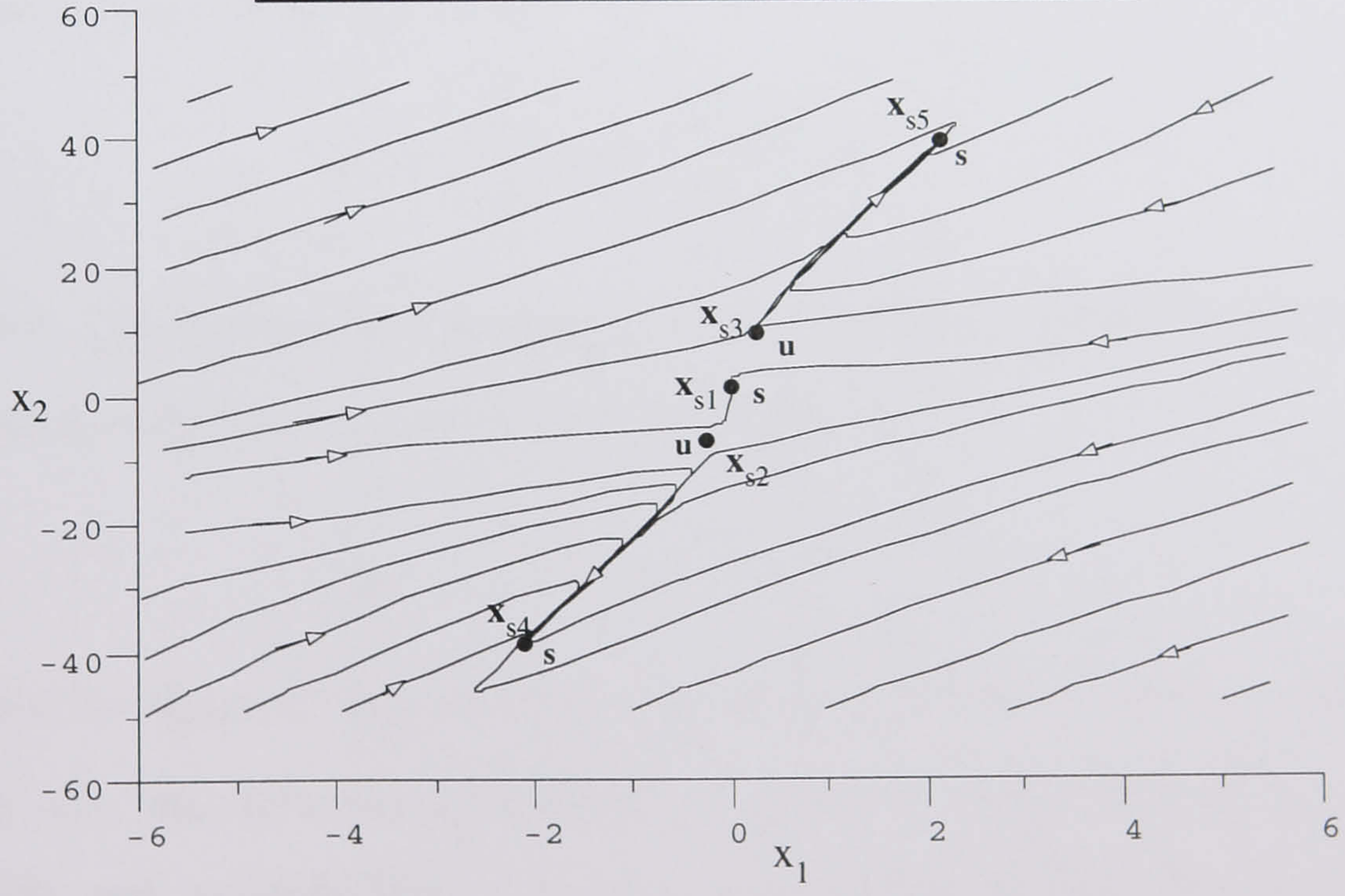

Multiple steady-states in the polynomial process in which all homogeneous terms are globally asymptotically stable.

FIGURE 5.1.4.

As demonstrated in Section 2.1 a power series expansion about a steady-state point produces the k-forms defined by Equation (1.2.6). Thus the first-order form, or the Jacobian, determines the k=1 eigenspectra, while for k>1 the eigenspectra are given by the sets

$$\chi_k\{R^2\} = \left\{ \begin{bmatrix} 1 \\ B \end{bmatrix} ; \begin{bmatrix} 1 \\ k/(1-x_{1s}) \end{bmatrix} ; \begin{bmatrix} 1 \\ 0 \end{bmatrix}_{(k-1)} : k \geq 2 \right\} \quad \text{and}$$

$$\Lambda_k\{R\} = \left\{ \frac{B^{k-1}x_{1s}}{k!}\left(B - \frac{k}{(1-x_{1s})}\right); \quad 0 \quad ; \; 0_{(k-1)} \; : \; k \geq 2 \right\}$$

which were derived in Example 2.2.1. Therefore, for k>1 there are always three distinct eigenmodes. Of the three, two are nilpotent and do not contribute significantly to the dynamic behavior. According to Corollary 5.1.1 the behavior in the directions defined by the two nilpotent invariants is influenced by the Jacobian dynamics.

The third spectral component, however, is idempotent and is responsible for the reaction complexity. The idempotent eigenmode is given by the eigenvector $\mathbf{v}=[1, B]^t$, and the corresponding eigenvalue

$$\lambda_k = \frac{B^{k-1}x_{1s}}{k!}\left(B - \frac{k}{(1 - x_{1s})}\right), \tag{5.2.1}$$

for k>1. Clearly the sign of λ_k depends on the dimensionless adiabatic temperature rise B, the steady-state value x_{1s}, and k. One can show that for all

$$B(1 - x_{1s}) < k < \infty \tag{5.2.2}$$

λ_k must be negative, implying that in the positive state-space each k-form is marginally stable, *i.e.*, the odd k-forms are marginally stable over the entire state-space. Thus when B=7.06 and x_{1s}=0.632312, λ_k is negative for all k>2.59 (integer value 2). Consequently, the CSTR process is bounded in the $\mathbf{v}=[1, 7.06]^t$ direction by the third- and higher-order power series terms. This nonlinear bound is also responsible for folding the trajectories in the positive space around the locally unstable steady-state. Hence, the final outcome of such behavior is the appearance of the stable limit cycle (see Figure 1.2.3). Therefore, for this particular choice of CSTR parameters the first three power

series terms adequately capture the entire CSTR behavior. By adding additional terms one only accomplishes a more accurate approximation and contributes insignificantly to the overall qualitative behavior.

Let us now consider the same CSTR process with a different set of parameters. We make the new process highly exothermic by allowing B=25.0 and Damköhler number Da=0.05, while keeping β=3.0 and x_{2c}=0.0. These parameters produce the three steady-states,

$$\mathbf{x}_{1s}=\begin{bmatrix} 0.0732365 \\ 0.457728 \end{bmatrix} ; \mathbf{x}_{2s}=\begin{bmatrix} 0.4420834 \\ 2.763021 \end{bmatrix} ; \mathbf{x}_{3s}=\begin{bmatrix} 0.9498191 \\ 5.936369 \end{bmatrix}.$$

with the Jacobian eigenspectra:

For $\mathbf{x}_{1s}$:
$$\begin{cases} X_1\{\mathbb{R}^2\} = \left\{\begin{bmatrix} 1 \\ -2.112079 \end{bmatrix}, \begin{bmatrix} 1 \\ -12.772 \end{bmatrix}\right\} \\ \Lambda_1\{\mathbb{R}\} = \{-1.2337 , -2.0144\} \end{cases}$$

For $\mathbf{x}_{2s}$:
$$\begin{cases} X_1\{\mathbb{R}^2\} = \left\{\begin{bmatrix} 1 \\ 17.43645 \end{bmatrix}, \begin{bmatrix} 1 \\ 2.56988 \end{bmatrix}\right\} \\ \Lambda_1\{\mathbb{R}\} = \{5.91598 , -0.65628\} \end{cases}$$

For $\mathbf{x}_{3s}$:
$$\begin{cases} X_1\{\mathbb{C}^2\} = \left\{\begin{bmatrix} 1 \\ 20.8847+i7.8757 \end{bmatrix}, \begin{bmatrix} 1 \\ 20.8847-i7.8757 \end{bmatrix}\right\} \\ \Lambda_1\{\mathbb{C}\} = \{-0.0912+i7.48049 , -0.0912-i7.48049\} \end{cases}.$$

The signs of the real eigenvalue parts show that the first and third steady-states are stable while the second is unstable. Thus, if we evaluate the power series expansion at the unstable steady-state $\mathbf{x}_{2s}$, then from Equation (5.2.2) it follows that λ_k is negative for all k>13. This implies that for the operating point chosen, the first three power series terms are now not sufficient to capture the complete CSTR dynamics, or that the process is now more complex. To illustrate this point we compute the phase portraits for ascending power series process approximations that begins with k=1. Thus, the first power series term is

the Jacobian $\mathbf{F}_1[\overleftrightarrow{\mathbf{x}}]$ defined in Equation (1.2.6) which also determines the first-order process approximation

$$\dot{\overleftrightarrow{\mathbf{x}}} = \mathbf{F}_1[\overleftrightarrow{\mathbf{x}}] \tag{5.2.3}$$

The trajectories for this approximation are illustrated in Figure 5.2.1, 1-order case. As illustrated, the unstable steady-state is at the origin and represents the translated process steady-state $\mathbf{x}_{2s}$. Consequently, we label the origin as $\overleftrightarrow{\mathbf{x}}_{2s}$. Observe how the saddle topology at $\overleftrightarrow{\mathbf{x}}_{2s}$ is supported by the stable and unstable invariants traversing across the state-space respectively from left to right and from top to bottom. Also, the state-space region outlined by the dashed lines corresponds to the original positive CSTR region of interest.

Next, by adding the quadratic term $\mathbf{F}_2[\overleftrightarrow{\mathbf{x}}]$ we obtain the approximation,

$$\dot{\overleftrightarrow{\mathbf{x}}} = \mathbf{F}_1[\overleftrightarrow{\mathbf{x}}] + \mathbf{F}_2[\overleftrightarrow{\mathbf{x}}] \,. \tag{5.2.4}$$

The phase portrait is given in Figure 5.2.1, 2-order case, and it illustrates the spectral blend of the first and second-order homogeneous invariants. The blending of the two k-forms has changed the stable invariant of the linear system into the stable manifold (SM), while the unstable invariant becomes the unstable manifold (UM). Furthermore, the additional steady-state $\overleftrightarrow{\mathbf{x}}_{1s}$ has been created along the UM path. The stable manifold also separates the state-space into two distinct regions: the unstable top, and the stable bottom regions. The unstable region results from both the linear and quadratic solutions being unstable above SM, while the stable region exists because the stable quadratic solutions bound the unstable linear solutions below SM. The splicing of the stable and unstable solutions is achieved at the steady-state $\overleftrightarrow{\mathbf{x}}_{1s}$, which represents the birth of the stable steady-state $\mathbf{x}_{1s}$.

As we increase the model approximation the state-space dynamics progressively approaches that of the original process. For example, for the 3-order approximation the stable dynamics at $\overleftrightarrow{\mathbf{x}}_{1s}$ changes from the nodal to focal, while for the 4-order case the steady-state $\overleftrightarrow{\mathbf{x}}_{1s}$ disappears and the new one, $\overleftrightarrow{\mathbf{x}}_{3s}$, is created. The new steady-state is the birth of the stable steady-state $\mathbf{x}_{3s}$. For the 5-order approximation both $\overleftrightarrow{\mathbf{x}}_{1s}$ and $\overleftrightarrow{\mathbf{x}}_{3s}$ are

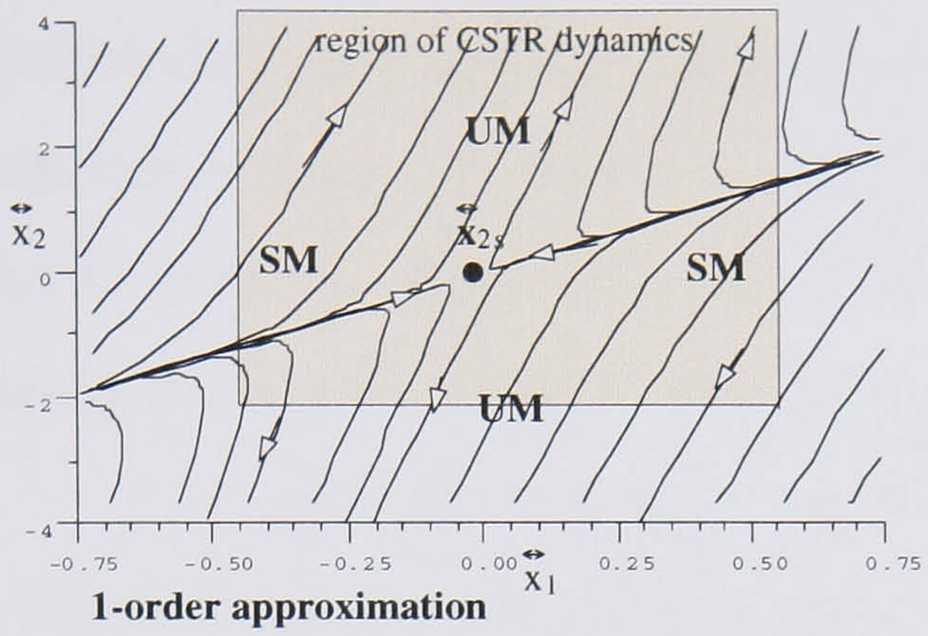

1-order approximation

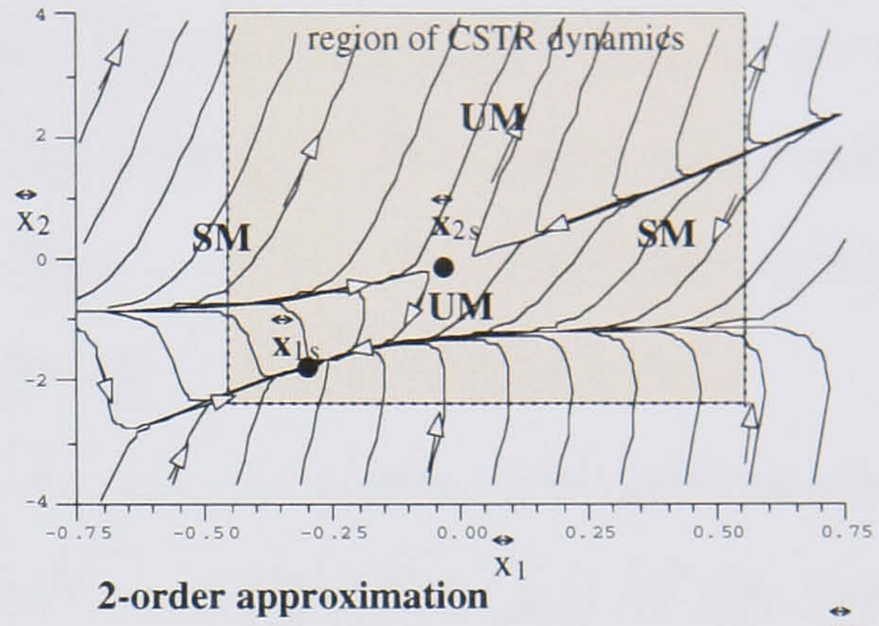

2-order approximation

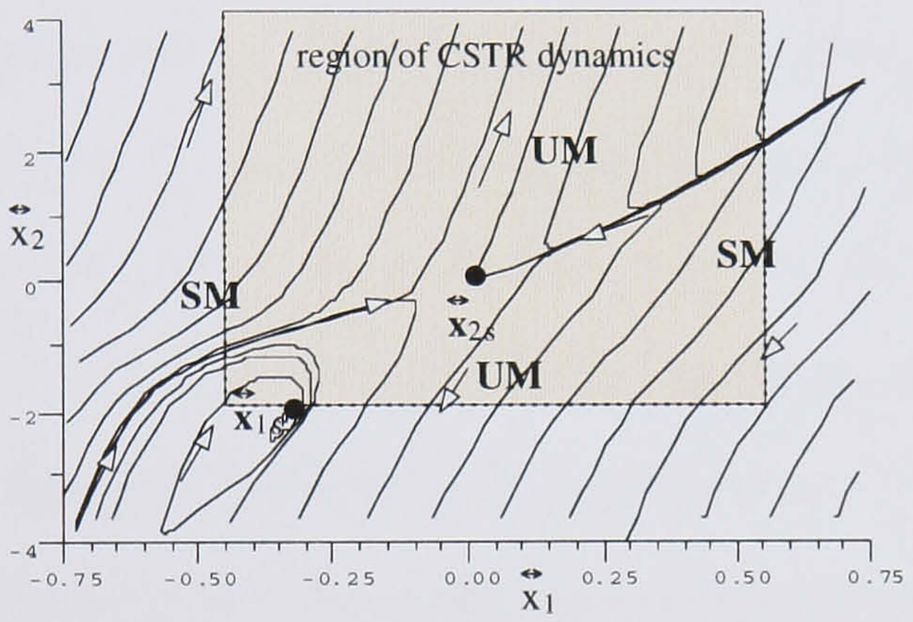

3-order approximation

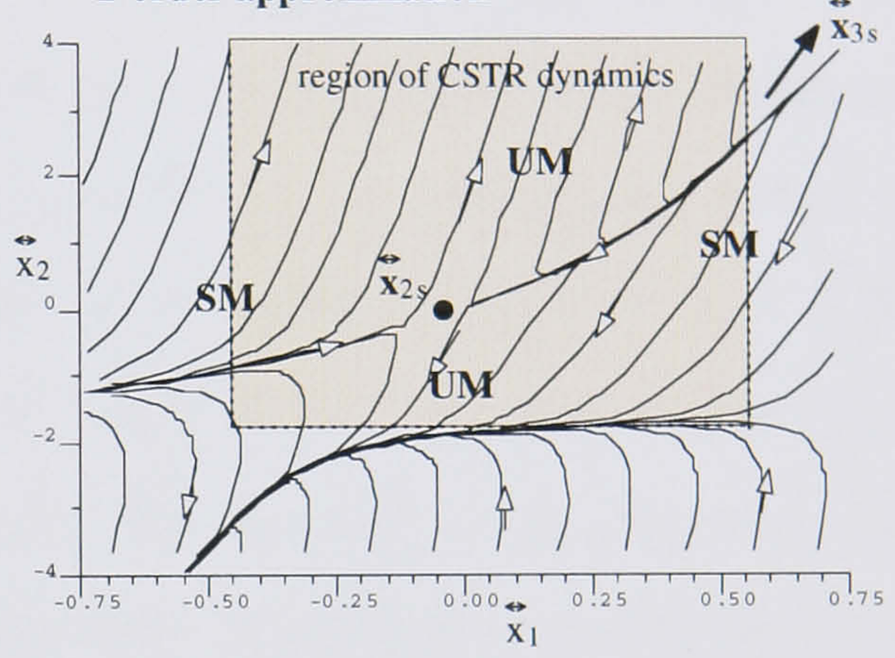

4-order approximation

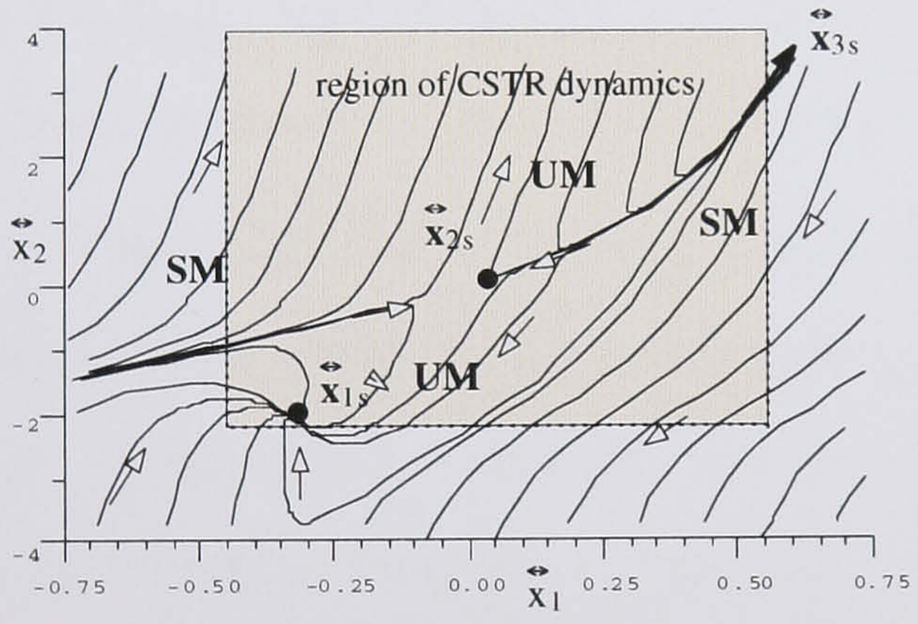

5-order approximation

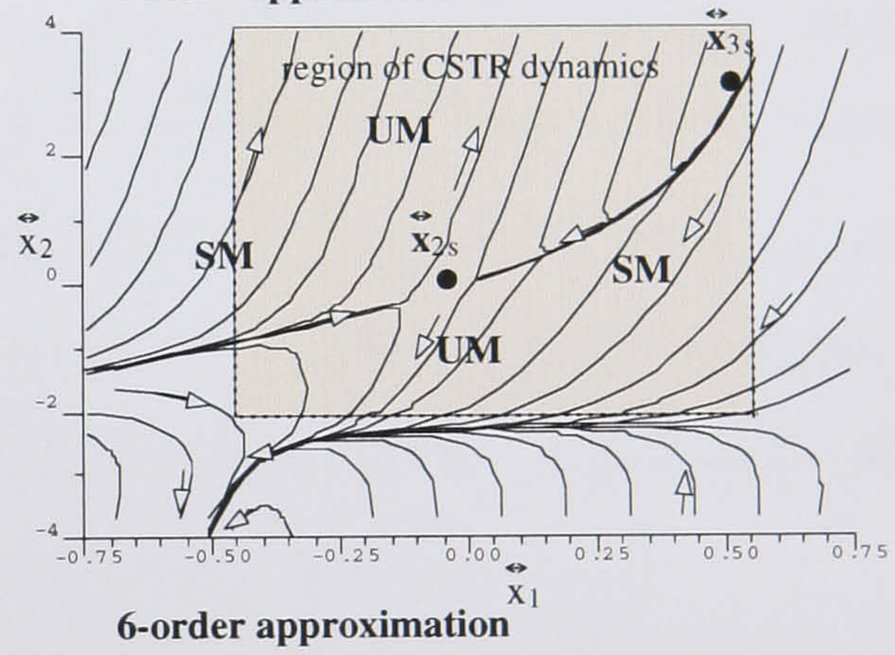

6-order approximation

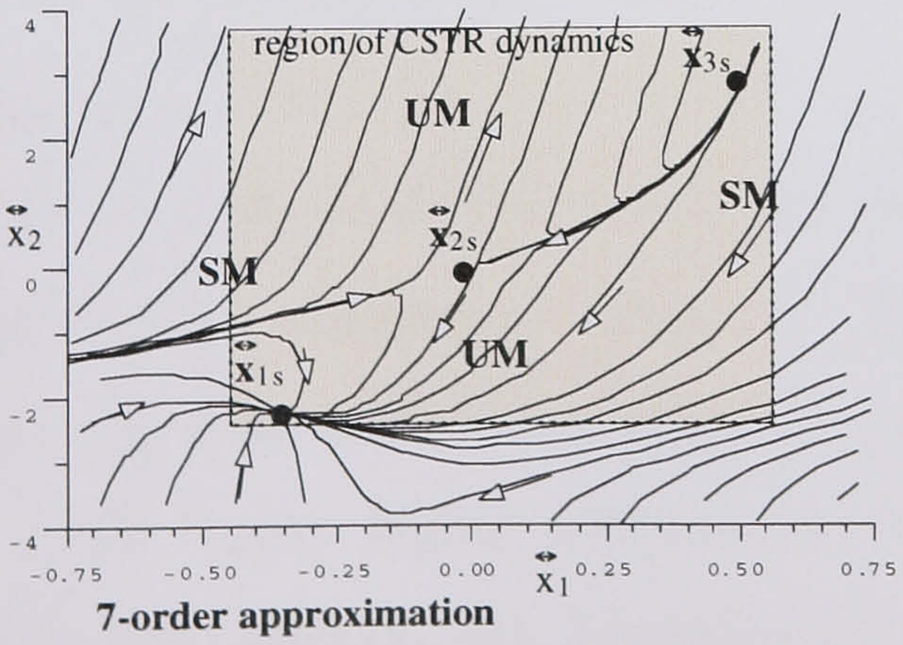

7-order approximation

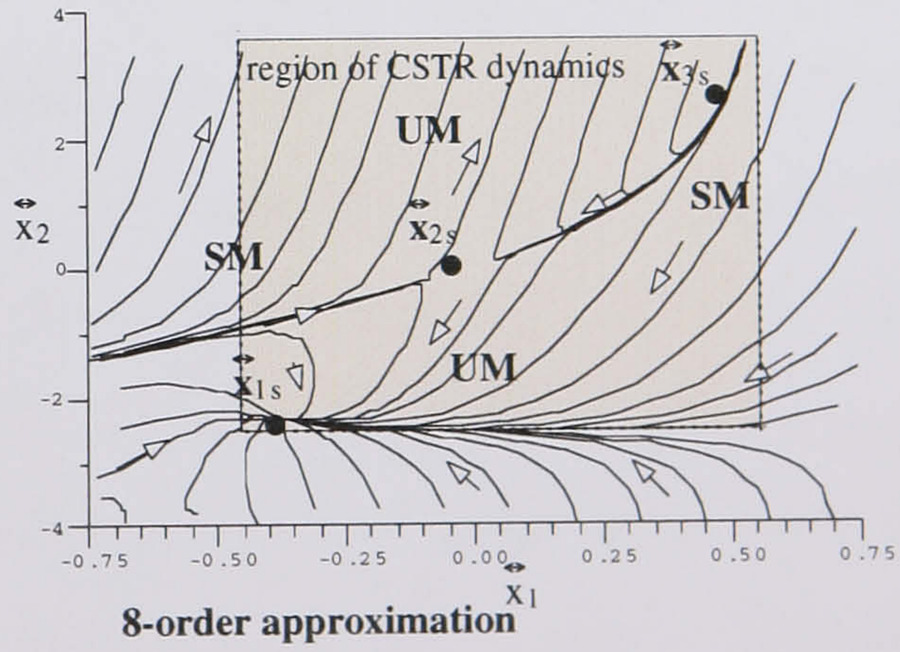

8-order approximation

State-space portraits of CSTR process approximations.

FIGURE 5.2.1.

present, while for the 6-order case the steady-state $\overleftrightarrow{\mathbf{x}}_{1s}$ once again disappears. However, for all model approximations of the orders seven or higher, both steady-states are present. Furthermore, the manifold anatomy of the 7-order approximation is computed in order to illustrate how the steady-states are created, Figure 5.2.2. The manifold equations, eigenfunctions, and the steady-states classifications are given in Appendix IV.

To complete the analysis we test the accuracy of the higher-order approximations. In Figure 5.2.3 the true process phase portrait is compared to that of the 9-order approximation. From the trajectories displayed it looks as if all of the CSTR features are captured by the 9-order approximation. However, the phase portraits are in this case deceiving since $\overleftrightarrow{\mathbf{x}}_{3s}$ is unstable and does not agree with the stable behavior of $\mathbf{x}_{3s}$. It turns out that not until the 12-order approximation is reached does the stable nature of $\overleftrightarrow{\mathbf{x}}_{3s}$ appear, see Table IV.1 in Appendix IV. Consequently the 12-order approximation is the minimal polynomial realization which captures the behavior of all three steady-states. The globally bounding CSTR behavior, however, is not yet captured. The reason is because λ_{12} remains positive, implying that in the $\mathbf{v}=[1, B]^t$ direction the approximating model is unbounded. This is in contradiction with the behavior of the original CSTR model which along the same direction is bounded since Equation (5.2.2) implies that all eigenvalues for $k>13$ are negative. Therefore, the first polynomial approximation which captures all dynamic features of the original model is of the degree 14.

These results show that the values for B and x_{1s} are critical for determining the degree of a polynomial approximation which adequately captures CSTR complexity and behavior. Clearly the more exothermic CSTR is, the higher is the required degree of the approximating polynomial. Moreover, from Equation (5.2.2) it follows that for CSTR processes with multiple steady-states, the steady-states with small conversion values ($x_{1s}<<1$) require higher polynomial approximations than the steady-states with high conversion values ($x_{1s}\approx 1$). For instance in the above example one requires $k>23$ in order to capture dynamics at $\overleftrightarrow{\mathbf{x}}_{1s}$, while for $\overleftrightarrow{\mathbf{x}}_{3s}$ the value is $k\geq 2$. In chemical and physical terms this implies that a CSTR operating at low conversions contains more unstable (*reactive*) nonlinear eigenmodes than at high conversions. Therefore, a CSTR operating at a low conversion is generally more excitable. As a result one would typically have to evaluate

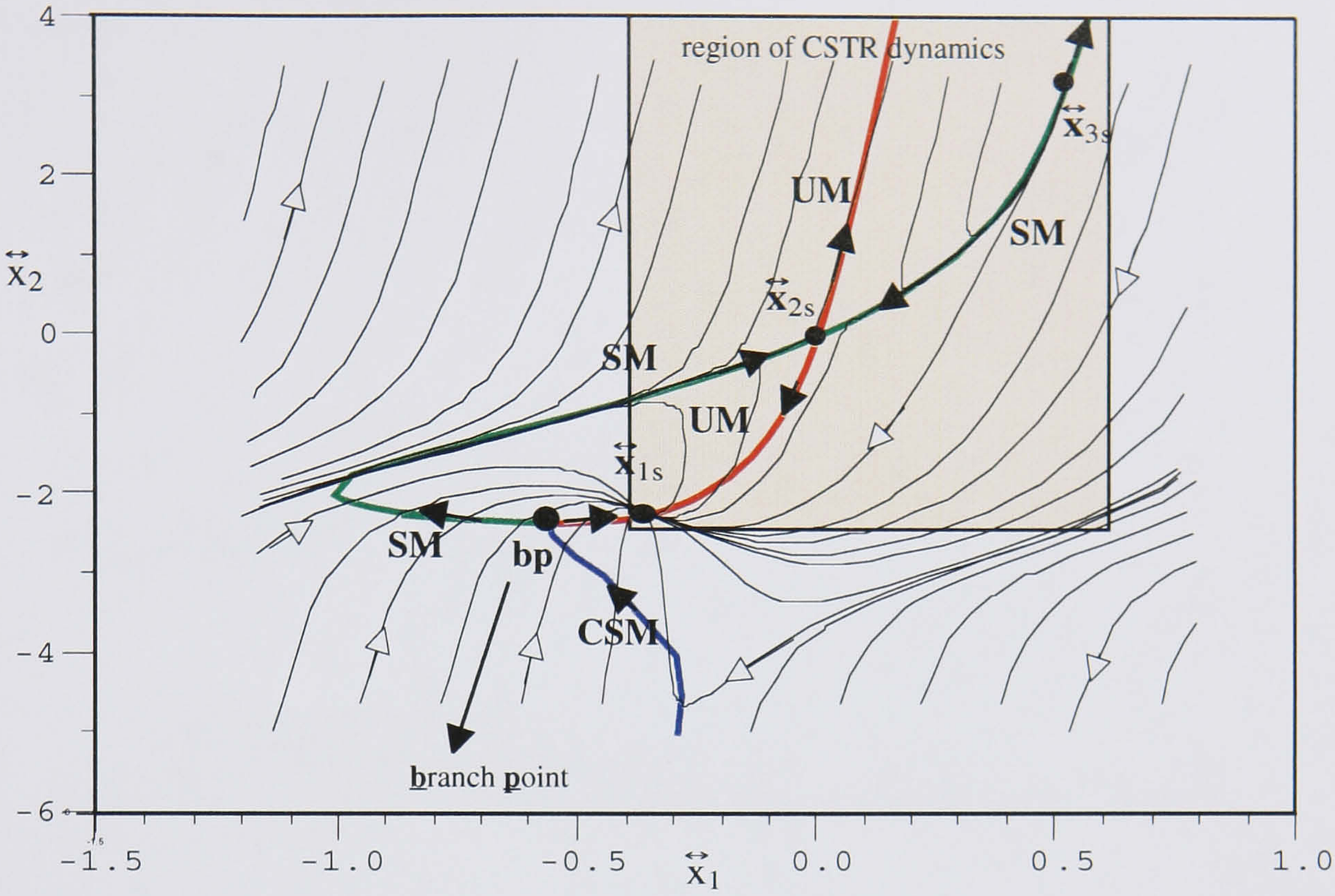

a) The manifilods in the 7-order approximation.

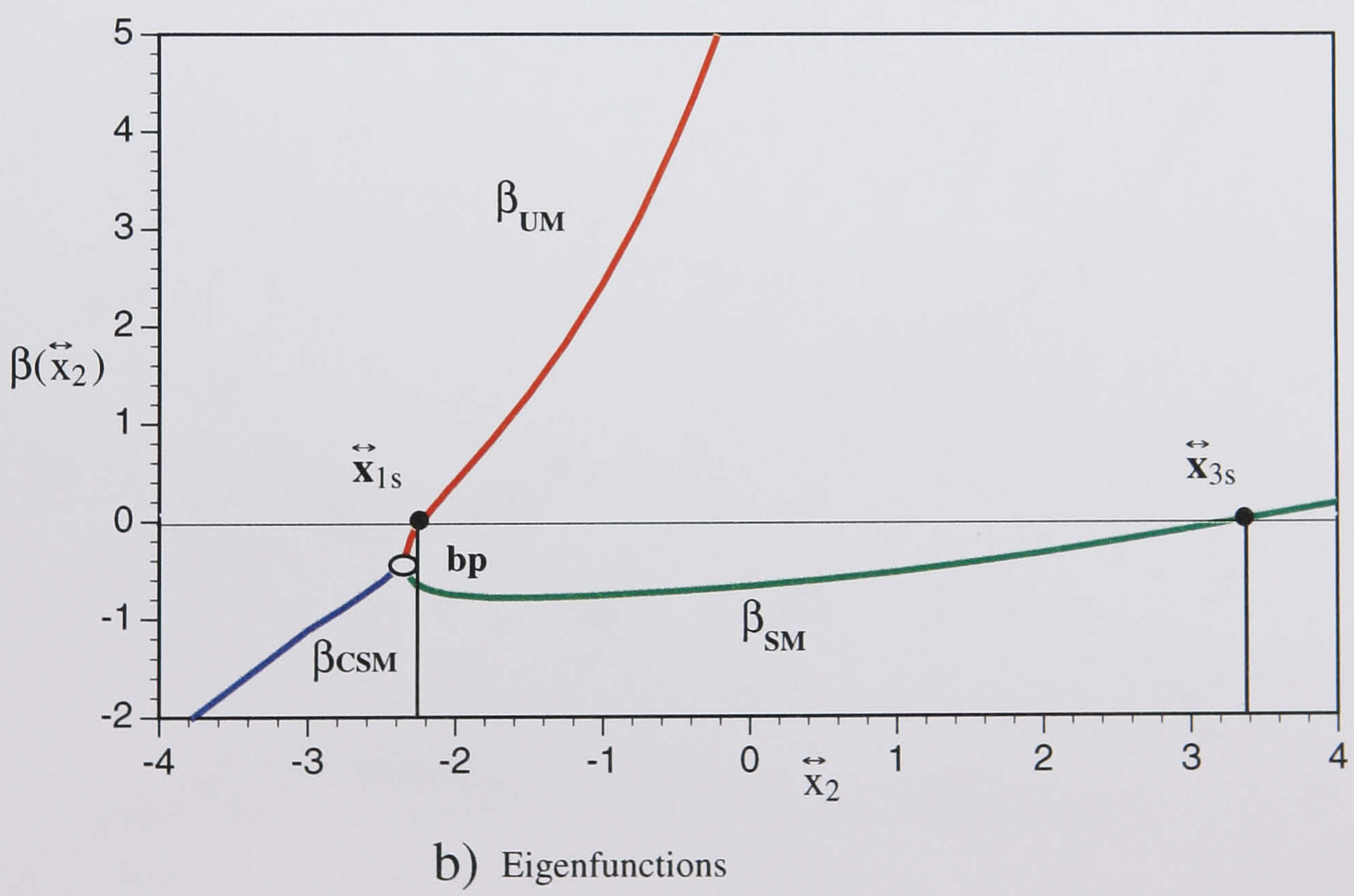

b) Eigenfunctions

The 7-order approximated CSTR spectra.

FIGURE 5.2.2.

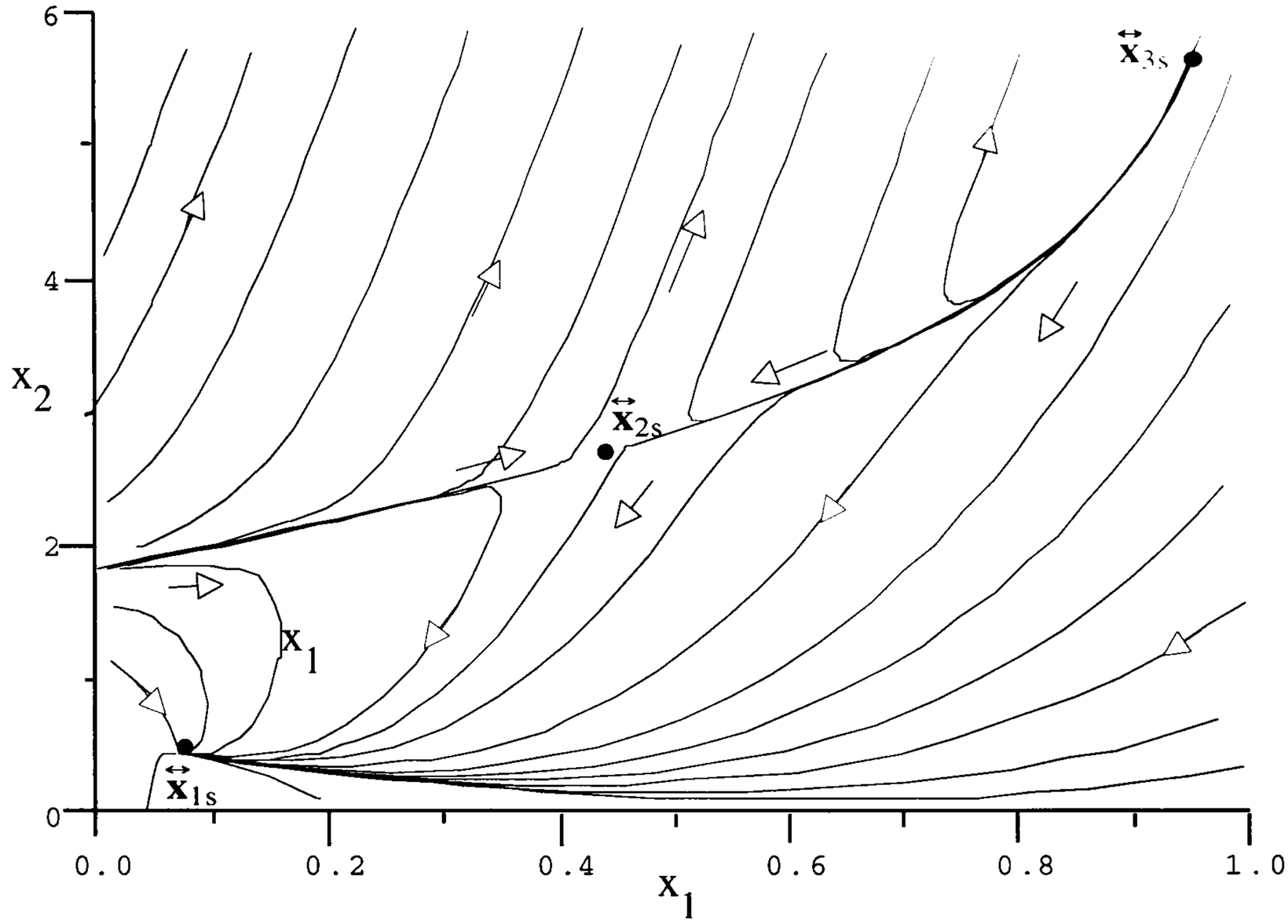

a) The 9-order power series approximation in the original CSTR coordinates.

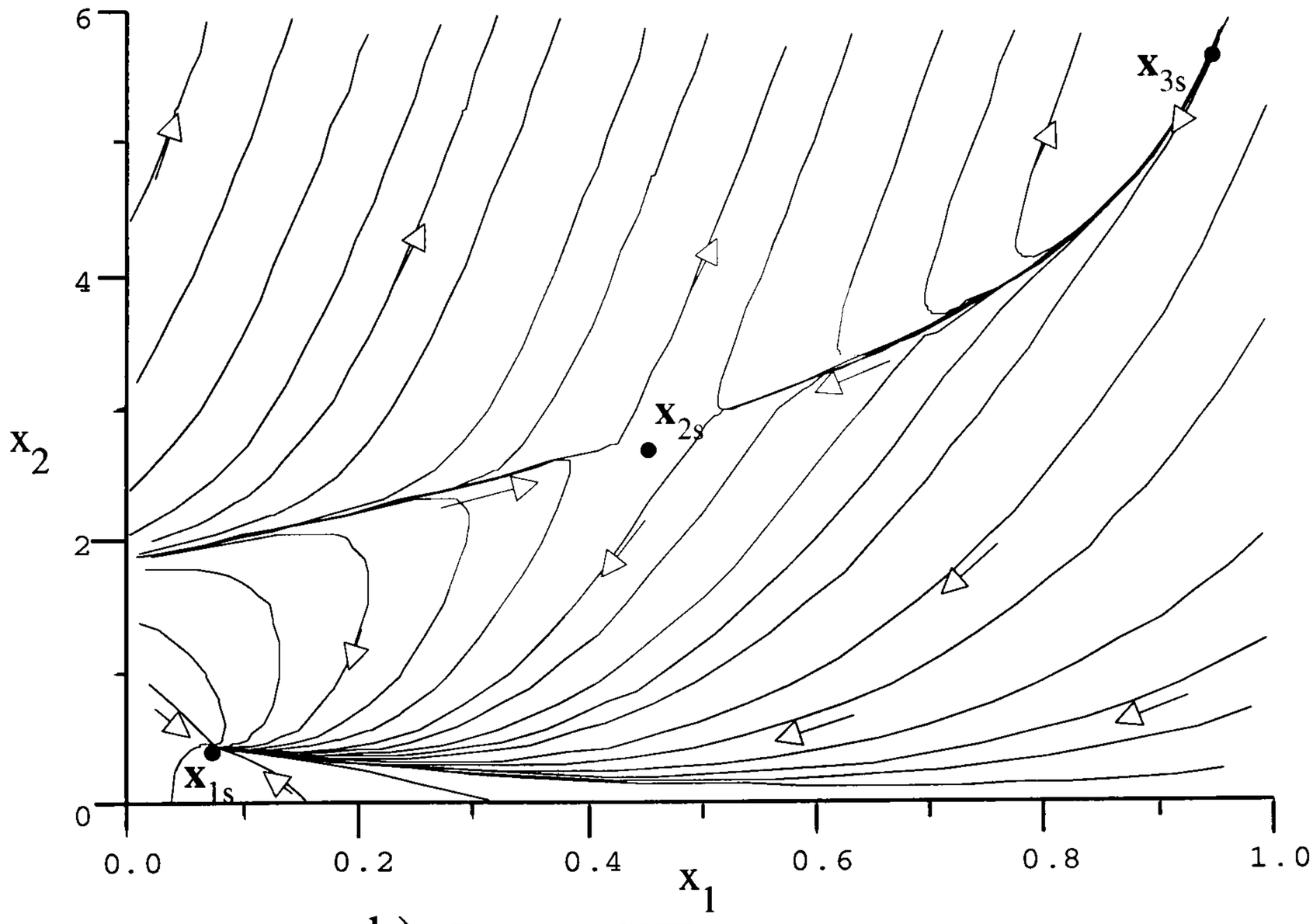

b) The exact CSTR equations.

Two CSTR representations.

FIGURE 5.2.3.

and analyze significantly more power series terms for process operations at lower conversions. However, for process operations with high conversions it is often enough to analyze first five power series terms.

5.3. GLOBAL CANCELONG OF PROCESS NONLINEARITIES

From the analysis presented it is evident that a CSTR model can be entirely characterized in terms of the k-form eigenspectra. It is also demonstrated that CSTR complexity and behavior depends on nonlinear idempotent eigenmodes while the nilpotent eigenmodes are of little dynamic significance. This is illustrated in Figure 5.2.1 in which the stable manifold direction is principally supported by the Jacobian stable eigenmode. In contrast, the unstable manifold direction is given by the unstable linear eigenmode as well as the higher-order unstable eigen solutions.

To appreciate further the significance of the idempotent eigenmodes we consider the following scalar function

$$g(\mathbf{x}) = -BDa\,(1-x_1)\,Exp\{x_2\} - \beta x_{2c} + (1+\beta)\,x_{2s} + Bx_{1s}\left((x_2-x_{2s}) - \frac{x_1-x_{1s}}{1-x_{1s}}\right) \qquad (5.3.1)$$

in which x_{1s} and x_{2s} refere to the steady-state coordinates. Next, by adding $g(\mathbf{x})$ to the normalized energy balance equation in Equation (1.2.4) we have

$$\begin{aligned} \frac{dx_1}{dt} &= -x_1 + Da\,(1-x_1)\,Exp\{x_2\} \\ \frac{dx_2}{dt} &= -\,Bx_{1s}\,\frac{x_1-x_{1s}}{1-x_{1s}} + (Bx_{1s}-1-\beta)(x_2-x_{2s})\,, \end{aligned} \qquad (5.3.2)$$

implying that the second equation is linearized. As before, we evaluate the power series expansion in terms of the translated coordinates to obtain

$$\dot{\overleftrightarrow{\mathbf{x}}} = \mathbf{F}[\overleftrightarrow{\mathbf{x}}+\mathbf{x}_s] = \sum_{k=1}^{\infty} \mathbf{F}_k[\overleftrightarrow{\mathbf{x}}] \qquad (5.3.3)$$

where now each

$$\mathbf{F}_k[\overleftrightarrow{\mathbf{x}}] = \frac{1}{k!}\left.\frac{\partial^k \mathbf{F}[\mathbf{x}]}{\partial \mathbf{x}^k}\right|_{\mathbf{x}=\mathbf{x}_s} \overleftrightarrow{\mathbf{x}}\, o\, (k)$$

$$= \begin{cases} \begin{bmatrix} \dfrac{-1}{1-x_{1s}} & x_{1s} \\ \dfrac{-Bx_{1s}}{1-x_{1s}} & \left(Bx_{1s}-1-\beta\right) \end{bmatrix} \begin{bmatrix} \overleftrightarrow{x}_1 \\ \\ \overleftrightarrow{x}_2 \end{bmatrix} & ; \quad \text{for } k=1 \\ \\ \left(\dfrac{-x_{1s}}{(k-1)!\,(1-x_{1s})}\, \overleftrightarrow{x}_1\, \overleftrightarrow{x}_2^{\,k-1} + \dfrac{x_{1s}}{k!}\overleftrightarrow{x}_2^{\,k}\right)\begin{bmatrix} 1 \\ 0 \end{bmatrix} & ; \quad \text{for } k>1 \ . \end{cases}$$

Therefore the Jacobian remains the same as in Equation (1.2.6), while the higher-order terms have changed since the second vector component is now 0. Consequently, the new k-form spectra are

$$\Sigma_k\{R^2\} = \left\{ \begin{bmatrix} 1 \\ k/(1-x_{1s}) \end{bmatrix} \ ; \ \begin{bmatrix} 1 \\ 0 \end{bmatrix}_{(k)} \ : \ k\geq 2 \right\} \quad \text{and}$$

$$\Lambda_k\{R\} = \{ \quad 0 \quad ; \quad 0_{(k)} \ : \ k\geq 2 \} \ ,$$

which implies that all eigenmodes are nilpotent. Thus, according to Corollary 5.1.1 the Jacobian spectra determines the entire process behavior. This is illustrated in Figure 5.3.1 in which the phase portrait of the original CSTR model and that of the CSTR version given in Equation (5.3.2) are compared. The parameter values for the simulations are B=25.0, Da=0.05, β=3, x_{2c}=0, and $\mathbf{x}_{2s}$=[0.4420834, 2.763021]^t. As can be seen, in the modified CSTR case the two stable steady-states have disappeared and the first-order hyperbolic nature of the steady-state $\mathbf{x}_{2s}$ is now present globally. For this reason the function g(**x**) is said to have *globally canceled* the CSTR process nonlinearities. Observe further that this function annihilates all idempotent spectral solutions. Thus, the resulting CSTR process must now be globally unstable.

We conclude by commenting on the parabolic curvature present in the phase portraits. As was noted earlier this curvature is responsible for the internal positive feedback which makes a CSTR excitable. Therefore, it is reasonable to expect that the

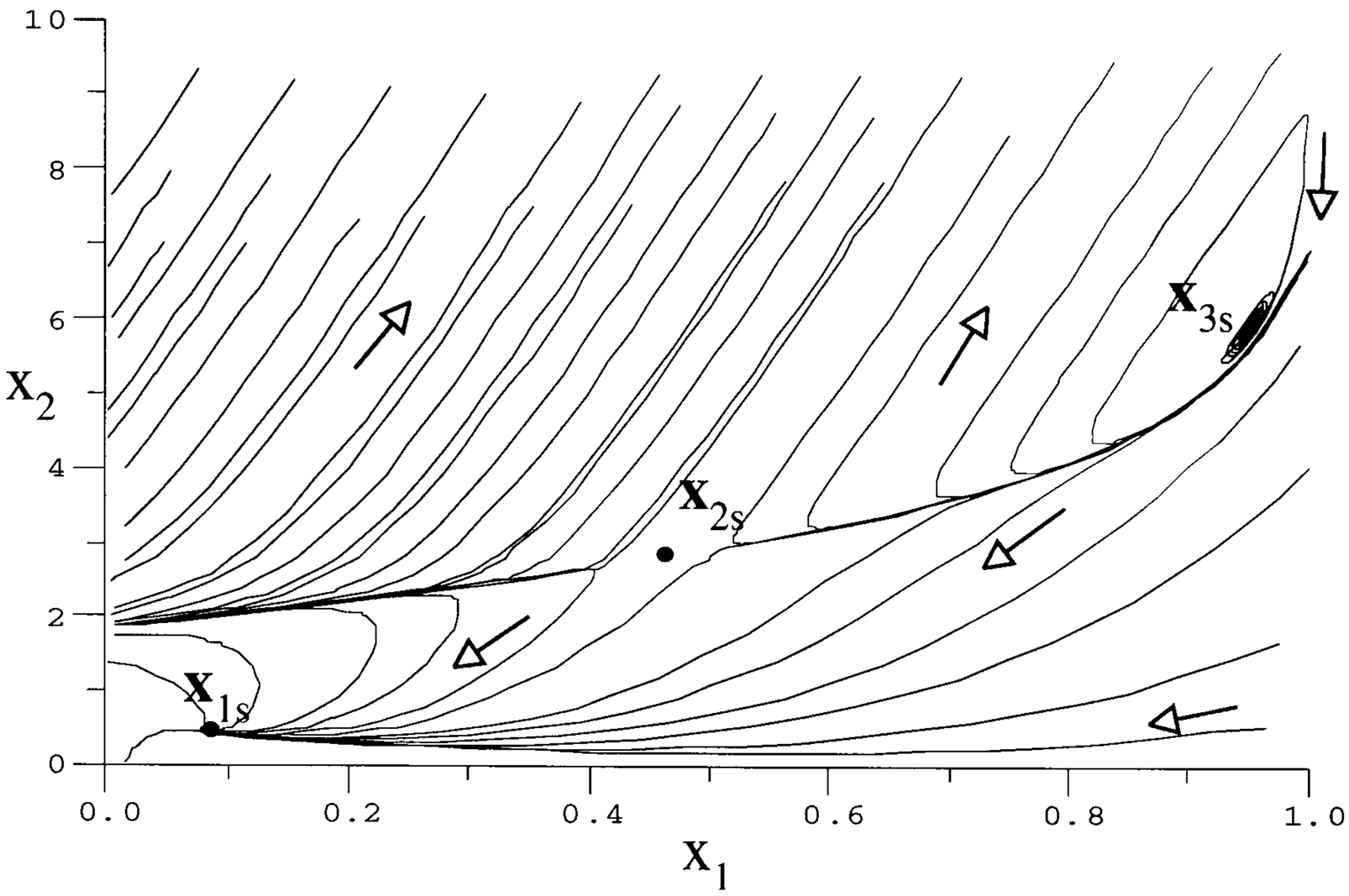

a) The behavior of the exact CSTR process model.

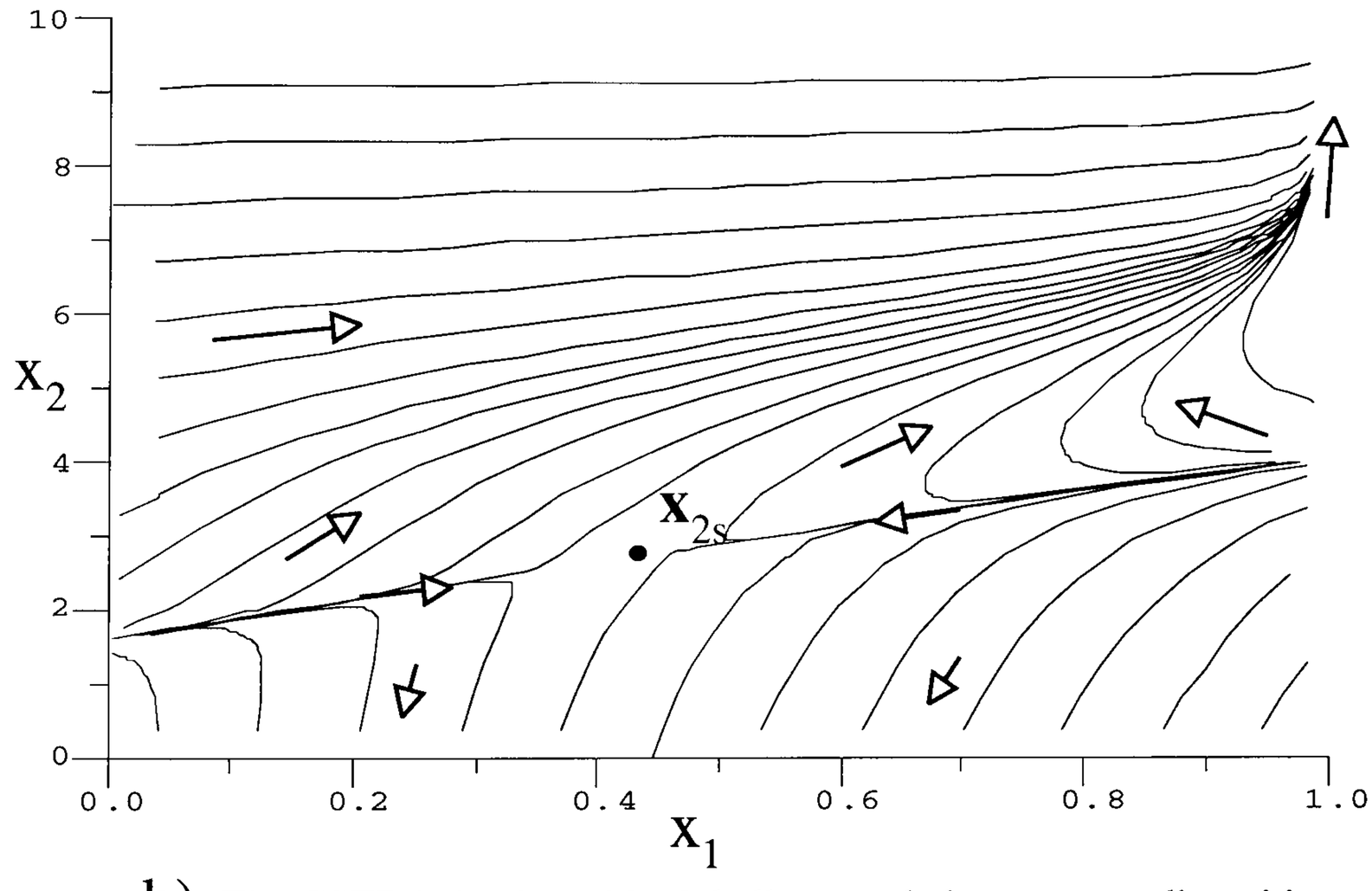

b) The CSTR behavior with globally canceled process nonlinearities.

Global cancaling of CSTR nonlinearities.

FIGURE 5.3.1.

more exothermic a reaction is, the larger are the parabolic excursions, and the more excitable a CSTR becomes. This can be verified by comparing Figures 1.2.3.a and 5.3.1.a. Moreover, since the CSTR eigenspectra have no complex higher-order eigen solutions, the curvature results from the spectral blend of the reactive low-order unstable and the high-order stable real eigenmodes.

5.4. APPLICATIONS

At this point it is possible to argue that both the nonlinear framework and the CSTR process analyzed are rather abstract, and that connections between the theory and the processes of industrial interest are still not clear. In addition, there is the question as to how the results presented for the two-dimensional CSTR model approximation can be used in the higher-dimensional cases. These concerns are now addressed by examining the dynamics of the three industrial CSTR models. The first two describe typical vinyl polymerizations, namely polymethylmethacrylate (PMMA) and polystyrene (PS) with initiator azoisobutyronitrile (AIBN). The third model, however, is a second-order CSTR scheme in which cyclopentenol is obtained from cyclopentadiene by acid-catalyzed electrophilic addition of water in dilute solution.

PMMA & PS Models:

The reaction equations for the two vinyl polymerization processes are derived by using the first-order kinetics assumptions and are described by the following three-dimensional nonlinear ODE,

$$\begin{bmatrix} \dot{x}_1 \\ \dot{x}_2 \\ \dot{x}_3 \end{bmatrix} = \mathbf{F}[\mathbf{x}] = \begin{bmatrix} 1\text{-}x_1\text{-}Da_p w\, x_1 Exp\left\{\dfrac{x_2}{1+x_2/\gamma_p}\right\} \\ -x_2+BDa_p w\, x_1 Exp\left\{\dfrac{x_2}{1+x_2/\gamma_p}\right\} - \beta(x_2-x_{2c}) \\ x_{3f}\text{-}x_3\text{-}Da_d x_3 Exp\left\{\dfrac{\gamma_d x_2}{1+x_2/\gamma_p}\right\} \end{bmatrix} \qquad (5.4.1)$$

where

$$w = \left(\frac{2fDa_d x_3}{Da_t G}\right)^{1/2} Exp\left\{\frac{x_2(\gamma_d-\gamma_t)}{2(1+x_2/\gamma_p)}\right\}$$

is dimensionless growing radical concentration, and x_1, x_2 and x_3 are respectively dimensionless monomer concentration, dimensionless temperature rise and dimensionless initiator concentration (Jaisinghani and Ray 1977). For definitions of all other parameters and their simulation values consult the original contribution and Table 5.4.1. Note that by assuming that initiator concentration in the reactor is nearly constant over a wide range of conversions, it is possible to eliminate the third equation in Equation (5.4.1). In this case the resulting models are two-dimensional and as such are similar to the previous exothermic CSTR example. The steady-state solutions for both the two and three-dimensional model realizations are presented in Table 5.4.1. For the parameters selected, both processes have three steady-states: two are stable and one unstable. Furthermore, since the polymer conversion $\hat{x}$ is related to the dimensionless monomer concentration as

$$\hat{x} = 1 - x_1 \qquad (5.4.2)$$

then the steady-states defined by the stable high conversion points $\mathbf{x}_{3s}$ are desirable for production. Unfortunately, from a practical point of view these steady-states may not always be accessible. The operating point $\mathbf{x}_{3s}$ may exhibit either a prohibitively high operating temperature, or due to a high conversion rate the fluid may become overly viscous for product extraction. Therefore, the next best solution is quite often the unstable $\mathbf{x}_{2s}$ steady-state, since the stable $\mathbf{x}_{1s}$ steady-state has a low conversion. In any event, the

Table 5.4.1: Vinyl polymerization process parameters

PS data

PS gel effect:

$$\ln G(x_1,T) = \ln\left(\frac{k_t}{k_{to}}\right) = \begin{cases} D_1+D_2x_1+D_3x_1^2+D_4x_1^3+ \\ (D_5+D_6x_1+D_7x_1^2+D_8x_1^3)T \end{cases}$$

where $T=T_f(1+x_2/\gamma_p)$ is absolute temperature, G is change in termination rate constant due to viscosity, k^* is pre-exponential rate constant and

D_1=-30.48225 , D_2=62.34226 , D_3=-38.48330
D_4=66.1756x10^{-1} , D_5=30.00541x10^{-3} , D_6=-35.37124x10^{-3}
D_7=-8.93976x10^{-3} , D_8=14.30559x10^{-3}

simulation parameters:

dimensionless heat generation parameterr : B=12.0 ; initiation efficiency: f=0.5 ; feed temperature : T_f=295^{O}K

dimensionless heat removal : β=6.0 ; initiator feed : x_{3f}=0.05

dimensionless coolant temeperature : x_{2c}=0

Damköhler numbers:
Da_p=2.58633x10^5 , Da_d=1.1632x10^{-5} , Da_t=3.00312x10^{11}

dimensionless activation energies:
γ_p=12.0432 , γ_d=4.36261 , γ_t=0.23796

steady-states:

two-dimensional realization

$$\mathbf{x}_{1s}=\begin{bmatrix}0.999877\\0.00021\end{bmatrix}\ (\text{stable node});\quad \mathbf{x}_{2s}=\begin{bmatrix}0.160821\\1.438591\end{bmatrix}\ (\text{unstable node});\quad \mathbf{x}_{3s}=\begin{bmatrix}0.003419\\1.708424\end{bmatrix}\ (\text{stable node})$$

three-dimensional realization

$$\mathbf{x}_{1s}=\begin{bmatrix}0.999638\\0.000619\\0.049999\end{bmatrix}\ (\text{stable node});\quad \mathbf{x}_{2s}=\begin{bmatrix}0.231537\\1.317364\\0.049896\end{bmatrix}\ (\text{unstable node});\quad \mathbf{x}_{3s}=\begin{bmatrix}0.001094\\1.712408\\0.0496\end{bmatrix}\ (\text{stable node})$$

PMMA data

PMMA gel effect:

$$\ln G(x_1,T) = \ln\left(\frac{k_t}{k_{to}}\right) = \begin{cases} C_1+C_2/T+C_3x_1/T+C_4x_1^2/T+ \\ C_5T^2+C_6x_1T^2 \end{cases}$$

where $T=T_f(1+x_2/\gamma_p)$ is absolute temperature, G is change in termination rate constant due to viscosity, k^* is pre-exponential rate constant and

C_1=51.55494x10^{-3} ; C_2=-77.63652x10^2 ; C_3=82.87584x10^2
C_4=-52.39329x10 ; C_5=10.53524x10^{-5} ; C_6=-10.53524x10^{-5}

simulation parameters:

dimensionless heat generation parameterr : B=12.0 ; initiation efficiency : f=0.8 ; feed temperature : T_f=295^{O}K

dimensionless heat removal : β=6.0 ; initiator feed : x_{3f}=0.05

dimensionless coolant temeperature : x_{2c}=0

Damköhler numbers:
Da_p=6.25506x10^5 ; Da_d=1.1632x10^{-5} ; Da_t=3.74703x10^{10}

dimensionless activation energies:
γ_p=10.7468 ; γ_d=4.89 ; γ_t=0.444

steady-states:

two-dimensional realization

$$\mathbf{x}_{1s}=\begin{bmatrix}0.999105\\0.001533\end{bmatrix}\ (\text{stable node});\quad \mathbf{x}_{2s}=\begin{bmatrix}0.223416\\1.331286\end{bmatrix}\ (\text{unstable node});\quad \mathbf{x}_{3s}=\begin{bmatrix}0.097116\\1.547799\end{bmatrix}\ (\text{stable focus})$$

three-dimensional realization

$$\mathbf{x}_{1s}=\begin{bmatrix}0.996842\\0.005412\\0.049999\end{bmatrix}\ (\text{stable node});\quad \mathbf{x}_{2s}=\begin{bmatrix}0.496018\\0.863968\\0.049971\end{bmatrix}\ (\text{unstable node});\quad \mathbf{x}_{3s}=\begin{bmatrix}0.017549\\1.6842\\0.049292\end{bmatrix}\ (\text{stable node})$$

---

* subscripts p, d and t designate respectively propagation, dissociation and termination components

steady-state structure for both polymerization processes is identical to the exothermic CSTR example considered in the previous sections. This is illustrated in Figures 5.4.1 and 5.4.2 in which the reaction dynamics describing respectively the two-dimensional PS and PMMA model realizations are depicted. We now analyze these dynamics by using the theory presented.

As before, we start by deriving the power series expansion at the unstable steady-state $\mathbf{x}_{2s}$. However, because the ODE model descriptions are now quite elaborate one can only numerically evaluate the power series terms. In Appendix V the power series approximations for the two and three-dimensional model realizations are presented in Tables A.V.1-4. For the two-dimensional case the approximation is of the order 5, while for the three-dimensional case 3-order is considered. The same tables also list the numerically evaluated k-form terms and their eigenspectra. These are now examined.

By inspecting the eigen-solutions for the two-dimensional model approximations in Tables A.V.1 and A.V.3, it is evident that the first-order eigenspectra are unstable. This is consistent with the fact that the power series is evaluated about the unstable steady-state $\mathbf{x}_{2s}$. The next spectral component is quadratic, which in both instances contains a rather significant idempotent eigenmode. By contrast, the 3-order eigenspectra shows that the cubic term is unstable in the PS case while it is marginally stable in the PMMA case. In addition, since in the PS case the cubic unstable direction has a large positive eigenvalue (6973.49), this suggests that it is more reactive. One can substantiet this further by examining the shapes of the parabolic trajectories attracted by the stable steady-state $\mathbf{x}_{3s}$. In the PS case, these trajectories have a much larger temperature deviation. From Table A.V.1 one can also see that in the PS case the 7-order eigenspectra has a strong stabilizing eigenmode, while the 5-order eigenspectrum is unstable. In contrast, for the PMMA process, Table A.V.3 shows a reverse in behavior characterizing the 5 and 7-order idempotent eigenmodes. In addition, the PMMA unstable eigenmodes are weaker, *i.e.*, the eigenvalue magnitudes are not as large as in the PS case. Nevertheless, for k>>7 all terms must eventually become stable in the positive state-space, *i.e.*, all eigenvalues must

become ≤0. This is also evident from Figures 5.4.1 and 5.4.2 because the trajectories are bounded.

The two-dimensional analysis shows that the PS process is significantly more reactive. This is evident during numerical computations because the PS equations are numerically more stiff. The stiff behavior can also be attributed to the magnitude of the activation energy values used in the vinyl models. One can verify from Table 5.4.1 that the dimensionless propagation activation energy for PS is larger than that for the PMMA process, which confirms our reactivity observation. The results also indicate that the stable manifold direction is determined by the stable first-order eigenvector, while the unstable manifold is in direction of the higher-order idempotent eigenvector $[1, B(=-12)]^t$. Therefore, the manifold structure is identical to that described earlier for the exothermic CSTR case. Observe, however, that in the latter case the idempotent eigenvector must be $[1, -B]^t$ since concentration variable has been replaced by the conversion variable, *i.e.*, Figures 5.4.1 and 5.4.2 are flipped from left to right when the conversion variable $\widehat{\mathbf{x}}$ is prescribed to the horizontal axis. Finally, note that the stable or unstable nature of power series terms is no longer predictable as in the exothermic CSTR case. The stabilizing trend of terms of order k>>7 remains the same but the spectral structure of the lower-order terms has now been scrambled by the growing dimensionless radical concentration which incorporates the gel and initiator effects. The inclusion of these effects gives rise to a less predictable eigenspectra structure.

When the initiator value is no longer constant, the third ODE in Equation (5.4.1) must be considered. For this case the k-forms and their spectra are given in Tables A.V.2 and A.V.4. The inspection of the spectra shows that again the first-order terms are unstable and that eigenvalues have about the same magnitudes as in the two-dimensional case. The quadratic and cubic spectra, however, indicate that the initiator dynamics have a destabilizing effect since most idempotent eigenmodes are unstable in the B direction, which also determines the second eigenvector component. If this eigenvector component is different from B, the eigenvector is nilpotent. Therefore, the initiator dynamics tends to

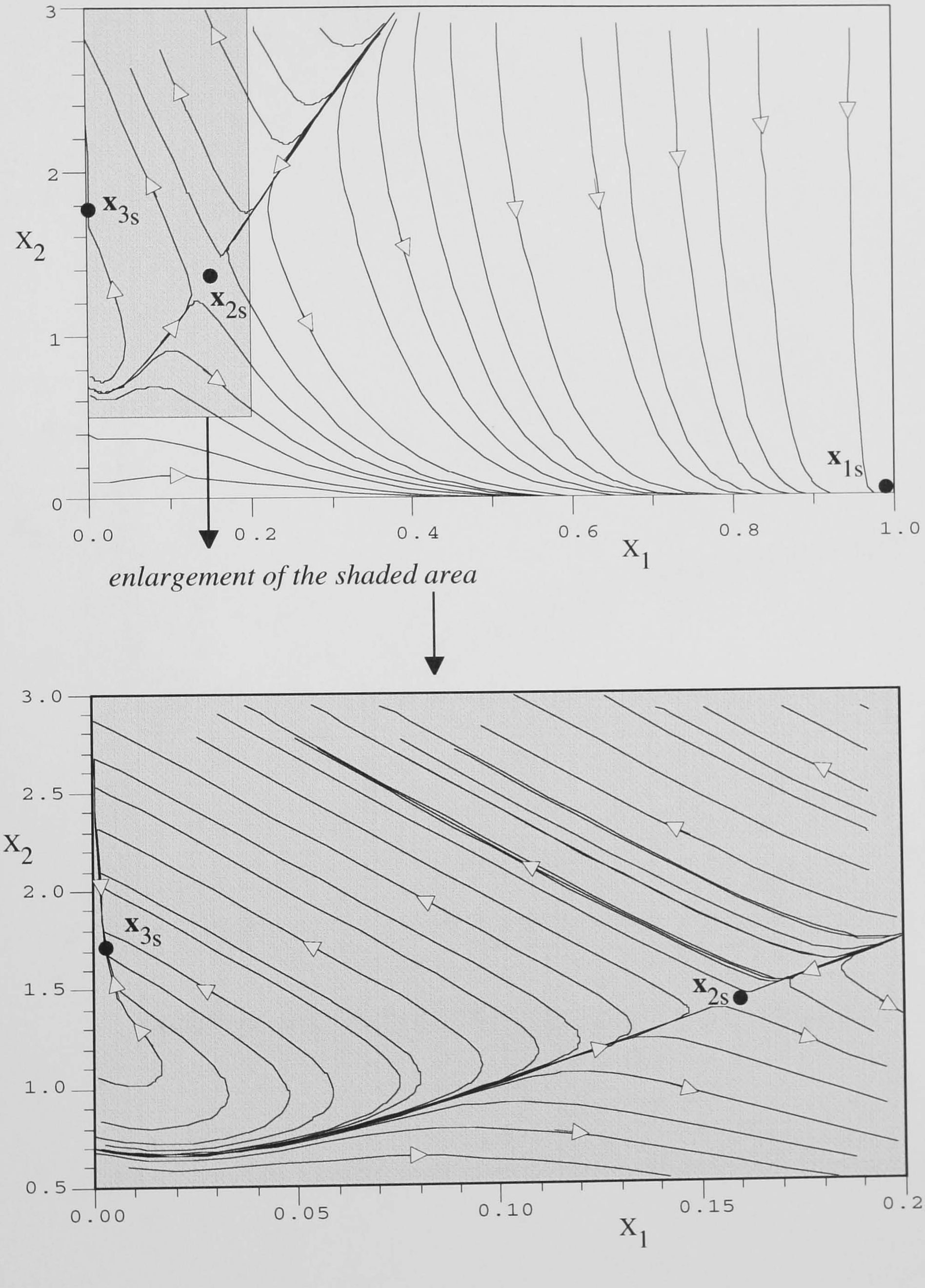

Simulation results for the CSTR polystyrene model.

FIGURE 5.4.1.

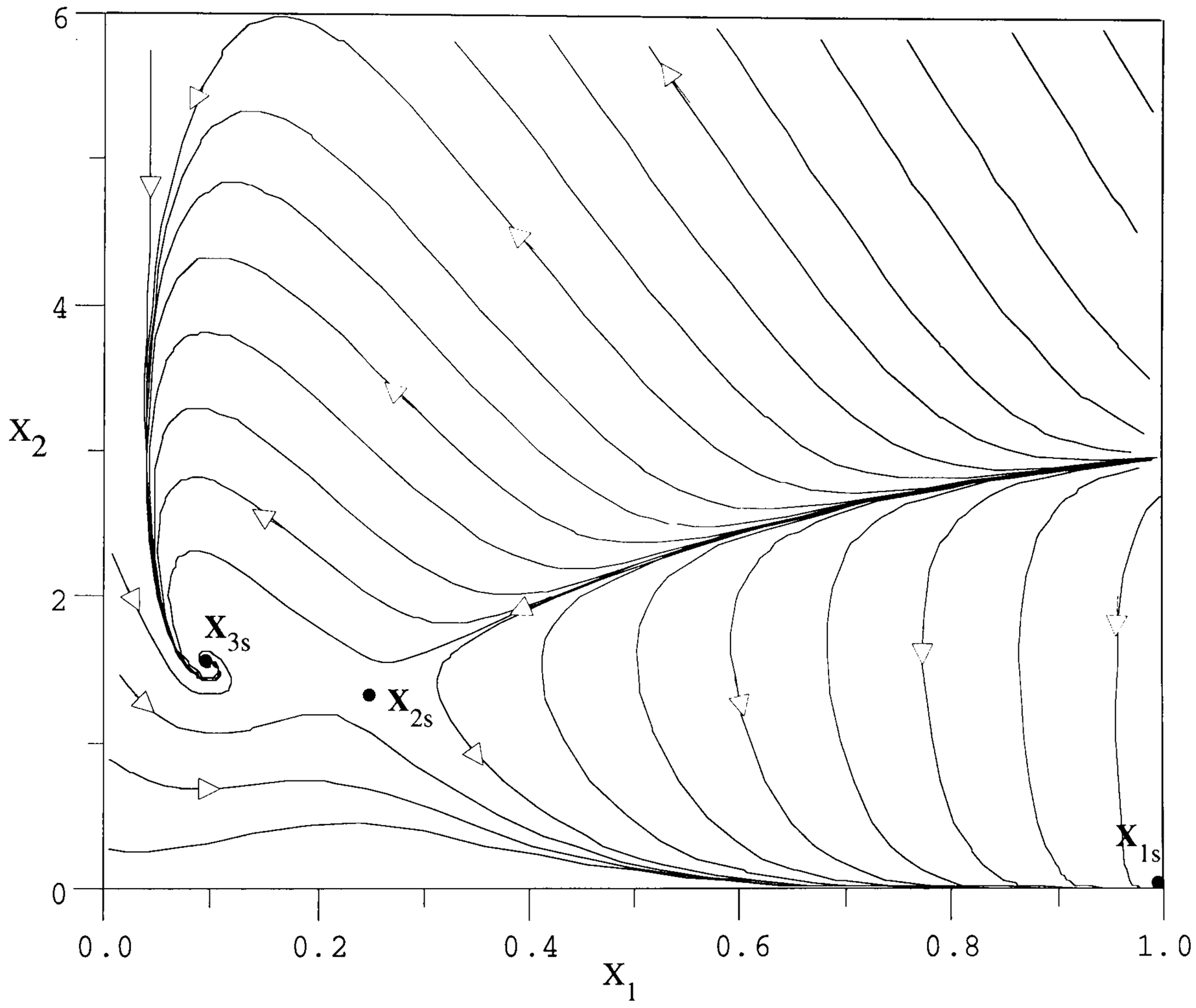

Simulation results for the CSTR polymethylmethacrylate model.

FIGURE 5.4.2.

increase the reactivity of the polymerization processes. This in turn increases the conversion values for the stable steady-states, while for the unstable steady-state, $\mathbf{x}_{2s}$, conversion decreases (see Table 5.4.1). In addition, note that the conversion value changes more for the PMMA case. This is because the two processes have different initiation efficiencies (f), Table 5.4.1. For the PS process f=0.5, while for PMMA f=0.8. The difference in f also reflects the character of the 3-order eigenspectra. For the PS process, the strong 3-order unstable eigenmode is essentially the same as in the two-dimensional instance. However, the 3-order PMMA eigenmode changes from stable to unstable, indicating that the initiator dynamics promotes more reactive PMMA polymerization. Nevertheless the higher-order spectra eventually become stabilizing, implying that the reaction dynamics remain bounded. Hence, the analysis for the third and higher-dimensional spectral structures is conceptually identical as for the two-dimensional case.

Cyclopentenol Model:

We now consider the second-order process in which cyclopentenol (Y) is obtained from cyclopentadiene (X) by the acid-catalyzed electrophilic addition of water in dilute solution. In this reaction the strong reactivity of the educt and the product also produce dicyclopentadiene (W) by Diels-Alder reaction as a side species, and cyclopentanediol (Z) as a consecutive species by addition of another water molecule. Therefore, the second-order reaction scheme is written as

$$X \xrightarrow{k_1} Y \xrightarrow{k_2} Z$$

$$2X \xrightarrow{k_3} W \quad ,$$

and has recently been proposed as a benchmark problem for nonlinear control system design (Engell and Klatt 1993, Chen *et al* 1995). The CSTR model description is given by the following three-dimensional nonlinear ODE system:

$$\frac{dx}{dt} = F(x_0 - x) - k_1 x - k_3 x^2$$
$$\frac{dy}{dt} = -Fy + k_1 x - k_2 y \qquad (5.4.3)$$
$$\frac{dT}{dt} = -\frac{1}{\rho C_p}\left(k_1 x \Delta H_{R_{xy}} + k_2 y \Delta H_{R_{yz}} + k_3 x^2 \Delta H_{R_{xw}}\right) + F(T_f - T) + \frac{Q_k}{\rho C_p V_r}.$$

The first two equations represent the concentrations of cyclopentadiene and the desired cyclopentenol product in terms of the normalized reactor inflow F, as well as the temperature dependent rate constants k_i's, i=1,2,3 , defined in Table 5.4.2.

The last expression is the energy balance equation in which T_f is the temperature of the inlet stream, Q_k is the heat removed by an external heat exchanger which is constant at the setpoint: the other relevant parameters are given in Table 5.4.3.

Table 5.4.2: Arrhenius' expressions for cyclopentenol process.

$$k_i = k_0 \, Exp\left(\frac{-E_A}{R(T+273.15)}\right), \quad \text{where}$$

$k_{0xy} = k_{0yz} = (1.287 \pm 0.04)\ 10^{12}\ h^{-1}$
$k_{0xw} = (9.043 \pm 0.27)\ 10^{9}$ l/mol h
$E_{Axy}/R = E_{Ayz}/R = 9758.3$ K
$E_{Axw}/R = 8560$ K

This process exhibits a peculiar input/output behavior when the reactor inflow F is used to control the process setpoint. Engell and Klatt (1993), and Chen *et al.* (1995) claim that this is a highly nonlinear chemical reactor, and show that as F varies the steady-state gain changes sign at the optimal conversion point. They also observe that at the optimal conversion point a linear controller with integral action does not provide a sufficient stabilization, and therefore they propose a nonlinear control strategy to improve the performance. In spite of these claims, however, we now show that for the inflow F at which the optimal steady-state is achieved, the process is weakly nonlinear.

Table 5.4.3: Cyclopentenol data.

reactor volume:
$V_r = 0.01\ m^3$
reaction enthalpies:
$\Delta H_{R_{xy}} = (4.2 \pm 2.36)$ kJ/mol X
$\Delta H_{R_{yz}} = -(11.0 \pm 1.926)$ kJ/mol Y
$\Delta H_{R_{xw}} = -(41.85 \pm 1.41)$ kJ/mol X
density $\rho = (0.9342 \pm 4.0\ 10^{-4})$ kg/l
heat cpacity $C_p = (3.01 \pm 0.04)$ kJ/kg K.

The steady-state point for maximum production of cyclopentenol is given by the parameters in Table 5.4.4 and is discussed by Chen *et al.* (1995). For these parameters

Table 5.4.4: Cyclopentenol operating point.

$x_{0s} = 5.1$ mol/l , $T_f = 104.9^oC$, $F = 14.19\ h^{-1}$, $Q_{ks} = -1113.5$ kJ/h
steady-state:
$x_s = 2.14$ mol/l , $y_s = 1.09$ mol/l , $T_s = 114.2^oC$.

one now evaluates the power series approximation of Equation (5.4.3) at the steady-state $\mathbf{x}_s=[x_s,y_s,T_s]^t$. Form this, the eigenspectra for the first five power series terms presented in Table A.V.5 are computed. The table indicates that $\mathbf{x}_s$ is now a stable focus, and has higher-order eigenspectra with eigenvalues that are orders of magnitude smaller than those obseved in the PS and PMMA spectra. In addition, Table A.V.5 shows that the first-order eigenvalues are significantly larger in magnitude than the higher-order ones, implying that the steady-state is surrounded by a weak nonlinear structure. Also, observe that the 3, 4 and 5-order eigenspectra have infinite spectral cardinality due to the nilpotent trivial subspace which exists for all solutions when T= 0. As a result, the spectral approach does not support the claim that the process operation is highly nonlinear.

5.5. CHAPTER V SUMMARY

Table 5.5.1 summarizes topics of significance covered in Chapter V. The topics in bold letters identify ideas that are conceived during the preparation of this thesis.

Table 5.5.1: Topics covered in Chapter V.

theory of polynomial processes
• **heterogeneous spectra** - **eigen-varieties and eigenfunctions** - **spectral blend** - **process manifolds and process anatomy** - **stability** - **controllability and stabilizability**
applications
• two-dimensional exothermic CSTR model - **analysis of reactor dynamics** - **reactor complexity** - **evolution of steady-states** - **reactive eigenmodes** - **global linearization** • industrial applications - vinyl polymerization - cyclopentenol polymerization

CHAPTER 6 - PROCESS CONTROL

6.1. PROBLEM FORMULATION

Until now the proposed nonlinear spectral framework has been used to study the complexity and the behavior present in unforced CSTR processes. We have demonstrated that this method globally quantifies the autonomous or zero-input process behavior, which in the process control literature is referred to as the open-loop response. Moreover, it was shown in Section 5.3 that by adding a certain type of function one can regulate the open-loop CSTR behavior in a way that makes the process appear globally linearized. These ideas now provide a basis for considering a process control problem defined by the following equation

$$\dot{\mathbf{x}} = \mathbf{F}[\mathbf{x}] + \mathbf{B}[[\mathbf{x}]]\mathbf{u} \,, \tag{6.1.1}$$

where $\mathbf{F}[\mathbf{x}]$ describes an open-loop nonlinear structure and $\mathbf{B}[[\mathbf{x}]]\mathbf{u}$ is generally a state dependent nonlinear control term with $\mathbf{u} \in \Re^n$, $1 \le n \le m$, and where as before m is the process dimension.

An interesting problem of this form is given by the exothermic CSTR formulation

$$\frac{dx_1}{dt} = -x_1 + Da\,(1-x_1)\,Exp\{x_2\}$$
$$\frac{dx_2}{dt} = -x_2 + BDa\,(1-x_1)\,Exp\{x_2\} - \beta[u + (x_2-x_{2c})] \qquad (6.1.2)$$

in which the control term

$$\mathbf{B}[[\mathbf{x}]]\,\mathbf{u} = -\beta \begin{bmatrix} 0 \\ 1 \end{bmatrix} u\,, \qquad (6.1.3)$$

implying that n=1. We will study this process for the case when u is defined by the polynomial realization

$$u(\mathbf{x}) = \sum_{k=1}^{r\leq\infty} \mathbf{g}^{t}_{p_{k,2}} \mathbf{z}_k(\mathbf{x}) \qquad (6.1.4)$$

where $\mathbf{g}_{p_{k,2}}$ is the k-form coefficient vector to be determined, and $\mathbf{z}_k(\mathbf{x})$ is an appropriate k-form vector. As defined, this nonlinear controller represents a state feedback regulator which regulates the reactor temperature by manipulating the coolant temperature x_{2c}.

6.2. Ideal or Unconstrained Control Design

We begin by observing that for $\mathbf{B}[[\mathbf{x}]]=\beta[0,\ 1]^t$ and any given B, Da, $\beta>0$ and $0<x_{1s}<1$, the entire CSTR process is state controllable, *i.e.*, for the specified control vector each power series term in Equation (1.2.6) satisfies the necessary state controllability condition. This follows from an observation that the process is two-dimensional, which further implies that a power series term is not state controllable if and only if u is restricted to one of its real eigenmodes which determine the ray type solutions defined by the subspaces $\Re^1$. Consequently, when a two-dimensional power series term is not state controllable a control vector is necessarily one of the real eigenvectors. However, it should be noted that for a power series term of order k>1, this necessary condition is not sufficient because the coupling among the process states must also be considered. Nevertheless, since the higher-order geometric spectra are

$$\Sigma_k\{\Re^2\} = \left\{ \begin{bmatrix} 1 \\ B \end{bmatrix} \ ; \ \begin{bmatrix} 1 \\ k/(1-x_{1s}) \end{bmatrix} \ ; \ \begin{bmatrix} 1 \\ 0 \end{bmatrix}_{(k-1)} : \ k\geq 2 \right\},$$

inspection shows that $[0, 1]^t$ is not an eigenvector and therefore all higher-order terms are state controllable. Similarly, for the first-order case, the same vector requires the Jacobian matrix

$$\begin{bmatrix} \dfrac{-1}{1-x_{1s}} & x_{1s} \\ \dfrac{-Bx_{1s}}{1-x_{1s}} & \left(Bx_{1s}-1-\beta\right) \end{bmatrix}$$

to have $x_{1s}=0$. Hence, the necessary state controllability conditions are then satisfied and, according to Theorem 4.5.2, one can design a polynomial state feedback that reassigns all eigenvalues in each of the power series terms. This further implies that each k-form is globally asymptotically stabilizable. A more rigorous proof of these claims can be obtained by considering the transformation sets

$$T_k = \left\{ \begin{bmatrix} 1 & 1 \\ 0 & B \end{bmatrix} ; \begin{bmatrix} 1 & 1 \\ B & k/(1-x_{1s}) \end{bmatrix} \right\} \text{ for } k\geq 2 \ ,$$

and evaluating the corresponding canonical representations.

We now continue with the following question: what is the simplest form of the polynomial structure (Equation (6.1.4)) which stabilizes all power series terms at any given steady-state $\mathbf{x}_s$? One possibility is given by the assumption that $u(\mathbf{x})$ depends only on the temperature

$$u(\mathbf{x})=\sum_{k=1}^{r\leq\infty} g_k(x_2-x_{2s})^k \ , \qquad (6.2.1)$$

where x_{2s} is the dimensionless temperature value at a steady-state. Then from Equation (1.2.6) it follows that the first r power series terms are

$$\mathbf{F}_k[\overleftrightarrow{\mathbf{x}}] = \begin{cases} \begin{bmatrix} \dfrac{-1}{1-x_{1s}} & x_{1s} \\ \dfrac{-Bx_{1s}}{1-x_{1s}} & \left(Bx_{1s}-1-\beta(1+g_1)\right) \end{bmatrix} \begin{bmatrix} \overleftrightarrow{x}_1 \\ \\ \overleftrightarrow{x}_2 \end{bmatrix} & ; \quad \text{for } k=1 \\ \left(\dfrac{-x_{1s}}{(k-1)!\,(1-x_{1s})} \overleftrightarrow{x}_1 \overleftrightarrow{x}_2^{\,k-1} + \dfrac{x_{1s}}{k!} \overleftrightarrow{x}_2^{\,k} \right) \begin{bmatrix} 1 \\ B \end{bmatrix} - \begin{bmatrix} 0 \\ \beta\, g_k \overleftrightarrow{x}_2^{\,k} \end{bmatrix} & ; \quad \text{for } k\leq r \ . \end{cases} \qquad (6.2.2)$$

while for k>r they remain as defined earlier. From these expressions, one can now determine for any g_k , $1 \le k \le r$, the local and global CSTR process behaviors. For instance, whenever a desired steady-state is unstable we would like to adjust g_1 so the forced, or closed-loop, first-order eigenvalues are all moved to the left side of the complex plane. In contrast, when a desired steady-state is first-order open-loop stable, one may wish to leave g_1 at 0. Similarly, for any $1<k \le r$, g_k is adjusted so the corresponding k-order term becomes stable. In any event, whatever gain adjustments are, the proposed controller has one restriction: it can only produce the closed-loop structure which has marginally stable higher-order terms. The reason is that for any $1<k \le r$, the regulated k-order term will always contain a nilpotent eigenmode determined by the eigenvector $[1, 0]^t$ of multiplicity k-1. Thus, by adjusting g_k, only two eigenmodes can be regulated. To verify this we select $\overleftrightarrow{x}_1$ as the projection state, and use it in Equation (6.2.2) to derive the higher-order characteristic value problems

$$v^{k-1}\left[\left(\frac{-x_{1s}}{(k-1)!\,(1-x_{1s})} + \frac{x_{1s}}{k!}\,v\right)(B - v) - \beta\, g_k v\right] = 0$$

with ; for $1<k \le r$, (6.2.3)

$$\lambda = v^{k-1}\left[\frac{-x_{1s}}{(k-1)!\,(1-x_{1s})} + \frac{x_{1s}}{k!}\,v\right]$$

where $v = \overleftrightarrow{x}_2 / \overleftrightarrow{x}_1$. Clearly v=0 and λ=0 are the solutions of multiplicity k-1. Therefore, by considering the control law in Equation (6.2.1) we have restricted the control degrees of freedom. Note that for k=1, two nonzero eigenvalues can always be assigned, implying that the first-order term can always be asymptotically stabilized.

We now demonstrate the control law considered by numerically simulating various CSTR behaviors for the process parameters B=25.0, Da=0.05, β=3.0, x_{2c}=0, and with the objective of stabilizing the unstable steady-state point $\mathbf{x}_{2s}$ depicted in Figure 5.2.3.b). The practical considerations for such a CSTR operation are discussed by Bruns and Bailey (1975). Thus, because $\mathbf{x}_{2s}$ is open-loop unstable, g_1 must be selected so it moves the closed-loop first-order eigenvalues to the left side of the complex plane. This is

accomplished by initially choosing g_1=0.5833 while keeping g_k=0 for the remaining 1<k≤r. From this it follows that

$$u(\mathbf{x}) \equiv u_p = g_1 (x_2 - x_{2s}), \tag{6.2.4}$$

where the subscript p designates the first-order control strategy, *i.e.*, proportional control. The resulting state-space behavior is depicted in Figure 6.2.1.a. The closed-loop first-order eigenvalues at the steady-state are also listed in the figure. The steady-state of interest, and the two additional steady-states, are all unstable. The two additional steady-states correspond to the stable steady-states of the open-loop structure which, as g_1 increases, converge to $\mathbf{x}_{2s}$ along the path of the stable manifold. Furthermore, as the stable steady-states move closer to $\mathbf{x}_{2s}$ they change qualitatively by becoming unstable. In the case considered, all three steady-states are unstable, while all higher-order closed-loop eigenmodes remain defined by the open-loop spectra. This implies that the closed-loop process is bounded and as such must have a stable limit cycle surrounding the three unstable steady-states. The limit cycle in this case is rather large and beyond the simulation boundary. The only evidence of its presence is the bundle of trajectories to the left of $\mathbf{x}_{1s}$.

By further increasing the first-order gain to g_1=2.0, the two unstable steady-states merge with the focally stable $\mathbf{x}_{2s}$ (Figure 6.2.1.b). Consequently, $\mathbf{x}_{2s}$ is stabilized and the control objective is accomplished. One can further argue that because the closed-loop system is bounded the process is also globally stabilized. This is true, except that a large reactive region identified by the parabolic trajectories is present due to the unregulated open-loop unstable higher-order eigenmodes. One can view this region as being the residue of the limit cycle basin. Observe that the residues from the stable manifold and the limit cycle orbit now combine and determine the *reaction boundary* which markedly separates the locally stable region from the parabolic or reactive region.

To reduce the parabolic excursions in the neighborhood of $\mathbf{x}_{2s}$ we need to enlarge the locally stable steady-state region. This is accomplished by increasing g_1 to 5.533. The corresponding simulation in Figure 6.2.1.c shows that the steady-state is now a stable

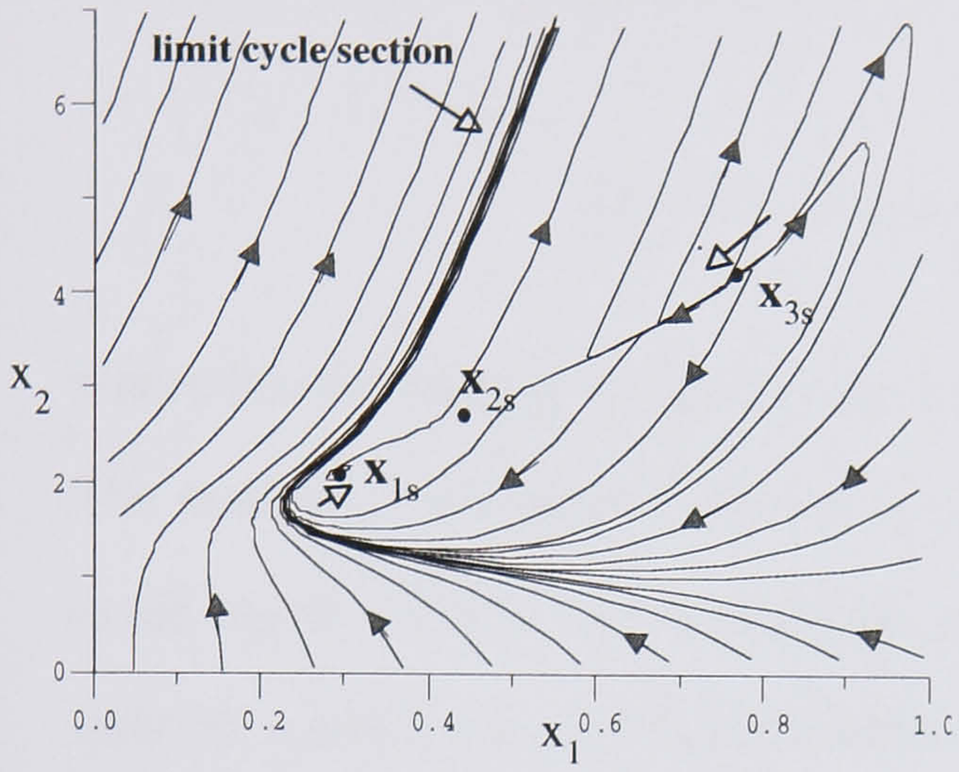

a) g_1=0.5833 ; $\mathbb{A}_1\{\mathbb{R}\}_{c\text{-}l} = \{3.71 ; -0.201\}$

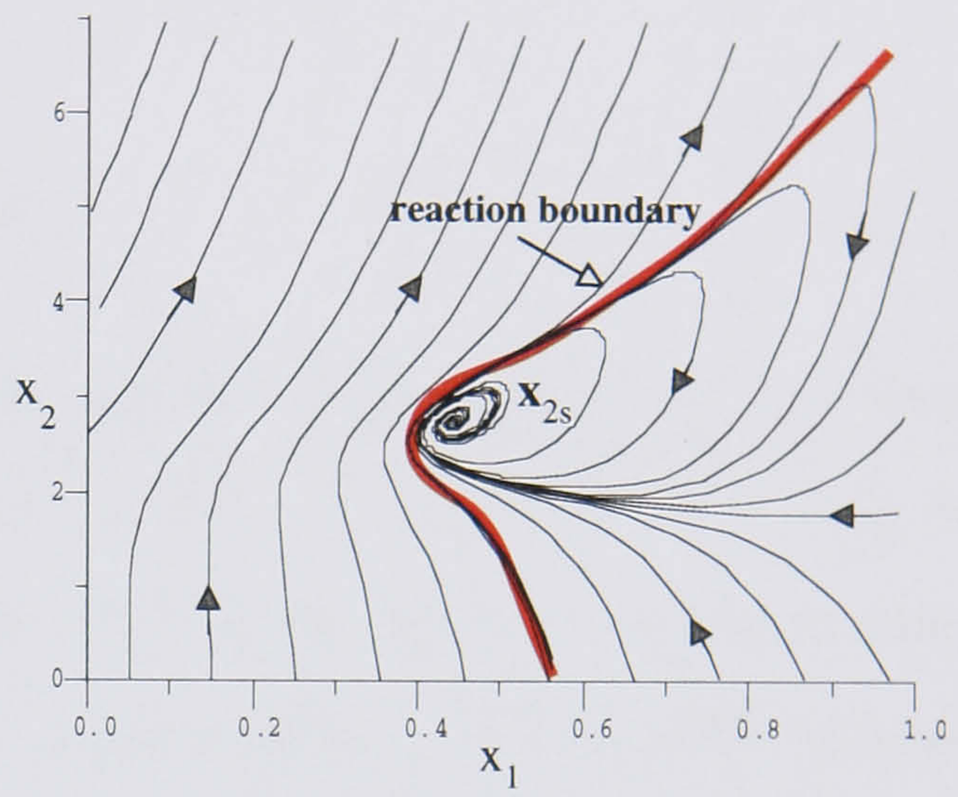

b) g_1=2.0 ; $\mathbb{A}_1\{\mathbb{R}\}_{c\text{-}l} = \{-0.37 + i2.595 ; -0.37 - i2.595\}$

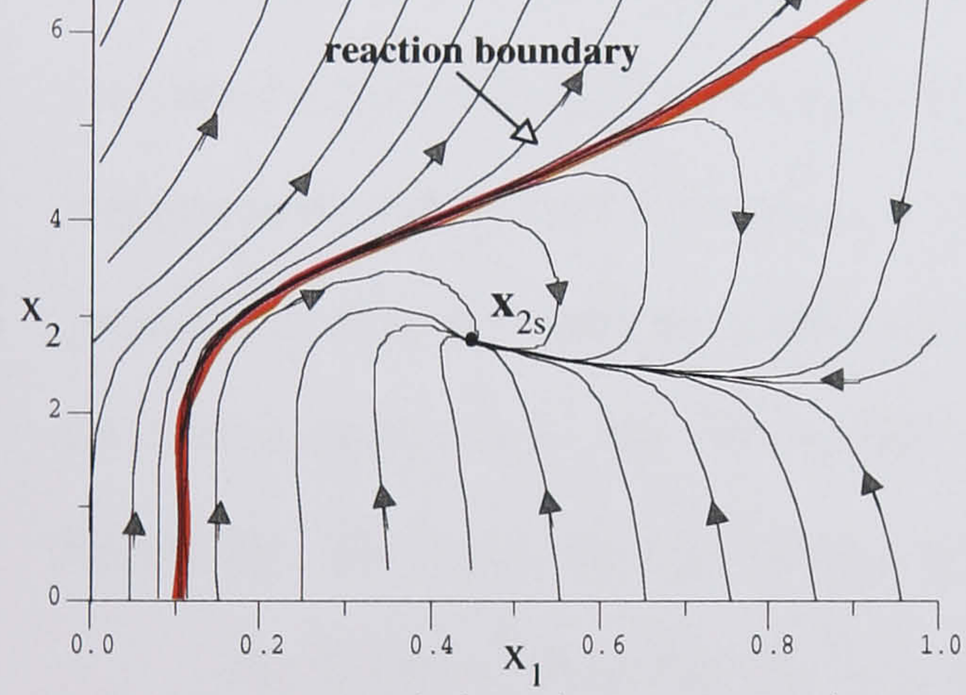

c) g_1=5.533 ; $\mathbb{A}_1\{\mathbb{R}\}_{c\text{-}l} = \{-8.176 ; -3.164\}$

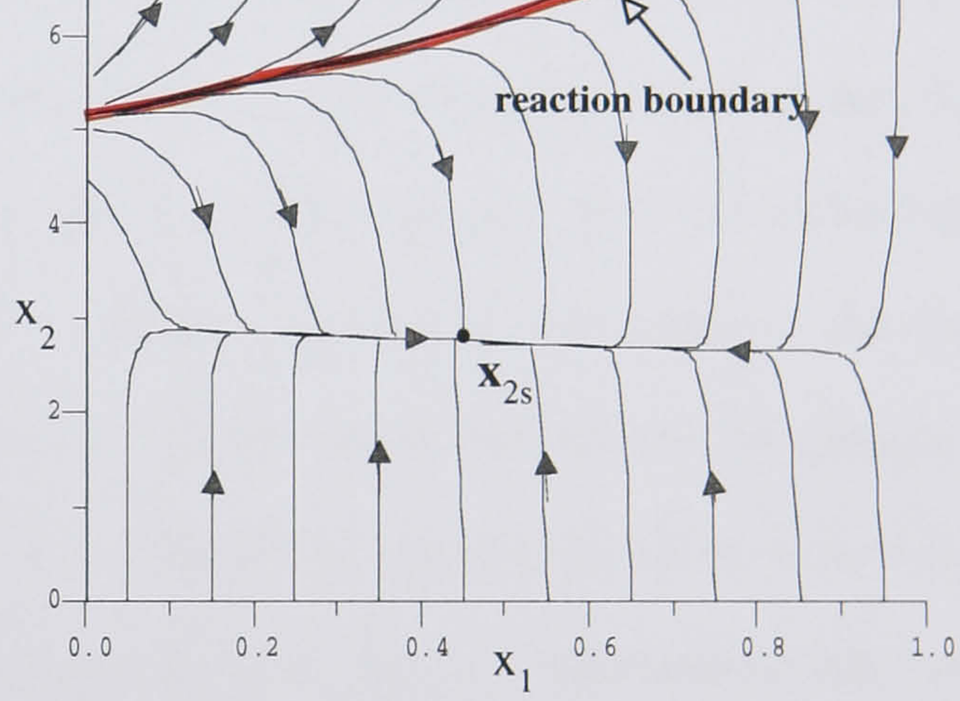

d) g_1=25.0 ; $\mathbb{A}_1\{\mathbb{R}\}_{c\text{-}l} = \{-67.815 ; -1.925\}$

The first-order open-loop eigenvalue set* is:

$$\mathbb{A}_1\{\mathbb{R}\}_{o\text{-}l} = \{5.91598 , -0.656282\}.$$

The closed-loop state-space responses for the first-order (proportional) controller $u_p = g_1(x_2 - 2.763021)$.

FIGURE 6.2.1.

* Subscripts o-l and c-l associated with eigenvalue sets are used to signify respectively open-loop and closed-loop values.

node and that the reaction boundary has shifted away from $\mathbf{x}_{2s}$. By increasing g_1 to 25.0, the boundary shifts even further (Figure 6.2.1.d). Hence, any further increases in g_1 will cause the first-order stabilized steady-state surrounding to grow in size which, in turn will push the reaction boundary to higher temperature values. This strategy, however, will never eliminate the presence of the open-loop unstable higher-order eigenmodes. Consequently the proportional controller cannot control the CSTR's parabolic behavior, or for that matter a parabolic behavior of any other continuous nonlinear phenomenon.

Since the higher-order open-loop unstable eigenmodes are present in the closed-loop configuration, independently of how large the first-order gain g_1 is, we now attempt to regulate them by considering a cubic law of the form

$$u_c = g_1(x_2\text{-}2.763021) + g_2(x_2\text{-}2.763021)^2 + g_3(x_2\text{-}2.763021)^3 \qquad (6.2.5)$$

in which g_1, g_2 and g_3 are constants to be determined. In the closed-loop configuration the new controller allows regulation of the first, second and third-order eigenspectra. As before, the objective is to adjust odd-order gains so that all odd controllable eigenmodes have eigenvalues in the left side of the complex plane. This follows from the fact that odd terms behave symmetrically around a steady-state. However, for the even-order terms the behavior is not symmetric, implying that the same gain objective will always produce an invariant segment which is unstable. Therefore, for the even-order eigenmodes we would like to place eigenvalues close to the imaginary axis. In this way the stabilizing dynamics of the odd terms becomes dominant while the instabilities created by the idempotent even eigenmodes are minimized. This is illustrated in Figure 6.2.2 where both the open and closed-loop eigenvalues are listed. Observe that the reaction boundary becomes less well defined as we compensate higher-order terms. This is because higher-order regulation schemes can promote a smoother interaction between the two regions.

To further improve the cubic control law, we proceed by regulating 4,5,..and higher-order eigenmodes. Alternatively we can also consider the exponential control law

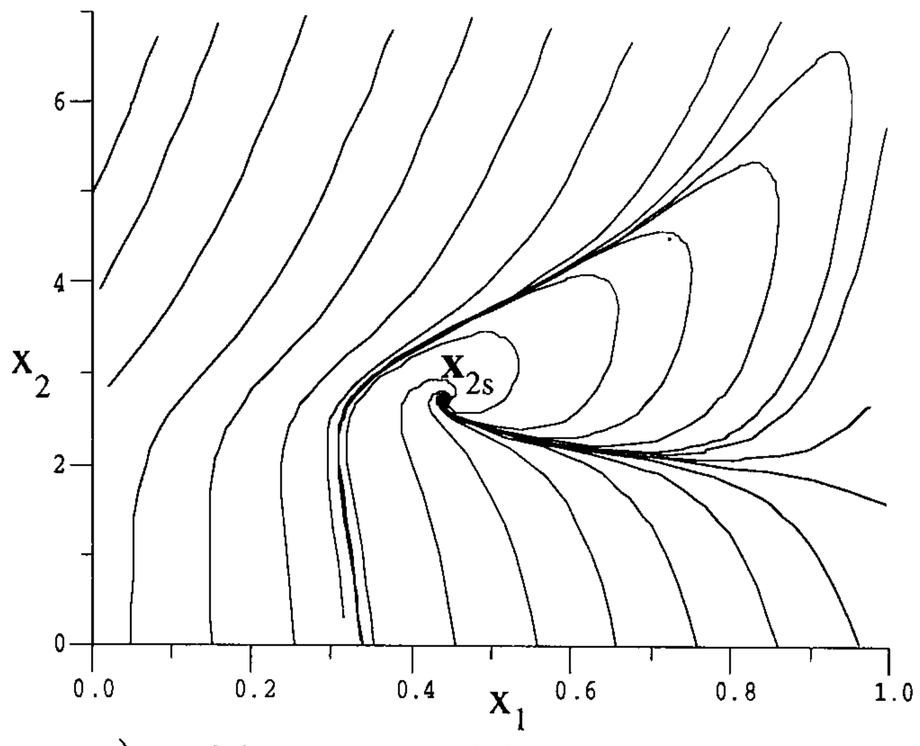

a) g_1=3.0 , g_2=0.0 , g_3=0.0

$\Lambda_1\{\mathbb{R}\}_{o\text{-}l}$ = {5.91598 , -0.656282}

$\Lambda_1\{\mathbb{R}\}_{c\text{-}l}$ = {-1.87+i2.958 , -1.87-i2.958}

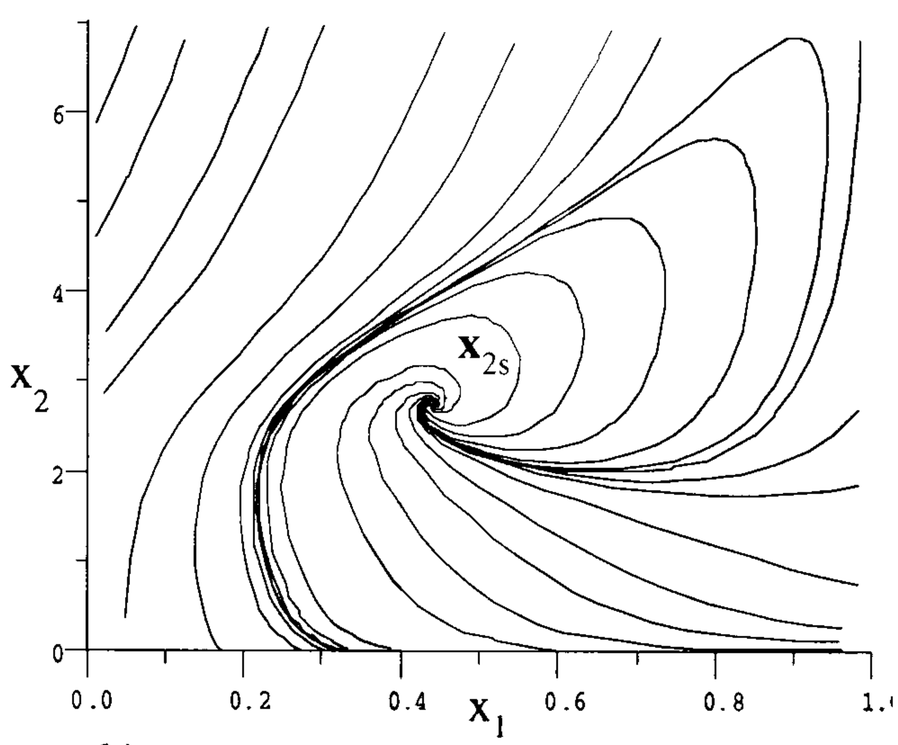

b) g_1=3.0 , g_2=1.1 , g_3=0.0

$\Lambda_2\{\mathbb{R}\}_{o\text{-}l}$ = {118.574 , 0 , 0}

$\Lambda_2\{\mathbb{R}\}_{c\text{-}l}$ = {-4.56+i14.659 , -4.56-i14.659 , 0}

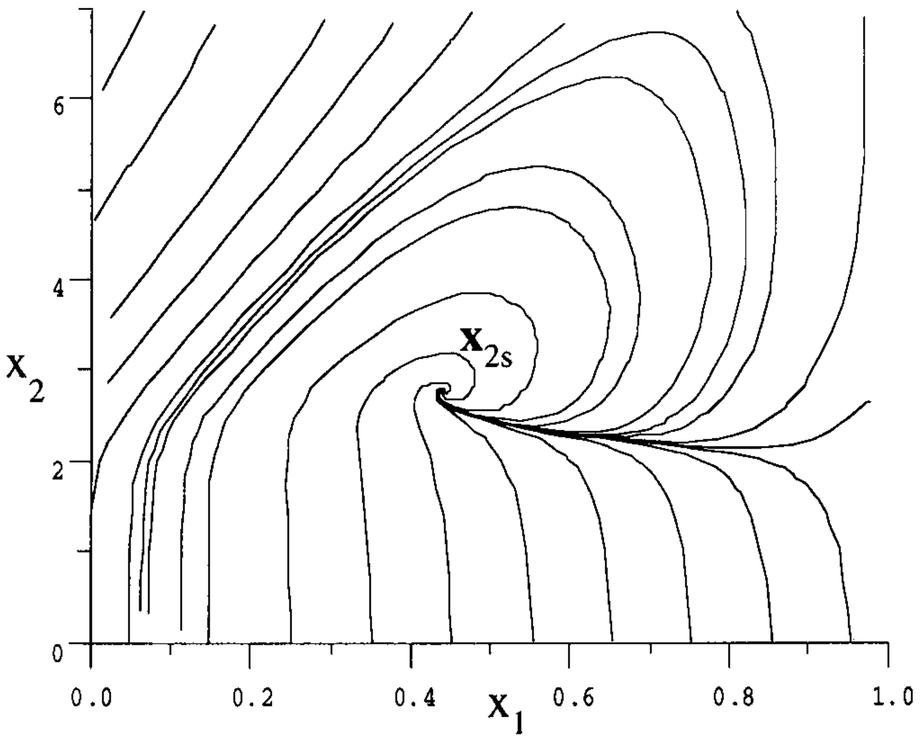

c) g_1=3.0 , g_2=0.0 , g_3=1.3333

$\Lambda_3\{\mathbb{R}\}_{o\text{-}l}$ = {905.238, 0 , $0_{(2)}$}

$\Lambda_3\{\mathbb{R}\}_{c\text{-}l}$ = {-307.171 , -93.945 , $0_{(2)}$}

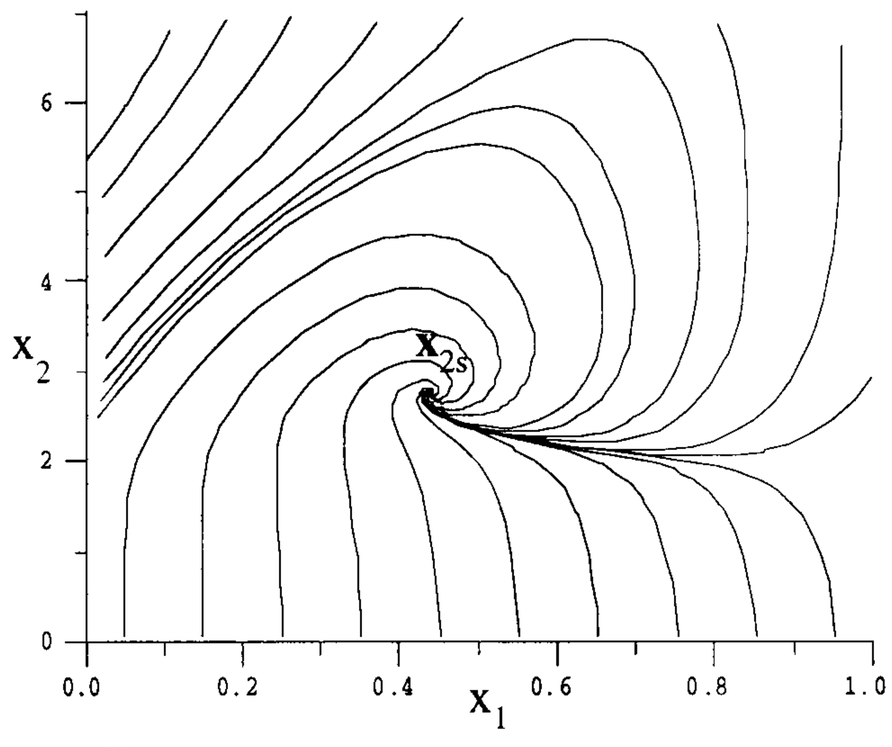

d) g_1=3.0 , g_2=1.1, g_3=1.3333 ;

The closed-loop state space responses for the cubic control law $u_c=g_1(x_2-2.763021)+g_2(x_2-2.763021)^2+g_3(x_2-2.763021)^3$.

FIGURE 6.2.2.

* Subscripts o-l and c-l associated with eigenvalue sets are used to signify respectively open-loop and closed-loop values.

$$u_e = RBx_{1s}(Exp(x_2\text{-}x_{2s}) - 1) = RBx_{1s}\left(\sum_{k=1}^{\infty} \frac{(x_2\text{-}x_{2s})^k}{k!}\right) , \qquad (6.2.6)$$

in which R is the regulation parameter, while the other symbols are as defined earlier. The power series expansion shows that for $r=\infty$ and $g_k=RBx_{1s}/k!$ this control law corresponds to Equation (6.2.1). Its performances are shown in Figure 6.2.3, and they resemble the simulations given in Figures 6.2.1-2. The limit cycle behavior exists for R=0.07 and R=0.15. As R further increases, the limit cycle collapses, and $\mathbf{x}_{2s}$ becomes stable. For R=0.3, the dynamics surrounding the steady-state are very much like the behaviors observed in Figure 6.2.2. Furthermore, since all eigenmodes are now regulated the reaction boundary disappears. For R=0.5 the reactive region is practically nonexistent, and the parabolic behavior is hardly evident. Nevertheless, one can argue that the exponential control strategy is not consistent with our gain design objective which is aimed at promoting the odd dynamics and canceling the even eigenmodes. For this reason we now write

$$Exp(x_2\text{-}x_{2s}) = Sinh(x_2\text{-}x_{2s}) + Cosh(x_2\text{-}x_{2s}) , \qquad (6.2.7)$$

and change the exponential control law into the hyperbolic form

$$u_h = Bx_{1s}(R_sSinh(x_2\text{-}x_{2s})+R_c(Cosh(x_2\text{-}x_{2s}) -1)) \qquad (6.2.8)$$

where R_s and R_c are the tuning parameters which respectively control odd and even power series terms. This hyperbolic controller contains all necessary features that meet our gain requirements.

So far we have studied the control forms in which the dimensionless temperature is the only independent variable. Clearly by allowing both process states to enter the control scheme defined in Equation (6.1.4), regulation of process eigenmodes is no longer constrained by Equation (6.2.3). In this case all eigenvalues in all power series terms can be arbitrarily reassigned, implying that the following design objective can be realized;

- *<u>all</u> odd degree eigenmodes are assigned eigenvalues in the left side of the complex plane,*
- *and <u>all</u> even degree eigenmodes are assigned eigenvalues close to the imaginary axis.*

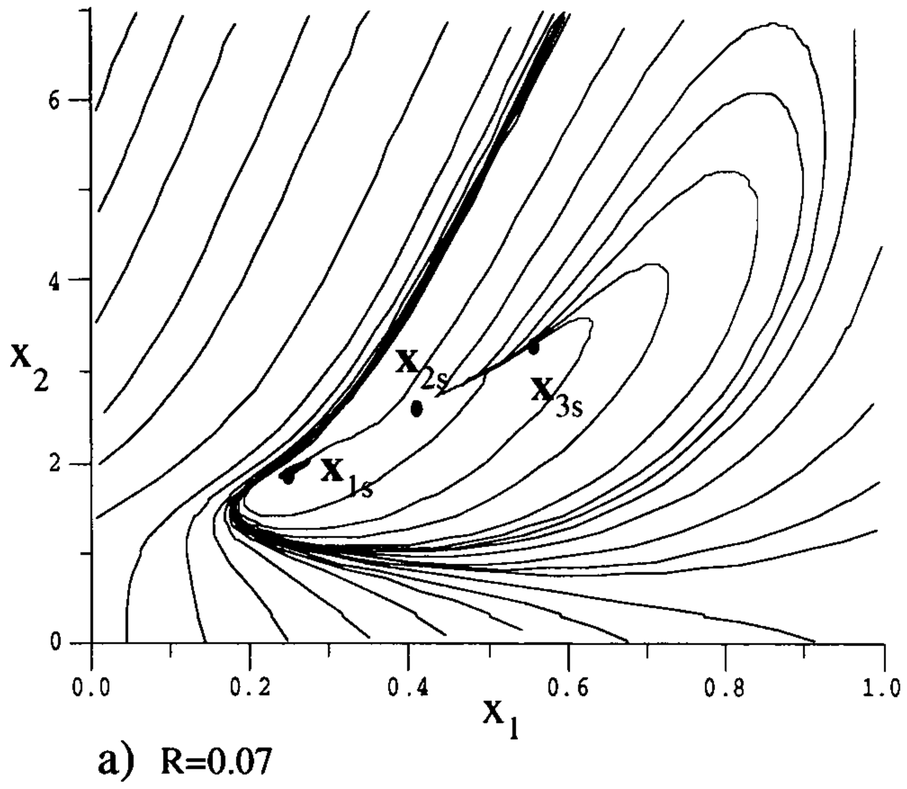

a) R=0.07

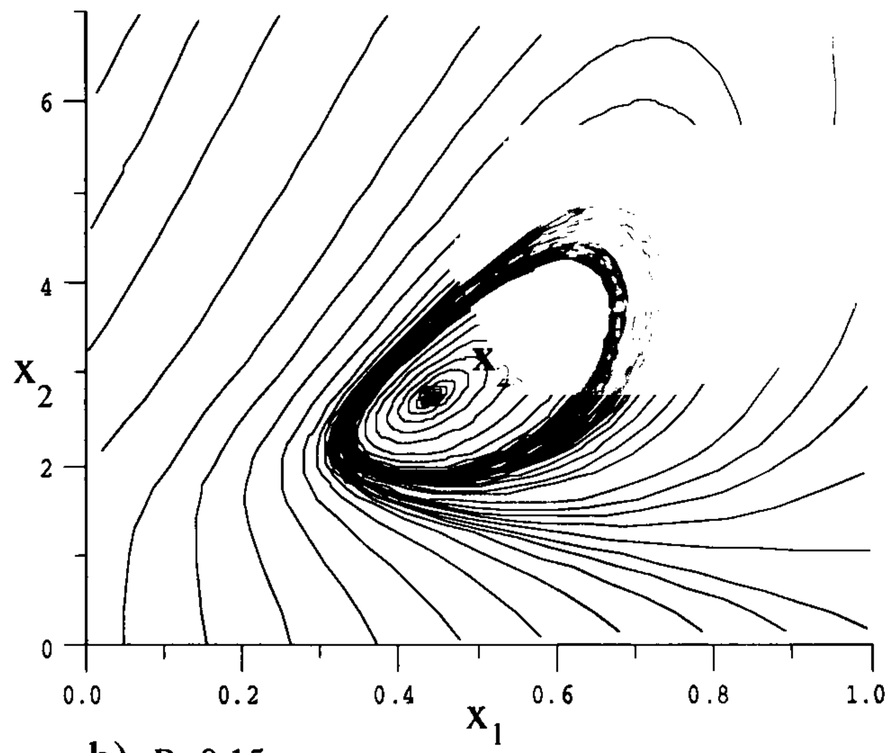

b) R=0.15

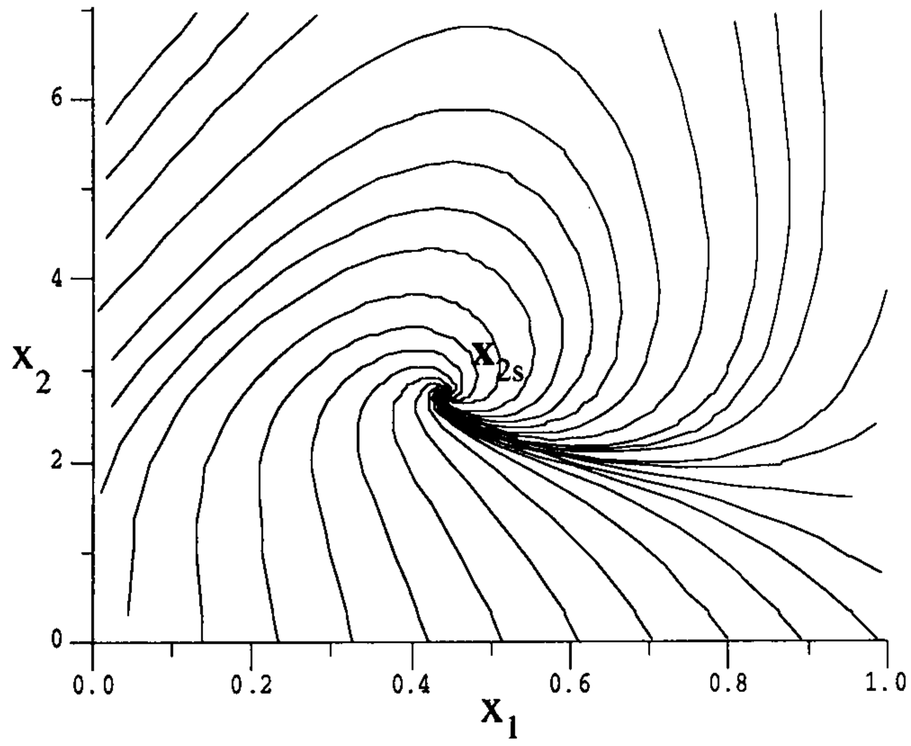

c) R=0.3

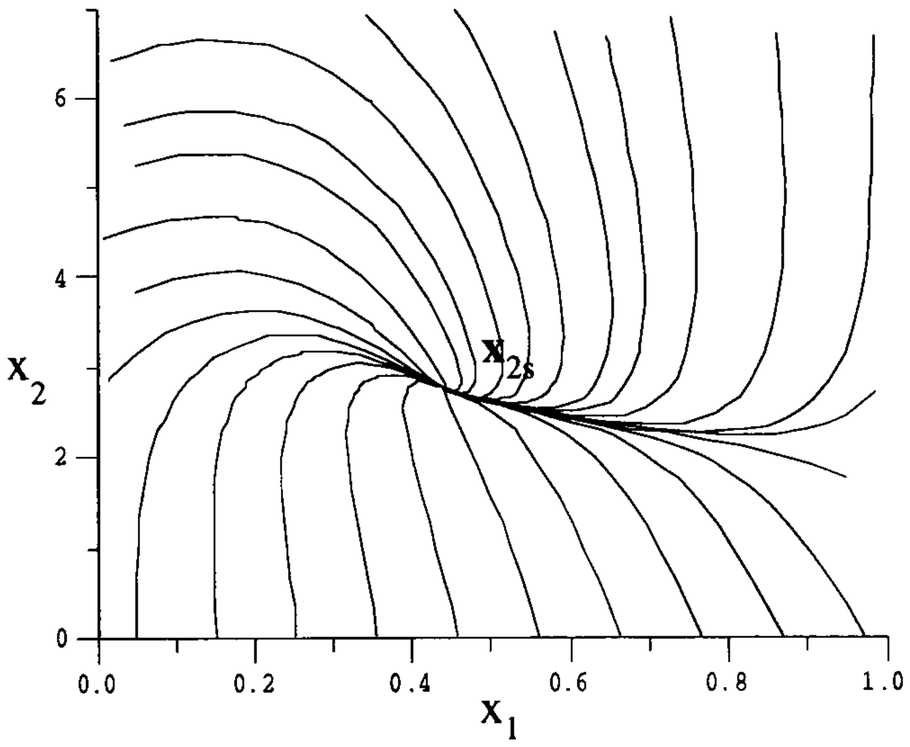

d) R=0.5

The closed-loop state-space responses for the exponential control $u_e=RBx_{1s}\{Exp(x_2-x_{2s}) - 1\}$ with B=25.0, x_{1s}=0.442083, x_{2s}=2.763021.

FIGURE 6.2.3.

An interesting control realization exists when

$$u(\mathbf{x})_{i/o} = g_1(x_2 - x_{2s}) - g(\mathbf{x})/\beta \qquad (6.2.9)$$

where $g(\mathbf{x})$ is the global linearization function defined by Equation (5.3.1). This type of the control function is receiving a significant attention among control researchers who study and apply differential geometry methods. Isidori (1989), Kravaris and Kantor (1990), Bequette (1991) refer to this type of control technique as the *input/output linearization* because u cancels out all process nonlinearities, *i.e.*, even as well as the odd. The simulation results for this control law are presented in Figure 6.2.4. Observe that now the steady-state is stabilized without presence of the limit cycle regime. This is because all higher-order eigenmodes (nonlinearities) are regulated in a way that their eigenvalues are zero. In fact, if we write Equation (6.2.9) in the power series form

$$u(\mathbf{x})_{i/o} = g_1(x_2 - x_{2s}) - \frac{B}{\beta}\sum_{k=2}^{\infty}\frac{1}{k!}\begin{bmatrix} \dfrac{k\,x_{1s}}{1-x_{1s}} & ; & -x_{1s} \end{bmatrix}\begin{bmatrix} (x_1-x_{1s})(x_2-x_{2s})^{k-1} \\ (x_2-x_{2s})^{k} \end{bmatrix}, \qquad (6.2.10)$$

then u is precisely of the form given in Equation (6.1.4), and is such that for $k \geq 2$ all higher-order CSTR eigenmodes are nilpotent. Therefore, g_1 is the only control parameter which determines both the local and global state-space behaviors. This is clearly illustrated in Figure 6.2.4 since the reactive region is not present for any g_1 which stabilizes $\mathbf{x}_{2s}$. Observe that the input/output linearization method applies essentially the same principle discussed in the rigid body rotation problem presented in Example 5.1.3.

We conclude this section by observing that the control formulation (Equation (6.1.2)) depends on an assumption in which control is not present in the dimensionless conversion equation. This restriction is imposed for no particular reason other than a convenience which makes control easier to implement. However, nothing precludes us from including the control formulation in the conversion equation. Therefore, for the general case, Equation (6.1.4) becomes

$$\mathbf{u}(\mathbf{x}) = \sum_{k=1}^{r\leq\infty} \mathbf{G}_{2xp_{k,2}} \mathbf{z}_k(\mathbf{x}) \qquad (6.2.11)$$

where $\mathbf{G}_{2xp_{j,2}}$ is an appropriate gain matrix for which the coefficients can be determined by using the same eigenvalue objectives that are previously discussed.

6.3. ROBUST CONTROL DESIGN

The ideal nonlinear control design method does not address all important control issues. No consideration has been given to a likely possibility that process parameters may change during operation. Also, in the idealized case the objective was to maximize the stable region surrounding a steady-state of interest. In practice, however, this objective may be quite excessive because process operators often need good and robust control over a specified operating region beyond which regulation is inconsequential. For instance, a CSTR operator may be interested to run the process of the last section only within the rectangular state-space region defined by

$$0.3\leq x_1\leq 0.675 \text{ and } 0.7\leq x_2\leq 3.5,$$

and illustrated with the shaded rectangle in Figure 6.3.1.a. In this case the closed-loop behavior and robustness need to be analyzed only within the region of interest. We now demonstrate how this is done for different control realizations.

In general, when the process parameters (as defined in the previous section) do not vary with time, control of a CSTR can be accomplished by applying a proportional controller as defined in Figure 6.3.1.b. However, this controller may no longer be adequate when the parameters such as the Damköhler number, Da, or the dimensionless heat transfer coefficients β change with time. For example, for a 25% increase in the Damköhler number, the performance is illustrated in Figure 6.3.1.c. As depicted, the reaction boundary is now within the operating region of interest. Observe that as Da increases the steady-state $\mathbf{x}_{2s}$ drifts to the right and pulls the boundary into the desired region. This makes the CSTR safety and operation quite unacceptable for the process

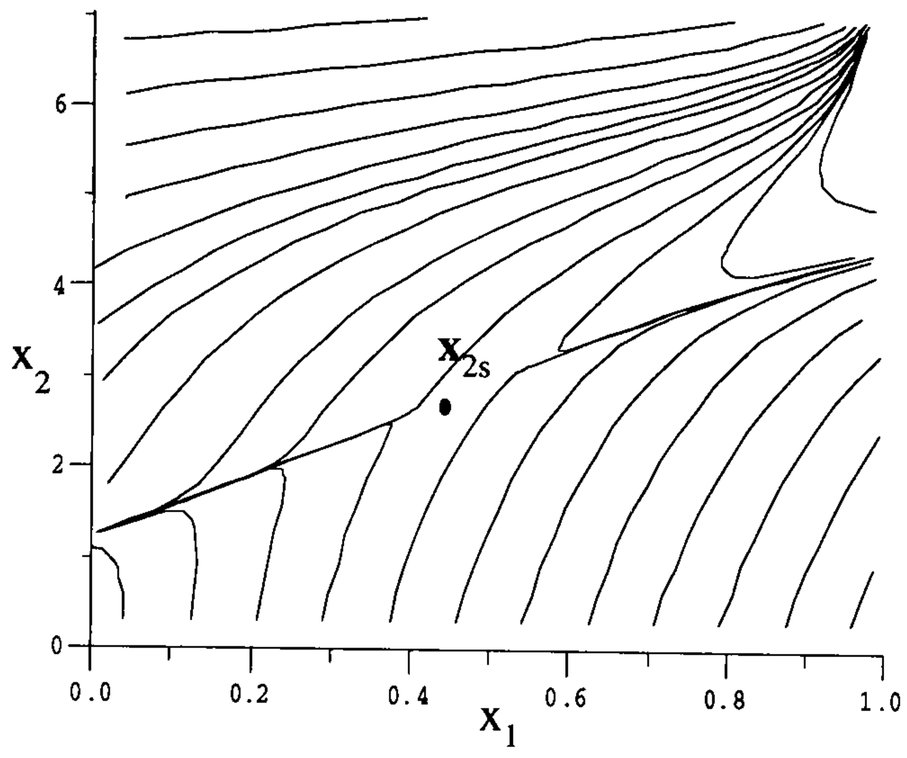

a) g_1=0.5833

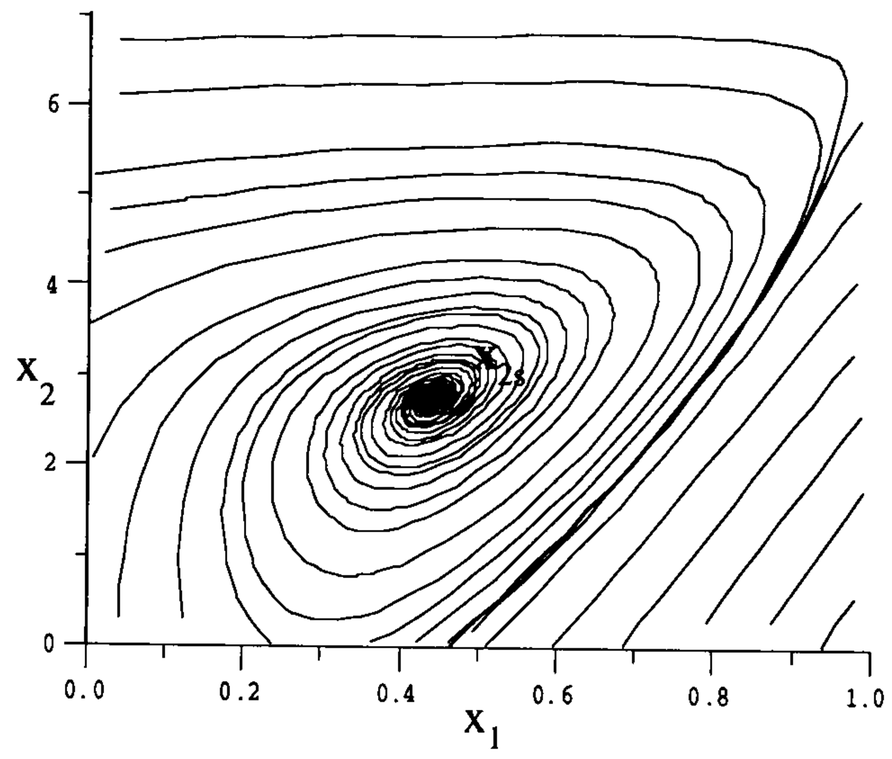

b) g_1=2.0

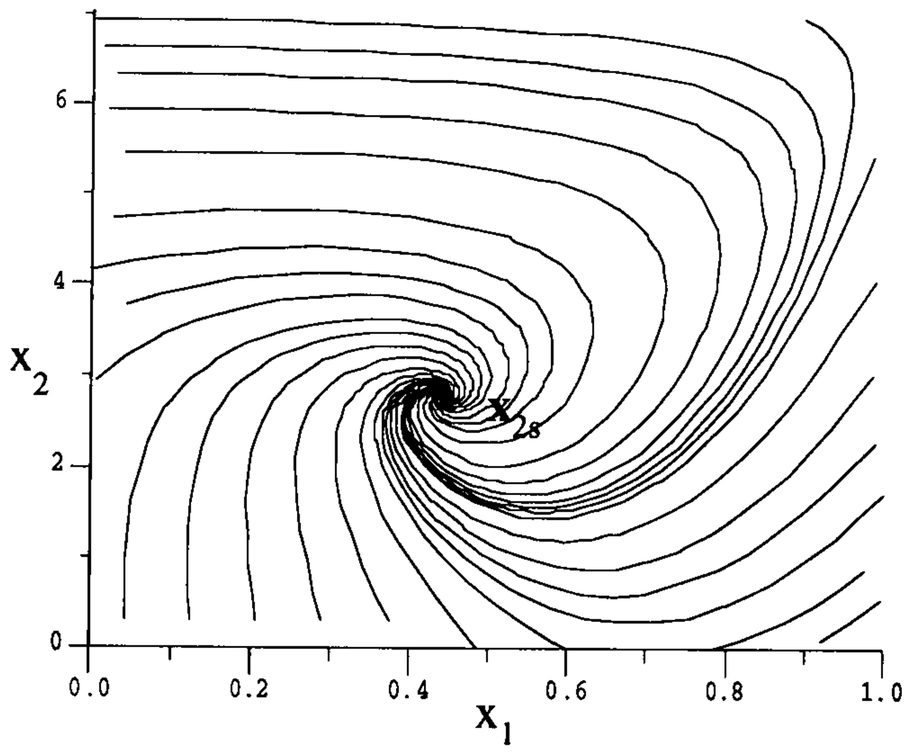

c) g_1=3.0

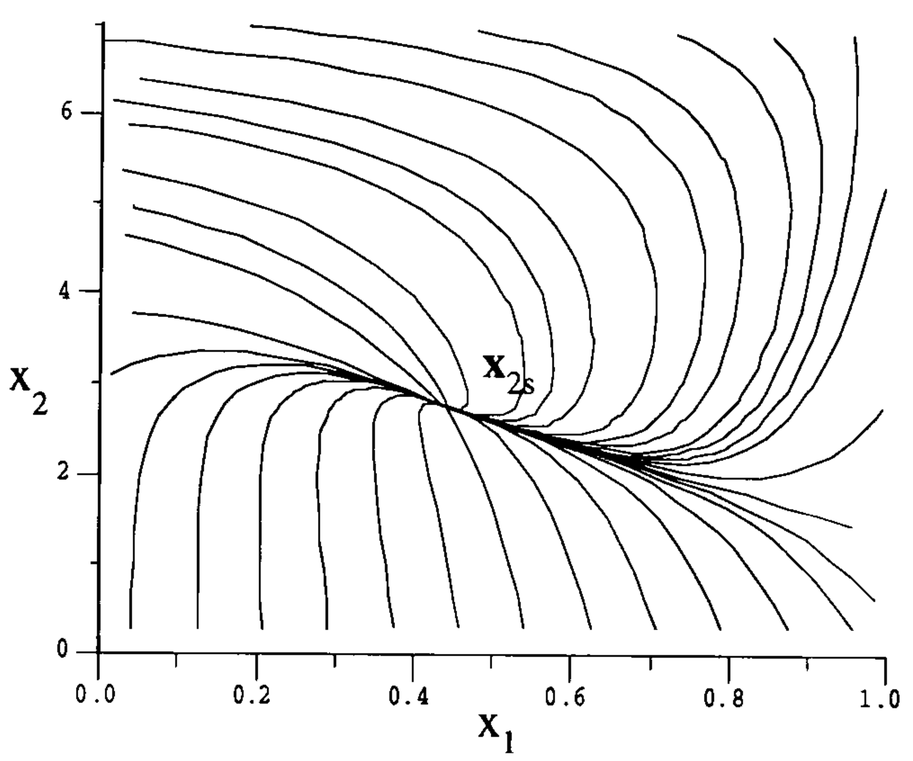

d) g_1=5.533

The closed-loop state-space responses for the input/output linearization control scheme $u_{i/o} = g_1(x_2-x_{2s}) - g(\mathbf{x})/3$.

FIGURE 6.2.4.

disturbances on the boundary. In contrast, when Da decreases the steady-state drifts to the left and pushes the boundary away from the desired region. Thus, as long as Da decreases and $\mathbf{x}_{2s}$ remains stable we need not be concerned about the process safety. On the other hand, when Da increases the process needs to be better regulated. The first obvious choice is to increase the first-order gain to g_1= 9.0, which is about a 60% change in the original g_1 setting. For this case the process responds as illustrated in Figure 6.3.1.d. As can be seen the behavior within the shaded region once again is acceptable.

From this discussion it follows that by increasing g_1 the first-order closed-loop eigenvalues are set deeper into the left side of the complex plane, and a solution with the larger degree of robustness is obtained. Nevertheless, in spite of the more robust solution for g_1=9.0 the local steady-state behavior is qualitatively almost identical to that of g_1=5.533. The only differences between the two realizations are that the process robustness in the g_1=5.533 case is affected by the appearance of the reactive boundary inside the region of interest, and that for the case of g_1=9.0 the first-order dynamics are promoted by faster solutions. This suggests that rather than changing the speed of the first-order response, one should be able to obtain a robust process realization by keeping g_1=5.533 and regulating the higher-order eigenmodes. To demonstrate this, we consider a cubic control law with g_1=5.533, and with the second and third-order gains defined in Figure 6.2.2. For this closed-loop process realization the operation again becomes robust inside the region of interest. This is illustrated in Figure 6.3.2 in which the performances of the exponential, hyperbolic and input/output linearization controllers are also depicted. Note that all control realizations considered in the figure have comparable first-order eigenvalues. This is verified in Table 6.3.1 where the sixth and lower-order closed-loop eigenvalues are listed. The table also shows that the input/output linearization controller suppresses all nonlinear eigenmodes, while the other nonlinear control realizations regulate higher-order modes. For instance, the cubic controller has stabilized the first three power series terms, while the remaining higher-order terms preserve the open-loop characteristics.

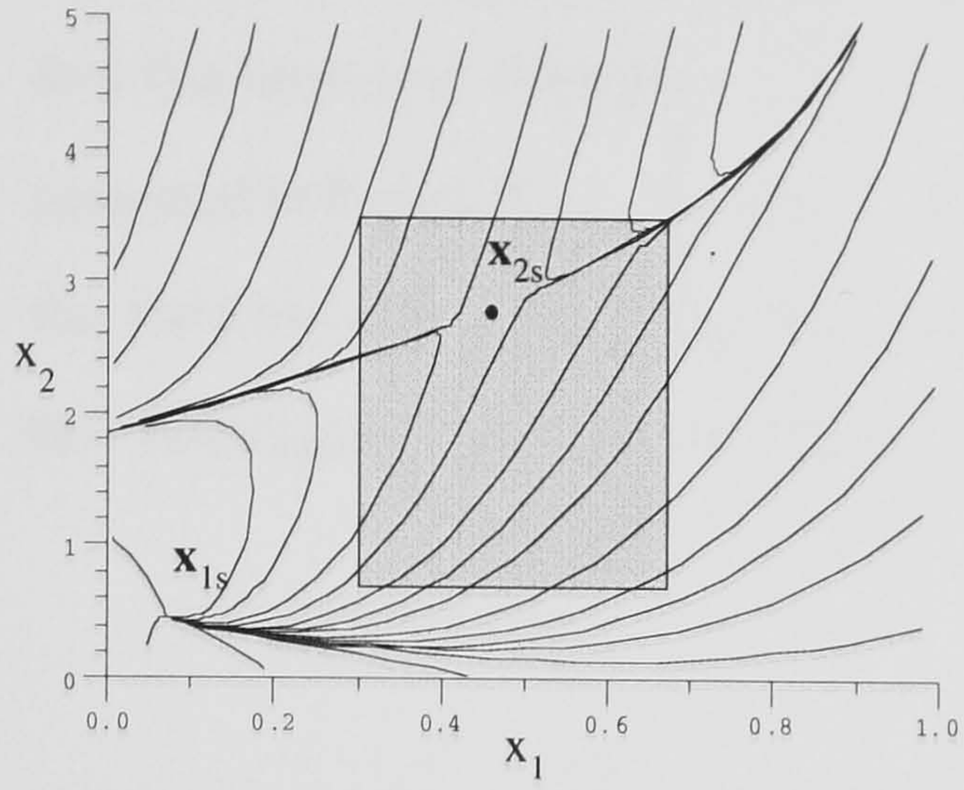

a) g_1=0.0 ; Da=0.05

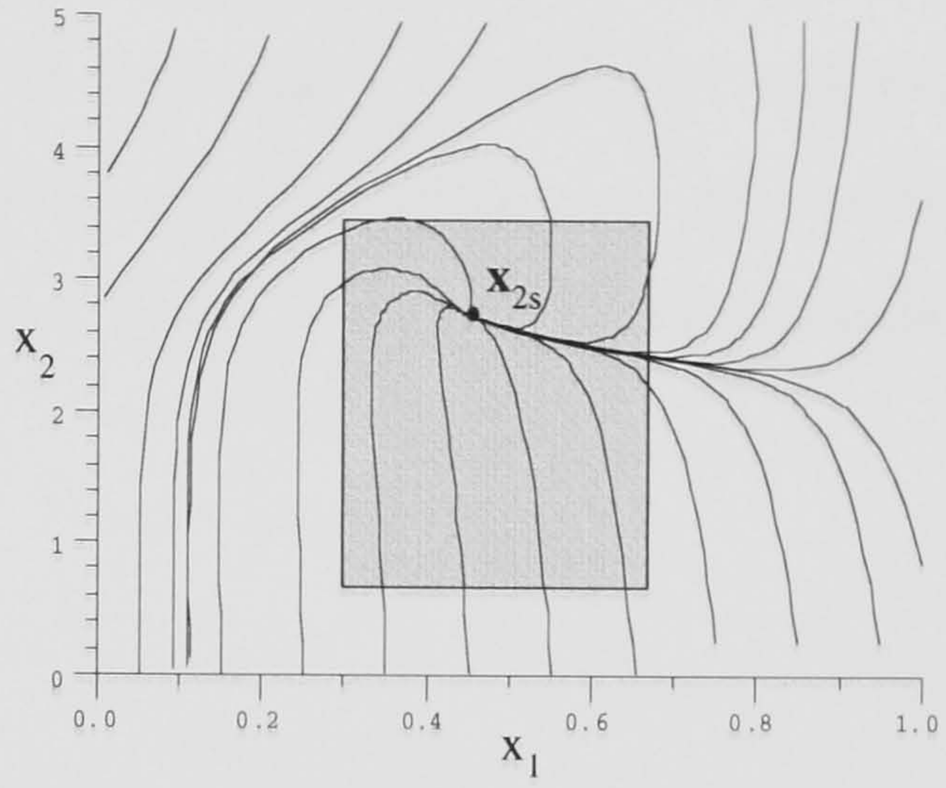

b) g_1=5.533 ; Da=0.05

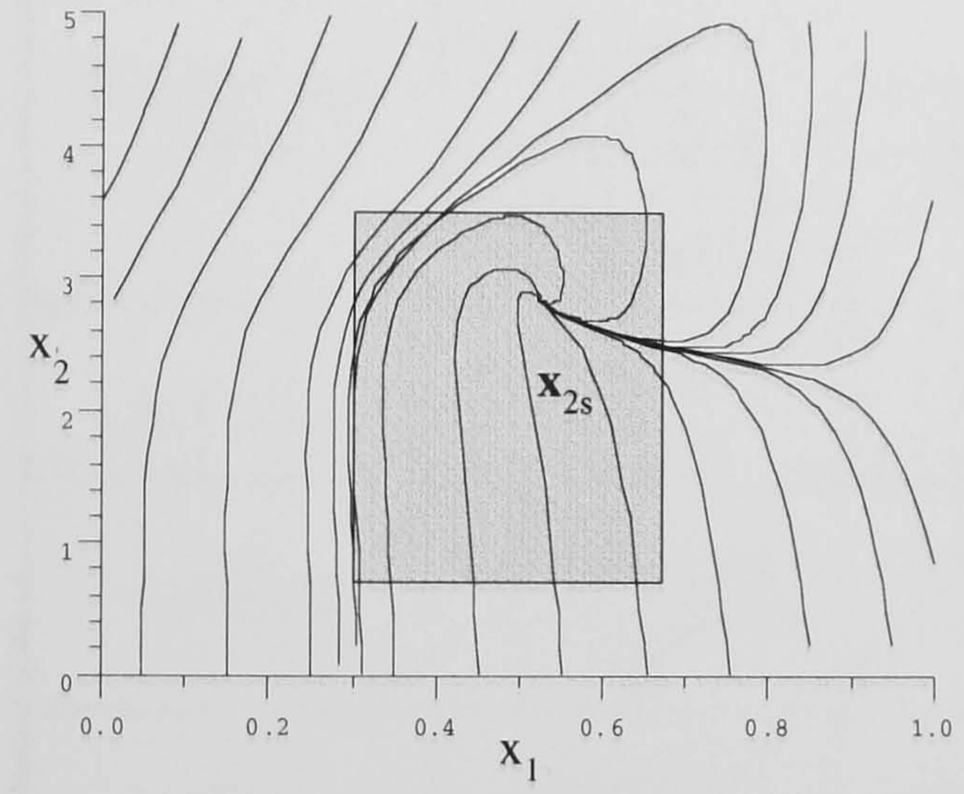

c) g_1=5.533 ; Da=0.0625

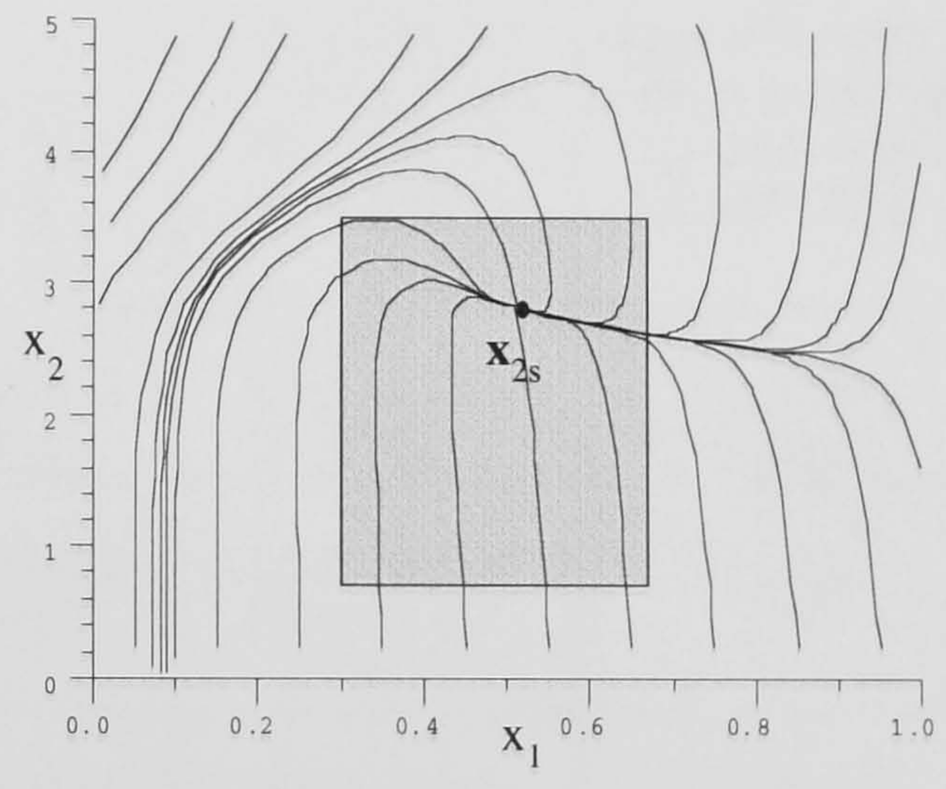

d) g_1=9.0 ; Da=0.0625

The open-loop and the closed-loop first-order regulated behaviors. The shaded region is of interest.

FIGURE 6.3.1.

It is now evident that one can combine various control realizations. For instance, when Da=0.05, the closed-loop performance for the exponential control law given by R=1.0 is illustrated in Figure 6.3.3.a. This control law outperforms all control realizations presented in Figure 6.3.2. However, this comparison is not entirely just. The reason is that the first-order dynamics are now accelerated, which is indicated by the closed-loop first-order eigenvalues listed in Table 6.3.2.

Table 6.3.1: The eigenvalues of the first six power series terms evaluated at $\mathbf{x}_{2s}$ for Da=0.05.

Eigenvalue Sets	**Cubic control with g_1=5.533, g_2=1.1 & g_3=1.3333**	**Exponential control with R=0.5**	**Hyperbolic control with R_s=0.5 & R_c=0.333**	**Input/Output Linearization control with g_1=5.533**
$\Lambda_1(K)_{c\text{-}l}$	{-8.176 ; -3.164}	{-8.14817 ; -3.17025}	{-8.14817 ; -3.17025}	{-8.176 ; -3.164}
$\Lambda_2(K)_{c\text{-}l}$	{-4.61+i4.597 ; -4.61-i4.597 ; 0}	{-7.49+i23.07 ; -7.49-i23.07 ; 0}	{-19.8+i0.051 ; -19.8-i0.051 ; 0}	{0 ; $0_{(2)}$}
$\Lambda_3(K)_{c\text{-}l}$	{-330.0 ; -83.78 ; $0_{(2)}$}	{135.7+i36.9 ; 135.7-i36.9 ; $0_{(2)}$}	{135.7+i36.9 ; 135.7-i36.9 ; $0_{(2)}$}	{0 ; $0_{(3)}$}
$\Lambda_4(K)_{c\text{-}l}$	{5131.87 ; 0 ; $0_{(3)}$}	{232.3+i686.5 ; 232.3-i686.5 ; $0_{(3)}$}	{505.5+i307.0 ; 505.5-i307.0 ; $0_{(3)}$}	{0 ; $0_{(4)}$}
$\Lambda_5(K)_{c\text{-}l}$	{23080 ; 0 ; $0_{(4)}$}	{-3.02+i1.54 ; -3.02-i1.54 ; $0_{(4)}$}x 10^3	{-3.02+i1.54 ; -3.02-i1.54 ; $0_{(4)}$}x 10^3	{0 ; $0_{(5)}$}
$\Lambda_6(K)_{c\text{-}l}$	{85419.2 ; 0 ; $0_{(5)}$}	{-9.27+i11.29 ; -9.27-i11.29 ; $0_{(5)}$}x 10^3	{-2.71+i11.6 ; -2.71-i11.6 ; $0_{(5)}$}x 10^3	{0 ; $0_{(6)}$}

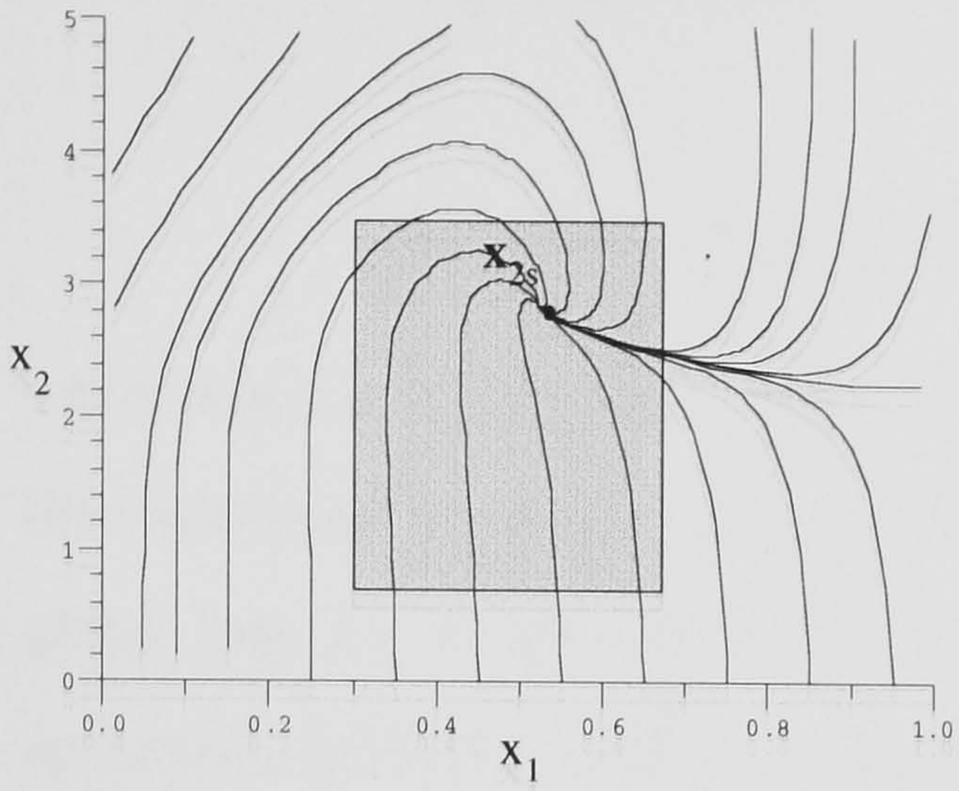

a) cubic control with g_1=5.533 , g_2=1.1 , g_3=1.3333 and Da=0.0625.

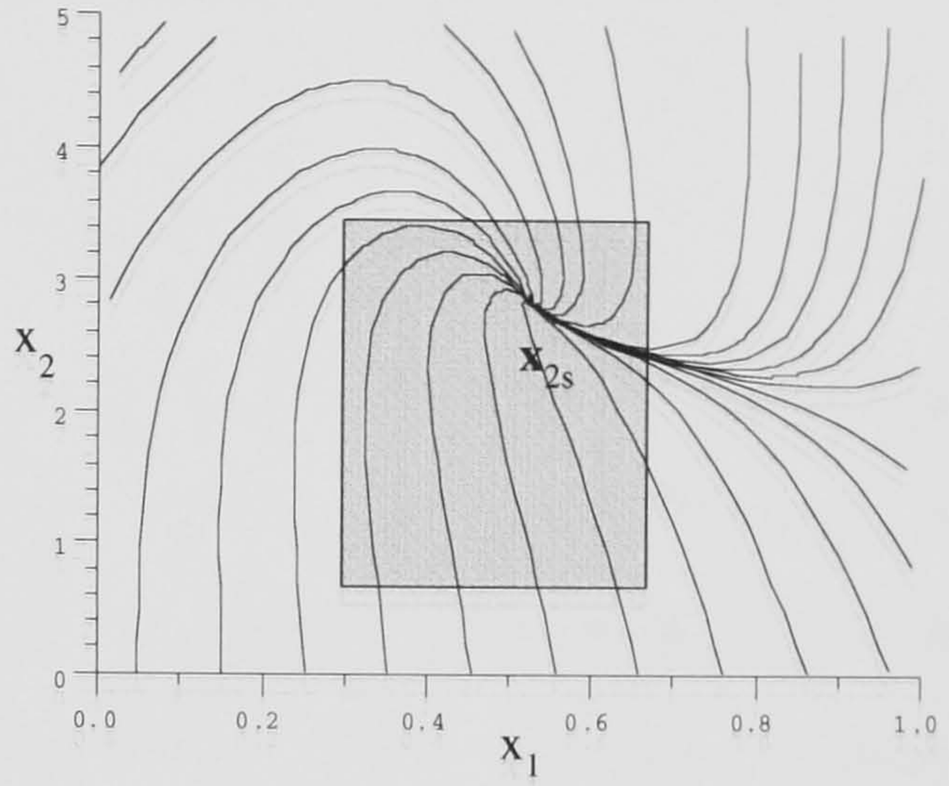

b) exponential control with R=0.5 and Da=0.0625.

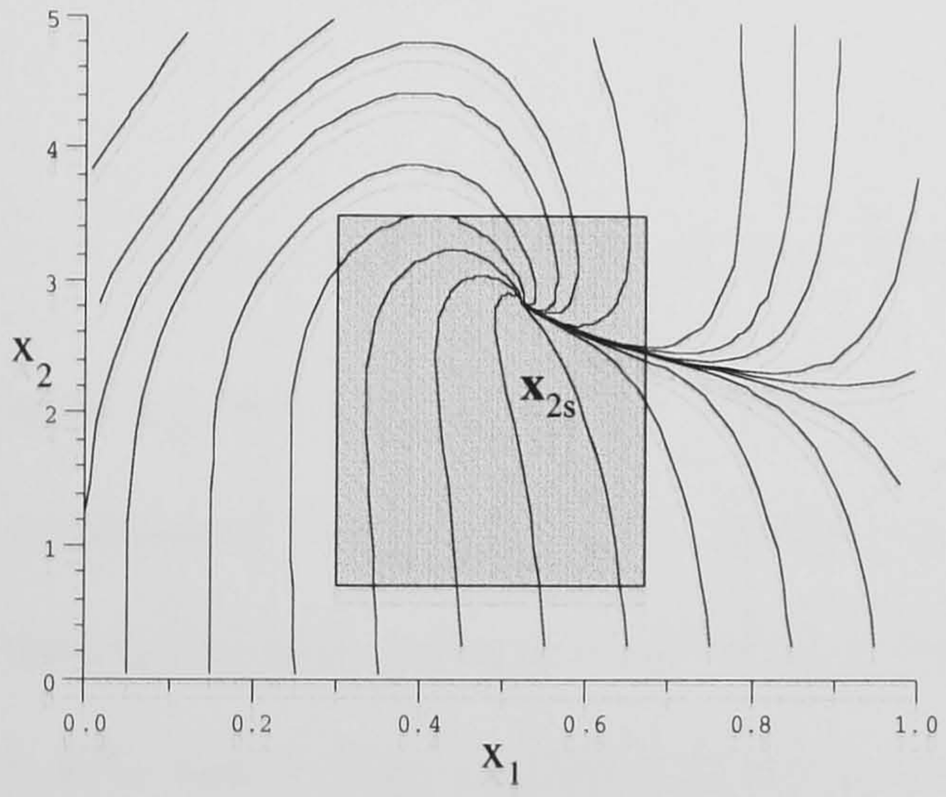

c) hyperbolic control with R_s=0.5 , R_c=0.333 and Da=0.0625.

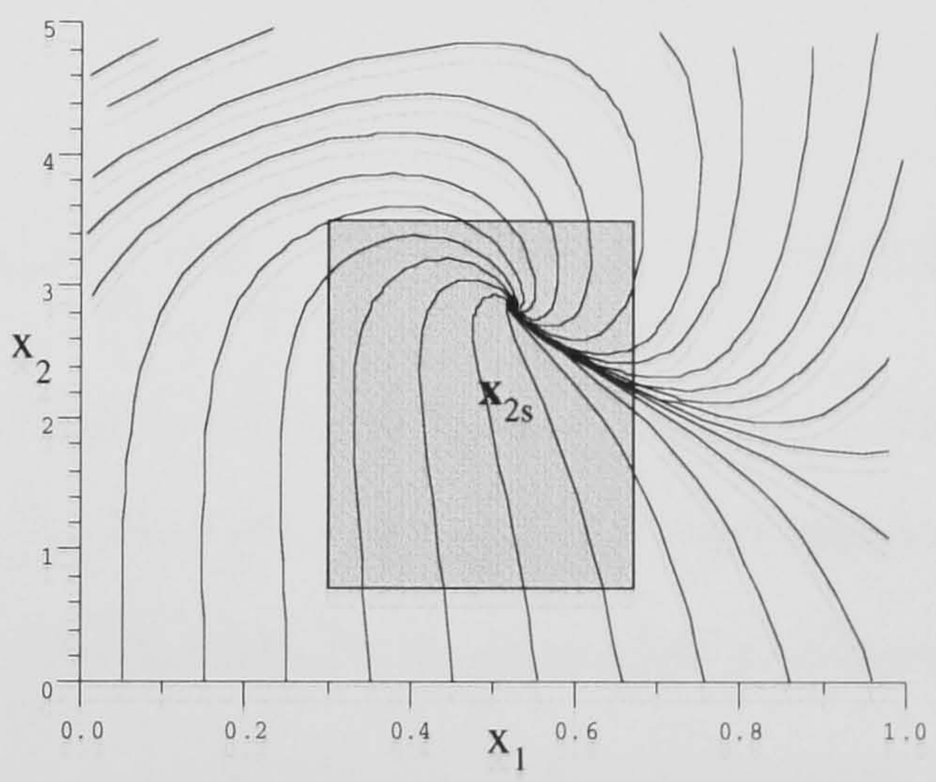

d) input/output linearization with g_1=5.533 and Da=0.0625.

The closed-loop behaviorof for different nonlinear control strategies. The shaded region is of interest.

FIGURE 6.3.2.

To make the new control realization first-order compatible with the previous strategies, we add the proportional term such that the regulation scheme becomes

$$u_{e+p} = RBx_{1s}(Exp(x_2-x_{2s}) -1) + g_1(x_2-x_{2s}) , \qquad (6.3.2)$$

where now g_1=-5.533, and as before B=25.0, x_{1s}=0.442 and x_{2s}=2.763. The resulting first-order dynamics are now similar to those depicted in Figure 6.3.2. Unfortunately, the global behavior of this control configuration has changed significantly due to the appearance of the new unstable steady-state $\mathbf{x}_s$ (Figure 6.3.3.b). The new state-space structure is the consequence of the first-order term being too weak with respect to the even-order terms. To overcome this we introduce the hyperbolic+proportional realization

$$u_{h+p} = Bx_{1s}(R_sSinh(x_2-x_{2s})+R_c(Cosh(x_2-x_{2s}) -1)) + g_1(x_2-x_{2s}) , \qquad (6.4.2)$$

with R_s=1.0 and R_c=0.75. This way the strength of the even degree terms is de-emphasized (see Table 6.3.2) and the unstable steady-state is eliminated. Furthermore, the closed-loop behaviors for both Da=0.05 and Da=0.0625 are illustrated in Figures 6.3.3.c and d. The overall behavior is now robust and similar to the behavior illustrated in Figure 6.3.2.

At this point one may ask why cannot we reduce the effect of the even-order terms by setting R_c=0? The answer is that if we do so, the open-loop even eigenmodes will remain unregulated.

The analysis and conclusions presented also apply for the parameter β. This is because according to the power series expression in Equation (1.2.5.a), the parameters β and Da mainly influence the first-order behavior. However, it is also possible to allow for variations in the dimensionless adiabatic temperature rise B. In this case all nonlinear

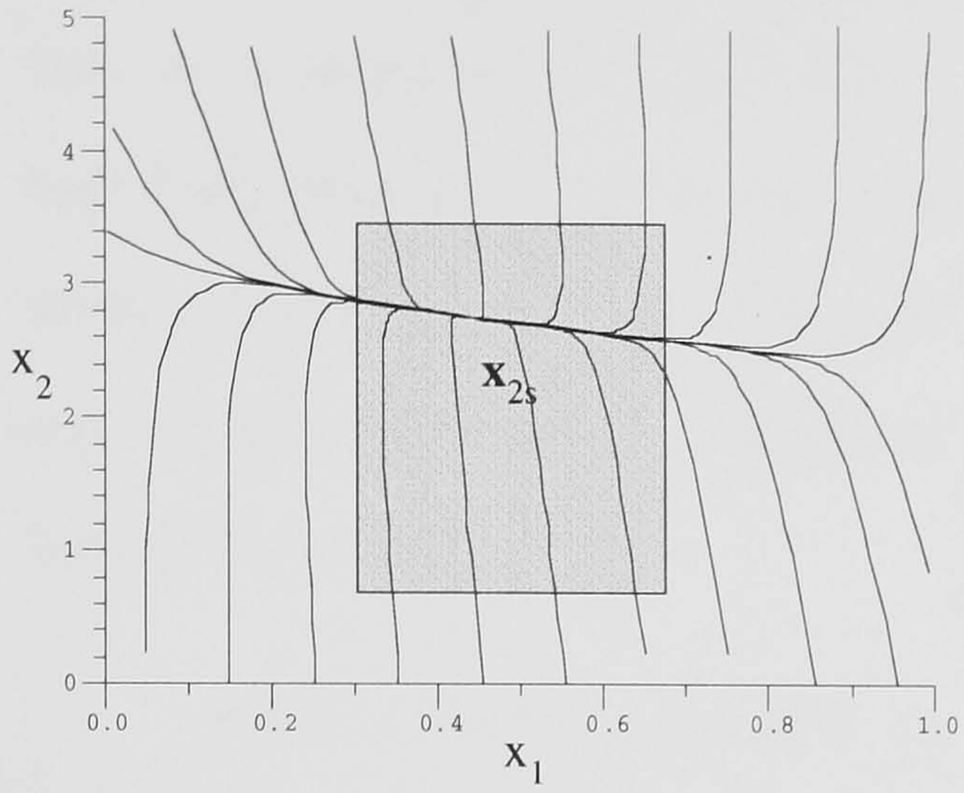

a) exponential control for Da=0.05 and R=1.0.

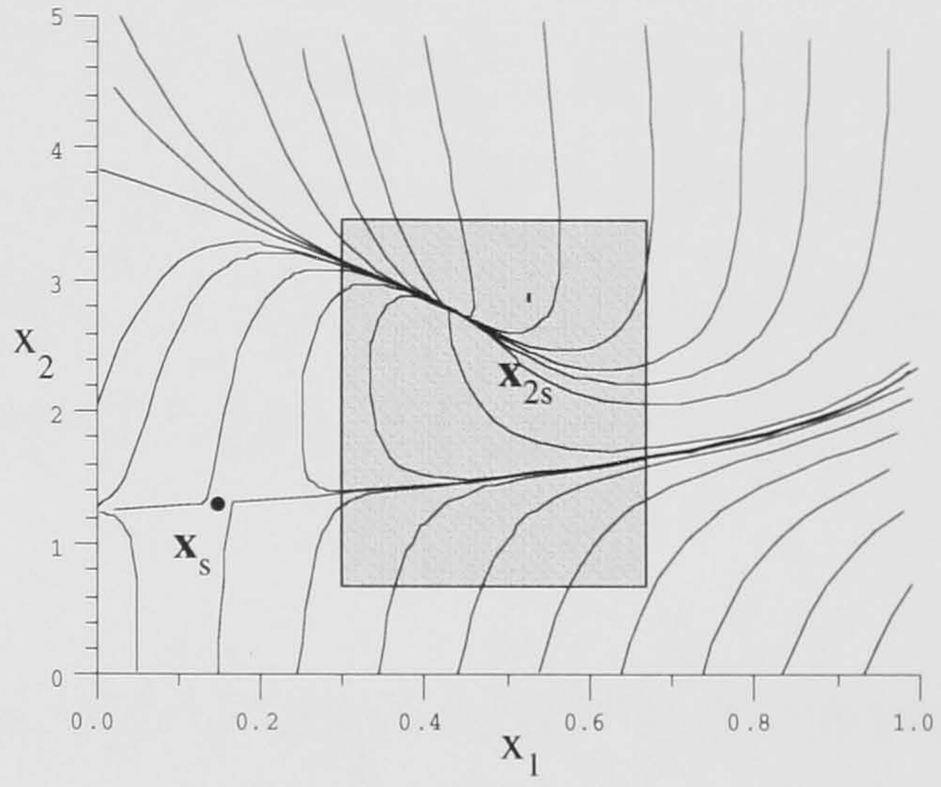

b) exponential+proportional control for Da=0.05 and R=1.0 ; g_1=-5.533.

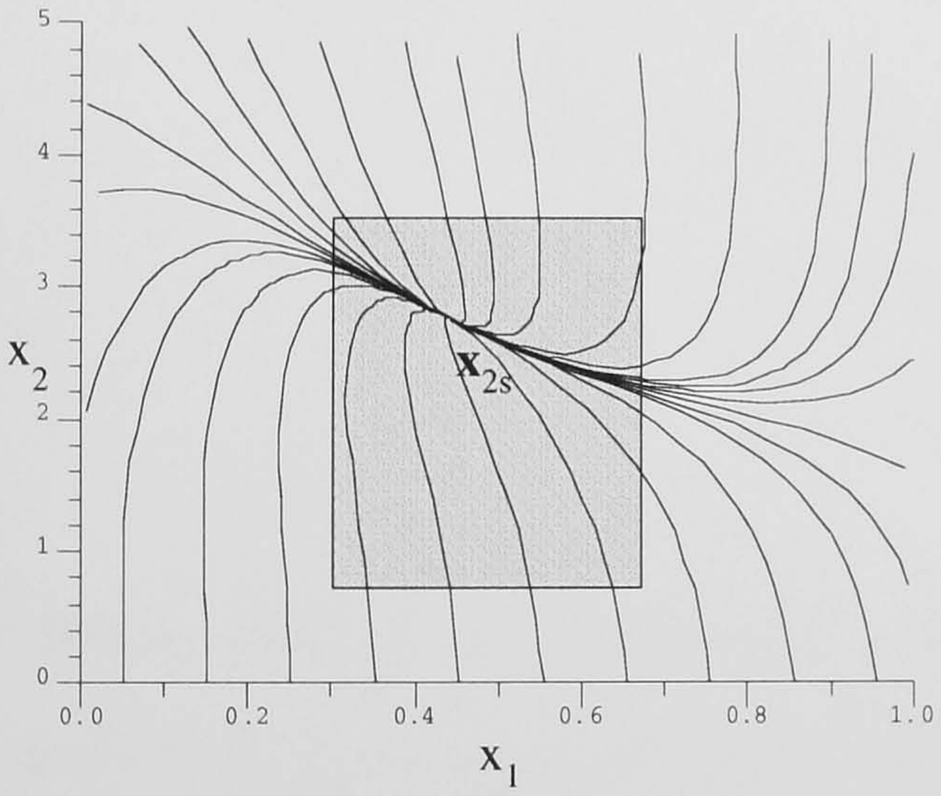

c) hyperbolic+proportional control for Da=0.05 and R_s=1.0, R_c=0.75, g_1=-5.533.

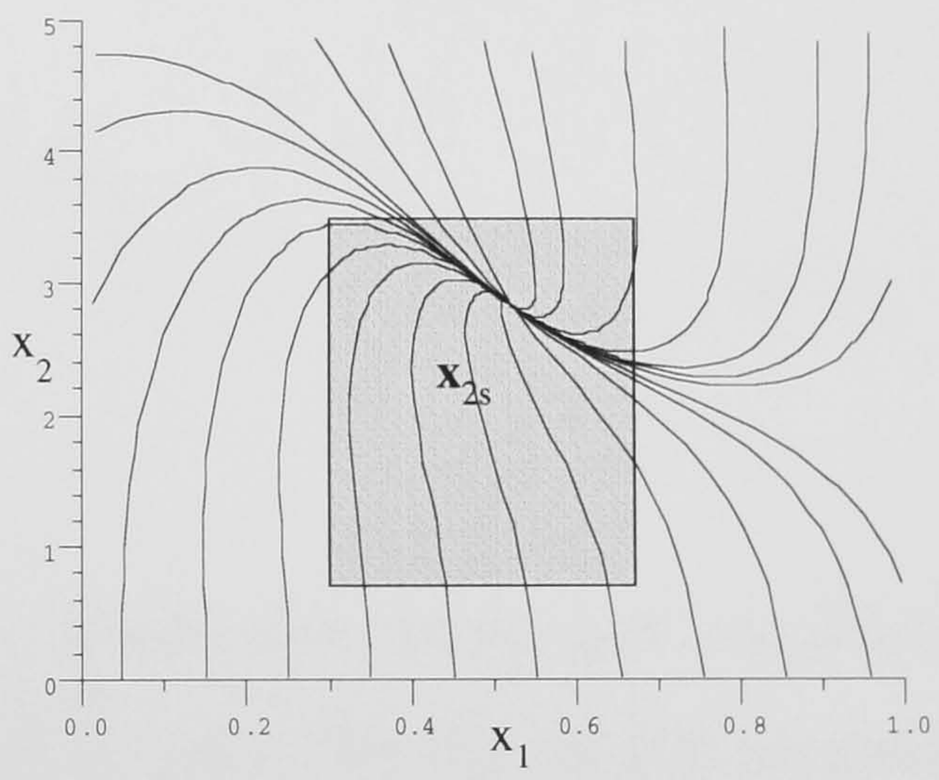

d) hyperbolic+proportional control for Da=0.0625 and R_s=1.0, R_c=0.75, g_1=-5.533.

The closed-loop behavior of the combined control strategies. The shaded region is of interest.

FIGURE 6.3.3.

eigenmodes are affected, and no longer are only the first-order dynamics of relevance. The control realizations u_{h+p} and $u_{i/o}$ illustrate this point in the simulation in Figure 6.3.4. Here B is increased from Da=0.05 to Da=0.0625. The simulation shows that the hyperbolic+proportional regulation scheme exhibits a greater robustness than input/output linearization strategy. This is because, in the latter case the higher-order nilpotent eigenmodes (see Table 6.3.3) are structurally unstable whenever the nonlinear eigenmodes become disturbed.

A final comment is regarding the steady-state drift which appears in all simulated results. This is not a concerning issue since it can be remedied by augmenting the CSTR equations with an integral control action. In this case, the process equations are

$$\begin{bmatrix} \dot{\mathbf{x}} \\ \dot{x}_3 \\ \dot{x}_4 \end{bmatrix} = \begin{bmatrix} \mathbf{F}[\mathbf{x}] - \beta \begin{bmatrix} 0 \\ 1 \end{bmatrix} (u + x_3 + x_4) \\ c_{1i}(x_1 - x_{1s}) \\ c_{2i}(x_2 - x_{2s}) \end{bmatrix} \tag{6.3.1}$$

where x_3 and x_4 are the integral control variables which assure that the open-loop process steady-state $x_s = [x_{1s}, x_{2s}]^t$ never drifts, and c_{1i} and c_{2i} are the specified integration constants. It is easy to verify that the steady-state for this case must always be $[x_{1s}, x_{2s}, x_{3s}, x_{4s}]^t$, and is such that the steady-state values x_{3s} and x_{4s} compensate for a drift. In effect, this procedure generalizes the classic proportional+integral control paradigm.

6.4. Comparison of Control Strategies

Despite the fact that the proposed robust control strategies perform well in the state-space, the question is which of these strategies is the best. This answer is not entirely evident from the state-space analysis because the impression is that all robust realizations posses similar trajectories within the region of interest. We now examine this with a greater detail by using the following procedure.

Table 6.3.2: The eigenvalues of the combined control strategies evaluated at x_{2s} for Da=0.05.

Eigenvalue Sets	Exponential control with R=1.0	Exponential+ proportional control with R=1.0 & g_1=-5.533	Hyperbolic+ proportional control with R_s=1.0, R_c=0.75 & g_1=-5.533	Input/Output Linearization control with g_1=5.533
$\Lambda_1(K)_{c\text{-}l}$	{-25.7384; -2.1581}	{-8.12147 ; -3.17607}	{-8.12147 ; -3.17607}	{-8.176 ; -3.164}
$\Lambda_2(K)_{c\text{-}l}$	{470.865 ; 2.5 ; 0}	{470.865 ; 2.5 ; 0}	{145.408 ; 6.07209 ; 0}	{0 ; $0_{(2)}$}
$\Lambda_3(K)_{c\text{-}l}$	{-5896.0 ; -6.70981 ; $0_{(2)}$}	{-5896.0 ; -6.70981 ; $0_{(2)}$}	{-5896.0 ; -6.70981 ; $0_{(2)}$}	{0 ; $0_{(3)}$}
$\Lambda_4(K)_{c\text{-}l}$	{46256.6 ; 22.7118 ; $0_{(3)}$}	{46256.6 ; 22.7118 ; $0_{(3)}$}	{-73.3+i884.6 ; -73.3-i884.6 ; $0_{(3)}$}	{0 ; $0_{(4)}$}
$\Lambda_5(K)_{c\text{-}l}$	{-228544.0 ; -100.576 ; $0_{(4)}$}	{-228544.0 ; -100.576 ; $0_{(4)}$}	{-228544.0 ; -100.576 ; $0_{(4)}$}	{0 ; $0_{(5)}$}
$\Lambda_6(K)_{c\text{-}l}$	{656597.0 ; 650.789 ; $0_{(5)}$}	{656597.0 ; 650.789 ; $0_{(5)}$}	{5.517+i17.02 ; 5.517+i17.02 ; $0_{(5)}$}x 10^3	{0 ; $0_{(6)}$}

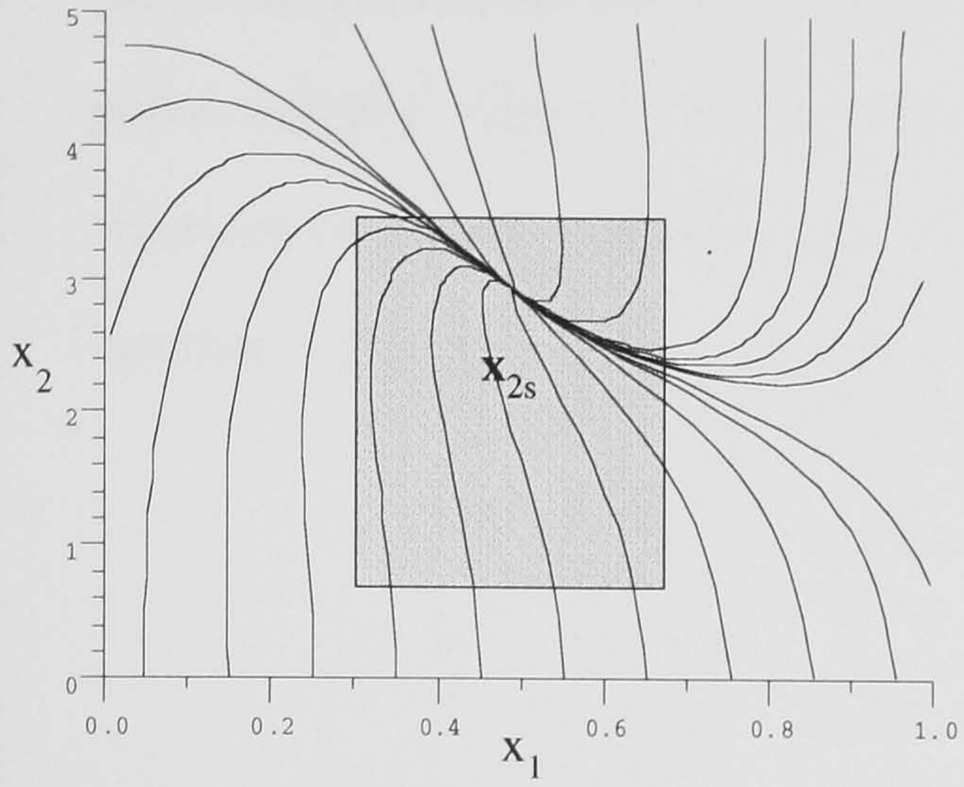

a) hyperbolic+proportional control for B=31.25, Da=0.05 and R_s=1.0, R_c=0.75, g_1=-5.533.

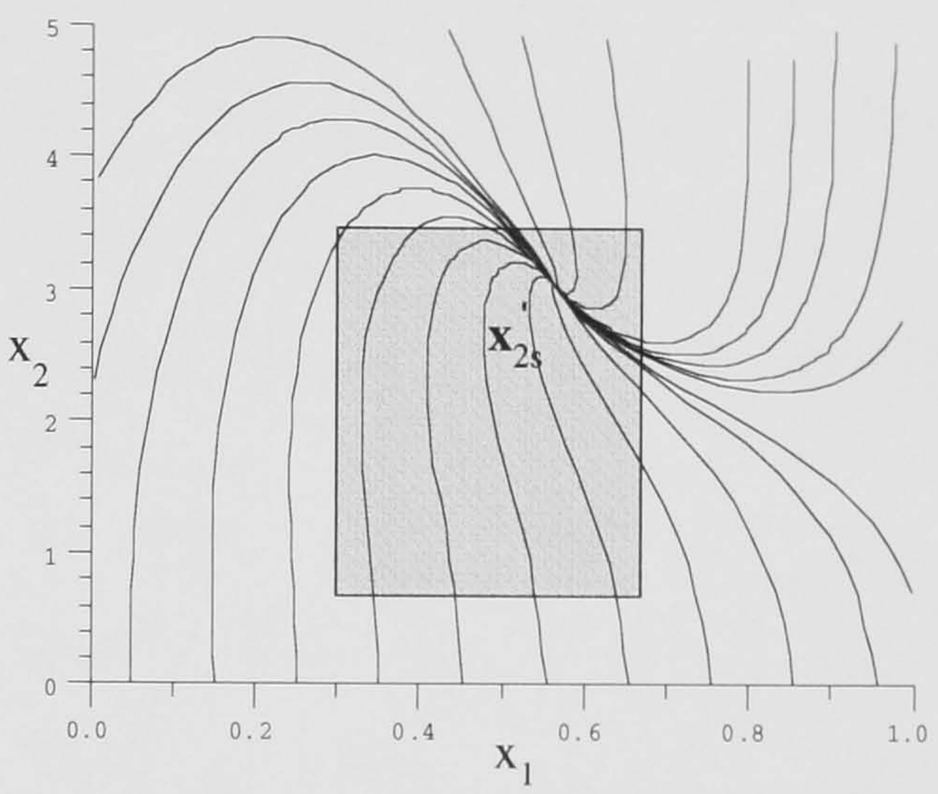

b) hyperbolic+proportional control for B=31.25, Da=0.0625 and R_s=1.0, R_c=0.75, g_1=-5.533.

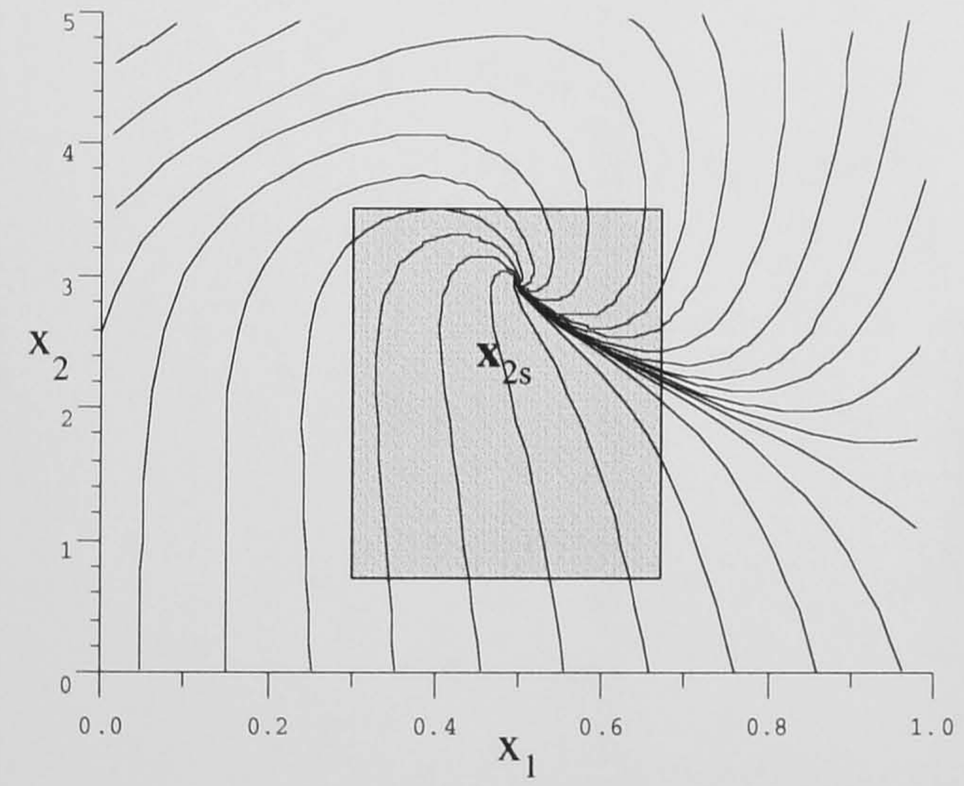

c) input/output linerization control for B=31.25, Da=0.05 and g_1 = 5.533.

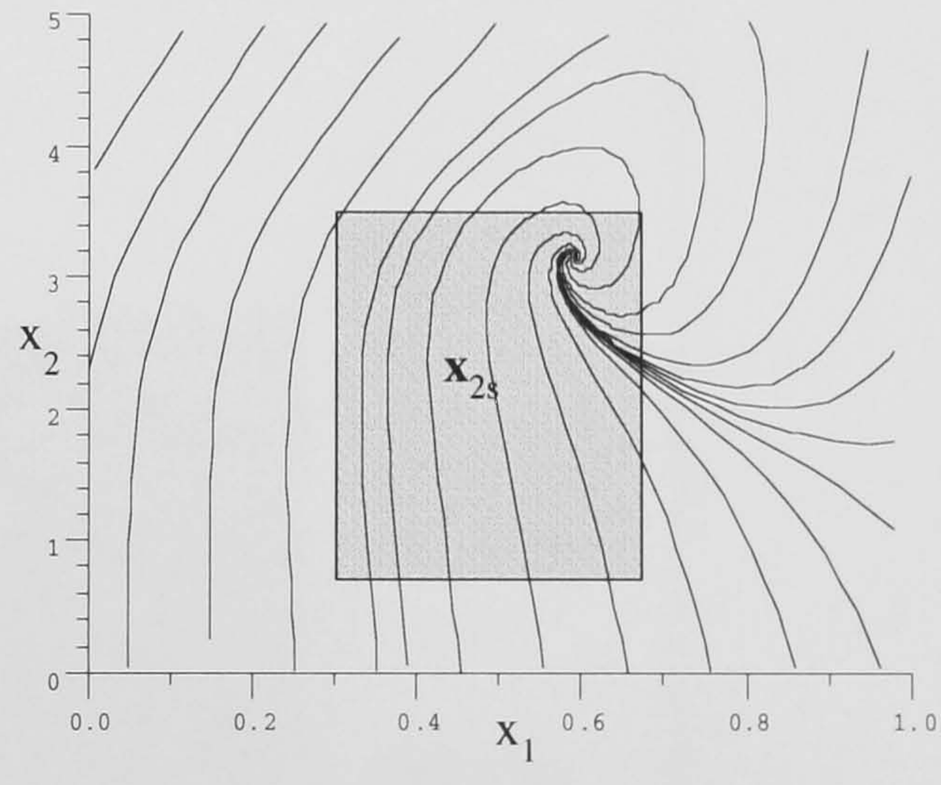

d) input/output linerization control for B=31.25, Da=0.0625 and g_1 = 5.533.

The closed-loop process robustness for various parameter variations. The shaded region is of interest.

FIGURE 6.3.4.

First, we select extreme points on the boundary of the region of interest. In the present case these are the four corner points illustrated in Figure 6.4.1. Next we apply the points as initial values for computing the solutions of $x_1(t)$ and $x_2(t)$, and then we let these solutions be the representative impulse responses for the sub-regions A, B, C and D. For instance, the first-order regulated CSTR process with $u_p(g_1=5.533)$ and parameters

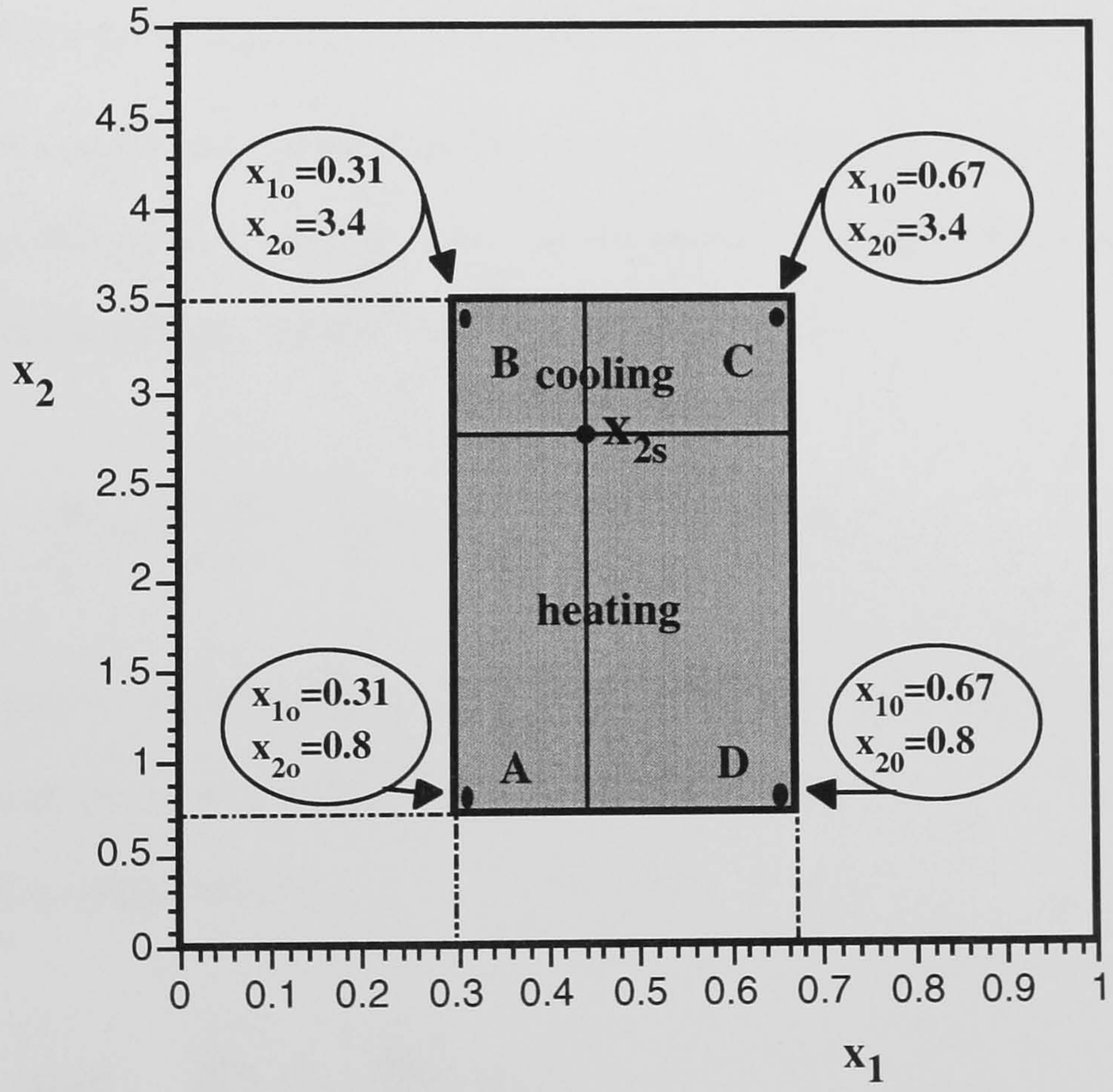

FIGURE 6.4.1: The four initial points used in control evaluations.

B=25.0, Da=0.05, β=3.0 and x_{2c}=0.0 has the representative impulse responses illustrated in Figure 6.4.2. In all the cases illustrated the transient response subsides, and the process settles at the steady-state $\mathbf{x}_{2s}$. However, the four impulse response solutions do not reveal much about the temporal behavior of $u_p(t)$. For the four regions these behaviors are obtained by using Equation (6.2.4), and are depicted in the Figure 6.4.3. They show that before the process comes to a rest, or u_p settles at 0, the control action is either positive or negative. It is negative whenever the controller needs to provide heat, and it is positive whenever it needs to cool the reaction. For example, from Figure 6.4.3 it is follows that in the regions A and D the controller needs to supply heat because the reactor temperatures are below the required value, x_{2s}=2.763021. In the regions B and C, the reactor temperatures exceed that of x_{2s} and the controller must provide cooling.

By evaluating a control function and determining its behavior we have not completely characterized a control law. An important practical control parameter is the speed of a control strategy, which is defined as

$$\frac{d\mathbf{u}}{dt} = \frac{\partial \mathbf{u}}{\partial \mathbf{x}} \frac{d\mathbf{x}}{dt} = \frac{\partial \mathbf{u}}{\partial \mathbf{x}} \dot{\mathbf{x}} = \frac{\partial \mathbf{u}}{\partial \mathbf{x}} \{\mathbf{F}[\mathbf{x}] + \mathbf{B}[[\mathbf{x}]]\, \mathbf{u}\}, \tag{6.4.1}$$

or as the product of the control gain matrix $\partial\mathbf{u}/\partial\mathbf{x}$ and the closed-loop process response $d\mathbf{x}/dt$. Because this is in general a vector quantity, we represent it in a scalar form by applying the Euclidean norm

$$\left\| \frac{d\mathbf{u}}{dt} \right\|_2 = \left\| \frac{\partial \mathbf{u}}{\partial \mathbf{x}} \dot{\mathbf{x}} \right\|_2 \leq \left\| \frac{\partial \mathbf{u}}{\partial \mathbf{x}} \right\|_2 \left\| \frac{d\mathbf{x}}{dt} \right\|_2 \tag{6.4.2}$$

where $\|\partial\mathbf{u}/\partial\mathbf{x}\|_2$ is the absolute control gain, and $\|d\mathbf{x}/dt\|_2$ is the absolute closed-loop response. Therefore, to provide a more detailed characterization of a control strategy, we also need to supply the information for the absolute control speed $\|d\mathbf{u}/dt\|_2$. For the proportional controller with g_1=5.533 the absolute gains are given in Figure 6.4.3, while

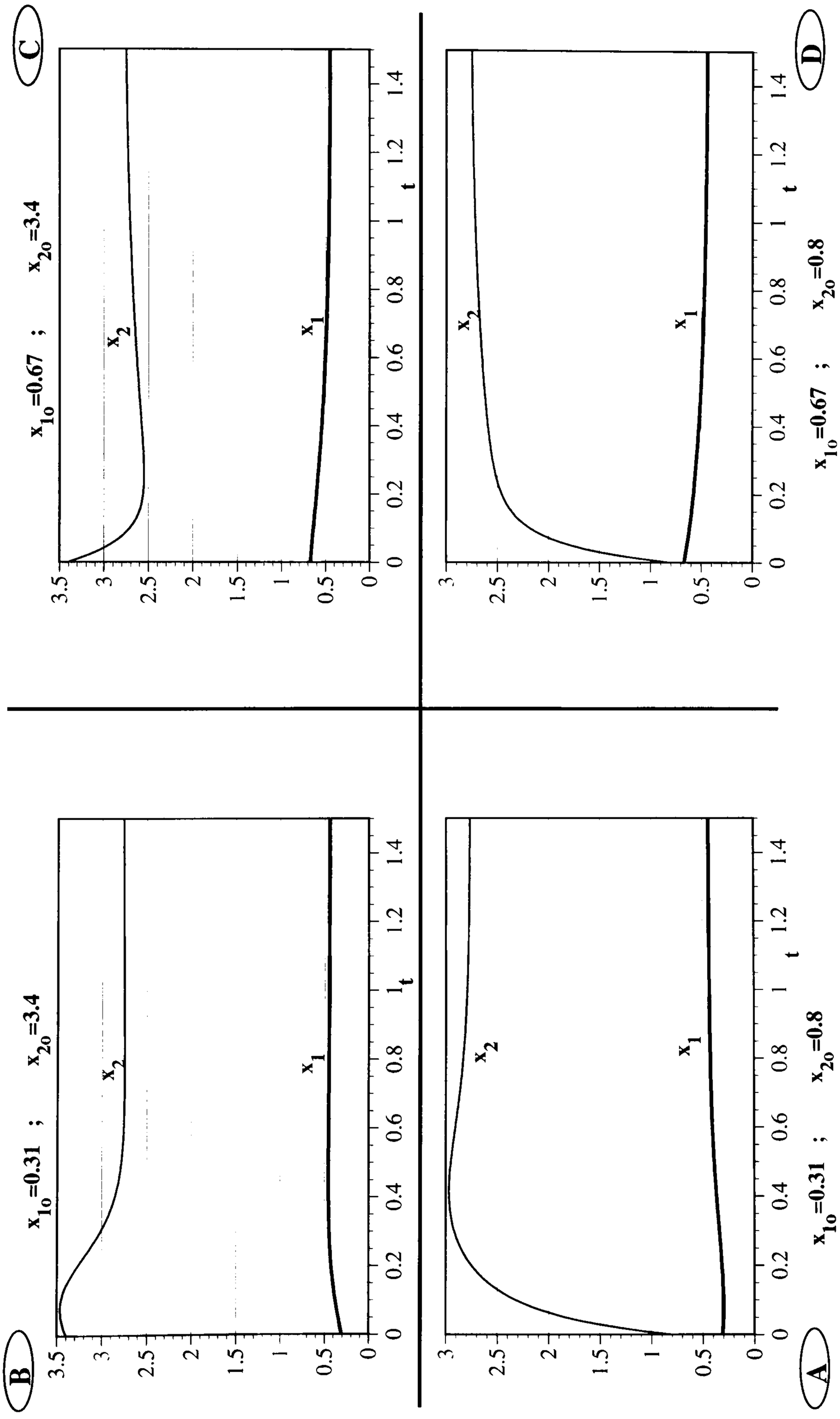

The representative impulse responses for the $u_p(g_1=5.533)$ regulated CSTR.

The parameters are B=25.0, Da=0.05, β=3.0, x_{2c}=0.0.

FIGURE 6.4.2.

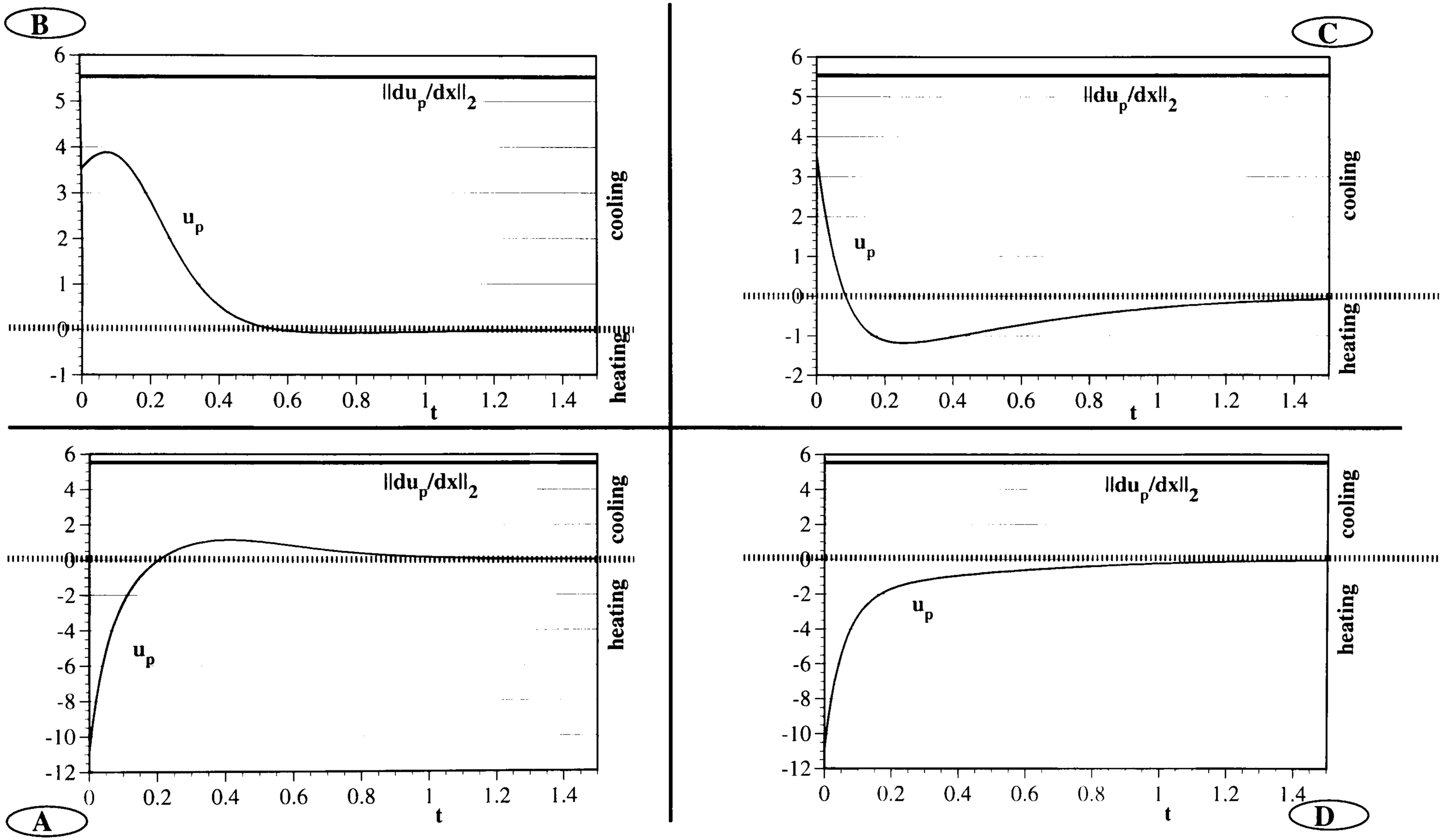

The proportional control actions and the control gains for the four corner points. The CSTR parameters are B=25.0, Da=0.05, β=3.0 and x_{2c}=0.0.

FIGURE 6.4.3.

the absolute speeds are shown in Figure 6.4.4. Note that the control gains are always constant because the law is proportional. Also, observe that since the speed requirements are greater in the regions A and D, the controller must have the ability to provide heating more rapidly than cooling.

One may now pose the question: what happens if the $u_p(g_1=5.533)$ control realization satisfies all the characteristics in Figure 6.4.3, except that it is slower than the requirements called for in Figure 6.4.4? In this event the closed-loop operation would not be robust in all regions of interest because the process can exhibit unpredictable behavior for the disturbances that demand a rapid control action. In other words, the less a control strategy keeps up with the closed-loop speed requirement, the more certain is occurrence of an unpredictable process behavior. It must be possible for the controller to respond with the required speed if the desired regulation is to be achieved.

By applying the procedure proposed we now compute the same results for all control strategies presented in Figures 6.3.2-4. In computing these solutions we have used the Damköhler value Da=0.0625. The simulation results are shown in Figures A.VI.1-8 in Appendix VI. For instance, in Figure A.VI.1, the representative time responses are depicted for the proportional control law with $g_1=5.533$. From the figure it is evident that it performs poorly in regions A and B. This is especially true in region B, where the reactive behavior is significant and causes a dramatic increase in both u_p and $\|du_p/dt\|_2$ over a short period of time. Therefore, in this region the closed-loop process operation becomes rather unrealistic because it is quite unlikely that any real control element could keep up with the required speed demand. However, for the cubic law described in Figure 6.3.2, the representative responses are as illustrated in Figure A.VI.2. In this case, the control values are more manageable and the maximum speed requirement has decreased substantially. Nevertheless, the control scheme still appears to be unrealistic since the required speeds remain large in the regions A and D. Next we compute characteristic responses for the hyperbolic control law. The results are illustrated in Figure A.VI.3.

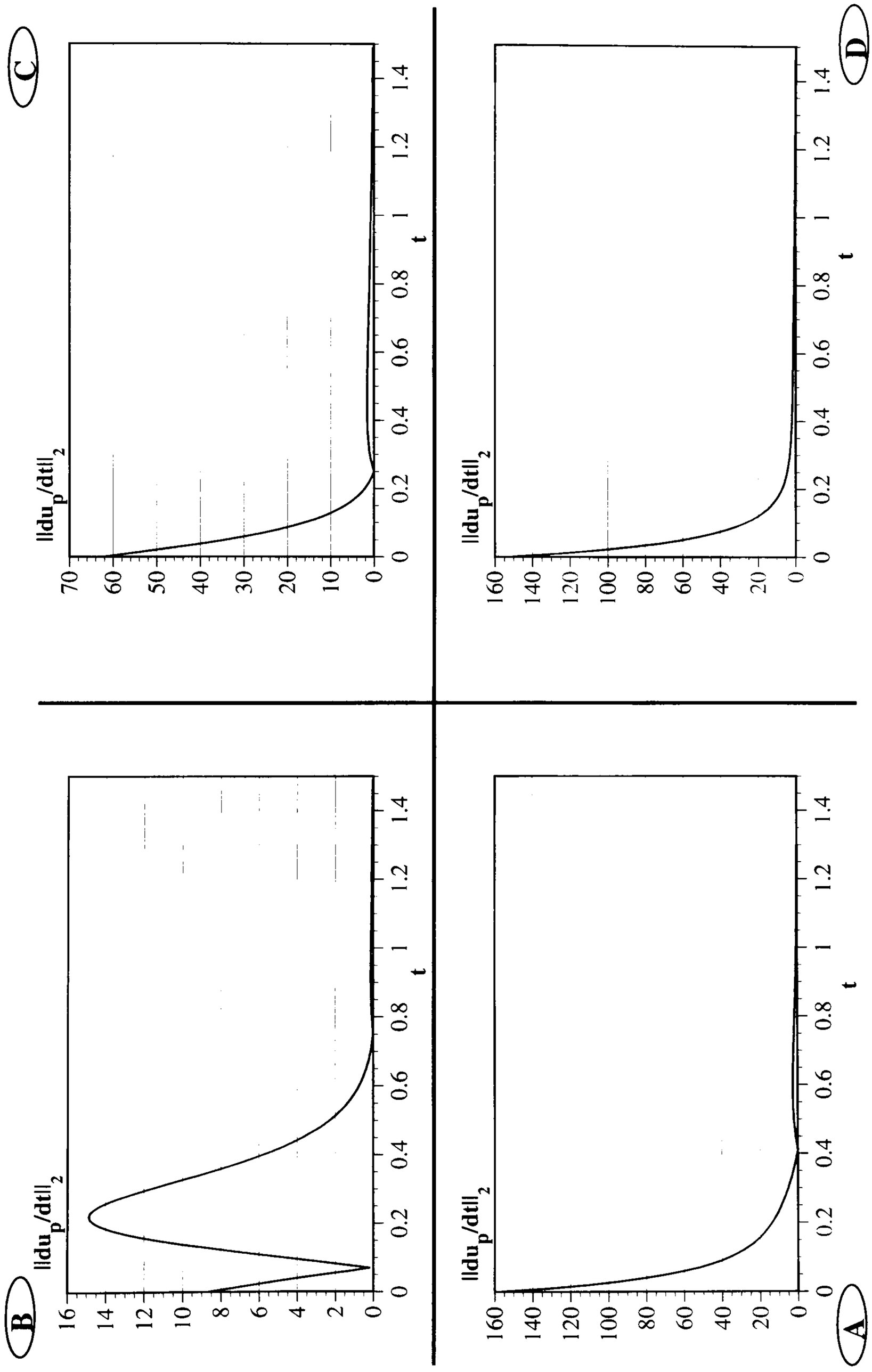

The required u_p control speeds for the four corner points. The CSTR parameters are B=25.0, Da=0.05, β=3.0 and x_{2c}=0.0.

FIGURE 6.4.4.

The u_h law has impulse responses similar to that of the u_c strategy, while the maximum speed requirements are significantly reduced.

Proceeding in this manner we analyze the remaining control realizations. We then look for the best control strategy by comparing the control speed results. That is, we look for the closed-loop realization for which the control speed requirements are least demanding in the four regions considered. By doing so we find that among the proposed control strategies there does not exist one single realization which provides the best solution in all four regions. In regions A and D the exponential control law works best, whereas in regions B and C the input/output linearization control is best. The two control realizations exhibit speed demands illustrated in Figure 6.4.5. Hence, from the control speed point of view, the combined control strategy provides the best overall control system for the CSTR problem considered.

It is also interesting to observe that the best nonlinear control realization in Figure 6.4.5 outperforms the u_p (g_1 =5.533) realization even in the ideal case (Figure 6.4.4). In addition, note that all nonlinear realizations have variable gains, and as such resemble continuous gain scheduling methods. Finally in Figures A.VI.6-8, the temporal responses which characterize the higher gain control strategies are depicted. The results show that the demand for control speed increase as gain increases.

6.5. CONSTRAINED CONTROL DESIGN

By using the control analysis presented we can easily address the constrained control problem. This is because any practical control realization is usually a subject to the following real constraints

$$|\mathbf{u}|_2 \leq u_{max}\,, \tag{C.1}$$

$$\left|\frac{\partial \mathbf{u}}{\partial \overleftrightarrow{\mathbf{x}}}\right|_2 \leq g_{max}\,, \text{ and} \tag{C.2}$$

$$\left|\frac{d\mathbf{u}}{dt}\right|_2 \leq r_{max}\,. \tag{C.3}$$

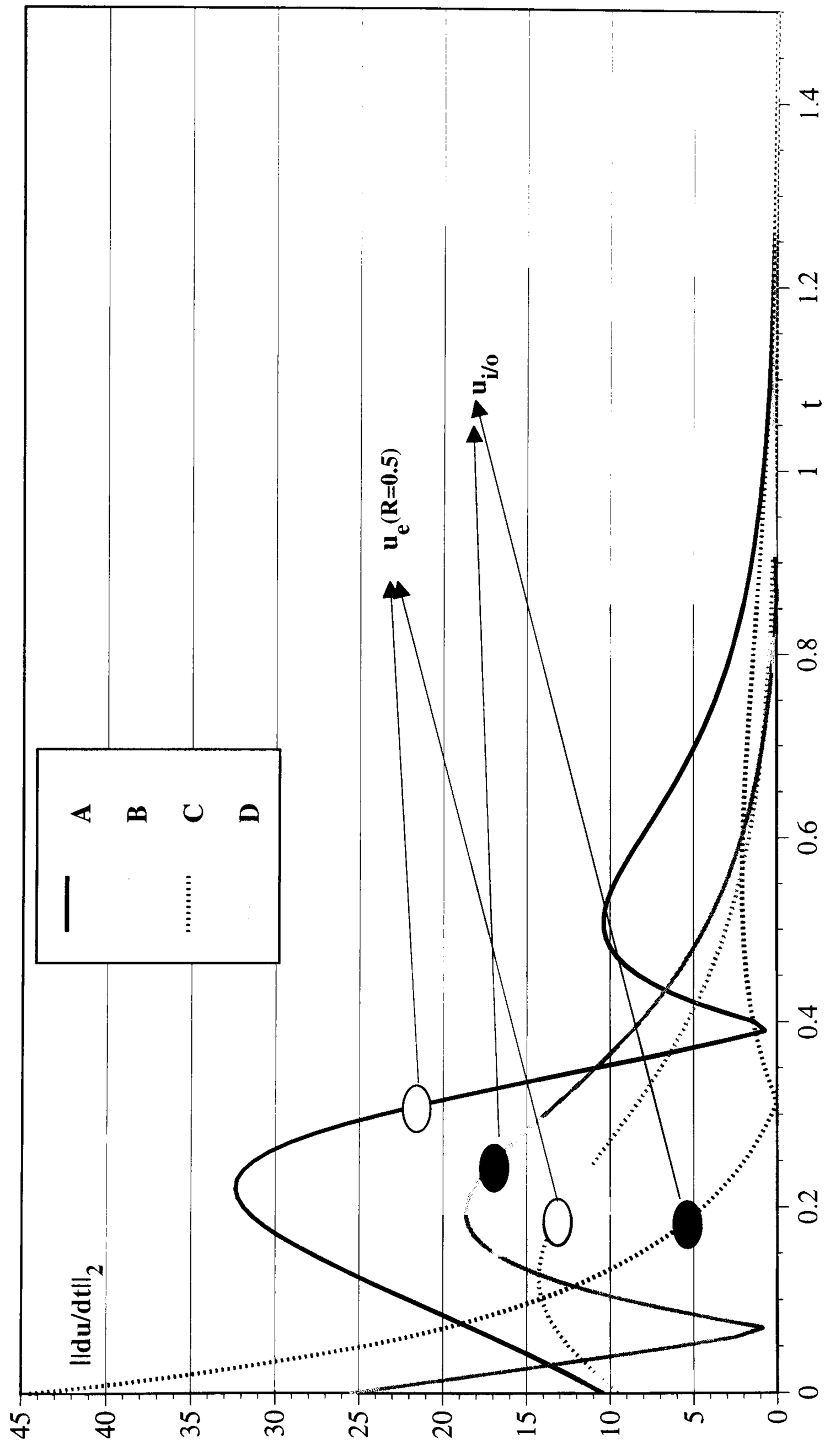

The four corner speed requirements for the combined control strategy with $u_{i/o}$ and u_e(R=0.5). The CSTR parameters are B=25.0, Da=0.0625, β=3.0 and x_{2c}=0.0.

FIGURE 6.4.5.

Thus, if for the control examples of the previous section we impose the real constraints u_{max}=8.0, g_{max}=14.0 and r_{max}=250.0, then according to the figures in Appendix VI only three control strategies meet these specifications. These are u_e(R=0.5), $u_{i/o}$, and u_{h+p} illustrated in Figures A.VI.4-6. If, however, the requirement for r_{max} is further reduced to 50.0, then the control combination in Figure 6.4.5 is the only possible solution. This shows that a control designer may often find a feasible control realization by correctly identifying and compensating open-loop process nonlinearities.

6.6. CHAPTER VI SUMMARY

Table 6.6.1 summarizes topics of significance covered in Chapter VI. The topics in bold letters identify ideas that are conceived during the preparation of this thesis.

Table 6.6.1: Topics covered in Chapter VI.

nonlinear state feedback control design for CSTR regulation
• two-dimensional control strategies - proportional - **cubic** - **exponential** - **hyperbolic** - input/output linearization - **combined control strategies**
• robustness and performance analysis - **impulse response characterization** - **control response characterization** - **control speed requirement**
• constrained control analysis
• **relations among control characteristics and nonlinear process structure**

CHAPTER 7 - POLYMETHYLMETHACRYLATE REACTOR CONTROL - CASE STUDY

7.1. TWO-DIMENSIONAL PMMA PROCESS MODEL

To demonstrate how the control results developed in Chapter 6 can be applied, we consider the two-dimensional polymethylmethacrylate (PMMA) process studied by Jasinghani and Ray (1977), and described in Section 5.4. The governing equations derived from Equation (5.4.1) are

$$\begin{bmatrix} \dot{x}_1 \\ \dot{x}_2 \end{bmatrix} = \begin{bmatrix} 1-x_1-Da_p w\, x_1 Exp\left\{\dfrac{x_2}{1+x_2/\gamma_p}\right\} \\ -x_2+BDa_p w\, x_1 Exp\left\{\dfrac{x_2}{1+x_2/\gamma_p}\right\} - \beta[u+(x_2-x_{2c})] \end{bmatrix} = \begin{bmatrix} f_1(\mathbf{x}) \\ f_2(\mathbf{x}) \end{bmatrix} - \begin{bmatrix} 0 \\ 1 \end{bmatrix} \beta u \qquad (7.1.1)$$

where the parameters are defined in Table 5.4.1, $\mathbf{b}=\beta[0,1]^t$ is the control vector and u is a control strategy. For the unstable steady-state

$$\mathbf{x}_{2s}=[0.223416,\ 1.331286]^t\ ,$$

the 5-order open-loop power series approximation and the corresponding eigenspectra are presented in Table A.V.3. The inspection of the geometric spectra indicates that **b** is not an eigenvector and the process is at least 5-order stabilizable. Thus, we can stabilize the first-order dynamics at $\mathbf{x}_{2s}$ by considering the proportional control law

$$u(\mathbf{x}) \equiv u_p(\mathbf{x}) = \frac{g_{11}}{\beta}(x_1 - x_{1s}) + \frac{g_{12}}{\beta}(x_2 - x_{2s}) = \frac{g_{11}}{\beta}\overleftrightarrow{x}_1 + \frac{g_{12}}{\beta}\overleftrightarrow{x}_2, \qquad (7.1.2)$$

where g_{11} and g_{12} are the coefficients to be determined, and where x_{1s}=0.223416 and x_{2s}=1.331286. This is accomplished by substituting the last expression into Equation (7.1.1), and then assigning the first-order closed-loop eigenvalues to the Jacobian matrix

$$\frac{\partial}{\partial \mathbf{x}}\left\{\begin{bmatrix} f_1(\mathbf{x}) \\ f_2(\mathbf{x}) \end{bmatrix} + \begin{bmatrix} 0 \\ 1 \end{bmatrix}\beta u_p\right\}\Bigg|_{\mathbf{x}=\mathbf{x}_{2s}} = \begin{bmatrix} 0.459375 & -0.827057 \\ -17.5125 - g_{11} & 2.92468 - g_{12} \end{bmatrix}. \qquad (7.1.3)$$

Now, by applying the Routh-Hurwitz criterion one can verify that for any stabilizing state feedback realization the conditions

$$g_{12} > 3.38406 \text{ and}$$

$$g_{11} < -\frac{13.1403 + 0.459375\, g_{12}}{0.827057}$$

must be met in order for both closed-loop eigenvalues to be negative. Hence, for the PMMA process considered, there does not exist a stabilizing state feedback realization at $\mathbf{x}_{2s}$ for which g_{11}=0. Instead, both state variables must be considered to achieve the first-order control objective. The Routh-Hurwitz conditions are satisfied for g_{11}=-35.0 and g_{12}=10.0, and the corresponding closed-loop state-space behavior is depicted in Figure 7.1.1.a. The results show that the process is stabilized at $\mathbf{x}_{2s}$, and contains the reaction boundary which separates the stable domain from the reactive region.

Next we consider the polynomial controller which forces all eigenmodes to be nilpotent inside the first three even-degree terms. That is, we cancel out nonlinearities due

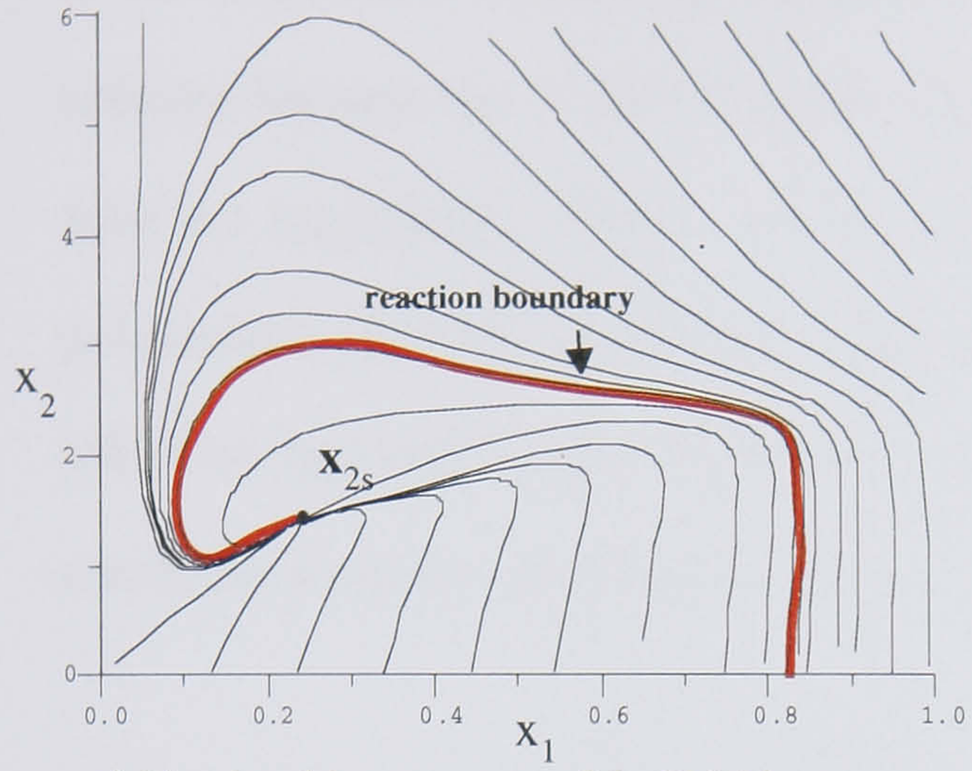

a) The closed-loop response of the PMMA process regulated by applying the proportional controller u_P with the gains g_{11}=-35.0 and g_{12}=10.0. The closed-loop first-order eigenvalues are:

$\mathbb{A}_1\{\mathbb{R}\}_{c\text{-}l} = \{ -3.30797 + i51986 \;\; ; \;\; -3.30797 - i51986\}$

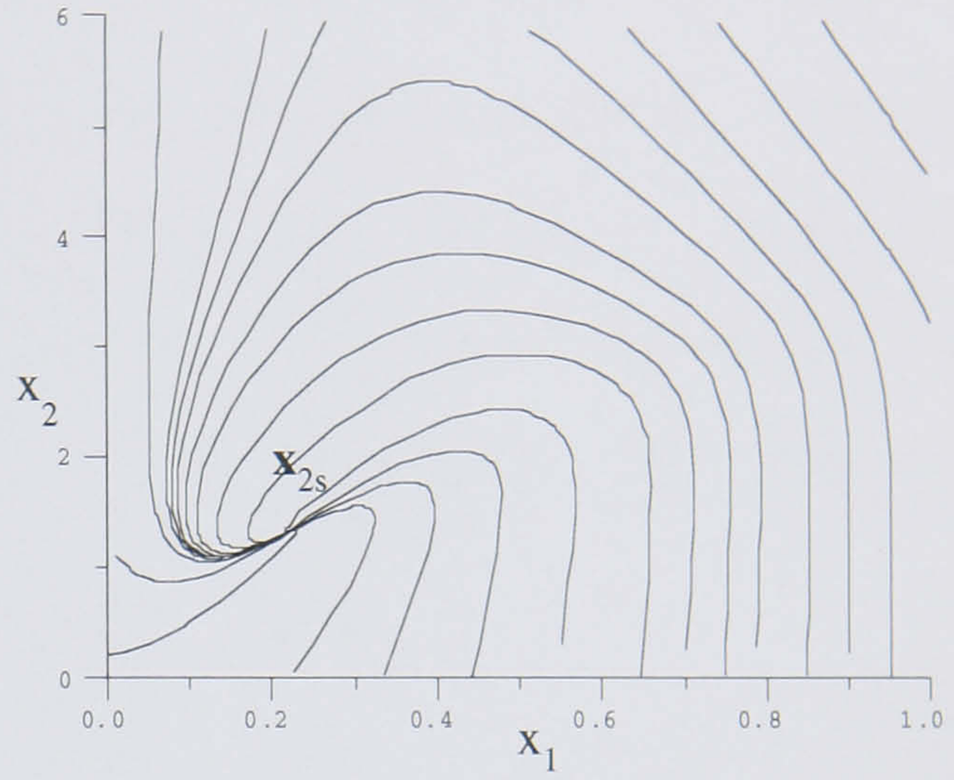

b) The closed-loop response of the PMMA process with the compensated first and second-order nonlinearities by using the u_s control law with the switching parameters L_2=1 and L_4=L_6=0.

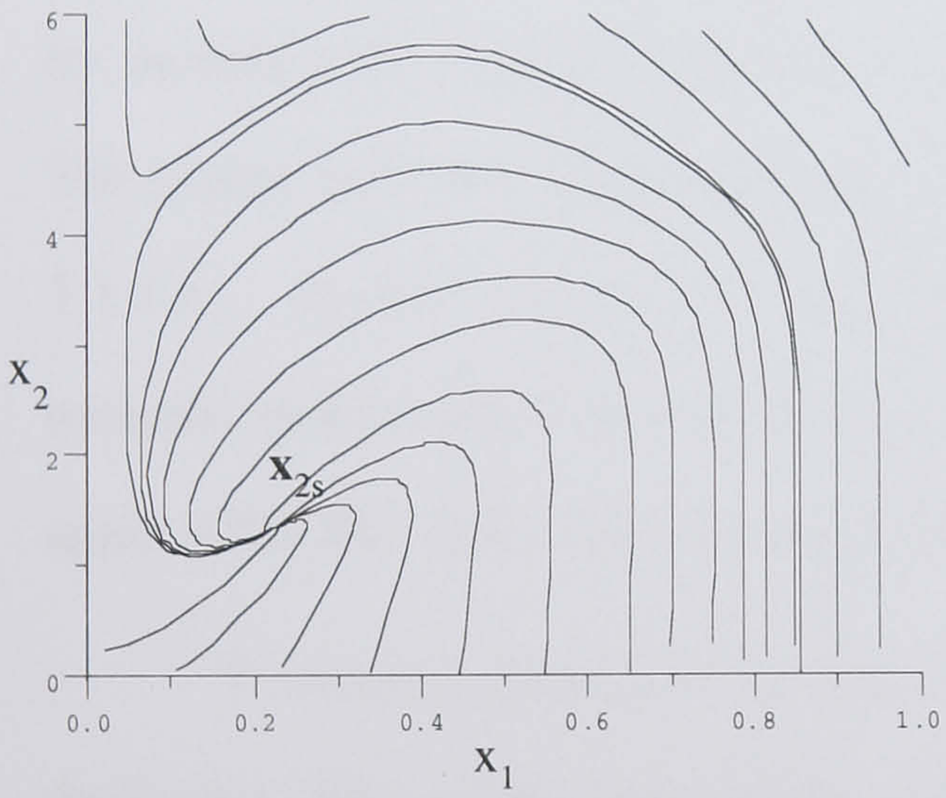

c) The closed-loop response of the PMMA process with the compensated first, second and fourth-order nonlinearities by using the u_s control law with the switching parameters L_2=L_4=1 and L_6=0.

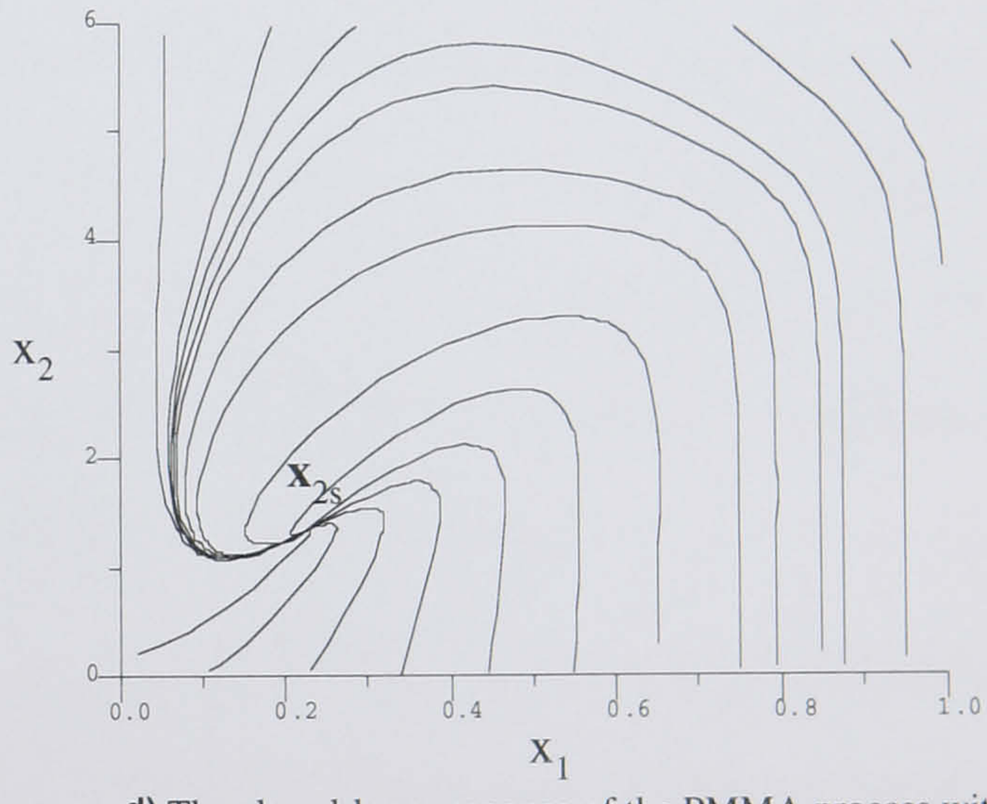

d) The closed-loop response of the PMMA process with the compensated first, second, fourth and sixth-order nonlinearities by using the u_s control law with the switching parameters: L_2=L_4=L_6=1.

The 2D-PMMA closed-loop performances obtained by the proportional and polynomial type controllers.

FIGURE 7.1.1.

to the even-order open-loop idempotent modes listed in Table A.V.3. This choice is selected because the 3- and 5-degree idempotent modes are already stable and, therefore, need no regulation. Thus, to accomplish this we consider the 6-order. even only, polynomial feedback realization defined in Table 7.1.1. Clearly this controller has no effect on any odd-degree eigenmode. Therefore, to assure that $\mathbf{x}_{2s}$ remains stable we create the 6-order polynomial control law

$$u(\mathbf{x}) \equiv u_s(\mathbf{x}) = u_p(\mathbf{x}) + u_{even}(\mathbf{x}). \tag{7.1.4}$$

For this control law the closed-loop state-space behaviors are also illustrated in Figure 7.1.1. In Figure 7.1.1.b the global behavior of the proportional only scheme is improved by including the regulated quadratic term. Observe that the reaction boundary thins out. The global behavior deteriorates once the regulated fourth-degree term is added (Figure 7.1.1.c). In this instance the regulation has increased the global complexity since the unstable steady-state is formed at higher temperature. This behavior, however, improves again when the sixth-order regulated term is included, Figure 7.1.1.d.

To obtain a better global regulation we can either continue to evaluate and regulate the higher-order power series terms, or we can consider the closed form nonlinear control law

$$u(\mathbf{x}) \equiv u_T(\mathbf{x}) = u_P(\mathbf{x}) - \frac{g_T(\mathbf{x})}{\beta}, \tag{7.1.5}$$

where $u_P(\mathbf{x})$ is defined in Equation (7.1.2), and where

$$g_T(\mathbf{x}) = \left[\frac{\partial f_2(\mathbf{x})}{\partial \mathbf{x}}\bigg|_{\mathbf{x}=\mathbf{x}_{2s}}\right] \overleftrightarrow{\mathbf{x}} - f_2(\mathbf{x}) \tag{7.1.6}$$

is defined in the same fashion as the globally linearizing function g(x), Equation (5.3.1). If we elect the first alternative numerical computations rapidly become unmanageable, and the question whether we have compensated enough terms remains. On the other hand, if

Table 7.1.1: The even only 6-order polynomial controller.

$$u_{even}(\mathbf{x}) = -\sum_{j=1}^{3} L_{2j} \frac{B + v_{2j}}{\beta\ (2j)!}\, \mathbf{c}_{2j}\, \mathbf{z}_{2j}(\overleftrightarrow{\mathbf{x}})$$

where for any subscript k=2j, L_k is the switching parameter that is either 0 or 1,

v_k is such that $\begin{bmatrix} 1 \\ v_k \end{bmatrix}$ is the nilpotent eigenvector in $\chi_k\{R^2\}_{open\text{-}loop}$,

and $\mathbf{c}_k = \left[\frac{\partial^k [f_1(\mathbf{x})]}{\partial \mathbf{x}^k}\right]_{1 \times (k+1)}\Big|_{\mathbf{x}=\mathbf{x}_{2s}}$.

k=2 => v_2=4.44204* and

$\mathbf{c}_2$= [11.5885 , 0.05745 , -0.60023] ;

which determines the 2-form closed-loop eigenvalue set

$$\Lambda_2\{R\} = \{0,\ 0_{(2)}\}$$

k=4 => v_4=5.22927* and

$\mathbf{c}_4$= [2.41768E3 , -6.44654E2 , 90,7274 , -12.6654 , 0.379176] ;

which determines the 4-form closed-loop eigenvalue set

$$\Lambda_4\{R\} = \{0,\ 0,\ 0,\ 0_{(2)}\}$$

k=6 => v_6=5.41075* and

$\mathbf{c}_6$= [2.21002E5 , -7.60057E3 , -17.1552E3 , 3.86273E3 , -4.25603E2 , 17.7079 , -0.273252] ;

which determines the 6-form closed-loop eigenvalue set

$$\Lambda_6\{R\} = \{0,\ 0,\ 0\ ,\ 0\ ,\ 0\ ,\ 0_{(2)}\}$$

*Note, v_{2j} is selected because it already satisfies a nilpotent solution of the open-loop characteristic equations. For this reason the last eigenvalue has multiplicity 2, *i.e.*, the corresponding closed-loop eigenvector must have multiplicity 2.

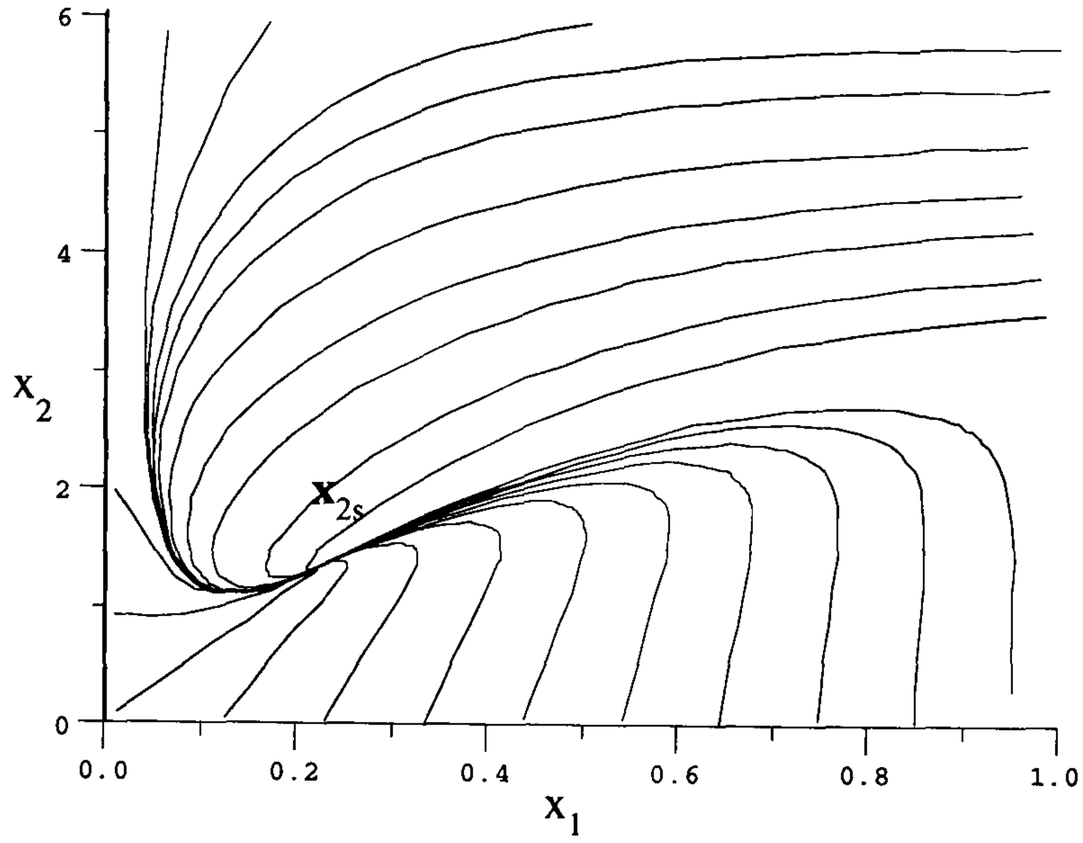

a) The closed-loop response created by using the u_T control law.

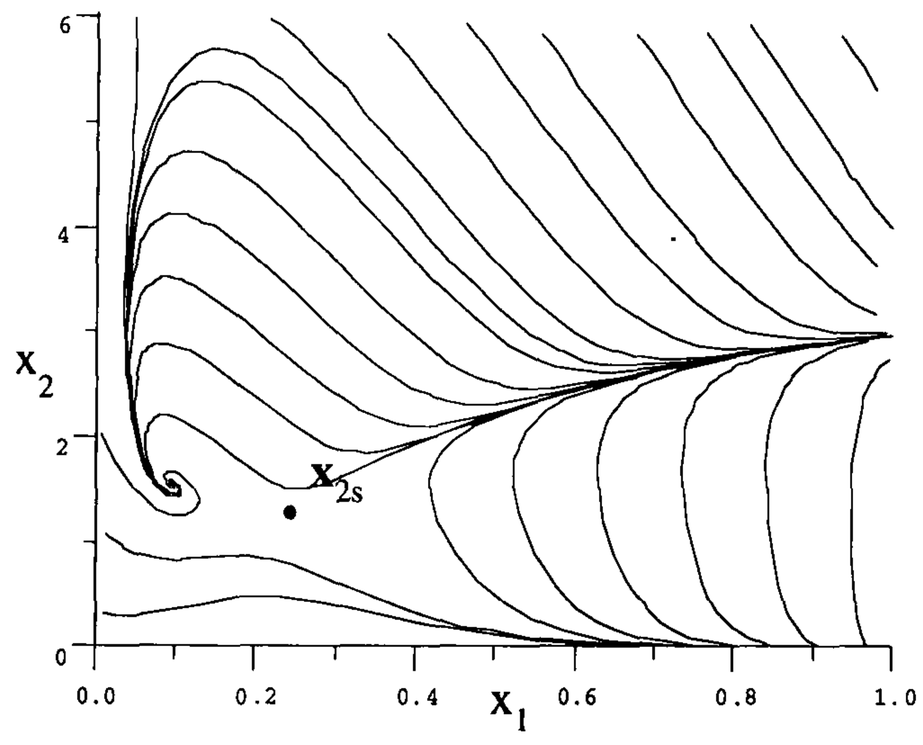

b) The open-loop response.

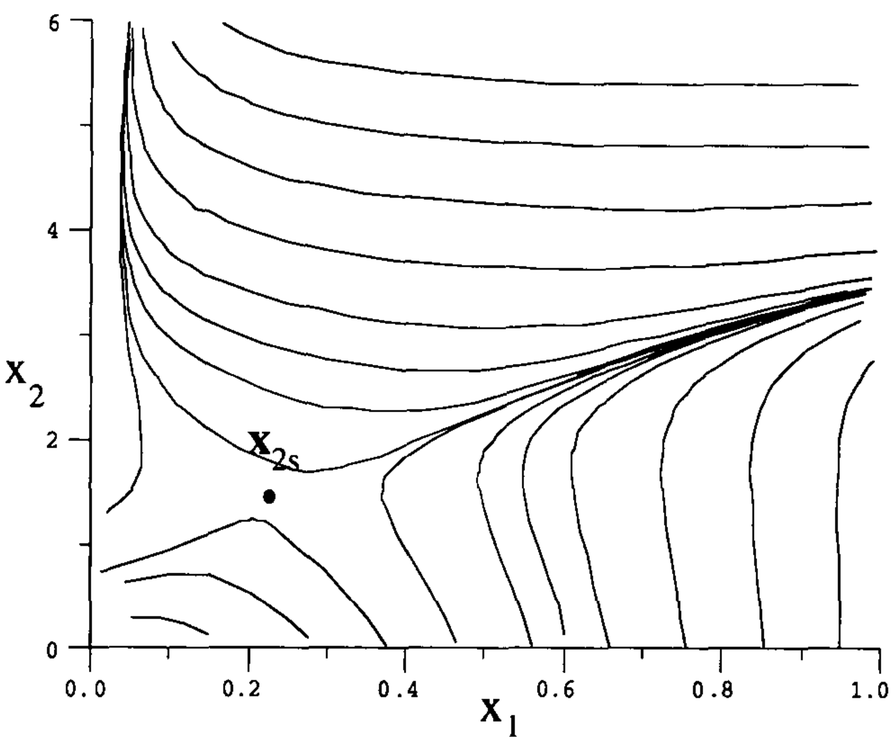

c) The closed-loop response with the u_T control law in which the first-order gains are set to 0. The effect of g_T is to eliminate parabolic behavior.

The 2D-PMMA process behavior obtained by applying the temperature input/output linearization control.

FIGURE 7.1.2.

we apply Equation (7.1.5), numerical computations are no longer an obstacle and the answer is immediate. The state-space behavior for the u_T control law is illustrated in Figure 7.1.2.a, and the closed-loop process eigenspectra are listed in Table 7.1.2. The results show that the u_T control law has the same effect on the process as the input/output linearization control illustrated in Figure 6.2.4. However, inspection of the closed-loop eigenspectra in Table 7.1.2 reveals that nonlinear eigenmodes are not all nilpotent, implying that $g_T(\mathbf{x})$ has not completely canceled all process nonlinearities. The spectra

Table 7.1.2: The close-loop 2D-PMMA eigenspectra for the temperature input/output linearization control law.

$$\mathcal{Z}_1\{\mathbb{R}^2\} = \left\{\begin{bmatrix} 1 \\ 4.5512 - i0.62857 \end{bmatrix} ; \begin{bmatrix} 1 \\ 4.5512 + i0.62857 \end{bmatrix}\right\}$$

$$\Lambda_1\{\mathbb{R}\} = \{ -3.30797 + i51986 \quad ; \quad -3.30797 - i51986 \}$$

$$\mathcal{Z}_2\{\mathbb{R}^2\} = \left\{\begin{bmatrix} 1 \\ 0 \end{bmatrix} ; \begin{bmatrix} 1 \\ 4.442039 \end{bmatrix} ; \begin{bmatrix} 1 \\ -4.346328 \end{bmatrix}\right\}$$

$$\Lambda_2\{\mathbb{R}\} = \{ 11.5885 \quad ; \quad 0 \quad ; \quad 0 \}$$

$$\mathcal{Z}_3\{\mathbb{C}^2\} = \left\{\begin{bmatrix} 1 \\ 0 \end{bmatrix} ; \begin{bmatrix} 1 \\ -70.2173 \end{bmatrix} ; \begin{bmatrix} 1 \\ 4.124744+i3.710989 \end{bmatrix} ; \begin{bmatrix} 1 \\ 4.124744-i3.710989 \end{bmatrix}\right\}$$

$$\Lambda_3\{\mathbb{R}\} = \{ -214.915 \quad ; \quad 0 \quad ; \quad 0 \quad ; \quad 0 \}$$

$$\mathcal{Z}_4\{\mathbb{C}^2\} = \left\{\begin{bmatrix} 1 \\ 0 \end{bmatrix} ; \begin{bmatrix} 1 \\ 26.4398 \end{bmatrix} ; \begin{bmatrix} 1 \\ 5.22927 \end{bmatrix} ; \begin{bmatrix} 1 \\ 0.866742+i6.73539 \end{bmatrix} ; \begin{bmatrix} 1 \\ 0.866742-i6.73539 \end{bmatrix}\right\}$$

$$\Lambda_4\{\mathbb{R}\} = \{ 2417.68 \quad ; \quad 0 \quad ; \quad 0 \quad ; \quad 0 \quad ; \quad 0 \}$$

$$\mathcal{Z}_5\{\mathbb{C}^2\} = \left\{\begin{bmatrix} 1 \\ 0 \end{bmatrix}; \begin{bmatrix} 1 \\ 22.2527 \end{bmatrix}; \begin{bmatrix} 1 \\ 5.32725-i2.54217 \end{bmatrix}; \begin{bmatrix} 1 \\ 5.32725+i2.54217 \end{bmatrix}; \begin{bmatrix} 1 \\ -7.2052-i5.90281 \end{bmatrix}; \begin{bmatrix} 1 \\ -7.2052+i5.90281 \end{bmatrix}\right\}$$

$$\Lambda_5\{\mathbb{R}\} = \left\{\begin{array}{ccccccc} -23750.4 & ; & 0 & ; & 0 & ; & 0 \quad ; \\ & & 0 & ; & 0 & & \end{array}\right\}$$

indicates that the nilpotent eigenvectors are only the eigenvectors with temperature components not equal to 0. Therefore, one can view the u_T control as the temperature only input/output linearization control. The open-loop PMMA process response and the effect of the $g_T(x)$ on the open-loop behavior are also depicted in Figure 7.1.2. From these figures it appears as if $g_T(x)$ has globally canceled all process nonlinearities.

7.2. THREE-DIMENSIONAL PMMA PROCESS MODEL

By adding the control term to the three-dimensional PMMA model described in Section 5.4 we obtain the following process equations

$$\begin{bmatrix} \dot{x}_1 \\ \dot{x}_2 \\ \dot{x}_3 \end{bmatrix} = \begin{bmatrix} 1\text{-}x_1\text{-}Da_p w\, x_1 Exp\left\{\dfrac{x_2}{1+x_2/\gamma_p}\right\} \\ -x_2+BDa_p w\, x_1 Exp\left\{\dfrac{x_2}{1+x_2/\gamma_p}\right\} - \beta[u + (x_2\text{-}x_{2c})] \\ x_{3f}\text{-}x_3\text{-}Da_d x_3 Exp\left\{\dfrac{\gamma_d x_2}{1+x_2/\gamma_p}\right\} \end{bmatrix} = \begin{bmatrix} f_1(\mathbf{x}) \\ f_2(\mathbf{x}) \\ f_3(\mathbf{x}) \end{bmatrix} - \begin{bmatrix} 0 \\ 1 \\ 0 \end{bmatrix} \beta u \qquad (7.2.1)$$

where $\mathbf{b}=\beta[0,1,0]^t$ is now the control vector and u is a control function. This process has the open-loop behavior characterized by the three steady-states which are defined in Table 5.4.1. Furthermore, since the process is three-dimensional it is not possible to provide the state-space visualization of the open-loop process behavior for all initial conditions of interest. Instead, we now consider the three-dimensional state-space representation for an arbitrarily selected one-dimensional initial value subset.

To select the initial value set, we proceed in the following way. Observe that for any fixed initiator state x_3, the process behavior for different initial pairs (x_{1o},x_{2o}) is described by the two-dimensional model realization studied in the preceding section. As a result, in the three-dimensional instance the simulations of interest are those in which the initial pair (x_{1o}, x_{2o}) is fixed while x_{3o} is varied. For example, one such simulation is accomplished by using the initial value set

$$\mathbf{S} \equiv \{x_{1o}=0.4,\ x_{2o}=1.5,\ \text{and}\ 0 \le x_{3o} < 1\},$$

which in the three-dimensional state-space defines a line orthogonal to the $x_1 x x_2$-plane. This is illustrated in Figure 7.2.1.a, where also the open-loop state responses are depicted for the initial conditions along the line **S.** As indicated, for all starting initiator values ≤ 0.00375, reactivity is poor and the process settles at the low conversion steady-state $\mathbf{x}_{1s}$. By contrast, for any $0.00375 < x_{3o} \le 1$ a stronger reaction occurs and the higher conversion steady-state is achieved. Observe that the reactive region again contains parabolic type trajectories which are responsible for large temperature swings. This is more clearly illustrated in Figure 7.2.1.b where the state-space projection onto the $x_1 x x_2$-plane is illustrated.

Next, suppose that, as before, we want to regulate the process so the open-loop unstable steady-state $\mathbf{x}_{2s}=[0.496018\ ,\ 0.863968\ ,\ 0.049971]^t$ becomes the operating point. For this steady-state the 3-order open-loop power series approximation and the corresponding eigenspectra are listed in Table A.V.4. By inspecting the eigenvector structure one can verify that the process is at least 3-order stabilizable, implying that the first-order dynamics at $\mathbf{x}_{2s}$ can be regulated by using the proportional control law

$$\begin{aligned} u(\mathbf{x}) \equiv u_P(\mathbf{x}) &= \frac{g_{11}}{\beta}(x_1 - x_{1s}) + \frac{g_{12}}{\beta}(x_2 - x_{2s}) + \frac{g_{13}}{\beta}(x_3 - x_{3s}) \\ &= \frac{g_{11}}{\beta}\overleftrightarrow{x}_1 + \frac{g_{12}}{\beta}\overleftrightarrow{x}_2 + \frac{g_{13}}{\beta}\overleftrightarrow{x}_3 \quad , \end{aligned} \tag{7.2.2}$$

where g_{11}, g_{12} and g_{13} are the coefficients to be determined, and where $x_{1s}=0.496018$, $x_{2s}=0.863968$ and $x_{3s}=0.049971$. For the purpose of this exercise we select $g_{11}=-45.0$, $g_{12}=10.0$ and $g_{13}=0.0$, which produce the closed-loop first-order eigenvalues

$$\Lambda_1\{R\}_{c\text{-}l} = \{-2.91916,\ -1.87303,\ -0.984116\}.$$

The closed-loop process is now stable at the state $\mathbf{x}_{2s}$ and the points defined by **S** must also be attracted by the same state (Figure 7.2.2.a). From the figure it is further evident

a)

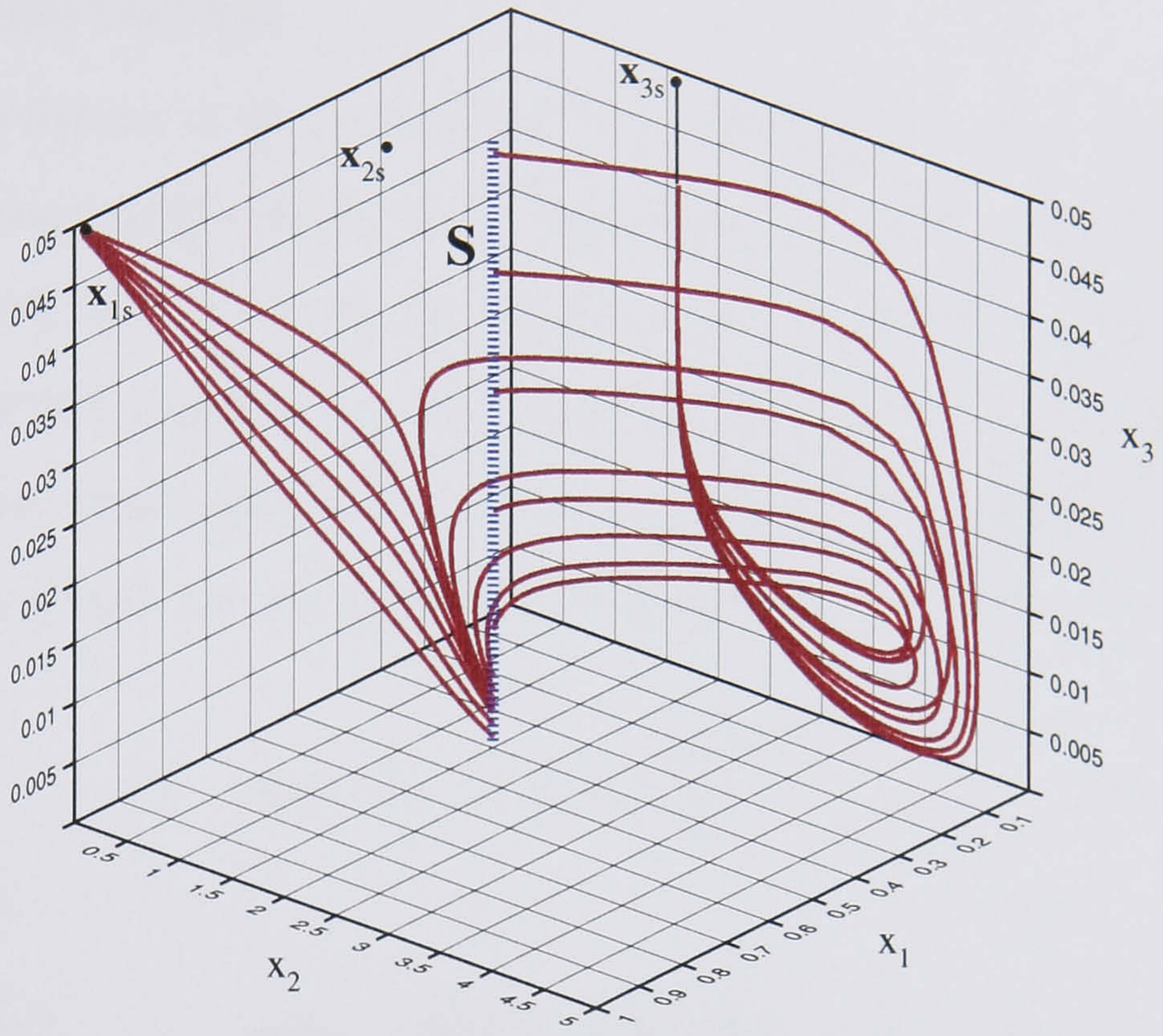

For initial initiator concentrations <0.00375 solutions converge to the low conversion steady-state $\mathbf{x}_{1s}$, while for initiator values >0.00375 solutions go to the high conversion steady-state $\mathbf{x}_{3s}$.

b)

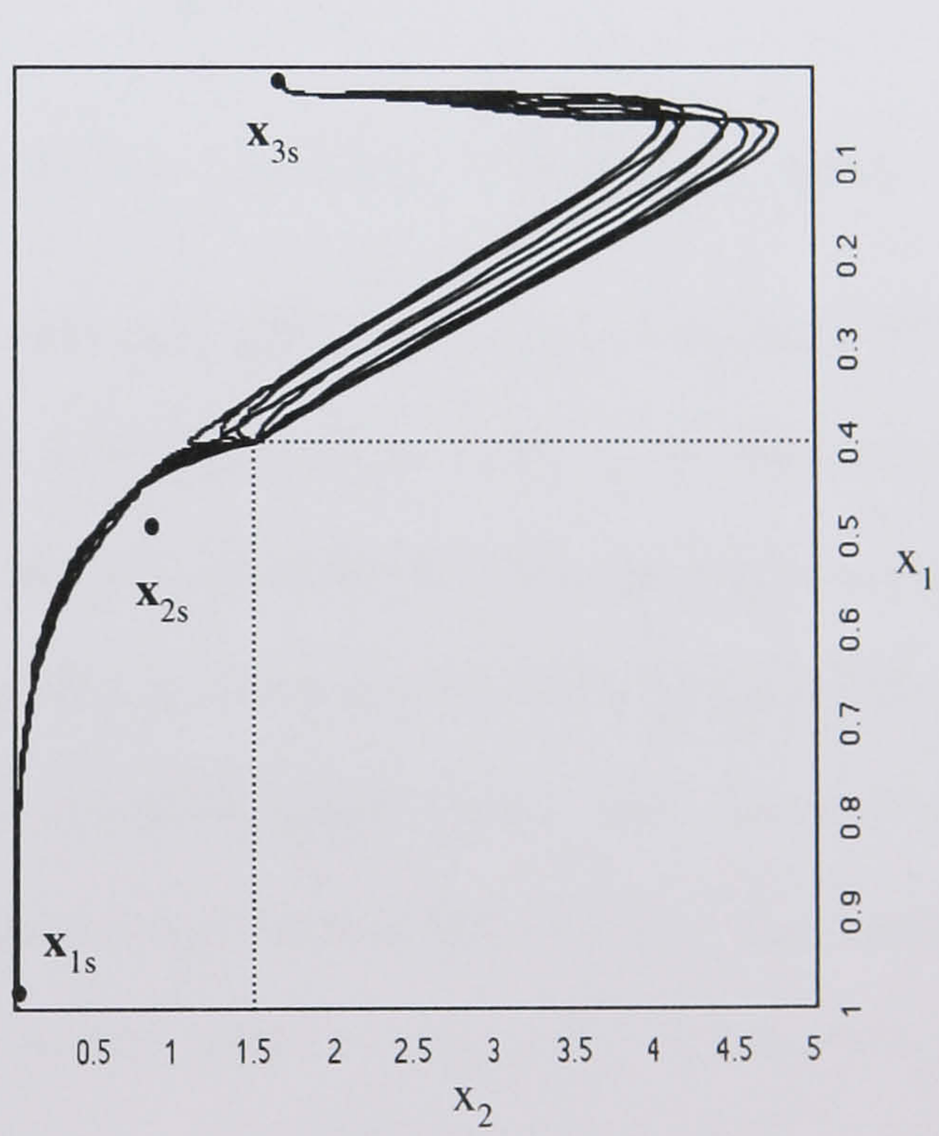

The 3D-PMMA open-loop process behavior.

FIGURE 7.2.1.

that the reactivity has subsided since the parabolic temperature excursions are not as great as in the open-loop case.

To obtain a control strategy which provides a greater degree of process robustness, we can either continue by increasing magnitudes of the proportional gains, or keep the existing first-order closed-loop dynamics and regulate the nonlinear terms. As before, the first choice will inevitably demand a higher control speed. Therefore, we consider the temperature input/output linearization strategy defined in Equations (7.1.5) and (7.1.6). For the parameters specified this control law becomes

$$u(\mathbf{x}) \equiv u_T(\mathbf{x}) = u_P(\mathbf{x}) - \frac{g_T(\mathbf{x})}{\beta} \tag{7.2.3}$$

where

$$u_P(\mathbf{x}) = \frac{-45.0}{\beta}\overleftrightarrow{x}_1 + \frac{10.0}{\beta}\overleftrightarrow{x}_2 \text{ , and}$$

$$g_T(\mathbf{x}) = -29.1456\overleftrightarrow{x}_1 + 3.79547\overleftrightarrow{x}_2 + 60.5128\overleftrightarrow{x}_3 - f_2(\mathbf{x}) \text{ .}$$

The closed-loop eigenspectra for the first three power series terms are listed in Table 7.2.1. By comparing the results in this table with the results in Table A.V.4 we note that for some closed-loop nilpotent eigenmodes which characterize the open-loop structure, the multiplicity has increased. In particular, the multiplicities have increased for all nilpotent eigenmodes in which eigenvectors have 0 temperature values. The closed-loop spectra also reveal that the higher-order idempotent eigenmodes have 0 for the temperature term, implying again that the temperature nonlinearities are canceled. Thus, the u_T controller significantly reduces the process reactivity. This is illustrated in the simulations shown in Figure 7.2.3. Observe that trajectories now converge to $\mathbf{x}_{2s}$ without experiencing large temperature swings. As a result, the u_T realization offers solutions which are globally less reactive than the proportional only realization.

To complete the three-dimensional case study we consider the cubic control law. In this instance we regulate the first three open-loop power series terms so that their closed-

a)

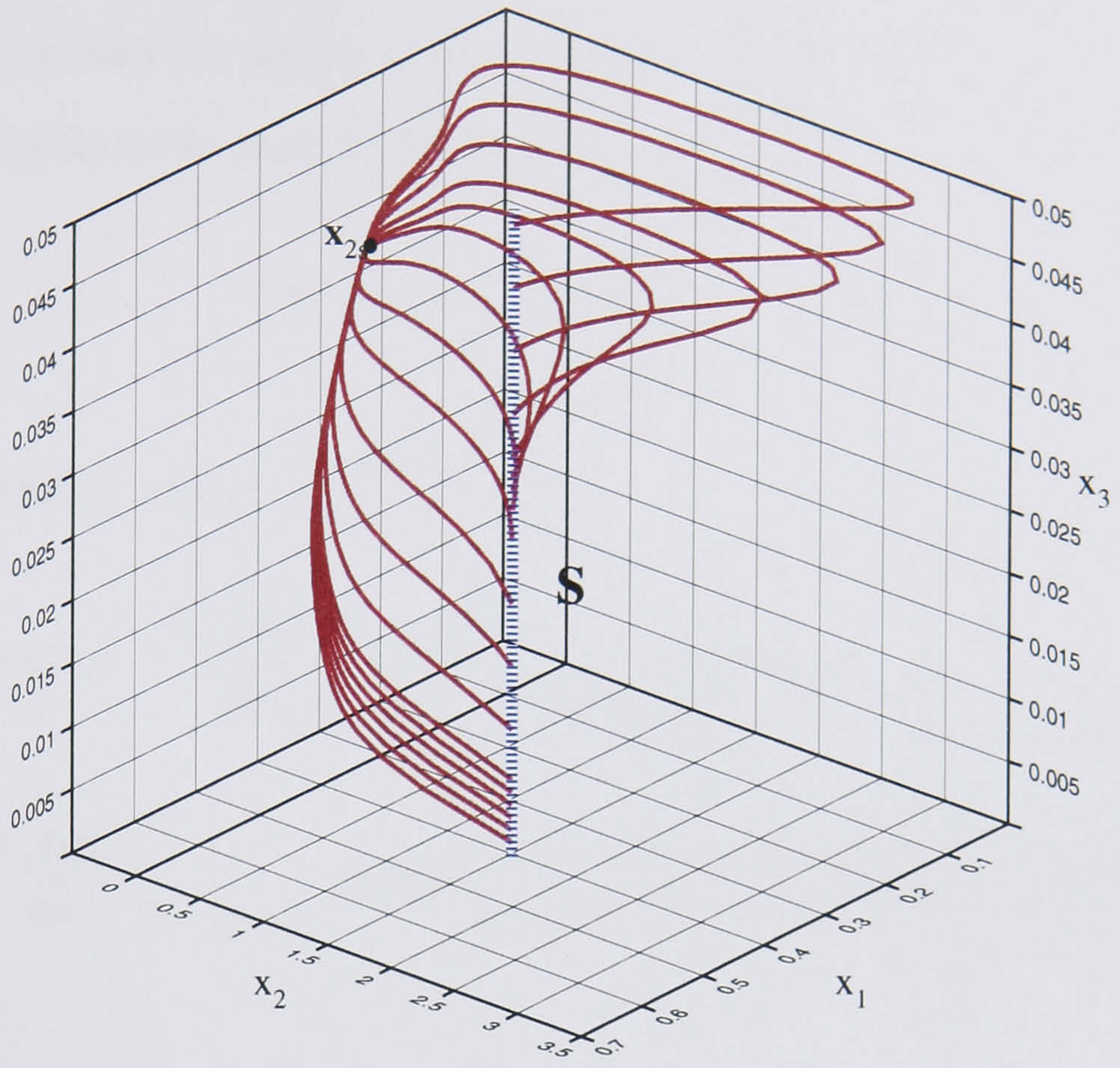

b)

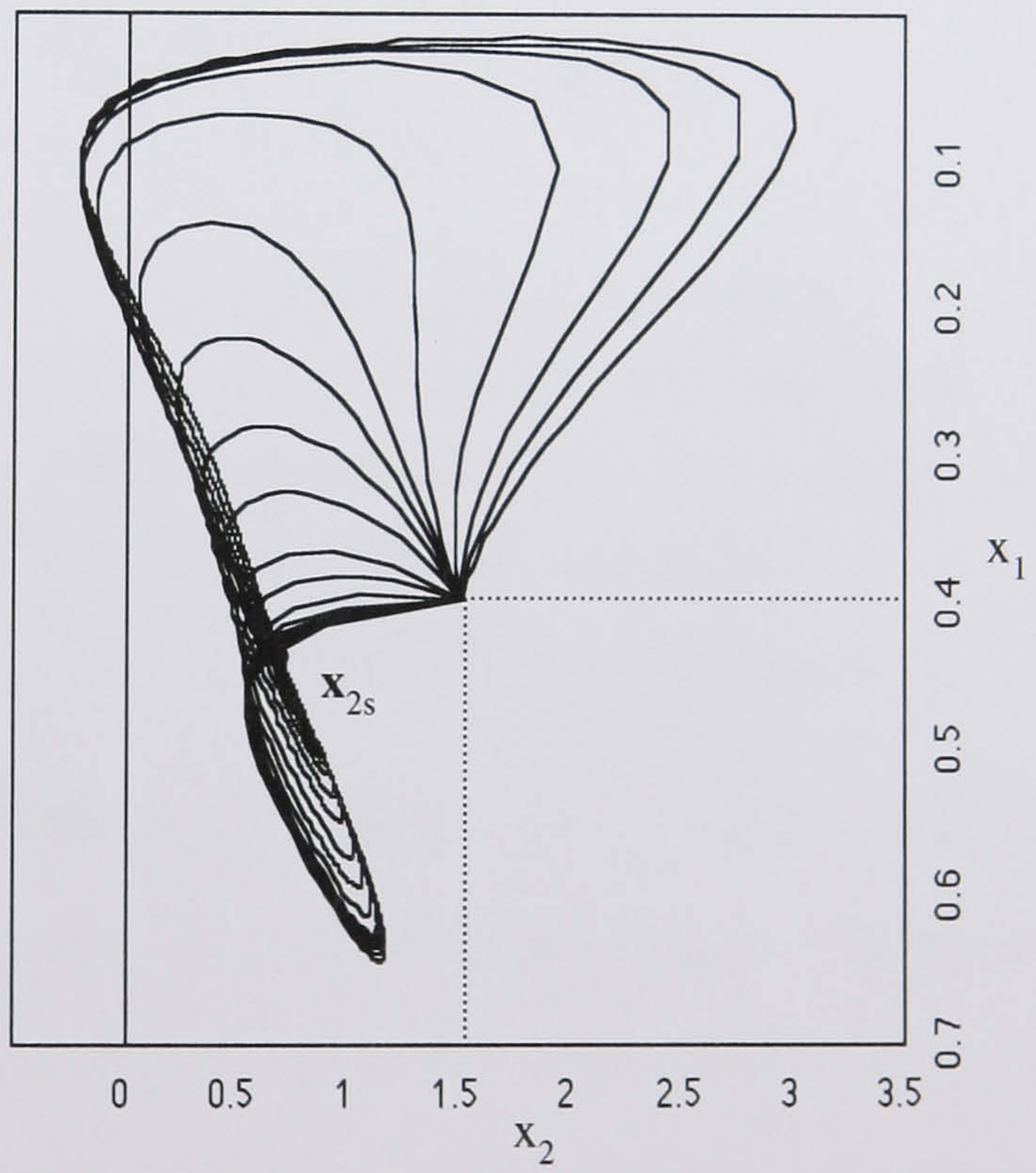

The 3D-PMMA closed-loop process behavior obtained by applying the proportional regulator u_p with g_{11}=-45.0, g_{12}=10.0 and g_{13}=0.0.

FIGURE 7.2.2.

loop eigenspectra are similar to those listed in Table 7.2.1. This is accomplished by considering the cubic controller defined by

$$\mathbf{u}(\mathbf{x}) \equiv \mathbf{u}_c(\mathbf{x}) = \sum_{k=1}^{3} \mathbf{u}_j(\mathbf{x}) \tag{7.2.4}$$

where

$$\mathbf{u}_1(\mathbf{x}) = \mathbf{u}_P(\mathbf{x}) = -\frac{45.0}{6}\overleftrightarrow{x}_1 + \frac{10}{6}\overleftrightarrow{x}_2 ,$$

$$\mathbf{u}_2(\mathbf{x}) = -\frac{(B + v_2)}{2!\beta}\left[\frac{\partial^2[f_1(\mathbf{x})]}{\partial \mathbf{x}^2}\right]_{1x7}\Bigg|_{\mathbf{x}=\mathbf{x}_{2s}} \mathbf{z}_2(\overleftrightarrow{\mathbf{x}}) \text{ with}$$

$$\left[\frac{\partial^2[f_1(\mathbf{x})]}{\partial \mathbf{x}^2}\right]_{1x7}\Bigg|_{\mathbf{x}=\mathbf{x}_{2s}} \mathbf{z}_2(\overleftrightarrow{\mathbf{x}}) = \begin{cases} (-10.485\overleftrightarrow{x}_1^2 + 6.68402\overleftrightarrow{x}_1\overleftrightarrow{x}_2 - 1.3904\overleftrightarrow{x}_2^2 + \\ 48.6042\overleftrightarrow{x}_1\overleftrightarrow{x}_3 - 18.0029\overleftrightarrow{x}_2\overleftrightarrow{x}_3 + 50.4566\overleftrightarrow{x}_3^2) \end{cases} ,$$

and,

$$\mathbf{u}_3(\mathbf{x}) = -\frac{(B + v_3)}{3!\beta}\left[\frac{\partial^3[f_1(\mathbf{x})]}{\partial \mathbf{x}^3}\right]_{1x10}\Bigg|_{\mathbf{x}=\mathbf{x}_{2s}} \mathbf{z}_3(\overleftrightarrow{\mathbf{x}}) \text{ with}$$

$$\left[\frac{\partial^3[f_1(\mathbf{x})]}{\partial \mathbf{x}^3}\right]_{1x10}\Bigg|_{\mathbf{x}=\mathbf{x}_{2s}} \mathbf{z}_3(\overleftrightarrow{\mathbf{x}}) = \begin{cases} (30.512\overleftrightarrow{x}_1^3 - 27.2075\overleftrightarrow{x}_1^2\overleftrightarrow{x}_2 - \\ 314.733\overleftrightarrow{x}_1^2\overleftrightarrow{x}_3 + 9.61498\overleftrightarrow{x}_1\overleftrightarrow{x}_2^2 + \\ 200.637\overleftrightarrow{x}_1\overleftrightarrow{x}_2\overleftrightarrow{x}_3 - 729.486\overleftrightarrow{x}_1\overleftrightarrow{x}_3^2 - \\ 1.76319\overleftrightarrow{x}_2^3 - 41.7362\overleftrightarrow{x}_2^2\overleftrightarrow{x}_3 + \\ 270.2\overleftrightarrow{x}_2\overleftrightarrow{x}_3^2 - 1514.58\overleftrightarrow{x}_3^3) \end{cases} ,$$

and for B=12.0, v_2=2.52974 and v_3=-2.01236. Observe that v_2 and v_3 are selected from the open-loop nilpotent eigenvectors listed in Table A.V.4. The proposed cubic control structure produces the closed-loop eigenspectra listed in Table 7.2.2. By comparing the eigenvalues in Tables 7.2.1 and 7.2.2 one can verify that the largest idempotent component magnitudes are comparable. This is confirmed in the closed-loop simulations illustrated in Figure 7.2.4 in which the parabolic behavior is practically nonexistent, just as in the case of the u_T control law.

Finally, to complete the three-dimensional control realizations we evaluate the performance of the strategies considered. This is accomplished by applying a control

analysis similar to that discussed in Section 6.4. However, for each control law we now evaluate the required control speeds for the following three initial conditions

$$\mathbf{x}_o = \left\{ \begin{bmatrix} 0.4 \\ 1.5 \\ 0.001 \end{bmatrix}; \begin{bmatrix} 0.4 \\ 1.5 \\ 0.05 \end{bmatrix}; \begin{bmatrix} 0.4 \\ 1.5 \\ 0.1 \end{bmatrix} \right\} .$$

The initial conditions for x_{1o} and x_{2o} are identical in all three instances, while for x_{3o} they vary. The simulation results are presented in Appendix VII (Figures A.VII.1-3). They show that the u_p control strategy has the most demanding control speed requirements. By contrast, the results for the other two regulation schemes are more reasonable since the control speed requirements are substantially reduced. Observe that from the speed point of view the best control strategy is the one which applies the u_T law for low initiator variations, $0.0 \leq x_3 \leq 0.06$, and the u_c regulation for high initiator values, $0.06 < x_3 \leq 0.1$. Thus, again the combined strategy is best.

By proceeding with regulation of higher-order eigenmodes, one can now derive various control strategies. Whether these strategies are of the polynomial, exponential, hyperbolic or combined types is immaterial as long as the control objective is accomplished feasibly. For example, in applications where a control scheme needs to regulate only the low-order eigenmodes the polynomial realization may be adequate. On the other hand, in applications where a large number of higher-order eigenmodes need to be regulated the exponential type controller may provide a better alternative. Clearly, when the process is linear the exponential control strategy is not appropriate because there is no need to regulate higher-order eigenmodes.

In conclusion, we have demonstrated that the two-dimensional nonlinear control results can easily be extended and applied in multivariate instances of dimension>2. However, one should keep in mind that although the extension appears to be conceptually straight forward, the computational requirements in higher-dimensions increase dramatically. This is quite obvious when analytic solutions are not possible.

Table 7.2.1: The close-loop 3D-PMMA eigenspectra for the temperature input/output linearization control law.

$$G_1\{R^3\} = \left\{ \begin{bmatrix} 1 \\ 4.8486 \\ 0.000304418 \end{bmatrix}; \begin{bmatrix} 1 \\ 3.63865 \\ 0.000521844 \end{bmatrix}; \begin{bmatrix} 1 \\ 3.63865 \\ 0.000521844 \end{bmatrix} \right\}$$

$$\Lambda_1\{R\} = \{-2.93451 ; -1.84724 ; -0.994559\} ; \quad |G_1\{R^3\}| = s_{1,3} = 3$$

$$G_2\{R^3\} = \left\{ \begin{bmatrix} 1 \\ 0 \\ 0 \end{bmatrix}; \begin{bmatrix} 1 \\ 0 \\ 0.181518 \end{bmatrix}_{(2)}; \begin{bmatrix} 1 \\ 0 \\ -1.1448 \end{bmatrix}_{(2)}; \begin{bmatrix} 1 \\ 2.52974 \\ -0.253847 \end{bmatrix}; \begin{bmatrix} 1 \\ -4.48486 \\ 0.450033 \end{bmatrix} \right\}$$

$$\Lambda_2\{R\} = \left\{ \begin{matrix} & & -5.24251 & ; & \\ 0_{(2)} & ; & 0_{(2)} & ; & 0 & ; & 0 \end{matrix} \right\} ; \quad |G_2\{R^3\}| = 5, \ s_{2,3} = 7$$

$$G_3\{C^3\} = \left\{ \begin{bmatrix} 1 \\ 0 \\ 0 \end{bmatrix}; \begin{bmatrix} 1 \\ -2.01236 \\ 0.128723 \end{bmatrix}; \begin{bmatrix} 1 \\ 2.29408 - i\ 1.01616 \\ -0.146743 + i\ 0.065 \end{bmatrix}; \begin{bmatrix} 1 \\ 2.29408 + i\ 1.01616 \\ -0.146743 - i\ 0.065 \end{bmatrix}; \begin{bmatrix} 1 \\ 0 \\ 0.0797 \end{bmatrix}_{(3)}; \begin{bmatrix} 1 \\ 0 \\ -0.280 + i\ 0.416 \end{bmatrix}_{(3)}; \begin{bmatrix} 1 \\ 0 \\ -0.280 - i\ 0.416 \end{bmatrix}_{(3)} \right\}$$

$$\Lambda_3\{C\} = \left\{ \begin{matrix} & & 30.512 & ; & \\ 0 & ; & 0 & ; & 0 & ; \\ 0_{(3)} & ; & 0_{(3)} & ; & 0_{(3)} & \end{matrix} \right\} ; |G_3\{R^3\}| = 7, \ s_{3,3} = 13$$

a)

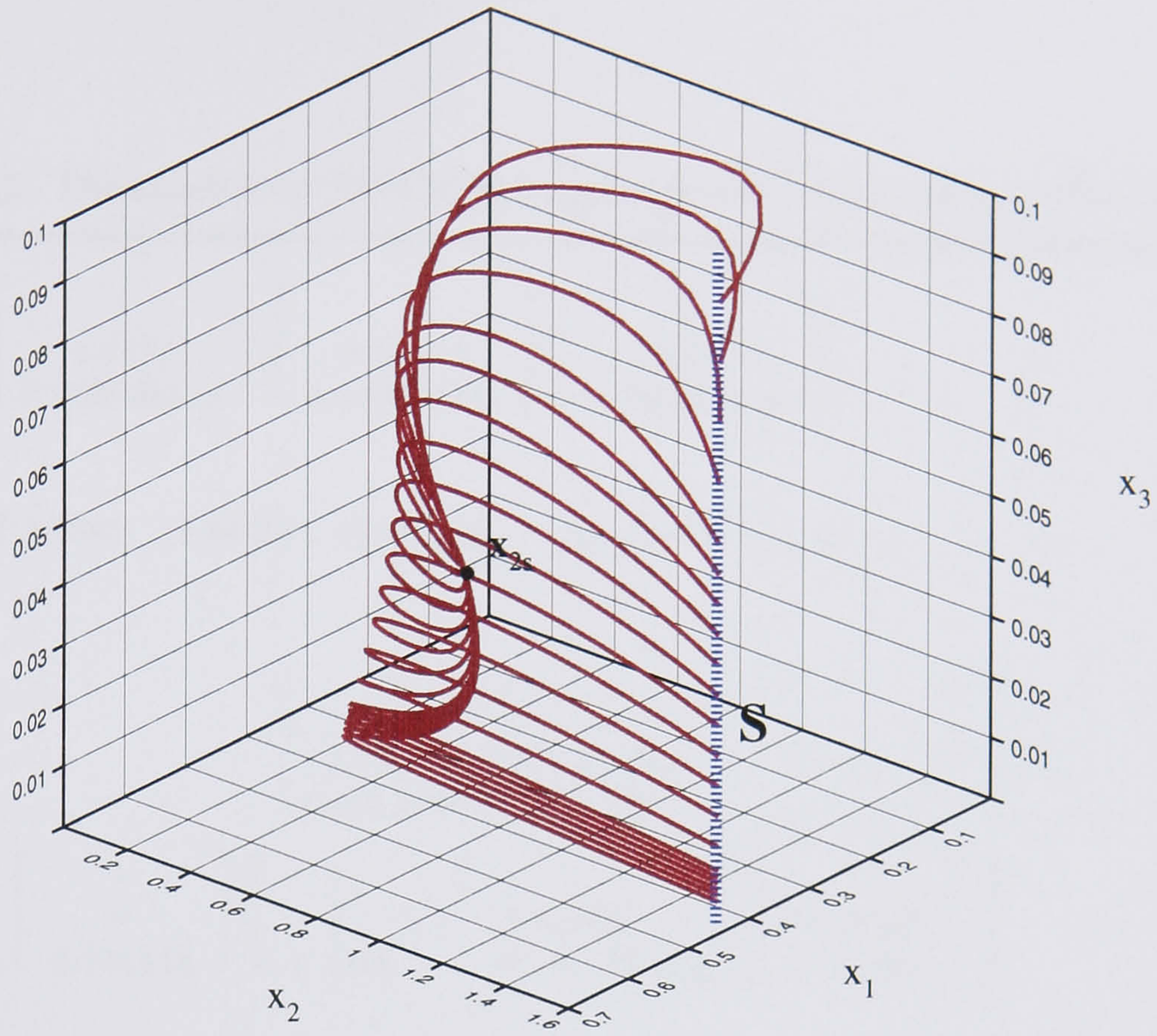

b)

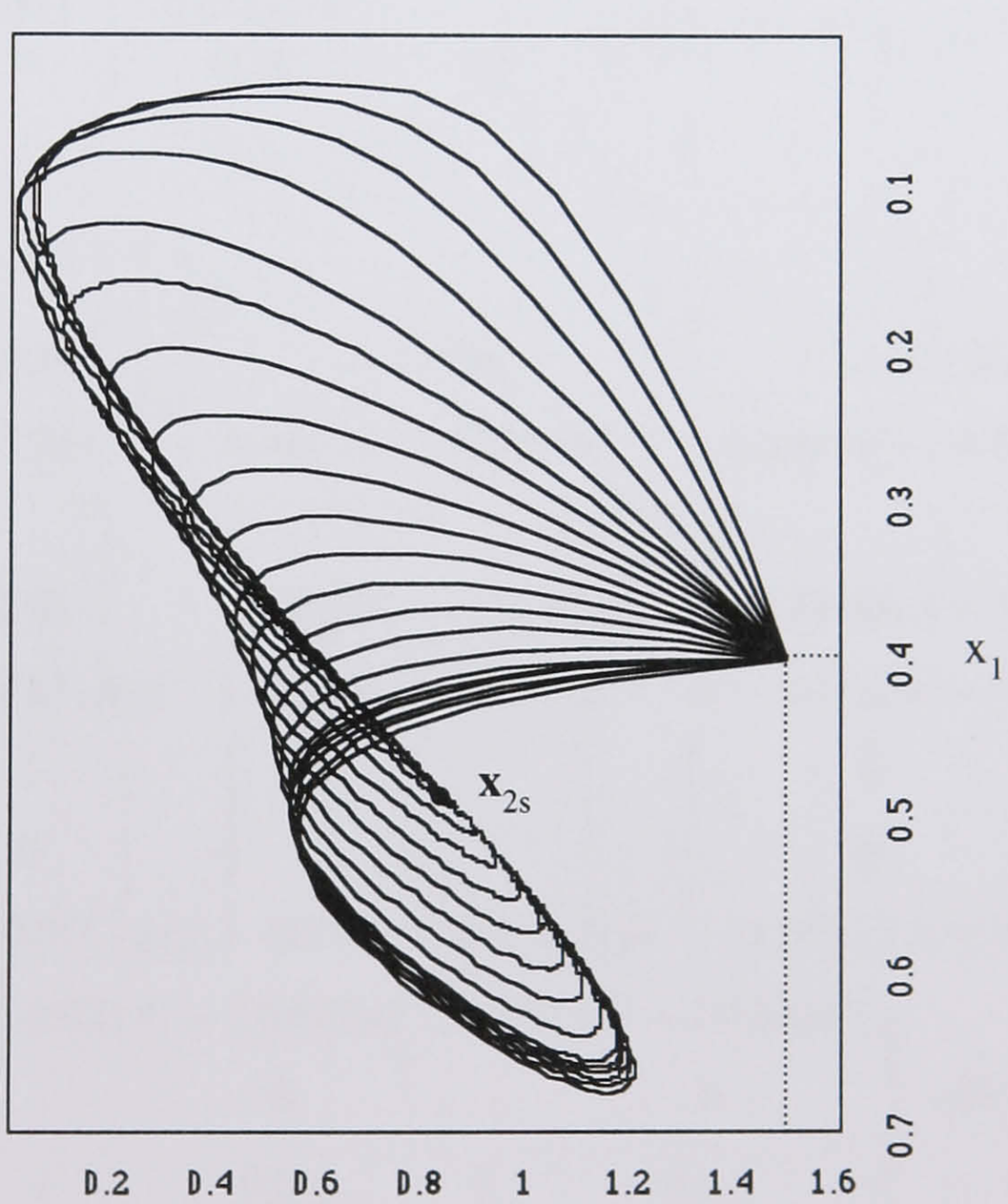

The 3D-PMMA closed-loop process behavior obtained by applying the temperature input/output linearization regulator u_T.

FIGURE 7.2.3.

Table 7.2.2: The close-loop 3D-PMMA eigenspectra for the cubic control law.

$$G_1\{R^3\} = \left\{ \begin{bmatrix} 1 \\ 4.8486 \\ 0.000304418 \end{bmatrix}; \begin{bmatrix} 1 \\ 3.63865 \\ 0.000521844 \end{bmatrix}; \begin{bmatrix} 1 \\ 3.63865 \\ 0.000521844 \end{bmatrix} \right\}$$

$$\Lambda_1\{R\} = \{-2.93451 \; ; -1.84724 \; ; \; -0.994559\} \; ; \quad |G_1\{R^3\}| = s_{1,3} = 3$$

$$G_2\{R^3\} = \left\langle \begin{bmatrix} 1 \\ 2.52974 \\ 0.0012697 \end{bmatrix}; \begin{bmatrix} 1 \\ 2.52974 \\ 0.1919 \end{bmatrix}; \begin{bmatrix} 1 \\ 0 \\ 0.181518 \end{bmatrix}; \begin{bmatrix} 1 \\ 0 \\ -1.1448 \end{bmatrix}; \begin{bmatrix} 1 \\ 2.52974 \\ -0.253847 \end{bmatrix}_{(2)}; \begin{bmatrix} 1 \\ -4.48486 \\ 0.450033 \end{bmatrix} \right\rangle$$

$$\Lambda_2\{R\} = \left\{ \begin{matrix} & -1.2351 & ; & -0.0142784 & \\ 0 & ; & 0 & ; & 0_{(2)} \end{matrix} \quad ; \quad 0 \right\} ; \quad |G_2\{R^3\}| = 6, \quad s_{2,3} = 7$$

$$G_3\{C^3\} = \left\langle \begin{bmatrix} 1 \\ -2.01236 \\ 0.12872261 \end{bmatrix}; \begin{bmatrix} 1 \\ -2.01236 \\ 0.48474 - i\,0.689845 \end{bmatrix}; \begin{bmatrix} 1 \\ -2.01236 \\ 0.48474 + i\,0.689845 \end{bmatrix}; \begin{bmatrix} 1 \\ -2.01236 \\ 0.128723 \end{bmatrix}_{(2)}; \begin{bmatrix} 1 \\ 2.29408 - i\,1.01616 \\ -0.146743 + i\,0.065 \end{bmatrix}; \begin{bmatrix} 1 \\ 2.29408 + i\,1.01616 \\ -0.146743 - i\,0.065 \end{bmatrix}; \begin{bmatrix} 1 \\ 0 \\ 0.0797 \end{bmatrix}_{(2)}; \begin{bmatrix} 1 \\ 0 \\ -0.280 + i\,0.416 \end{bmatrix}_{(2)}; \begin{bmatrix} 1 \\ 0 \\ -0.280 - i\,0.416 \end{bmatrix}_{(2)} \right\rangle$$

$$\Lambda_3\{C\} = \left\{ \begin{matrix} 23.0785 ; & -0.02151 + i\,0.00247 & ; & -0.02151 + i\,0.00247 \\ 0_{(2)} & ; & 0 & ; & 0 \\ 0_{(2)} & ; & 0_{(2)} & ; & 0_{(2)} \end{matrix} \right\} ; |G_3\{R^3\}| = 9, \quad s_{3,3} = 13$$

a)

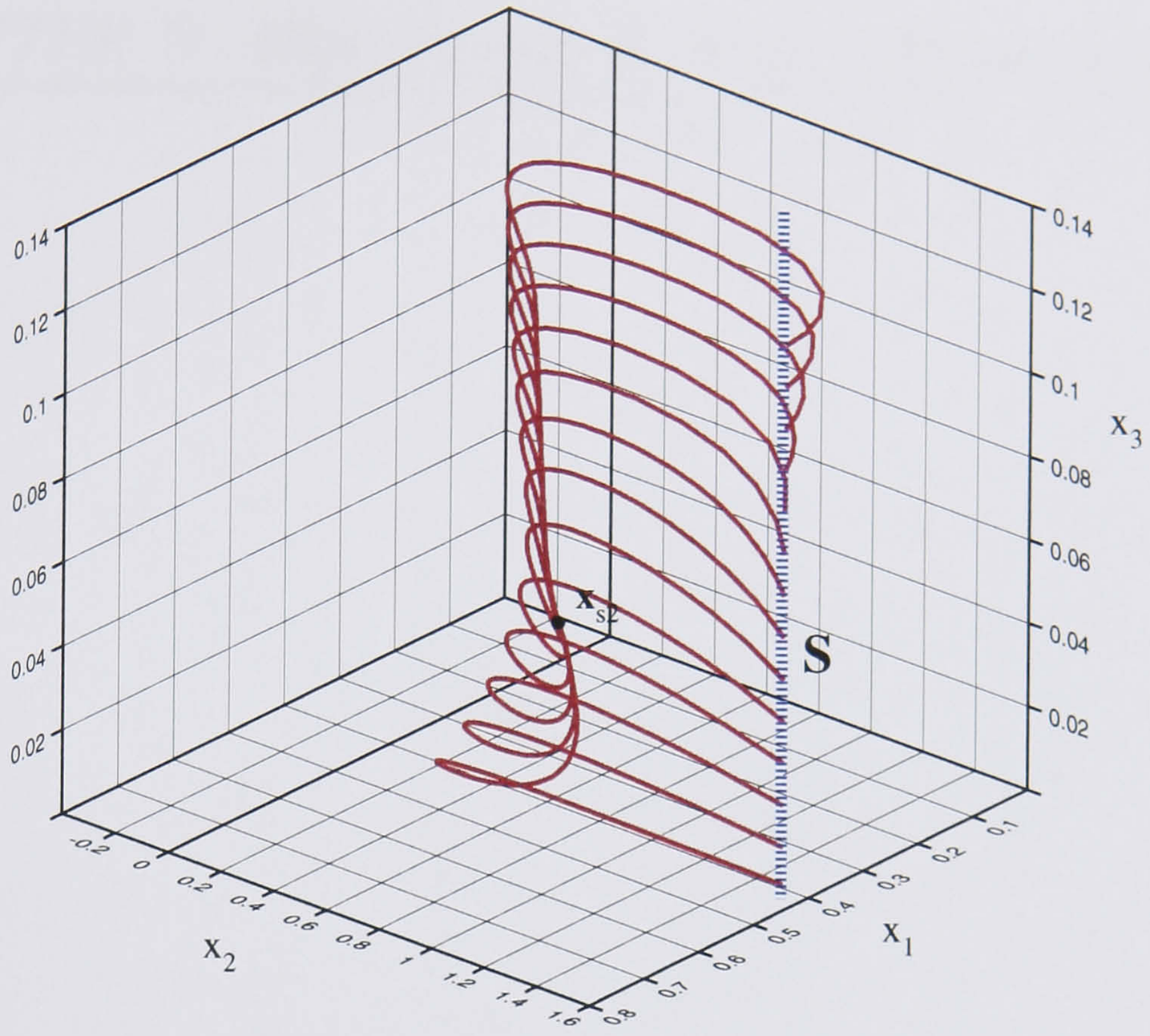

b)

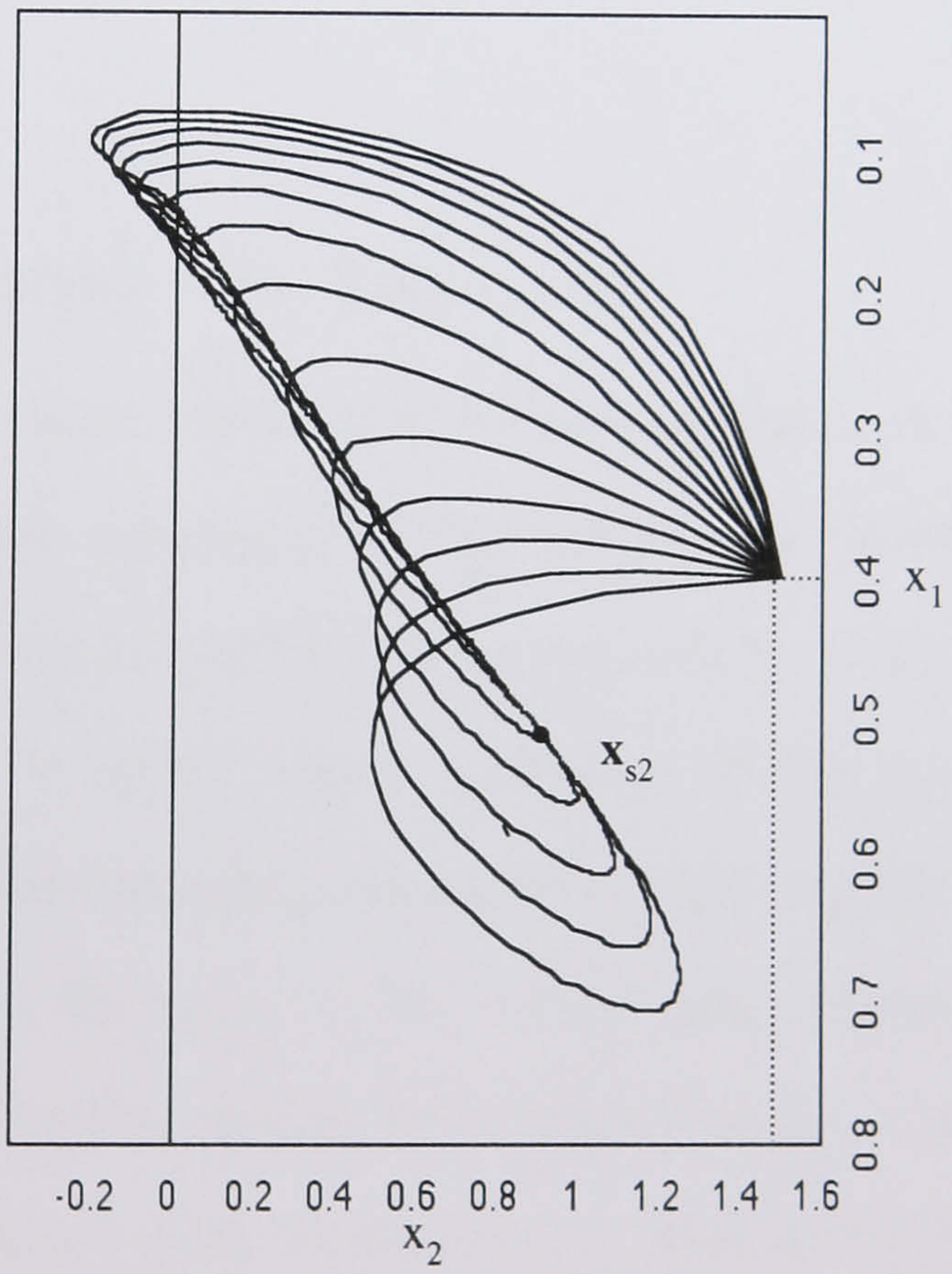

The 3D-PMMA closed-loop process behavior obtained by applying the cubic regulator u_c.

FIGURE 7.2.4.

CHAPTER 8 - DISCUSSION AND CONCLUSIONS

8.1. CONTRIBUTIONS TO THEORY

In this thesis a new mathematical framework based on a concept of nonlinear spectra is used to examine algebraic properties and dynamic behavior of chemical reaction systems. First a theoretical foundation is presented and results are then applied to analyze and control behaviors of several highly exothermic CSTR processes. Through this exercise it is demonstrated that most linear systems design concepts have natural extensions into a nonlinear domain. The eigenvectors, eigenvalues, eigenmodes and eigenspectrum are all familiar linear systems design tools which through a projection operation are introduced into the proposed nonlinear framework. Moreover, the linear algebra notions such as the degrees of freedom, linear independence (dependence) and linear basis are used to formulate similar concepts for nonlinear multivariate k-form structures. It is also shown that this framework offers a useful method for characterizing process nonlinearities which can be presented by algebraic combinations of the k-form modules, and as such provides a new twist to a number of nonlinear issues. In particular, Fundamental Spectral

Theorem introduced in Chapter 2 completely characterizes a k-form structural complexity, and forms a basis for understanding general algebraic structure and dynamic behavior of nonlinear systems. The results of this theorem have the same significance for nonlinear systems as the linear algebra results have for linear systems. This is discussed in Chapters 2, 3, 4 and 5.

The theory is also used to study mathematical and physical relations between eigenspectra, linear or nonlinear, and a nonlinear ODE process description. We show that a global dynamic behavior and control of polynomial systems can be studied by the same eigenspectra methods used in the theory of linear systems. As a result, the stability and control properties of nonlinear systems are formulated by using the familiar linear systems formalism. For example, the concepts such as the asymptotic stability in the large (global asymptotic stability), marginal stability, periodic stability and state controllability are all extended into a nonlinear framework. Hence, these concepts are physically identical in both linear and nonlinear cases. However, mathematically they are treated somewhat differently. In a nonlinear case understanding of global system properties in general demands a more intricate analysis since there are a greater number of eigenmodes which need to be accounted for. This is discussed in Chapters 3, 4 and 5.

It is also demonstrated that algebraic relations which determine process eigenspectra can be used to look at a way in which global process complexity and behavior emerge from local levels. This knowledge is particularly of significance when we need to understand how a nonlinear process changes, or adapts, to external forces. For instance, this information is used in Chapters 6 and 7 to examine closed-loop process properties for different nonlinear control realizations. In addition, it was used to demonstrate how a control speed is related to open-loop process characteristics. As a result, the analytic method presented offers a significant contribution to the theory of nonlinear systems, especially since other currently available nonlinear methods provide only limited answers to the issues considered.

8.2. On Applications of Nonlinear Spectral Technique

Although the focus of the thesis is on analysis and control of exothermic CSTR processes, the proposed spectral method applies to a much broader class of chemical engineering problems. In particular, it can be used to study global nonlinear behavior of any chemical reaction system (*e.g.*, plug flow or batch), as well as global behavior of distillation and separation processes. In addition, it can be applied to study different behaviors of a combustion system (Gray 1990). All these processes exhibit either, or both, the time and space dependent nonlinearities which in a constant pressure environment are chiefly temperature determined by Arrhenius' law. Therefore, any analytic method that in these cases properly identifies and characterizes open-loop process properties offers a valuable design tool. This was clearly demonstrated for the cyclopentenol model discussed in Chapter 5. In this particular case the spectral method was used to show that in spite of earlier reports which claim that the process is highly nonlinear, operating conditions at the steady-state of interest are at most weakly nonlinear. It is also worth mentioning that the spectral method can be applied to a large variety of physical and biological processes. For example, it can be used to analyze a structural complexity and behavior of the classic Hodgkin and Huxley model (1952 a.&b.). This model describes a nerve cell's response to constant electric stimulation and has nonlinear characteristics similar to those found in chemical reaction processes.

The results also provide a strong justification for a need of nonlinear analysis in process design efforts. This is because we can now apply the proposed spectral technique to show quantitatively and qualitatively why for given open-loop system characteristics some control strategies perform better than others. For instance, it is well known that widely accepted first-order regulation schemes (*i.e.*, PID controllers), can be applied in a number of nonlinear instances. This is easy to verify when process nonlinearities are weak. However, when nonlinearities are strong, as is the case in highly exothermic CSTR processes, the first-order control realizations often exhibit serious limitations. By contrast, the nonlinear controllers proposed and examined in Chapters 6 and 7 (*i.e.*,

polynomial, exponential, input/output, *etc.*) are less limiting because they have ability to incorporate a global process information. Thus, rather than attempting to control a nonlinear process by using a high gain first-order regulation scheme. a process designer can apply the spectral framework to obtain a nonlinear regulation strategy that fits more naturally within a nonlinear setting. Such control realizations often perform with less effort and are more efficient. These observations were previously in general intuitive and seldom quantitative.

The CSTR results presented in Chapters 5, 6 and 7 also raise some interesting design questions. First, all control realizations reported are designed to stabilize an open-loop unstable CSTR steady-state. This control objective was deliberately selected in order to demonstrate how different nonlinear control realizations perform under the most demanding operating conditions. However, it should be quite evident that the method applies to any control objective, even when the objective is to enhance a process performance around an open-loop stable steady-state. By doing so one can improve on a process safety and reliability. For instance, it is quite possible that a realization of one of the nonlinear control strategies presented in the thesis would have prevented the Bhopal thermal runaway incident.

Another important design issue is that of a process dimensionality. Although the theory presented is general, the CSTR results primarily address two and three-dimensional process descriptions for which visualizations of the state-space are unambiguous. However, when a dimensionality increases (*e.g.*, CSTR copolymer systems) such visualizations become more obscure and the question is: how does one gain confidence in the method proposed for a multivariate process of a dimension >3? A simple satisfactory answer presently is not available, and is a subject for future investigations. Nevertheless, it should be emphasized that the proposed spectral framework already provides a good road-map which shows what has to be done in any dimension. Clearly, as was done for the vinyl and cyclopentenol process models in Chapter 5, the first step is to evaluate spectral sets and to identify critical eigenmodes. These modes can then be regulated by one

of the techniques described in the thesis. For example, in higher dimensions a reasonable initial regulation approach is given by the recursive pole placement algorithm presented in Chapter 4.

8.3. FUTURE DIRECTIONS

Despite the fact that today most industrial process applications successfully utilize first-order design methods, demands for more sophisticated modeling and control methods are increasing daily as technology and society grow in complexity. The justifications for this are not only driven by economic reasons, but also by a need for a better process and model understanding. For example, even in cases when a process of interest is linear it is often not easy to confirm accuracy of a model proposed. In a nonlinear case this task is even more difficult. Consequently, any theory which elucidates various nonlinear issues is increasingly becoming important in modeling and control efforts. Therefore, it is appropriate to conclude by presenting some ideas on future directions of the work presented.

In the present work the k-form spectra were used to fully characterize homogeneous polynomial nonlinearities. However, the research on nonlinear characterization of heterogeneous polynomials is far from being completed. There are numerous important questions for which currently there are either partial or no answers. For instance, of what significance are the eigenmode multiplicities on formations of process manifolds? In Example 5.1.1 in Chapter 5, it was demonstrated that in the simple two-dimensional case the eigenmode multiplicity branches polynomial eigenspectra by creating parallel manifolds: what happens in more complex situations? Moreover, it would be useful to have a better understanding of relations between the homogeneous invariants (*i.e.*, k- form eigenmodes) and other state-space invariants (*e.g.*, steady-states, process manifolds, limit cycles, chaotic attractors, *etc.*). Also, an important theoretical and practical question is: what nonlinearities, other than those of the polynomial type, can

be characterized by using the spectral method? As an example of nonlinearities not treated in the thesis, and which are of a considerable importance in chemistry and biology, are the ones that are defined by the rational functions. These can also be characterized by using the method proposed.

From the results presented we can further conclude that a considerable research effort is needed in the area of algorithm development. Presently there are no algorithms that in a systematic way address numeric evaluations of power series terms and their spectra. Thus, computation of eigenspectra is often a time consuming exercise, which in higher dimensional cases can also become unreliable and confusing. As a result, better algorithms are needed for computing process eigenspectra more rapidly and more reliably. In addition, this would enhance our ability to understand and apply the method in instances when a model dimension >3.

From the process analysis and design point of views we have covered quite extensively various stability and control issues. Nevertheless, the research on understanding properties of different nonlinear control strategies (*e.g.*, polynomial, exponential, input/output, *etc.*) and how they blend with different global open-loop characteristics needs to be continued. Furthermore, in evaluating a performance and feasibility of a control strategy we have used a measure defined by the control speed du/dt. However, of a considerable practical importance are also higher-order dynamic moments (*e.g.*, control acceleration d^2u/dt^2). Moreover, in addition to the robustness results presented there is a need for a better understanding of adaptive control issues caused by uncertainty in model parameters, as well as a presence of an external noise. And finally, the present study does not consider the case in which an observer is included in process descriptions. As a result, the nonlinear process observability should also be examined in the context of the spectral framework. Ultimately, one would like to be able to combine both the controllability and observability criteria for a state feedback realization.

APPENDIX I

SPECTRAL SETS FOR EXAMPLE 3.4.1

For the 4-dimensional skew-symmetric cubic model we have that $s_{3,4}=40$, and the degree of freedom is $p_{3,4}=20$. Therefore, any 20 eigenvectors form an algebraic basis while the remaining 20 are algebraically dependent. All eigenvectors are computed by solving the characteristic equation using the Newton's method.

$$\Lambda_3\{C\} = \left\{ \begin{array}{c} i\ 0.5816977100\ ;\ -i\ 0.5816977100\ ; \\ i\ 4.7886536247\ ;\ -i\ 4.7886536247\ ; \\ -0.3030068281 + i\ 0.6540346567\ ;\ -0.3030068281 - i\ 0.6540346567\ ; \\ 0.3030068281 - i\ 0.6540346567\ ;\ 0.3030068281 + i\ 0.6540346567\ ; \\ 0.6684942287 - i\ 0.1563646526\ ;\ 0.6684942287 + i\ 0.1563646526\ ; \\ -0.6684942287 + i\ 0.1563646526\ ;\ -0.6684942287 - i\ 0.1563646526\ ; \\ 0.3183525219 - i\ 0.2384632232\ ;\ 0.3183525219 + i\ 0.2384632232\ ; \\ -0.3183525219 + i\ 0.2384632232\ ;\ -0.3183525219 - i\ 0.2384632232\ ; \\ 0.7913874549 - i\ 0.2587704301\ ;\ 0.7913874549 + i\ 0.2587704301\ ; \\ -0.7913874549 + i\ 0.2587704301\ ;\ -0.7913874549 - i\ 0.2587704301\ ; \\ -0.2401839983 + i\ 0.5452212257\ ;\ -0.2401839983 - i\ 0.5452212257\ ; \\ 0.2401839983 - i\ 0.5452212257\ ;\ 0.2401839983 + i\ 0.5452212257\ ; \\ -2.4508866524 + i\ 2.9659249474\ ;\ -2.4508866524 - i\ 2.9659249474\ ; \\ 2.4508866524 - i\ 2.9659249474\ ;\ 2.4508866524 + i\ 2.9659249474\ ; \\ 0.7456003562 + i\ 0.1844854245\ ;\ 0.7456003562 - i\ 0.1844854245\ ; \\ -0.7456003562 - i\ 0.1844854245\ ;\ -0.7456003562 + i\ 0.1844854245\ ; \\ 0.9079837399 - i\ 0.7922002008\ ;\ 0.9079837399 + i\ 0.7922002008\ ; \\ -0.9079837399 + i\ 0.7922002008\ ;\ -0.9079837399 - i\ 0.7922002008\ ; \\ -0.2513426308 + i\ 0.5549623252\ ;\ -0.2513426308 - i\ 0.5549623252\ ; \\ 0.2513426308 - i\ 0.5549623252\ ;\ 0.2513426308 + i\ 0.5549623252\ ; \end{array} \right\}$$

and

$$X_3\{C^4\} = \left\{ \begin{bmatrix} 1 \\ -0.5363913556 - i\ 0.6852873335 \\ -i\ 0.3485319470 \\ 0.5363913556 - i\ 0.6852873335 \end{bmatrix}; \begin{bmatrix} 1 \\ -0.5363913556 + i\ 0.6852873335 \\ i\ 0.3485319470 \\ 0.5363913556 + i\ 0.6852873335 \end{bmatrix}; \right.$$

$$\begin{bmatrix} 1 \\ 1.9662136656 - i\ 1.5390042921 \\ i\ 2.8691816198 \\ -1.9662136656 - i\ 1.5390042921 \end{bmatrix}; \begin{bmatrix} 1 \\ 1.9662136656 + i\ 1.5390042921 \\ -i\ 2.8691816198 \\ -1.9662136656 + i\ 1.5390042921 \end{bmatrix};$$

$$\begin{bmatrix} 1 \\ -0.6180419404 - i\ 0.6955166029 \\ -0.4292713353 + i\ 0.0554128919 \\ 0.4641306031 - i\ 0.6186853448 \end{bmatrix}; \begin{bmatrix} 1 \\ -0.6180419404 + i\ 0.6955166029 \\ -0.4292713353 - i\ 0.0554128919 \\ 0.4641306031 + i\ 0.6186853448 \end{bmatrix};$$

$$\begin{bmatrix} 1 \\ -0.4641306031 + i\ 0.6186853448 \\ 0.4292713353 - i\ 0.0554128919 \\ 0.6180419404 + i\ 0.6955166029 \end{bmatrix}; \begin{bmatrix} 1 \\ -0.4641306031 - i\ 0.6186853448 \\ 0.4292713353 + i\ 0.0554128919 \\ 0.6180419404 - i\ 0.6955166029 \end{bmatrix};$$

$$\begin{bmatrix} 1 \\ -0.2277581873 - i\ 0.9737177250 \\ 0.9604318557 + i\ 0.4794832863 \\ 0.6856275933 + i\ 0.8259832774 \end{bmatrix}; \begin{bmatrix} 1 \\ -0.2277581873 + i\ 0.9737177250 \\ 0.9604318557 - i\ 0.4794832863 \\ 0.6856275933 - i\ 0.8259832774 \end{bmatrix};$$

$$\begin{bmatrix} 1 \\ -0.6856275933 - i\ 0.8259832774 \\ -0.9604318557 - i\ 0.4794832863 \\ 0.2277581873 + i\ 0.9737177250 \end{bmatrix}; \begin{bmatrix} 1 \\ -0.6856275933 + i\ 0.8259832774 \\ -0.9604318557 + i\ 0.4794832863 \\ 0.2277581873 - i\ 0.9737177250 \end{bmatrix};$$

$$\begin{bmatrix} 1 \\ 0.7826349144 + i\ 0.2009393579 \\ 0.6300260965 + i\ 0.5059260334 \\ 0.5995153081 + i\ 0.8003632895 \end{bmatrix}; \begin{bmatrix} 1 \\ 0.7826349144 - i\ 0.2009393579 \\ 0.6300260965 - i\ 0.5059260334 \\ 0.5995153081 - i\ 0.8003632895 \end{bmatrix};$$

$$\begin{bmatrix} 1 \\ -0.5995153081 - i\ 0.8003632895 \\ -0.6300260965 - i\ 0.5059260334 \\ -0.7826349144 - i\ 0.2009393579 \end{bmatrix}; \begin{bmatrix} 1 \\ -0.5995153081 + i\ 0.8003632895 \\ -0.6300260965 + i\ 0.5059260334 \\ -0.7826349144 + i\ 0.2009393579 \end{bmatrix};$$

$$\begin{bmatrix} 1 \\ 0.2619406467 + i\ 0.3844352645 \\ 0.1657046968 - i\ 0.8145643585 \\ 0.7139057902 + i\ 0.8033974440 \end{bmatrix}; \begin{bmatrix} 1 \\ 0.2619406467 - i\ 0.3844352645 \\ 0.1657046968 + i\ 0.8145643585 \\ 0.7139057902 - i\ 0.8033974440 \end{bmatrix};$$

$$\begin{bmatrix} 1 \\ -0.7139057902 - i\ 0.8033974440 \\ -0.1657046968 + i\ 0.8145643585 \\ -0.2619406467 - i\ 0.3844352645 \end{bmatrix}; \begin{bmatrix} 1 \\ -0.7139057902 + i\ 0.8033974440 \\ -0.1657046968 - i\ 0.8145643585 \\ -0.2619406467 + i\ 0.3844352645 \end{bmatrix}; \left. \right\}$$

.....

continue on the next page

$$\left(\begin{bmatrix} 1 \\ -0.5949905567 - i\ 0.7167918201 \\ 0.8334668679 - i\ 0.4160976529 \\ -0.9151375845 - i\ 0.4031416650 \end{bmatrix}; \begin{bmatrix} 1 \\ -0.5949905567 + i\ 0.7167918201 \\ 0.8334668679 + i\ 0.4160976529 \\ -0.9151375845 + i\ 0.4031416650 \end{bmatrix};\right.$$

$$\begin{bmatrix} 1 \\ 0.9151375845 + i\ 0.4031416650 \\ -0.8334668679 + i\ 0.4160976529 \\ 0.5949905567 + i\ 0.7167918201 \end{bmatrix}; \begin{bmatrix} 1 \\ -0.5949905567 - i\ 0.7167918201 \\ 0.8334668679 - i\ 0.4160976529 \\ -0.9151375845 - i\ 0.4031416650 \end{bmatrix};$$

$$\begin{bmatrix} 1 \\ -1.2464798689 + i\ 1.2803423970 \\ 2.2913478042 + i\ 0.2957807747 \\ -1.2104286034 - i\ 1.7764753649 \end{bmatrix}; \begin{bmatrix} 1 \\ -1.2464798689 - i\ 1.2803423970 \\ 2.2913478042 - i\ 0.2957807747 \\ -1.2104286034 + i\ 1.7764753649 \end{bmatrix};$$

$$\begin{bmatrix} 1 \\ 1.2104286034 + i\ 1.7764753649 \\ -2.2913478042 - i\ 0.2957807747 \\ 1.2464798689 - i\ 1.2803423970 \end{bmatrix}; \begin{bmatrix} 1 \\ 1.2104286034 - i\ 1.7764753649 \\ -2.2913478042 + i\ 0.2957807747 \\ 1.2464798689 + i\ 1.2803423970 \end{bmatrix};$$

$$\begin{bmatrix} 1 \\ 0.3153755041 - i\ 0.2468513874 \\ 0.2401885332 - i\ 0.9707261599 \\ 0.7082621994 + i\ 0.9048674849 \end{bmatrix}; \begin{bmatrix} 1 \\ 0.3153755041 + i\ 0.2468513874 \\ 0.2401885332 + i\ 0.9707261599 \\ 0.7082621994 - i\ 0.9048674849 \end{bmatrix};$$

$$\cdots\cdots \begin{bmatrix} 1 \\ -0.7082621994 - i\ 0.9048674849 \\ -0.2401885332 + i\ 0.9707261599 \\ -0.3153755041 + i\ 0.2468513874 \end{bmatrix}; \begin{bmatrix} 1 \\ -0.7082621994 + i\ 0.9048674849 \\ -0.2401885332 - i\ 0.9707261599 \\ -0.3153755041 - i\ 0.2468513874 \end{bmatrix};$$

$$\begin{bmatrix} 1 \\ -0.3903802939 + i\ 0.4009855666 \\ 0.2398135117 + i\ 1.1788653745 \\ 0.7758932040 - i\ 1.0342643877 \end{bmatrix}; \begin{bmatrix} 1 \\ -0.3903802939 - i\ 0.4009855666 \\ 0.2398135117 - i\ 1.1788653745 \\ 0.7758932040 + i\ 1.0342643877 \end{bmatrix};$$

$$\begin{bmatrix} 1 \\ -0.7758932040 + i\ 1.0342643877 \\ -0.2398135117 - i\ 1.1788653745 \\ 0.3903802939 - i\ 0.4009855666 \end{bmatrix}; \begin{bmatrix} 1 \\ -0.7758932040 - i\ 1.0342643877 \\ -0.2398135117 + i\ 1.1788653745 \\ 0.3903802939 + i\ 0.4009855666 \end{bmatrix};$$

$$\begin{bmatrix} 1 \\ 1.1987165927 - i\ 0.3077671792 \\ -0.9649745006 - i\ 0.7748976192 \\ -0.9109301659 - i\ 0.4125605764 \end{bmatrix}; \begin{bmatrix} 1 \\ 1.1987165927 + i\ 0.3077671792 \\ -0.9649745006 + i\ 0.7748976192 \\ -0.9109301659 + i\ 0.4125605764 \end{bmatrix};$$

$$\left.\begin{bmatrix} 1 \\ 0.9109301659 + i\ 0.4125605764 \\ 0.9649745006 + i\ 0.7748976192 \\ -1.1987165927 + i\ 0.3077671792 \end{bmatrix}; \begin{bmatrix} 1 \\ 0.9109301659 - i\ 0.4125605764 \\ 0.9649745006 - i\ 0.7748976192 \\ -1.1987165927 - i\ 0.3077671792 \end{bmatrix}.\right)$$

APPENDIX II

EIGENVECTOR POOLS FOR EXAMPLE 4.3.1

The eigenvector solutions outlined in plain boxes are used to form the algebraic basis and the matrix Γ which produces the unstable cubic state feedback realization. The solution in the shaded box of the eigenvector pool λ=-1, is used to construct the algebraic basis which yields the globally stabilizing feedback structure.

Eigenvector pools:

$$P_3\{C^3|\lambda=-1\}=\left\{\begin{bmatrix}1\\0\\0\end{bmatrix};\begin{bmatrix}1\\5.645751\\0\end{bmatrix};\begin{bmatrix}1\\0.3542487\\0\end{bmatrix};\begin{bmatrix}1\\0\\0.4142136\end{bmatrix};\begin{bmatrix}1\\0\\-2.414214\end{bmatrix};\boxed{\begin{bmatrix}1\\0.734695\\-2.286523\end{bmatrix}};\ \boxed{\begin{bmatrix}1\\0.4656943\\0.4254655\end{bmatrix}};\begin{bmatrix}1\\-0.2668613+i\,2.334425\\2.597195+i\,0.6708414\end{bmatrix};\begin{bmatrix}1\\-0.2668613-i\,2.334425\\2.597195-i\,0.6708414\end{bmatrix}\right\}$$

$$P_3\{C^3|\lambda=-2\}=\left\{\begin{bmatrix}1\\0\\0\end{bmatrix};\begin{bmatrix}1\\5.44949\\0\end{bmatrix};\begin{bmatrix}1\\0.5505103\\0\end{bmatrix};\begin{bmatrix}1\\0\\0.7320508\end{bmatrix};\begin{bmatrix}1\\0\\-2.732051\end{bmatrix};\begin{bmatrix}1\\0.9160221\\-2.495938\end{bmatrix};\ \boxed{\begin{bmatrix}1\\0.8240486\\0.57033\end{bmatrix}};\begin{bmatrix}1\\-0.536702+i\,2.271175\\2.62947+i\,0.9845724\end{bmatrix};\begin{bmatrix}1\\-0.536702-i\,2.271175\\2.62947-i\,0.9845724\end{bmatrix}\right\}$$

$$P_3\{C^3|\lambda=-3\}=\left\{\begin{bmatrix}1\\0\\0\end{bmatrix};\begin{bmatrix}1\\5.236068\\0\end{bmatrix};\begin{bmatrix}1\\0.763932\\0\end{bmatrix};\begin{bmatrix}1\\0\\1\end{bmatrix};\begin{bmatrix}1\\0\\-3\end{bmatrix};\begin{bmatrix}1\\1.080683\\-2.656784\end{bmatrix};\ \boxed{\begin{bmatrix}1\\1.165663\\0.5646482\end{bmatrix}};\begin{bmatrix}1\\-0.7898392+i\,2.260396\\2.712735+i\,1.266155\end{bmatrix};\begin{bmatrix}1\\-0.7898392-i\,2.260396\\2.712735-i\,1.266155\end{bmatrix}\right\}$$

$$P_3\{C^3|\lambda=-5\}=\left\{\begin{bmatrix}1\\0\\0\end{bmatrix};\begin{bmatrix}1\\4.732051\\0\end{bmatrix};\boxed{\begin{bmatrix}1\\1.267949\\0\end{bmatrix}};\begin{bmatrix}1\\0\\1.44949\end{bmatrix};\begin{bmatrix}1\\0\\-3.44949\end{bmatrix};\begin{bmatrix}1\\1.379951\\-2.88982\end{bmatrix};\ \begin{bmatrix}1\\1.714037\\0.3557992\end{bmatrix};\begin{bmatrix}1\\-1.213661+i\,2.310522\\2.933677+i\,1.719419\end{bmatrix};\begin{bmatrix}1\\-1.213661-i\,2.310522\\2.933677-i\,1.719419\end{bmatrix}\right\}$$

$$P_3\{C^3|\lambda=-8\}=\left\{\begin{bmatrix}1\\0\\0\end{bmatrix};\boxed{\begin{matrix}1\\3\\0\end{matrix}}_{(2)};\begin{bmatrix}1\\0\\2\end{bmatrix};\begin{bmatrix}1\\0\\-4\end{bmatrix};\begin{bmatrix}1\\1.78667\\-3.098164\end{bmatrix};\begin{bmatrix}1\\2.291671\\-0.1122157\end{bmatrix};\begin{bmatrix}1\\-1.705837+i\,2.430973\\3.271857+i\,2.226005\end{bmatrix};\begin{bmatrix}1\\-1.705837-i\,2.430973\\3.271857-i\,2.226005\end{bmatrix}\right\}$$

$$P_3\{C^3|\lambda=-13\}=\left\{\begin{bmatrix}1\\0\\0\end{bmatrix};\begin{bmatrix}1\\3+i\,2.236068\\0\end{bmatrix};\begin{bmatrix}1\\3-i\,2.236068\\0\end{bmatrix};\begin{bmatrix}1\\0\\2.741657\end{bmatrix};\begin{bmatrix}1\\0\\-4.741657\end{bmatrix};\begin{bmatrix}1\\2.424003\\-3.161579\end{bmatrix};\boxed{\begin{matrix}1\\2.907286\\-1.051561\end{matrix}};\begin{bmatrix}1\\-2.332311+i\,2.63383\\3.773236+i\,2.226005\end{bmatrix};\begin{bmatrix}1\\-2.332311-i\,2.849794\\3.773236-i\,2.849794\end{bmatrix}\right\}$$

$$P_3\{C^3|\lambda=-21\}=\left\{\begin{bmatrix}1\\0\\0\end{bmatrix};\begin{bmatrix}1\\3+i\,3.605551\\0\end{bmatrix};\begin{bmatrix}1\\3-i\,3.605551\\0\end{bmatrix};\begin{bmatrix}1\\0\\3.690416\end{bmatrix};\boxed{\begin{matrix}1\\0\\-5.690416\end{matrix}};\begin{bmatrix}1\\3.432699+i\,0.2955507\\-2.777759+i\,1.058241\end{bmatrix};\begin{bmatrix}1\\3.432699-i\,0.2955507\\-2.777759-i\,1.058241\end{bmatrix};\begin{bmatrix}1\\-3.099366+i\,2.919651\\4.444426+i\,3.59229\end{bmatrix};\begin{bmatrix}1\\-3.099366-i\,2.919651\\4.444426-i\,3.59229\end{bmatrix}\right\}$$

$$P_3\{C^3\lambda=-34\}=\left\{\begin{bmatrix}1\\0\\0\end{bmatrix};\begin{bmatrix}1\\3+i\,5.09902\\0\end{bmatrix};\begin{bmatrix}1\\3-i\,5.09902\\0\end{bmatrix};\boxed{\begin{matrix}1\\0\\4.91608\end{matrix}};\begin{bmatrix}1\\0\\-6.91608\end{bmatrix};\begin{bmatrix}1\\4.394659+i\,0.7364631\\-3.664843+i\,2.290858\end{bmatrix};\begin{bmatrix}1\\4.394659-i\,0.7364631\\-3.664843-i\,2.290858\end{bmatrix};\begin{bmatrix}1\\-4.061326+i\,3.30631\\5.331509+i\,4.502744\end{bmatrix};\begin{bmatrix}1\\-4.061326-i\,3.30631\\5.331509-i\,4.502744\end{bmatrix}\right\}$$

$$P_3\{C^3|\lambda=-89\}=\left\{\boxed{\begin{matrix}1\\0\\0\end{matrix}};\begin{bmatrix}1\\3+i\,9\\0\end{bmatrix};\begin{bmatrix}1\\3-i\,9\\0\end{bmatrix};\begin{bmatrix}1\\0\\8.486833\end{bmatrix};\begin{bmatrix}1\\0\\-10.48683\end{bmatrix};\begin{bmatrix}1\\7.125024+i\,1.924152\\-6.291362+i\,5.00007\end{bmatrix};\begin{bmatrix}1\\7.125024-i\,1.924152\\-6.291362-i\,5.00007\end{bmatrix};\begin{bmatrix}1\\-6.79169+i\,4.468606\\7.958029+i\,7.025327\end{bmatrix};\begin{bmatrix}1\\-6.79169-i\,4.468606\\7.958029-i\,7.025327\end{bmatrix}\right\}$$

APPENDIX III

EIGENVECTOR POOLS FOR EXAMPLE 4.4.1

The eigenvectors outlined by using plain boxes create the quadratic basis $B_2\{R^3\}^{selected}$ which yields the unstable state feedback design. The solutions in shaded boxes are used to obtain the stabilizing quadratic basis. Observe, also, that the eigenvector pools contain the two-dimensional trivial subspace defined by the second pool component. Furthermore, since for any $\mathbf{x}=[1,-1,r\in R]^t$ we have $\mathbf{B}[\mathbf{x}]=0$, then the trivial subspace annihilates any control u. Thus, no solutions within the trivial subspace are permitted to enter the quadratic basis and the Γ-matrx defined as

$$\Gamma = \begin{bmatrix} \mathbf{z}(\mathbf{v}_{\lambda=-1})^t \\ \mathbf{z}(\mathbf{v}_{\lambda=-2})^t \\ \mathbf{z}(\mathbf{v}_{\lambda=-3})^t \\ \mathbf{z}(\mathbf{v}_{\lambda=-5})^t \\ \mathbf{z}(\mathbf{v}_{\lambda=-7})^t \\ \mathbf{z}(\mathbf{v}_{\lambda=-11})^t \end{bmatrix}$$

where $\mathbf{z}(\mathbf{v})=[1,v_2,v_3,v_2^2,v_2v_3,v_3^2]^t$ for each $\mathbf{v}=[1,v_2,v_3]^t$ selected. For the quadratic basis $B_2\{R^3\}^{selected}$ we have

$$\Gamma = \begin{bmatrix} 1 & 0 & 0 & 0 & 0 & 0 \\ 1 & 0 & -2.7320508 & 0 & 0 & 7.4641016 \\ 1 & 0 & 1 & 0 & 0 & 1 \\ 1 & 4.7320508 & 0 & 22.3923048 & 0 & 0 \\ 1 & 1.6548929 & -3.0439060 & 2.7386705 & -5.0373384 & 9.2653638 \\ 1 & 2.6997951 & -0.6507048 & 7.2888940 & -1.7567698 & 0.42341682 \end{bmatrix}$$

while for $B_2\{R^3\}^{selected}_{new}$

$$\Gamma_{new} = \begin{bmatrix} 1 & 0 & 0 & 0 & 0 & 0 \\ 1 & 0 & -2.7320508 & 0 & 0 & 7.4641016 \\ 1 & 0 & 1 & 0 & 0 & 1 \\ 1 & 4.7320508 & 0 & 22.3923048 & 0 & 0 \\ 1 & 2 & 0 & 4 & 0 & 0 \\ 1 & 2.1700006 & -3.1799530 & 4.7089027 & -6.9005000 & 10.1121011 \end{bmatrix}.$$

Eigenvector pools:

$$P_3\{C^3|\lambda=-1\} = \left\langle \begin{bmatrix} 1 \\ 0 \\ 0 \end{bmatrix}; \begin{bmatrix} 1 \\ -1 \\ r \end{bmatrix} r\in\mathbb{R}; \begin{bmatrix} 1 \\ -0.2668613 + i\,2.3344247 \\ 2.5971954 + i\,0.6708414 \end{bmatrix}; \begin{bmatrix} 1 \\ -0.2668613 - i\,2.3344247 \\ 2.5971954 - i\,0.6708414 \end{bmatrix} \right.$$
$$\left. \begin{bmatrix} 1 \\ 0.4656943 \\ 0.4254655 \end{bmatrix}; \begin{bmatrix} 1 \\ 0.7346950 \\ -2.2865230 \end{bmatrix}; \begin{bmatrix} 1 \\ 5.6457513 \\ 0 \end{bmatrix}; \right.$$
$$\left. \begin{bmatrix} 1 \\ 0.3542486 \\ 0 \end{bmatrix}; \begin{bmatrix} 1 \\ 0 \\ 0.4142135 \end{bmatrix}; \begin{bmatrix} 1 \\ 0 \\ -2.4142135 \end{bmatrix} \right\rangle$$

$$P_3\{C^3|\lambda=-2\} = \left\langle \begin{bmatrix} 1 \\ 0 \\ 0 \end{bmatrix}; \begin{bmatrix} 1 \\ -1 \\ r \end{bmatrix} r\in\mathbb{R}; \begin{bmatrix} 1 \\ -0.5367020 + i\,2.2711751 \\ 2.6294704 + i\,0.9845723 \end{bmatrix}; \begin{bmatrix} 1 \\ -0.5367020 - i\,2.2711751 \\ 2.6294704 - i\,0.9845723 \end{bmatrix}; \right.$$
$$\left. \begin{bmatrix} 1 \\ 0.8240486 \\ 0.5703300 \end{bmatrix}; \begin{bmatrix} 1 \\ 0.9160221 \\ -2.4959375 \end{bmatrix}; \begin{bmatrix} 1 \\ 5.4494897 \\ 0 \end{bmatrix}; \right.$$
$$\left. \begin{bmatrix} 1 \\ 0.5505102 \\ 0 \end{bmatrix}; \begin{bmatrix} 1 \\ 0 \\ 0.7320508 \end{bmatrix}; \boxed{\begin{bmatrix} 1 \\ 0 \\ -2.7320508 \end{bmatrix}} \right\rangle$$

$$P_3\{C^3|\lambda=-3\} = \left\langle \begin{bmatrix} 1 \\ 0 \\ 0 \end{bmatrix}; \begin{bmatrix} 1 \\ -1 \\ r \end{bmatrix} r\in\mathbb{R}; \begin{bmatrix} 1 \\ -0.7898392 + i\,2.2603960 \\ 2.7127345 + i\,1.2661549 \end{bmatrix}; \begin{bmatrix} 1 \\ -0.7898392 - i\,2.2603960 \\ 2.7127345 - i\,1.2661549 \end{bmatrix}; \right.$$
$$\left. \begin{bmatrix} 1 \\ 1.1656625 \\ 0.5646482 \end{bmatrix}; \begin{bmatrix} 1 \\ 1.0806825 \\ -2.6567839 \end{bmatrix}; \begin{bmatrix} 1 \\ 5.2360679 \\ 0 \end{bmatrix}; \begin{bmatrix} 1 \\ 0.7639320 \\ 0 \end{bmatrix}; \boxed{\begin{bmatrix} 1 \\ 0 \\ 1 \end{bmatrix}}; \begin{bmatrix} 1 \\ 0 \\ -3 \end{bmatrix} \right\rangle$$

$$P_3\{C^3|\lambda=-5\} = \left\langle \begin{bmatrix} 1 \\ 0 \\ 0 \end{bmatrix}; \begin{bmatrix} 1 \\ -1 \\ r \end{bmatrix} r\in\mathbb{R}; \begin{bmatrix} 1 \\ -1.2136606 + i\,2.3105216 \\ 2.9336773 + i\,1.7194189 \end{bmatrix}; \begin{bmatrix} 1 \\ -1.2136606 - i\,2.3105216 \\ 2.9336773 - i\,1.7194189 \end{bmatrix}; \right.$$
$$\left. \begin{bmatrix} 1 \\ 1.7140369 \\ 0.3557992 \end{bmatrix}; \begin{bmatrix} 1 \\ 1.3799509 \\ -2.8898204 \end{bmatrix}; \boxed{\begin{bmatrix} 1 \\ 4.7320508 \\ 0 \end{bmatrix}}; \right.$$
$$\left. \begin{bmatrix} 1 \\ 1.2679491 \\ 0 \end{bmatrix}; \begin{bmatrix} 1 \\ 0 \\ 1.4494897 \end{bmatrix}; \begin{bmatrix} 1 \\ 0 \\ -3.4494897 \end{bmatrix} \right\rangle$$

$$P_3\{C^3|\lambda=-7\}=\left\{\begin{bmatrix}1\\0\\0\end{bmatrix};\begin{bmatrix}1\\-1\\r\end{bmatrix}r\in\mathbb{R};\begin{bmatrix}1\\-1.5555207+i\,2.3893135\\3.1618072+i\,2.0731163\end{bmatrix};\begin{bmatrix}1\\-1.5555207-i\,2.3893135\\3.1618072-i\,2.0731163\end{bmatrix};\right.$$
$$\left.\begin{bmatrix}1\\2.1228153\\0.0536248\end{bmatrix};\begin{bmatrix}1\\1.6548929\\-3.0439060\end{bmatrix};\begin{bmatrix}1\\4\\0\end{bmatrix};\begin{bmatrix}1\\2\\0\end{bmatrix};\begin{bmatrix}1\\0\\1.8284271\end{bmatrix};\begin{bmatrix}1\\0\\-3.8284271\end{bmatrix}\right\}$$

$$P_3\{C^3|\lambda=-11\}=\left\{\begin{bmatrix}1\\0\\0\end{bmatrix};\begin{bmatrix}1\\-1\\r\end{bmatrix}r\in\mathbb{R};\begin{bmatrix}1\\-2.1015645+i\,2.5547178\\3.5819956+i\,2.6222565\end{bmatrix};\begin{bmatrix}1\\-2.1015645-i\,2.5547178\\3.5819956-i\,2.6222565\end{bmatrix};\right.$$
$$\begin{bmatrix}1\\2.6997951\\-0.6507048\end{bmatrix};\begin{bmatrix}1\\2.1700006\\-3.1799530\end{bmatrix};\begin{bmatrix}1\\3+i\,1.73205\\0\end{bmatrix};$$
$$\left.\begin{bmatrix}1\\3-i\,1.73205\\0\end{bmatrix};\begin{bmatrix}1\\0\\2.4641016\end{bmatrix};\begin{bmatrix}1\\0\\-4.4641016\end{bmatrix}\right\}$$

APPENDIX IV

CSTR MANIFOLDS AND STEADY-STATES

To compute CSTR manifolds we select the projection state to be the translated dimensionless temperature variable $\overleftrightarrow{x}_2$, and use it to derive the heterogeneous eigenvalue problem for the approximating CSTR model given in Equation (1.2.6). At a steady-state $\mathbf{x}_s=[x_{1s}, x_{2s}]^t$ the characteristic equation is

$$\sum_{j=1}^{k} \mathbf{F}_j[\mathbf{v}]\, \overleftrightarrow{x}_2^{k-1} - \beta(\overleftrightarrow{x}_2)\, \mathbf{v} = 0 \qquad \text{(A.IV.1)}$$

where k signifies the highest power series term considered, $\mathbf{v}=[v_1, 1]^t$ is such that $\overleftrightarrow{x}_1=v_1\overleftrightarrow{x}_2$ and

$$\beta(\overleftrightarrow{x}_2) = \sum_{j=1}^{k} \lambda_j\, \overleftrightarrow{x}_2^{j-1} \qquad \text{(A.IV.2)}$$

with

$$\lambda_j = \begin{cases} Bx_{1s} - 1 - \beta - \dfrac{Bx_{1s}}{1-x_{1s}} v_1 \; ; & \text{for } j=1 \\ \dfrac{Bx_{1s}}{j!}\left(1 - \dfrac{j}{1-x_{1s}} v_1\right) \; ; & \text{for } j>1 \end{cases} . \qquad \text{(A.IV.3)}$$

Equation (A.IV.1) can further be simplified to obtain

$$a_2(\overleftrightarrow{x}_2)\, v_1^2 + a_1(\overleftrightarrow{x}_2)\, v_1 + a_0(\overleftrightarrow{x}_2) = 0 \qquad \text{(A.IV.4)}$$

where

$$a_0(\overleftrightarrow{x}_2) = x_{1s} \sum_{j=1}^{k} \frac{\overleftrightarrow{x}_2^{j-1}}{j!}$$

$$a_1(\overleftrightarrow{x}_2) = 1 + \beta - B\, x_{1s} - \frac{1}{1-x_{1s}} - \sum_{j=2}^{k} \left[\frac{x_{1s}\overleftrightarrow{x}_2^{j-1}}{(1-x_{1s})(j-1)!} + \frac{Bx_{1s}\overleftrightarrow{x}_2^{j-1}}{j!} \right]$$

$$a_2(\overleftrightarrow{x}_2) = \frac{Bx_{1s}}{1-x_{1s}} \sum_{j=1}^{k} \frac{\overleftrightarrow{x}_2^{j-1}}{(j-1)!}$$

The last expression is quadratic in v_1 and as such produces two manifold solutions for any specified projection state $\overleftrightarrow{x}_2$ and any truncation value k. Thus, the complete CSTR dynamics from the temperature point of view is determined by two manifolds. For example, for k=7 these are presented in Figure 5.2.2.a) as the stable (SM) and unstable (UM) manifolds, while the corresponding eigenfunctions are depicted in Figure 5.2.2.b). Observe that the two real manifolds which emerge out of the steady-state $\overleftrightarrow{x}_{2s}$ become complex for $\overleftrightarrow{x}_2$<-2.35. The branch point (bp) separates the two solutions. In addition, note that the sign change in eigenfunctions β_{UM} and β_{SM} implies the presence of the steady- states $\overleftrightarrow{x}_{1s}$ and $\overleftrightarrow{x}_{3s}$. The evolution and stability character of these steady-states for different k values are listed in Table A. IV.1.

Table A.IV.1: Evolution of CSTR steady-states.

k-order approximation	$\overleftrightarrow{x}_{1s}$	accuracy: $\|x_{1s} - (\overleftrightarrow{x}_{1s} + x_{2s})\|$	$\overleftrightarrow{x}_{3s}$	accuracy: $\|x_{3s} - (\overleftrightarrow{x}_{3s} + x_{2s})\|$
1	not existent	-	not existent	-
2	$\begin{bmatrix} -0.263613 \\ -1.647585 \end{bmatrix}$ stable node	0.666073	not existent	-
3	$\begin{bmatrix} -0.344664 \\ -2.154152 \end{bmatrix}$ stable focus	0.153063	not existent	-
4	not existent	-	$\begin{bmatrix} 1.377565 \\ 8.609787 \end{bmatrix}$ unstable node	5.505585
5	$\begin{bmatrix} -0.328936 \\ -2.055854 \end{bmatrix}$ stable node	0.252611	$\begin{bmatrix} 0.684234 \\ 4.276468 \end{bmatrix}$ unstable node	1.11715
6	not existent	-	$\begin{bmatrix} 0.566591 \\ 3.541195 \end{bmatrix}$ unstable node	0.372526
7	$\begin{bmatrix} -0.357788 \\ -2.23618 \end{bmatrix}$ stable node	0.069991	$\begin{bmatrix} 0.529056 \\ 3.306602 \end{bmatrix}$ unstable focus	0.134949
8	$\begin{bmatrix} -0.373821 \\ -2.336381 \end{bmatrix}$ stable node	0.031483	$\begin{bmatrix} 0.515337 \\ 3.220856 \end{bmatrix}$ unstable focus	.048112
9	$\begin{bmatrix} -0.367638 \\ -2.297742 \end{bmatrix}$ stable node	0.007646	$\begin{bmatrix} 0.510295 \\ 3.189344 \end{bmatrix}$ unstable focus	0.0162
10	$\begin{bmatrix} -0.369156 \\ -2.30723 \end{bmatrix}$ stable node	0.001962	$\begin{bmatrix} 0.508534 \\ 3.17834 \end{bmatrix}$ unstable focus	0.005055
11	$\begin{bmatrix} -0.368779 \\ -2.304869 \end{bmatrix}$ stable node	0.000429	$\begin{bmatrix} 0.507965 \\ 3.174782 \end{bmatrix}$ unstable focus	0.001452
12	$\begin{bmatrix} -0.36886 \\ -2.305378 \end{bmatrix}$ stable node	0.000085	$\begin{bmatrix} 0.507796 \\ 3.173727 \end{bmatrix}$ stable focus	0.000384
13	$\begin{bmatrix} -0.368844 \\ -2.305277 \end{bmatrix}$ stable node	0.000015	$\begin{bmatrix} 0.50775 \\ 3.17344 \end{bmatrix}$ stable focus	0.000094
14	$\begin{bmatrix} -0.368847 \\ -2.305295 \end{bmatrix}$ stable node	0.000002	$\begin{bmatrix} 0.50773 \\ 3.173368 \end{bmatrix}$ stable focus	0.000021

$x_{1s} = \begin{bmatrix} 0.0732365 \\ 0.457728 \end{bmatrix}$, $x_{2s} = \begin{bmatrix} 0.4420834 \\ 2.763021 \end{bmatrix}$ and $x_{3s} = \begin{bmatrix} 0.9498191 \\ 5.936369 \end{bmatrix}$ are the original CSTR steady-state points for the parameter values B=25.0, Da=0.05, and β=3.0. The norm $\|x_{is} - (\overleftrightarrow{x}_{is} + x_{2s})\|$, where i=1 or 3, defines the measure which shows how close are the steady-state solutions for different k approximations to the original steady-states.

APPENDIX V

POWER SERIES AND SPECTRAL SETS FOR VINYL AND CYCLOPENTENOL EXAMPLES

The first four tables provide evaluated power series terms and the eigenspectra for the two vinyl CSTR processes examined in Section 5.4. For the cyclopentenol process only the numerically evaluated eigenspectra are listed in Table A.V.5.

Table A.V.1: 2D-PS case: numerically evaluated k-forms and their spectra at the unstable steady-state $\mathbf{x}_{2s}=[0.160821, 1.438591]^t$.

Two-dimensional PS power series approximation:	**PS eigenspectra:**
Two-dimensional CSTR model $\mathbf{F}[\mathbf{x}] \approx \sum_{i=1}^{5} \frac{1}{i!}\mathbf{F}_i[\mathbf{x}] + o6$, with $\mathbf{F}_1[\mathbf{x}] = \begin{bmatrix} 9.81606 & -1.8025 \\ -129.793 & 14.63 \end{bmatrix}\begin{bmatrix} x_1 \\ x_2 \end{bmatrix}$ $\mathbf{F}_2[\mathbf{x}] = \begin{bmatrix} 1 \\ -12 \end{bmatrix}\begin{bmatrix} -1.3714E2 & 4.5701E1 & -3.56744 \end{bmatrix}\begin{bmatrix} x_1^2 \\ x_1x_2 \\ x_2^2 \end{bmatrix}$ $\mathbf{F}_3[\mathbf{x}] = \begin{bmatrix} 1 \\ -12 \end{bmatrix}\begin{bmatrix} 1.33420E3 & -8.54314E2 & 1.33021E2 & -6.42348 \end{bmatrix}\begin{bmatrix} x_1^3 \\ x_1^2x_2 \\ x_1x_2^2 \\ x_2^3 \end{bmatrix}$ $\mathbf{F}_4[\mathbf{x}] = \begin{bmatrix} 1 \\ -12 \end{bmatrix}\begin{bmatrix} 5.93992E3 & 1.07246E4 & -3.24755E3 & 3.11694E2 & -1.03336E1 \end{bmatrix}\begin{bmatrix} x_1^4 \\ x_1^3x_2 \\ x_1^2x_2^2 \\ x_1x_2^3 \\ x_2^4 \end{bmatrix}$ $\mathbf{F}_5[\mathbf{x}] = \begin{bmatrix} 1 \\ -12 \end{bmatrix}\begin{bmatrix} -1.0339E6 & 7.54969E4 & 4.89205E4 & -9.2703E3 & 6.07512E2 & -1.44431E1 \end{bmatrix}\begin{bmatrix} x_1^5 \\ x_1^4x_2 \\ x_1^3x_2^2 \\ x_1^2x_2^3 \\ x_1x_2^4 \\ x_2^5 \end{bmatrix}$	$\mathbb{X}_1\{\mathbb{R}^2\} = \left\{\begin{bmatrix} 1 \\ -9.92551 \end{bmatrix}; \begin{bmatrix} 1 \\ 7.25478 \end{bmatrix}\right\}$ $\Lambda_1\{\mathbb{R}\} = \{ 27.7067 ; -3.26067\}$ $\mathbb{X}_2\{\mathbb{R}^2\} = \left\{\begin{bmatrix} 1 \\ -12 \end{bmatrix}; \begin{bmatrix} 1 \\ 4.79732 \end{bmatrix}; \begin{bmatrix} 1 \\ 8.01325 \end{bmatrix}\right\}$ $\Lambda_2\{\mathbb{R}\} = \{ -599.632 ; 0 ; 0\}$ $\mathbb{X}_3\{\mathbb{C}^2\} = \left\{\begin{bmatrix} 1 \\ -12 \end{bmatrix}; \begin{bmatrix} 1 \\ 2.285 \end{bmatrix}; \begin{bmatrix} 1 \\ 9.21184\text{-}i2.4581 \end{bmatrix}; \begin{bmatrix} 1 \\ 9.21184\text{+}i2.4581 \end{bmatrix}\right\}$ $\Lambda_3\{\mathbb{R}\} = \{ 6973.49 ; 0 ; 0 ; 0\}$ $\mathbb{X}_4\{\mathbb{C}^2\} = \left\{\begin{bmatrix} 1 \\ -12 \end{bmatrix}; \begin{bmatrix} 1 \\ -0.48062 \end{bmatrix}; \begin{bmatrix} 1 \\ 8.47442 \end{bmatrix}; \begin{bmatrix} 1 \\ 11.0847\text{-}i4.27282 \end{bmatrix}; \begin{bmatrix} 1 \\ 11.0847\text{+}i4.27282 \end{bmatrix}\right\}$ $\Lambda_4\{\mathbb{R}\} = \left\{\begin{matrix} -55970.5 ; 0 ; 0 ; \\ 0 ; 0 \end{matrix}\right\}$ $\mathbb{X}_5\{\mathbb{C}^2\} = \left\{\begin{bmatrix} 1 \\ -12 \end{bmatrix}; \begin{bmatrix} 1 \\ -3.76131 \end{bmatrix}; \begin{bmatrix} 1 \\ 8.98716\text{-}i1.21819 \end{bmatrix}; \begin{bmatrix} 1 \\ 8.98716\text{+}i1.21819 \end{bmatrix}; \begin{bmatrix} 1 \\ 13.9246\text{-}i6.1225 \end{bmatrix}; \begin{bmatrix} 1 \\ 13.9246\text{+}i6.1225 \end{bmatrix}\right\}$ $\Lambda_5\{\mathbb{R}\} = \left\{\begin{matrix} 310959.0 ; 0 ; 0 ; 0 ; \\ 0 ; 0 \end{matrix}\right\}$ All k-forms for k>5 have only one idempotent eigenvector which always is given by the solution $[1,-12]^t$. For k=6,7 one can show that eigenvalues corresponding to this eigenvector are $\lambda_6 = -997547.0$, $\lambda_7 = -1.29889E6$

Table A.V.2: 3D-PS case: numerically evaluated k-forms and their spectra at the unstable steady-state $\mathbf{x}_{2s}$=[0.231537,1.317364, 0.049896]^t.

Three-dimensional PS power series approximation:	**PS eigenspectra:**
Three-dimensional CSTR model $\mathbf{F}[\mathbf{x}] \approx \sum_{i=1}^{3} \frac{1}{i!}\mathbf{F}_i[\mathbf{x}] + o4$, with $\mathbf{F}_1[\mathbf{x}] = \begin{bmatrix} 8.5175 & -1.70961 & -7.70052 \\ -114.21 & 13.5153 & 92.4062 \\ 0.0 & -0.000365 & -1.00207 \end{bmatrix} \begin{bmatrix} x_1 \\ x_2 \\ x_3 \end{bmatrix}$ $\mathbf{F}_2[\mathbf{x}] = \begin{bmatrix} -129.33x_1^2 + 41.64x_1x_2 - 3.51x_2^2 + 190.74x_1x_3 - 34.26x_2x_3 + 77.16x_3^2 \\ -12(-129.33x_1^2 + 41.64x_1x_2 - 3.51x_2^2 + 190.74x_1x_3 - 34.26x_2x_3 + 77.16x_3^2) \\ - 0.0012x_2^2 - 0.0146x_2x_3 \end{bmatrix}$ $\mathbf{F}_3[\mathbf{x}] = \begin{bmatrix} 1787.76x_1^3 - 837.08x_1^2x_2 - 3887.94x_1^2x_3 + 126.01x_1x_2^2 - 2867.07x_1x_3^2 + \\ 1251.99x_1x_2x_3 - 6.61x_2^3 - 105.73x_2^2x_3 + 515.0x_2x_3^2 - 2319.71x_3^3 \\ -12(1787.76x_1^3 - 837.08x_1^2x_2 - 3887.94x_1^2x_3 + 126.01x_1x_2^2 - 2867.07x_1x_3^2 + \\ 1251.99x_1x_2x_3 - 6.61x_2^3 - 105.73x_2^2x_3 + 515.0x_2x_3^2 - 2319.71x_3^3) \\ (- 0.004025x_2^3 - 0.07465x_2^2x_3) \end{bmatrix}$	$G_1\{R^3\} = \left\{ \begin{bmatrix} 1 \\ -9.76468 \\ 0.0001362 \end{bmatrix}; \begin{bmatrix} 1 \\ 6.83555 \\ -0.00114919 \end{bmatrix}; \begin{bmatrix} 1 \\ 0.0041394 \\ 1.23531 \end{bmatrix} \right\}$ $\Lambda_1\{R\} = \{ 25.2102045 ; -3.1774410 ; -1.0020689 \}$; $\left\|G_1\{R^3\}\right\| = s_{1,3} = 3$ $G_2\{R^3\} = \left\{ \begin{bmatrix} 1 \\ -12. \\ 0.0001574 \end{bmatrix}; \begin{bmatrix} 1 \\ -12. \\ -9.3708760 \end{bmatrix}; \begin{bmatrix} 1 \\ -12. \\ 1.5705248 \end{bmatrix}; \begin{bmatrix} 1 \\ 0 \\ 0.5539125 \end{bmatrix}; \begin{bmatrix} 1 \\ 0 \\ -3.0258244 \end{bmatrix}; \begin{bmatrix} 1 \\ 5.1372758 \\ -0.4351283 \end{bmatrix}; \begin{bmatrix} 1 \\ 409.4144585 \\ -34.6774951 \end{bmatrix} \right\}$ $\Lambda_2\{R\} = \begin{Bmatrix} -567.7337492 & ; & 0.0974952 & ; & 0.0310329 & ; \\ 0 & ; & 0 & ; & 0 & ; & 0 \end{Bmatrix}$; $\left\|G_2\{R^3\}\right\| = s_{2,3} = 7$ $G_3\{C^3\} = \left\{ \begin{bmatrix} 1 \\ -12 \\ 0.00016 \end{bmatrix}; \begin{bmatrix} 1 \\ -12 \\ 0.9295 \end{bmatrix}; \begin{bmatrix} 1 \\ -12 \\ -2.4149 - i\ 3.6571 \end{bmatrix}; \begin{bmatrix} 1 \\ -12 \\ -2.4149027 + i\ 3.6571 \end{bmatrix}; \begin{bmatrix} 1 \\ -63.8070 \\ 3.4406 \end{bmatrix}; \begin{bmatrix} 1 \\ 5.4231 - i\ 0.4157 \\ -0.2924 + i\ 0.0224 \end{bmatrix}; \begin{bmatrix} 1 \\ 5.4231 + i\ 0.4157 \\ -0.2924 - i\ 0.0224 \end{bmatrix}; \begin{bmatrix} 1 \\ 0 \\ 0.3464 \end{bmatrix}_{(2)}; \begin{bmatrix} 1 \\ 0 \\ -0.7912 + i\ 1.2642 \end{bmatrix}_{(2)}; \begin{bmatrix} 1 \\ 0 \\ -0.7912 - i\ 1.2642 \end{bmatrix}_{(2)} \right\}$ $\Lambda_3\{C\} = \begin{Bmatrix} 6900.54 ; & -0.5444 & ; & -1.937 + i\ 0.22 & ; & -1.937 - i\ 0.22 \\ 0 & ; & 0 & ; & 0 & ; \\ 0_{(2)} & ; & 0_{(2)} & ; & 0_{(2)} & ; \end{Bmatrix}$; $\left\|G_3\{R^3\}\right\| = 10,\ s_{3,3} = 13$

Table A.V.3: 2D-PMMA case: numerically evaluated k-forms and their spectra at the unstable steady-state $\mathbf{x}_{2s}=[0.223416, 1.331286]^t$.

Two-dimensional PMMA power series approximation:	**PMMA eigenspectra:**
Two-dimensional CSTR model $\mathbf{F}[\mathbf{x}] \approx \sum_{i=1}^{5} \frac{1}{i!}\mathbf{F}_i[\mathbf{x}] + o6$, with $\mathbf{F}_1[\mathbf{x}] = \begin{bmatrix} 0.459375 & -0.827057 \\ -17.5125 & 2.92468 \end{bmatrix}\begin{bmatrix} x_1 \\ x_2 \end{bmatrix}$ $\mathbf{F}_2[\mathbf{x}] = \begin{bmatrix} 1 \\ -12 \end{bmatrix}\begin{bmatrix} 11.5885 & 0.05745 & -0.60023 \end{bmatrix}\begin{bmatrix} x_1^2 \\ x_1x_2 \\ x_2^2 \end{bmatrix}$ $\mathbf{F}_3[\mathbf{x}] = \begin{bmatrix} 1 \\ -12 \end{bmatrix}\begin{bmatrix} -2.14915E2 & 54.5303 & -6.16098 & -0.0994223 \end{bmatrix}\begin{bmatrix} x_1^3 \\ x_1^2x_2 \\ x_1x_2^2 \\ x_2^3 \end{bmatrix}$ $\mathbf{F}_4[\mathbf{x}] = \begin{bmatrix} 1 \\ -12 \end{bmatrix}\begin{bmatrix} 2.41768E3 & -6.44654E2 & 90.7274 & -12.6654 & 0.379176 \end{bmatrix}\begin{bmatrix} x_1^4 \\ x_1^3x_2 \\ x_1^2x_2^2 \\ x_1x_2^3 \\ x_2^4 \end{bmatrix}$ $\mathbf{F}_5[\mathbf{x}] = \begin{bmatrix} 1 \\ -12 \end{bmatrix}\begin{bmatrix} -2.37504E4 & 4.38509E3 & 1.01819E2 & -40.7858 & -6.53084 & 0.353079 \end{bmatrix}\begin{bmatrix} x_1^5 \\ x_1^4x_2 \\ x_1^3x_2^2 \\ x_1^2x_2^3 \\ x_1x_2^4 \\ x_2^5 \end{bmatrix}$	$\mathbb{X}_1\{\mathbb{R}^2\} = \left\{\begin{bmatrix} 1 \\ -6.32733 \end{bmatrix}; \begin{bmatrix} 1 \\ 3.34651 \end{bmatrix}\right\}$ $\Lambda_1\{\mathbb{R}\} = \{ 5.69244 \; ; \; -2.30838 \}$ $\mathbb{X}_2\{\mathbb{R}^2\} = \left\{\begin{bmatrix} 1 \\ -12 \end{bmatrix}; \begin{bmatrix} 1 \\ 4.442039 \end{bmatrix}; \begin{bmatrix} 1 \\ -4.346328 \end{bmatrix}\right\}$ $\Lambda_2\{\mathbb{R}\} = \{ -37.7674 \; ; \; 0 \; ; \; 0 \}$ $\mathbb{X}_3\{\mathbb{C}^2\} = \left\{\begin{bmatrix} 1 \\ -12 \end{bmatrix}; \begin{bmatrix} 1 \\ -70.2173 \end{bmatrix}; \begin{bmatrix} 1 \\ 4.124744+i3.710989 \end{bmatrix}; \begin{bmatrix} 1 \\ 4.124744-i3.710989 \end{bmatrix}\right\}$ $\Lambda_3\{\mathbb{R}\} = \{ -264.11 \; ; \; 0 \; ; \; 0 \; ; \; 0 \}$ $\mathbb{X}_4\{\mathbb{C}^2\} = \left\{\begin{bmatrix} 1 \\ -12 \end{bmatrix}; \begin{bmatrix} 1 \\ 26.4398 \end{bmatrix}; \begin{bmatrix} 1 \\ 5.22927 \end{bmatrix}; \begin{bmatrix} 1 \\ 0.866742+i6.73539 \end{bmatrix}; \begin{bmatrix} 1 \\ 0.866742-i6.73539 \end{bmatrix}\right\}$ $\Lambda_4\{\mathbb{R}\} = \left\{\begin{matrix} 2206.95 \; ; \; 0 \; ; \; 0 \; ; \\ 0 \; ; \; 0 \end{matrix}\right\}$ $\mathbb{X}_5\{\mathbb{C}^2\} = \left\{\begin{bmatrix} 1 \\ -12 \end{bmatrix}; \begin{bmatrix} 1 \\ 22.2527 \end{bmatrix}; \begin{bmatrix} 1 \\ 5.32725-i2.54217 \end{bmatrix}; \begin{bmatrix} 1 \\ 5.32725+i2.54217 \end{bmatrix}; \begin{bmatrix} 1 \\ -7.2052-i5.90281 \end{bmatrix}; \begin{bmatrix} 1 \\ -7.2052+i5.90281 \end{bmatrix}\right\}$ $\Lambda_5\{\mathbb{R}\} = \left\{\begin{matrix} -1787.61 \; ; \; 0 \; ; \; 0 \; ; \; 0 \; ; \\ 0 \; ; \; 0 \end{matrix}\right\}$ All k-forms for k>5 have **only one** idempotent **eigen**vector which always is given by the solution $[1,-12]^t$. For **k=6,7 one can show** that eigenval**ues** corresponding to **this** eigenvector are $\lambda_6 = -31778.4, \; \lambda_7 = 93250.4.$

Table A.V.4: 3D-PMMA case: numerically evaluated k-forms and their spectra at the unstable steady-state $\mathbf{x}_{2S}=[0.49601, 0.86396, 0.04997]^t$.

Three-dimensional PMMA power series approximation:	**PMMA eigenspectra:**
Three-dimensional CSTR model $\mathbf{F}[\mathbf{x}] \approx \sum_{i=1}^{3} \frac{1}{i!}\mathbf{F}_i[\mathbf{x}] + o4$, with $\mathbf{F}_1[\mathbf{x}] = \begin{bmatrix} 1.4288 & -0.899622 & -5.04274 \\ -29.1456 & 3.79547 & 60.5128 \\ 0.0 & -0.0001214 & -1.00058 \end{bmatrix} \begin{bmatrix} x_1 \\ x_2 \\ x_3 \end{bmatrix}$ $\mathbf{F}_2[\mathbf{x}] = \begin{bmatrix} -10.485x_1^2 + 6.68402x_1x_2 - 1.3904x_2^2 + 48.6042x_1x_3 - 18.0029x_2x_3 + 50.4566x_3^2 \\ -12(-10.485x_1^2 + 6.68402x_1x_2 - 1.3904x_2^2 + 48.6042x_1x_3 - 18.0029x_2x_3 + 50.4566x_3^2) \\ -0.0004876x_2^2 - 0.004859x_2x_3 \end{bmatrix}$ $\mathbf{F}_3[\mathbf{x}] = \begin{bmatrix} 30.512x_1^3 - 27.2075x_1^2x_2 - 314.733x_1^2x_3 + 9.61498x_1x_2^2 - 729.486x_1x_3^2 + \\ 200.637x_1x_2x_3 - 1.76319x_2^3 - 41.7362x_2^2x_3 + 270.2x_2x_3^2 - 1514.58x_3^3 \\ -12(30.512x_1^3 - 27.2075x_1^2x_2 - 314.733x_1^2x_3 + 9.61498x_1x_2^2 - 729.486x_1x_3^2 + \\ 200.637x_1x_2x_3 - 1.76319x_2^3 - 41.7362x_2^2x_3 + 270.2x_2x_3^2 - 1514.58x_3^3) \\ (-0.0018727x_2^3 - 0.0292765x_2^2x_3) \end{bmatrix}$	$G_1\{R^3\} = \left\{ \begin{bmatrix} 1 \\ -7.15704 \\ 0.000098 \end{bmatrix}; \begin{bmatrix} 1 \\ 4.52388 \\ 0.00033452 \end{bmatrix}; \begin{bmatrix} 1 \\ 0.00116101 \\ 0.481551 \end{bmatrix} \right\}$ $\Lambda_1\{R\} = \{ 7.86694 ; -2.64267 ; -1.00058 \}$; $\lvert G_1\{R^3\} \rvert = s_{1,3} = 3$ $G_2\{R^3\} = \left\{ \begin{bmatrix} 1 \\ -12. \\ 0.00024139 \end{bmatrix}; \begin{bmatrix} 1 \\ -12. \\ -6.1783 \end{bmatrix}; \begin{bmatrix} 1 \\ -12. \\ 0.933179 \end{bmatrix}; \begin{bmatrix} 1 \\ 0 \\ 0.181518 \end{bmatrix}; \begin{bmatrix} 1 \\ 0 \\ -1.1448 \end{bmatrix}; \begin{bmatrix} 1 \\ 2.52974 \\ -0.253847 \end{bmatrix}; \begin{bmatrix} 1 \\ -4.48486 \\ 0.450033 \end{bmatrix} \right\}$ $\Lambda_2\{R\} = \left\{ \begin{matrix} -145.424 & ; & 0.0348419 & ; & -0.00846672 \\ 0 & ; & 0 & ; & 0 \end{matrix} \right\}$; $\lvert G_2\{R^3\} \rvert = s_{2,3} = 7$ $G_3\{C^3\} = \left\{ \begin{bmatrix} 1 \\ -12 \\ 0.00067 \end{bmatrix}; \begin{bmatrix} 1 \\ -12 \\ 0.44343 \end{bmatrix}; \begin{bmatrix} 1 \\ -12 \\ -1.533 - i\,2.185 \end{bmatrix}; \begin{bmatrix} 1 \\ -12 \\ -1.533 + i\,2.185 \end{bmatrix}; \begin{bmatrix} 1 \\ -2.01236 \\ 0.128723 \end{bmatrix}; \begin{bmatrix} 1 \\ 2.29408 - i\,1.01616 \\ -0.146743 + i\,0.065 \end{bmatrix}; \begin{bmatrix} 1 \\ 2.29408 + i\,1.01616 \\ -0.146743 - i\,0.065 \end{bmatrix}; \begin{bmatrix} 1 \\ 0 \\ 0.0797 \end{bmatrix}_{(2)}; \begin{bmatrix} 1 \\ 0 \\ -0.280 + i\,0.416 \end{bmatrix}_{(2)}; \begin{bmatrix} 1 \\ 0 \\ -0.280 - i\,0.416 \end{bmatrix}_{(2)} \right\}$ $\Lambda_3\{C\} = \left\{ \begin{matrix} 797.07 & ; & 0.51 & ; & -0.81 + i\,0.16 & ; & -0.81 - i\,0.16 \\ 0 & ; & 0 & ; & 0 & ; & \\ 0_{(2)} & ; & 0_{(2)} & ; & 0_{(2)} & ; & \end{matrix} \right\}$; $\lvert G_3\{R^3\} \rvert = 10,\ s_{3,3} = 13$

Table A.V.5: Cyclopentenol eigenspectra.

CYCLOPENTENOL EIGENSPECTRA

$$G_1\{C^3\} = \left\{ \begin{bmatrix} -0.555 \\ 0.977 \\ 0.374 \end{bmatrix}; \begin{bmatrix} 1.056- \text{ i } 1.007 \\ -0.241- \text{ i } 0.714 \\ -11.86+ \text{ i}4.501 \end{bmatrix}; \begin{bmatrix} 1.056+ \text{ i } 1.007 \\ -0.241+ \text{ i } 0.714 \\ -11.86- \text{ i}4.501 \end{bmatrix} \right\}$$

$$\Lambda_1\{C\} = \{-36.942 \; ; \; -17.503+\text{i } 8.955 \; ; \; -17.503-\text{i } 8.955\}$$

$$|G_1\{C^3\}| = s_{1,3} = 3$$

$$G_2\{C^3\} = \left\{ \begin{bmatrix} 0 \\ 1 \\ 0 \end{bmatrix}_{(2)}; \begin{bmatrix} 0.524 \\ 1 \\ -1.509 \end{bmatrix}; \begin{bmatrix} 0.977 \\ 1 \\ -12.037 \end{bmatrix}; \begin{bmatrix} 1.424 \\ 1 \\ -21.027 \end{bmatrix}; \begin{bmatrix} -0.523 - \text{i } 0.156 \\ 1 \\ -0.674 + \text{i } 2.656 \end{bmatrix}; \begin{bmatrix} -0.523 + \text{i } 0.156 \\ 1 \\ -0.674 - \text{i } 2.656 \end{bmatrix} \right\}$$

$$\Lambda_2\{C\} = \left\{ \begin{matrix} 0_{(2)} \; ; \; 0.756 \; ; \; 4.628 \; ; \; 4.769 \\ 1.186 - \text{i } 3.891 \; ; \; 1.186 + \text{i } 3.891 \end{matrix} \right\}$$

$$|G_2\{C^3\}| = 6 \quad , \quad s_{2,3} = 7$$

$$G_3\{C^3\} = \left\{ \begin{bmatrix} r \\ 1 \\ 0 \end{bmatrix} r \in \mathbb{R}; \begin{bmatrix} 1.935 \\ 1 \\ -52.263 \end{bmatrix}; \begin{bmatrix} 0.497 + \text{i } 0.0019 \\ 1 \\ -4.430 - \text{i } 0.749 \end{bmatrix}; \begin{bmatrix} 0.497 - \text{i } 0.0019 \\ 1 \\ -4.430+ \text{i } 0.749 \end{bmatrix}; \begin{bmatrix} -0.422 + \text{i } 0.267 \\ 1 \\ -1.952 - \text{i } 3.433 \end{bmatrix}; \begin{bmatrix} -0.4228 - \text{i } 0.267 \\ 1 \\ -1.952 + \text{i } 3.433 \end{bmatrix} \right\}$$

$$\Lambda_3\{C\} = \left\{ \begin{matrix} 0 \; [\infty] \; ; \; -4.785 \; ; \; -0.319 - \text{i } 0.118 \; ; \; -0.319 + \text{i } 0.118 \\ 0.256 - \text{i } 0.608 \; ; \; 0.256 + \text{i } 0.6086 \end{matrix} \right\}$$

$$|G_3\{C^3\}| = \infty \quad , \quad s_{3,3} = 13$$

$$G_4\{C^3\} = \left\{ \begin{bmatrix} r \\ 1 \\ 0 \end{bmatrix}_{(2)} r \in \mathbb{R}; \begin{bmatrix} 2.0102 \\ 1 \\ -81.0206 \end{bmatrix}; \begin{bmatrix} -0.310 + \text{i } 0.331 \\ 1 \\ -3.221 - \text{i } 3.565 \end{bmatrix}; \begin{bmatrix} -0.310 - \text{i } 0.331 \\ 1 \\ -3.221 + \text{i } 3.565 \end{bmatrix}; \begin{bmatrix} 0.4203 + \text{i } 0.056 \\ 1 \\ -4.754 + \text{i } 1.923 \end{bmatrix}; \begin{bmatrix} 0.4203 - \text{i } 0.056 \\ 1 \\ -4.754 - \text{i } 1.923 \end{bmatrix} \right\}$$

$$\Lambda_4\{C\} = \left\{ \begin{matrix} 0_{(2)}[\infty] \; ; \; 7.734 \; ; -0.053 + \text{i } 0.059 \; ; -0.053 - \text{i } 0.059 \; ; \\ 0.01306 - \text{i } 0.043 \; ; \; 0.013 + \text{i } 0.043 \end{matrix} \right\}$$

$$|G_4\{C^3\}| = \infty \quad , \quad s_{4,3} = 21$$

$$G_5\{C^3\} = \left\{ \begin{bmatrix} r \\ 1 \\ 0 \end{bmatrix}_{(3)} r \in \mathbb{R}; \begin{bmatrix} 2.028 \\ 1 \\ -116.282 \end{bmatrix}; \begin{bmatrix} 0.357 + \text{i } 0.132 \\ 1 \\ -5.398 + \text{i } 1.857 \end{bmatrix}; \begin{bmatrix} 0.357 - \text{i } 0.132 \\ 1 \\ -5.398 - \text{i } 1.857 \end{bmatrix}; \begin{bmatrix} -0.1901 + \text{i } 0.361 \\ 1 \\ -4.413 - \text{i } 3.209 \end{bmatrix}; \begin{bmatrix} -0.1901 - \text{i } 0.361 \\ 1 \\ -4.413 + \text{i } 3.209 \end{bmatrix} \right\}$$

$$\Lambda_5\{C\} = \left\{ \begin{matrix} 0_{(3)}[\infty] \; ; \; -17.384 \; ; \; -0.00015 + \text{i } 0.00478 \; ; \; -0.00015 - \text{i } 0.00478 \\ 0.0045241 - \text{i } 0.0055886 \; ; \; 0.0045241 + \text{i } 0.0055886 \end{matrix} \right\}$$

$$|G_5\{C^3\}| = \infty \quad , \quad s_{5,3} = 31$$

APPENDIX VI

CHARACTERISTIC RESPONSES FOR VARIOUS CONTROL STRATEGIES

The control strategies simulated are:

- <u>proportional control</u>

$$u_p = g_1 (x_2 - x_{2s})$$
with g_1=5.533 or 9.0

- <u>cubic control</u>

$$u_c = g_1(x_2 - x_{2s}) + g_2(x_2 - x_{2s})^2 + g_3(x_2 - x_{2s})^3$$
with g_1=5.533, g_2=1.1 and g_3=1.333

- <u>exponential control</u>

$$u_e = RBx_{1s}(Exp(x_2-x_{2s}) -1)$$
with R=0.5 or 1.0

- <u>hyperbolic control</u>

$$u_h = Bx_{1s}(R_sSinh(x_2-x_{2s})+R_c(Cosh(x_2-x_{2s}) -1))$$
with R_s=0.5 and R_c=0.333

- <u>input/output linearization control</u>

$$u_{i/o}= g_1(x_2-x_{2s}) - g(\mathbf{x})/\beta$$
where $g(\mathbf{x})$ is defined in Equation (5.3.1)

- <u>proportional+ hyperbolic control</u>

$$u_{h+p} = Bx_{1s}(R_sSinh(x_2-x_{2s})+R_c(Cosh(x_2-x_{2s}) -1)) + g_1(x_2-x_{2s})$$
with g_1=5.533, R_s=1.0 and R_c=0.75

These control strategies are numerically simulated for the exothermic CSTR parameters B=25.0, Da=0.0625, β=3.0 and x_{2c}=0.0, and the steady-state values x_{1s}=0.4420834 and x_{2s}=2.763021. The simulation results are presented in Figures A.VI.1-8.

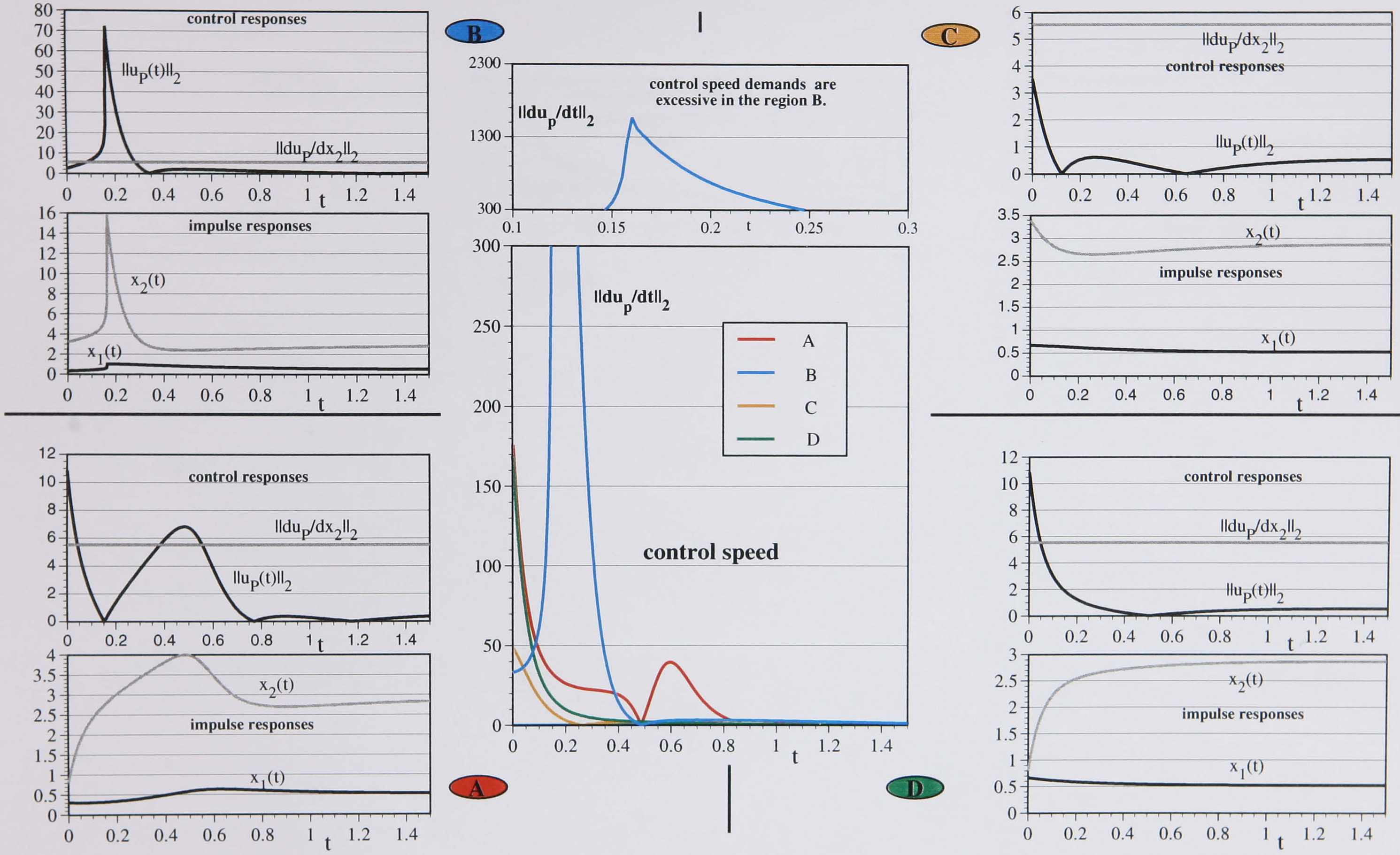

State and control time responses for the first-order controller $u_p(g_1=5.533)$.

FIGURE A.VI.1.

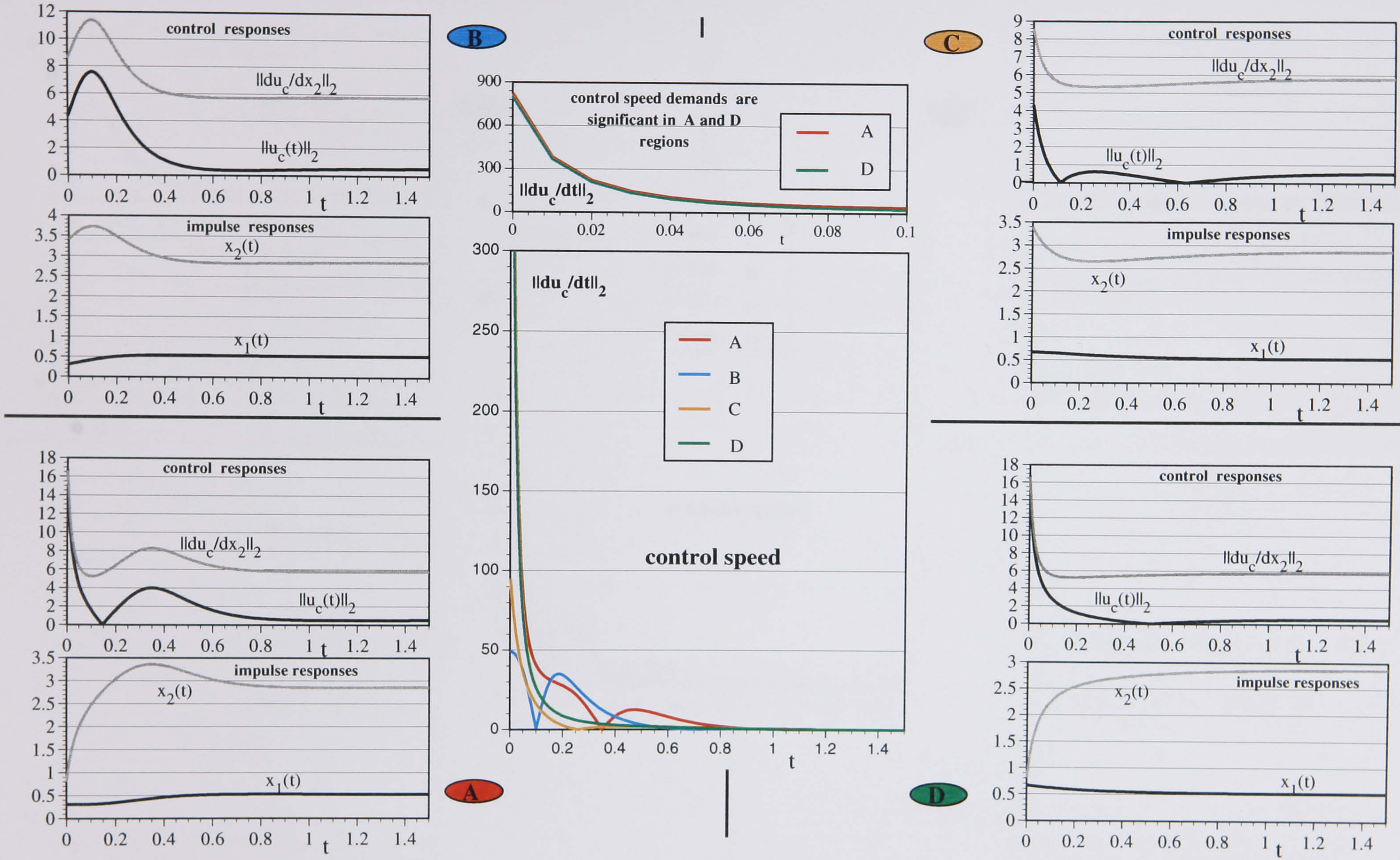

State and control time responses for the cubic controller u_c.

FIGURE A.VI.2.

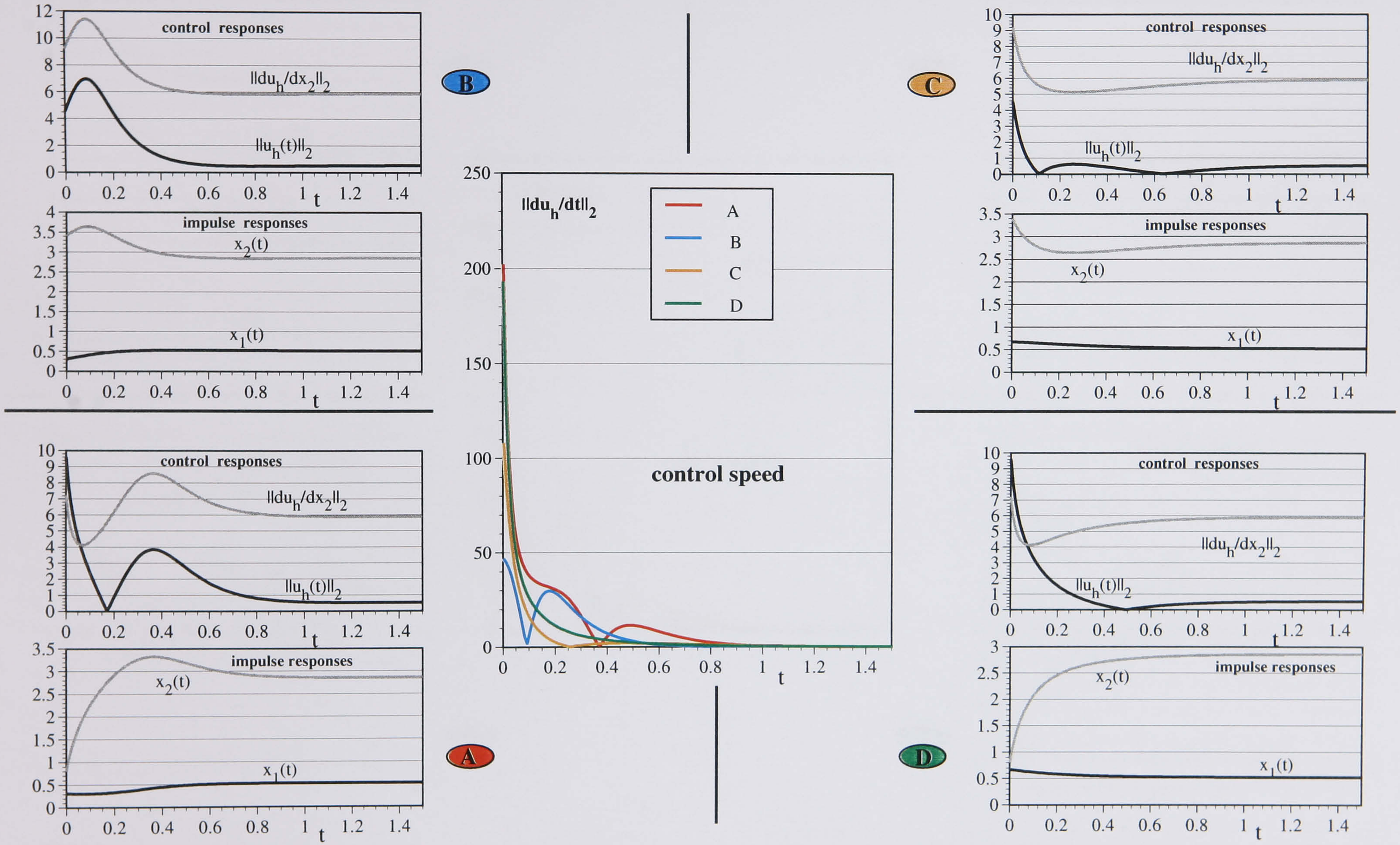

State and control responses for the hyperbolic controller $u_h(R_s=0.5 \& R_c=0.333)$.

FIGURE A.VI.3.

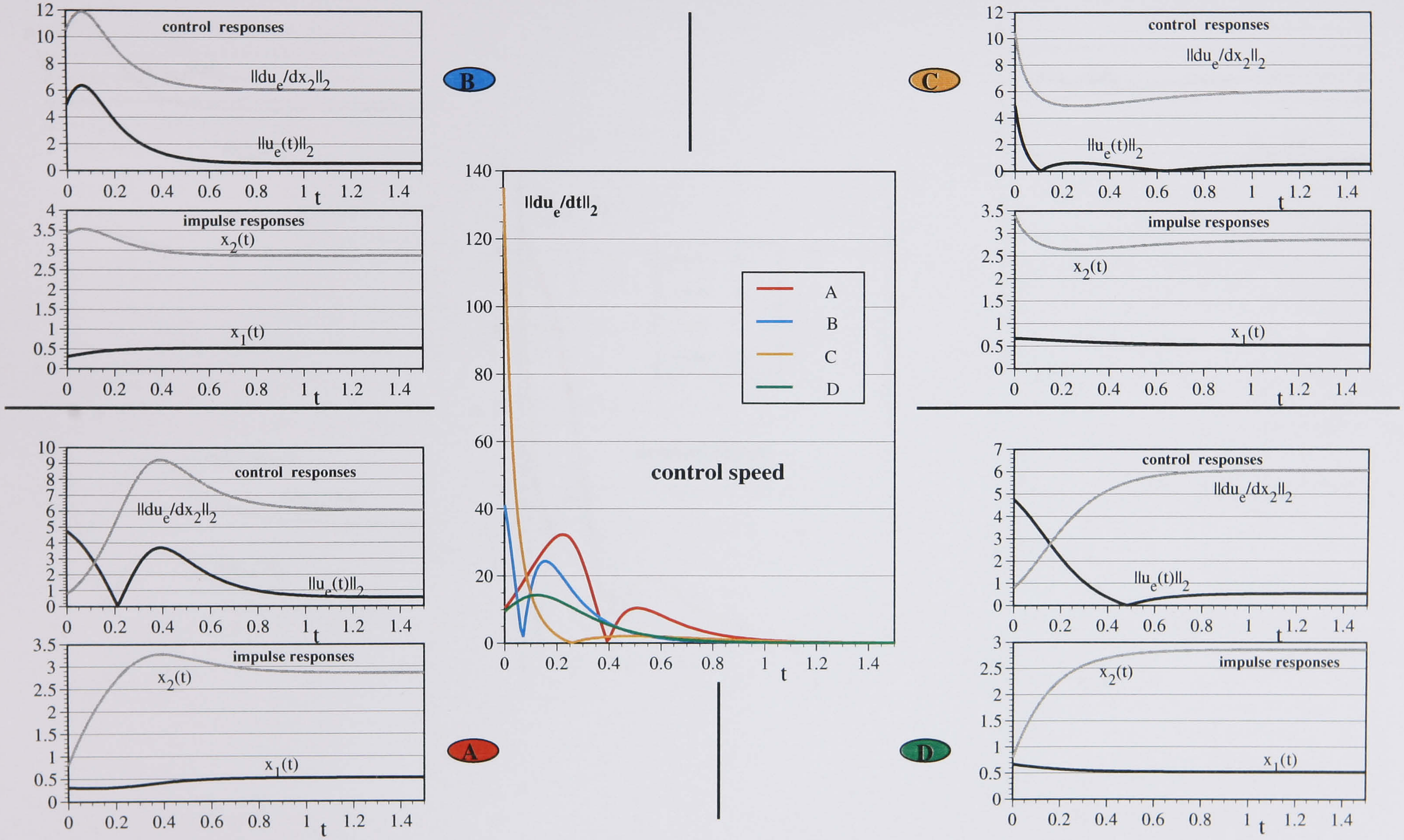

State and control responses for the exponential controller u_e(R=0.5).

FIGURE A.VI.4.

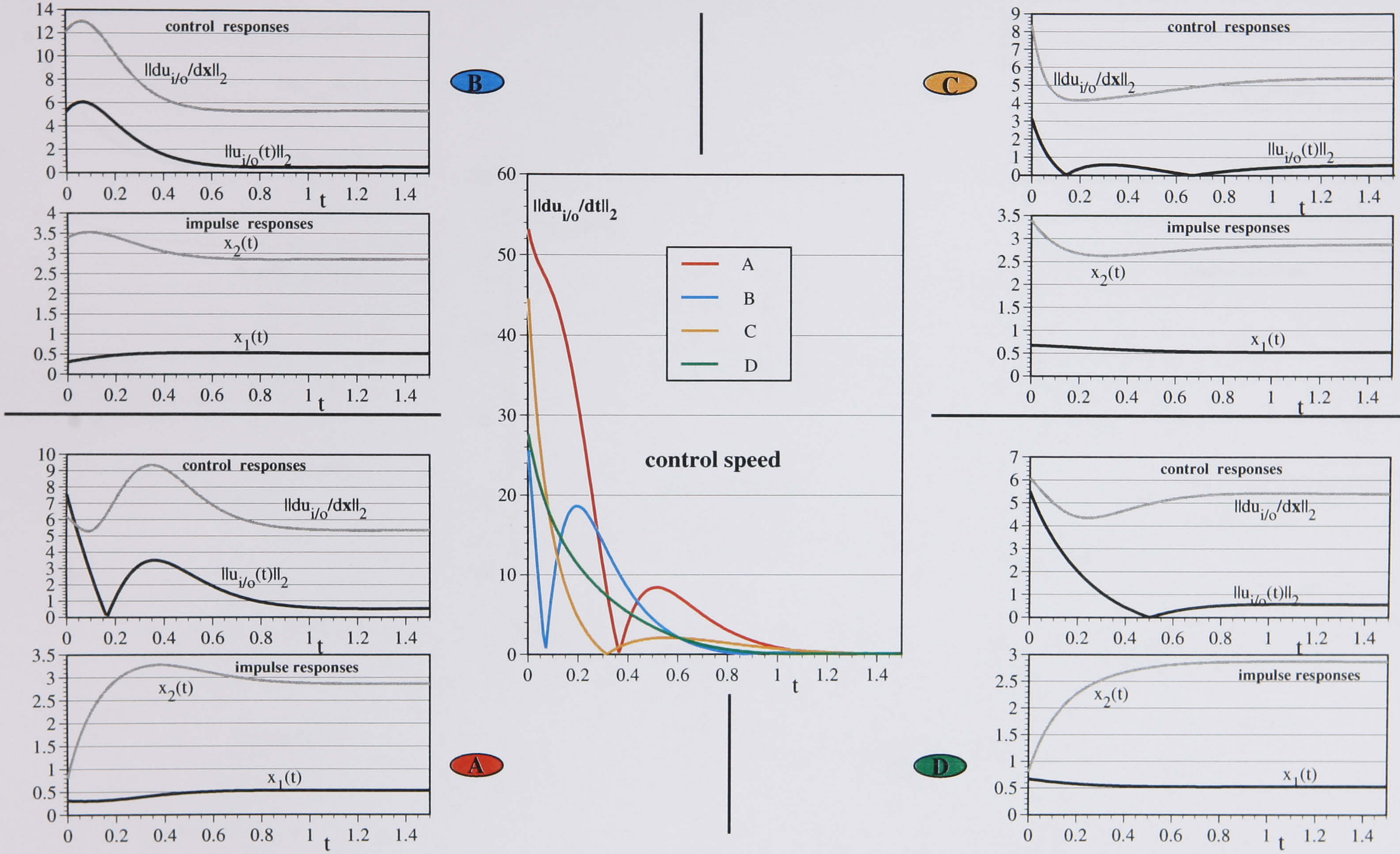

State and control responses for the input/output controller $u_{i/o}$.

FIGURE A.VI.5.

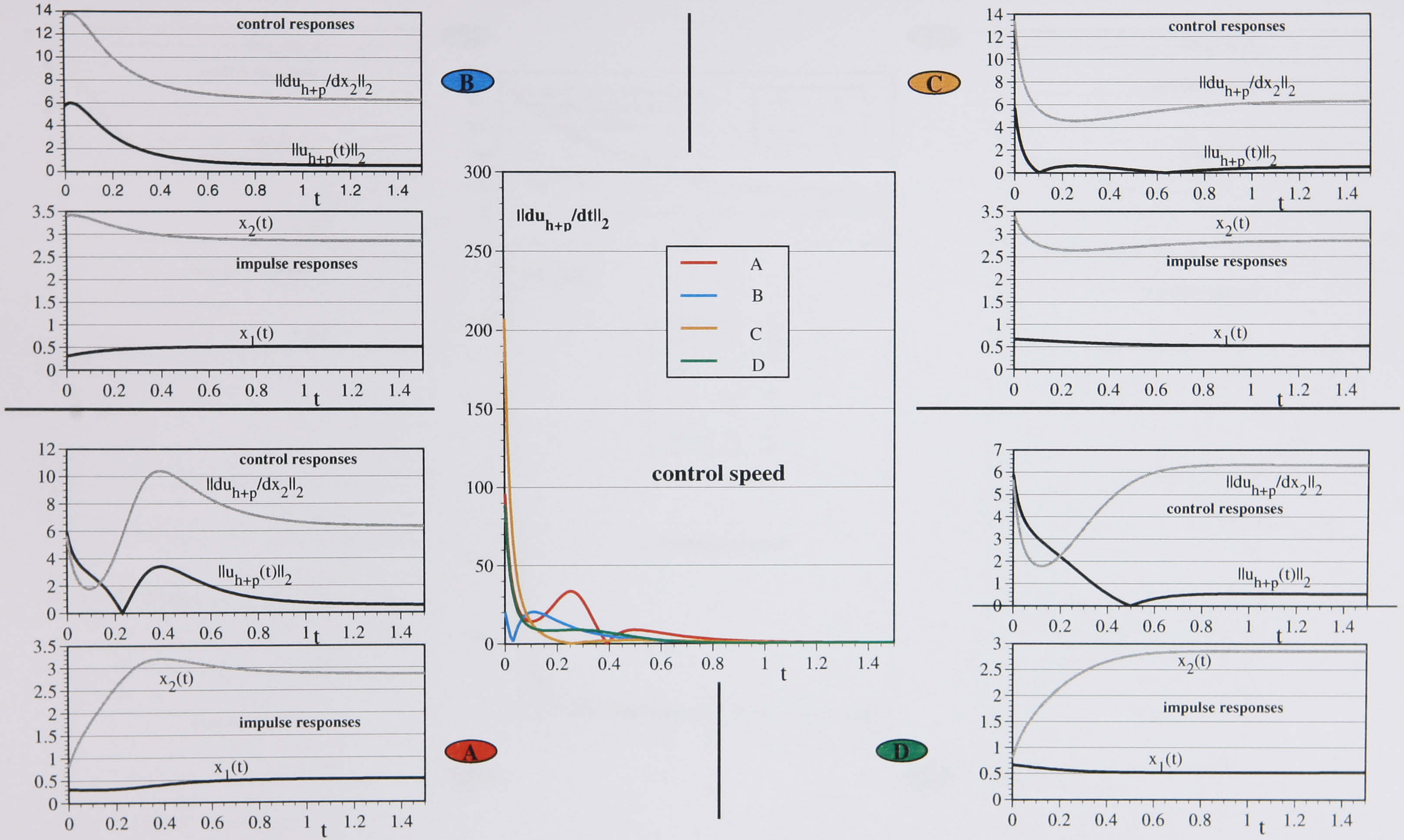

State and control time responses for the hyperbolic + proportional controller u_{h+p}.

FIGURE A.VI.6.

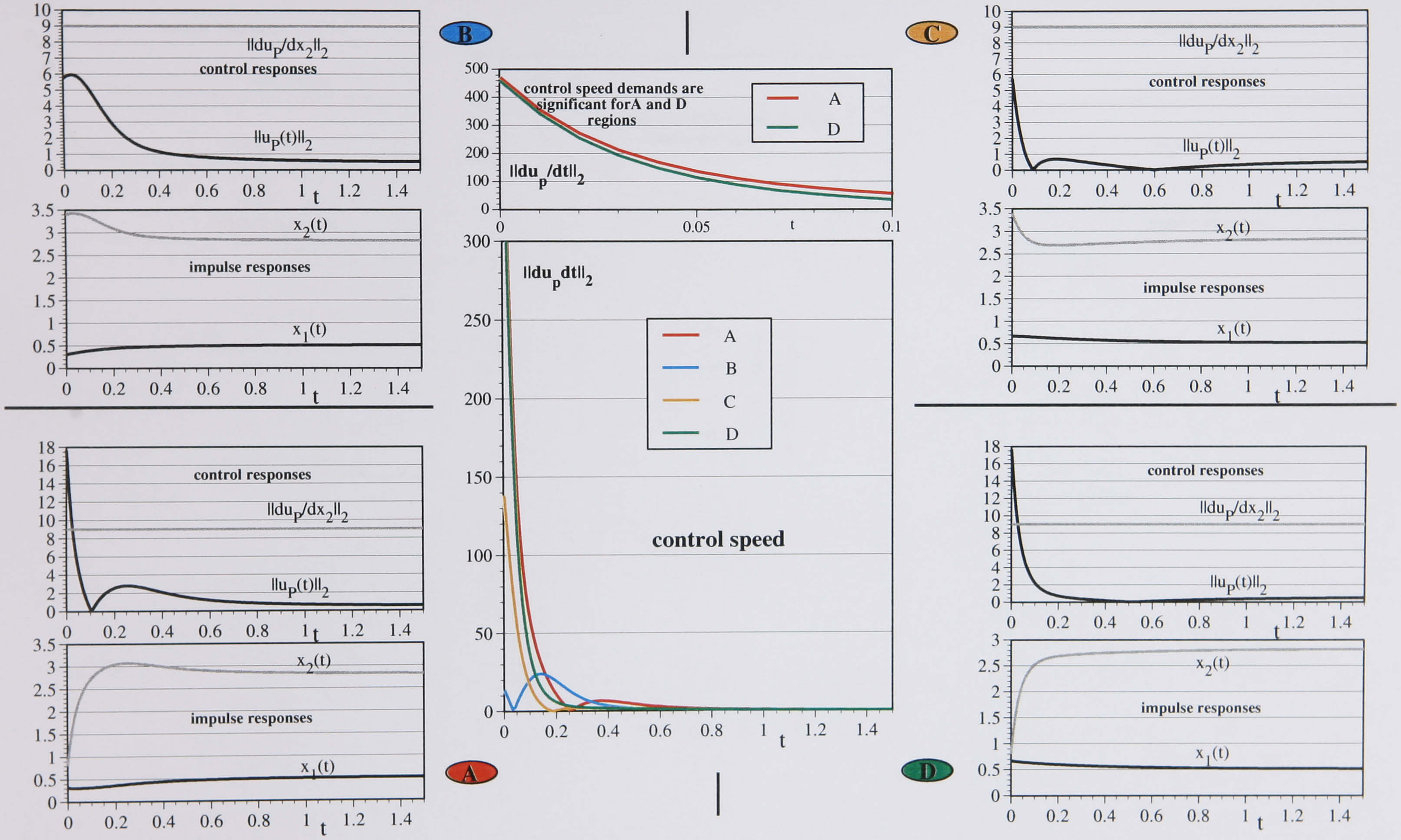

State and control time responses for the first-order controller $u_p(g_1=9.0)$.

FIGURE A.VI.7.

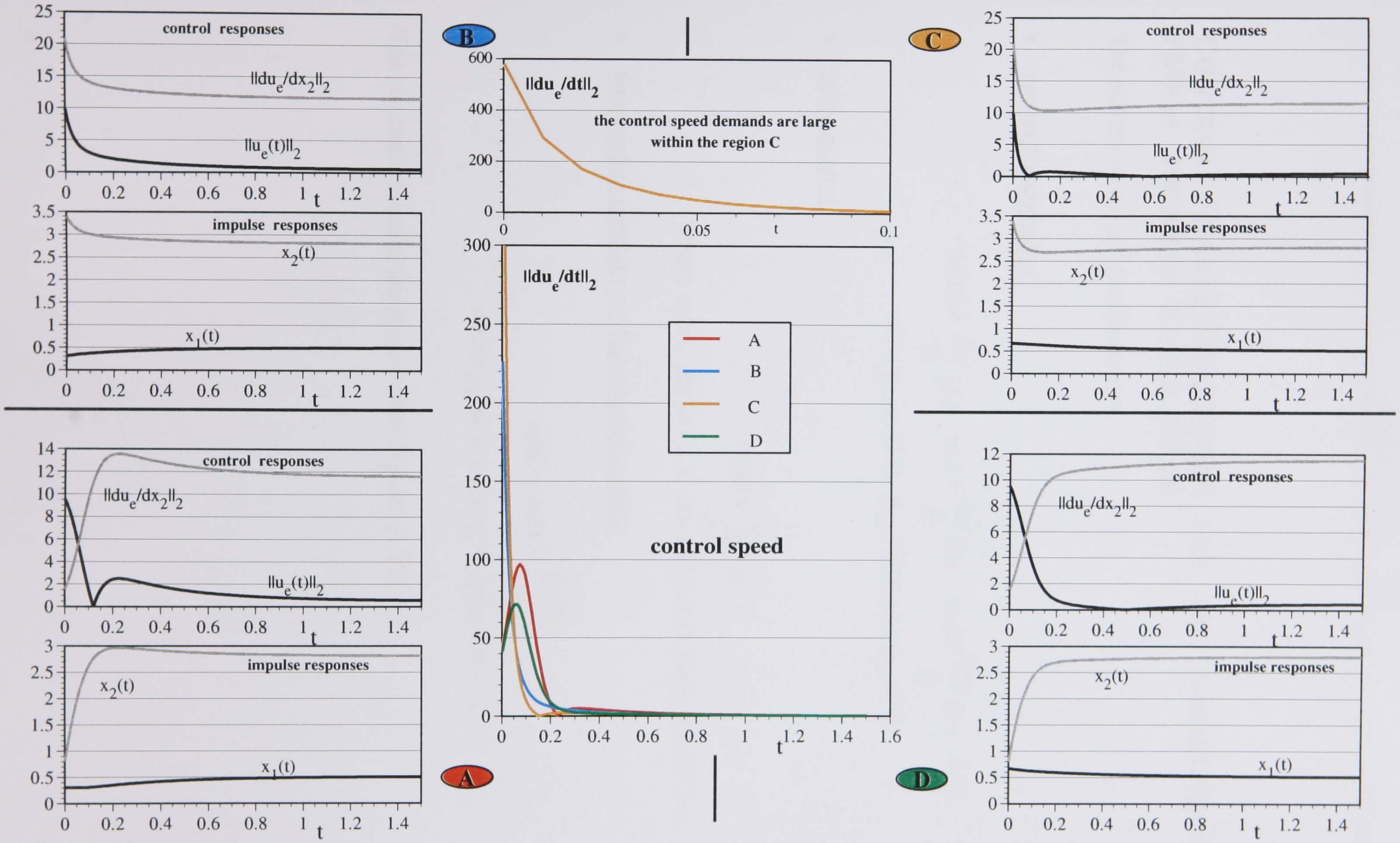

State and control time responses for the exponential controller u_e(R=1.0).

FIGURE A.VI.8.

APPENDIX VII

CONTROL CHARACTERIZATIONS FOR THE 3-DIMENSIONAL PMMA PROCESS REGULATION

The control strategies considered are:

- <u>proportional control</u>

$$u_P(\mathbf{x}) = \frac{g_{11}}{\beta}(x_1 - x_{1s}) + \frac{g_{12}}{\beta}(x_2 - x_{2s}) + \frac{g_{13}}{\beta}(x_3 - x_{3s})$$

with g_{11}=-45.0, g_{12}=10.0 and g_{13}=0.0

- <u>cubic control</u>

$$u_c(\mathbf{x}) = \sum_{k=1}^{3} u_j(\mathbf{x})$$

where $u_j(\mathbf{x})$, for j=1,2,3, are defined in Equation (7.2.4)

- <u>temperature input/output linearization control</u>

$$u_T(\mathbf{x}) = u_P(\mathbf{x}) - \frac{g_T(\mathbf{x})}{\beta}$$

where $g_T(\mathbf{x})$ is defined in Equation (7.2.3)

The simulation results are presented in Figures A.VII.1-3.

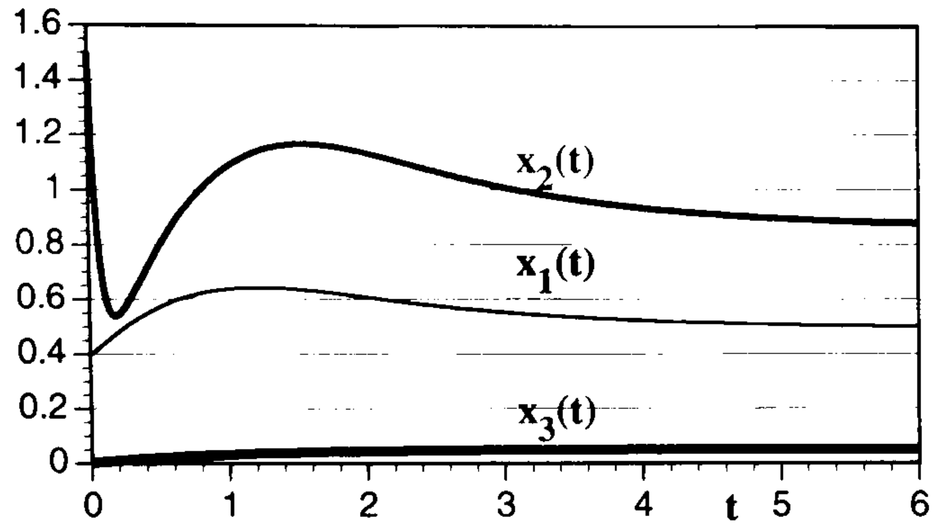

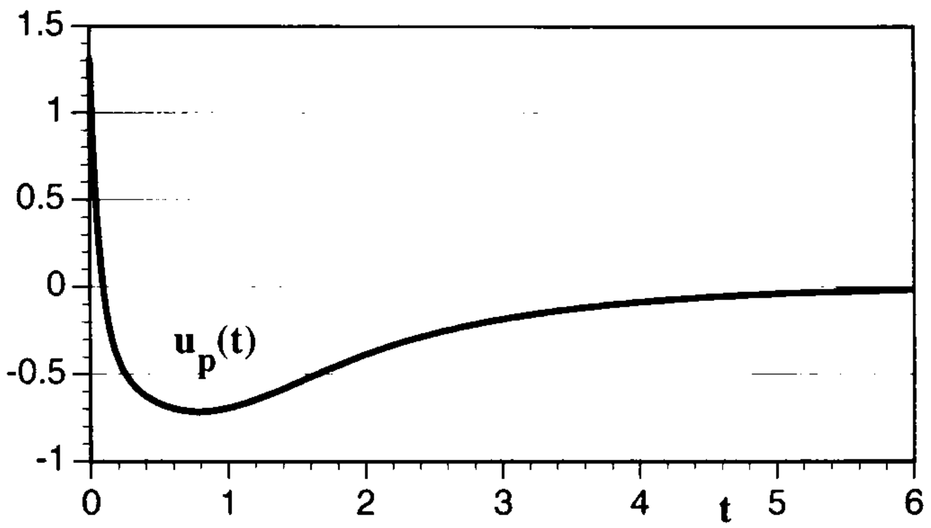

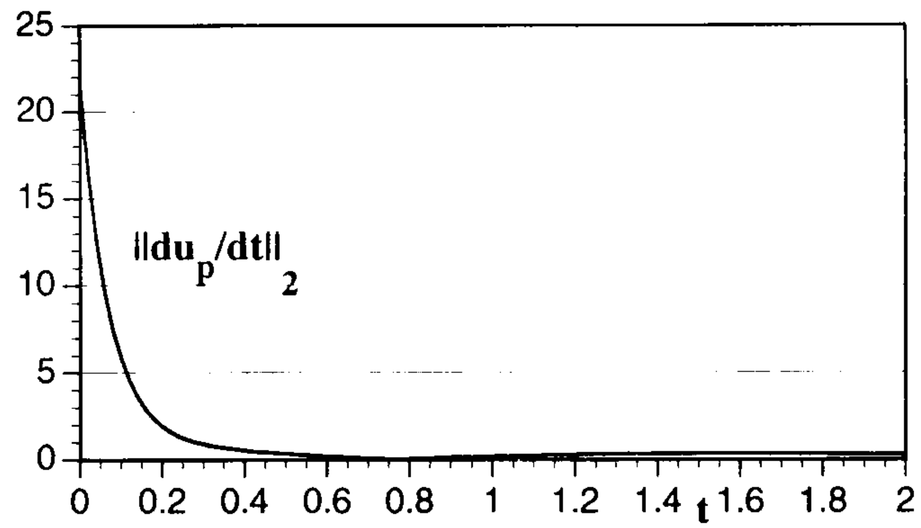

a) x_{1o}=0.4, x_{2o}=1.5, x_{3o}=0.001

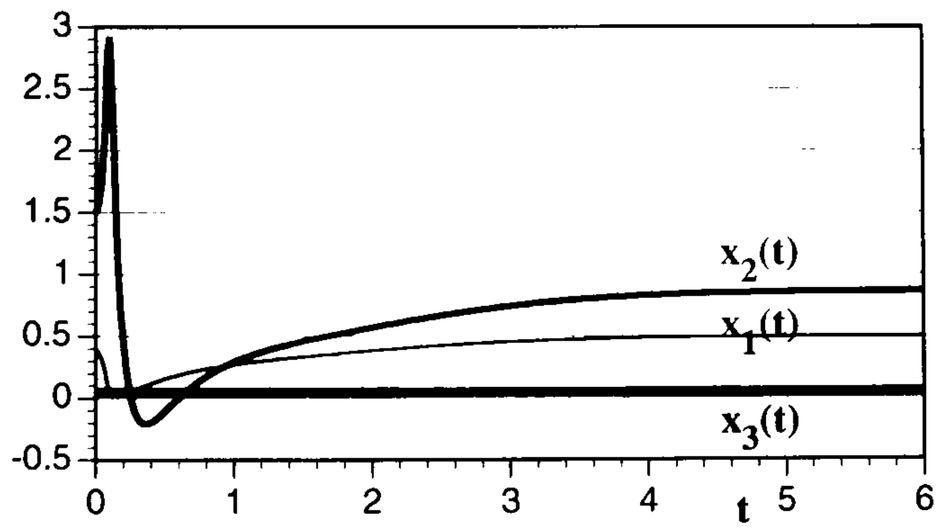

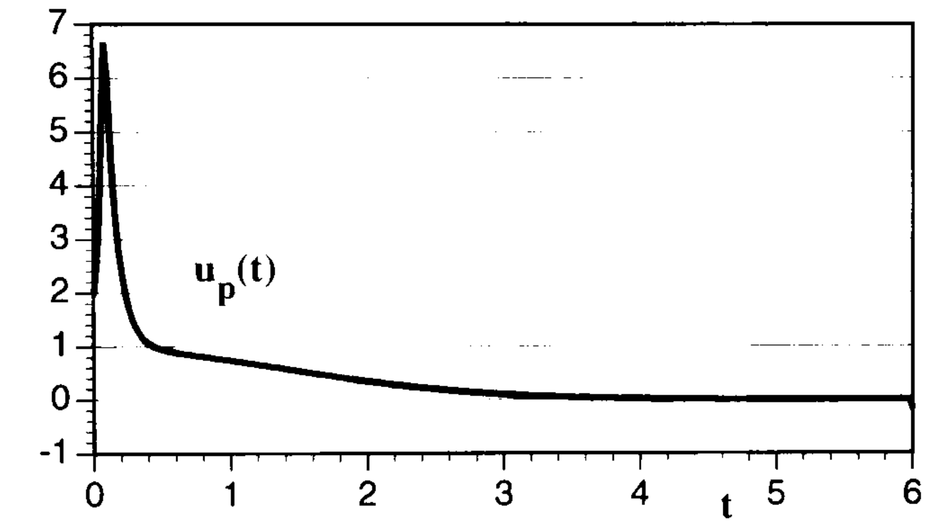

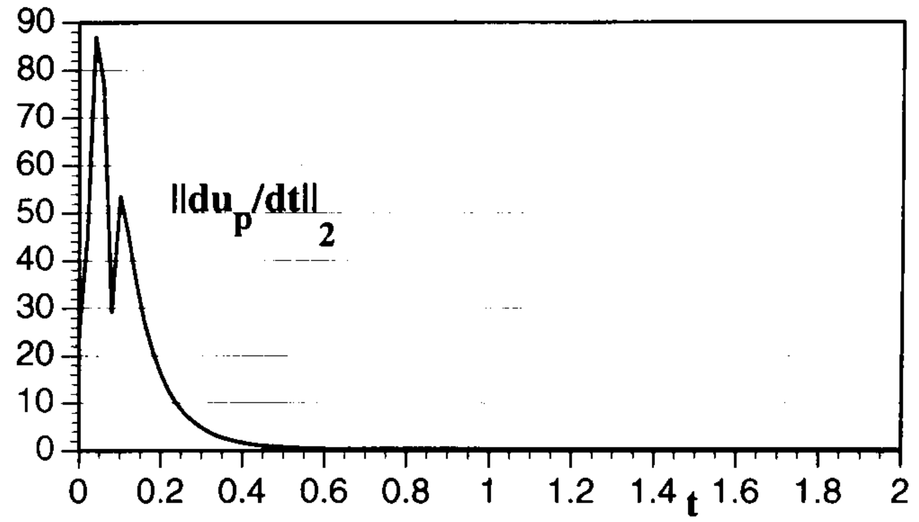

b) x_{1o}=0.4, x_{2o}=1.5, x_{3o}=0.05

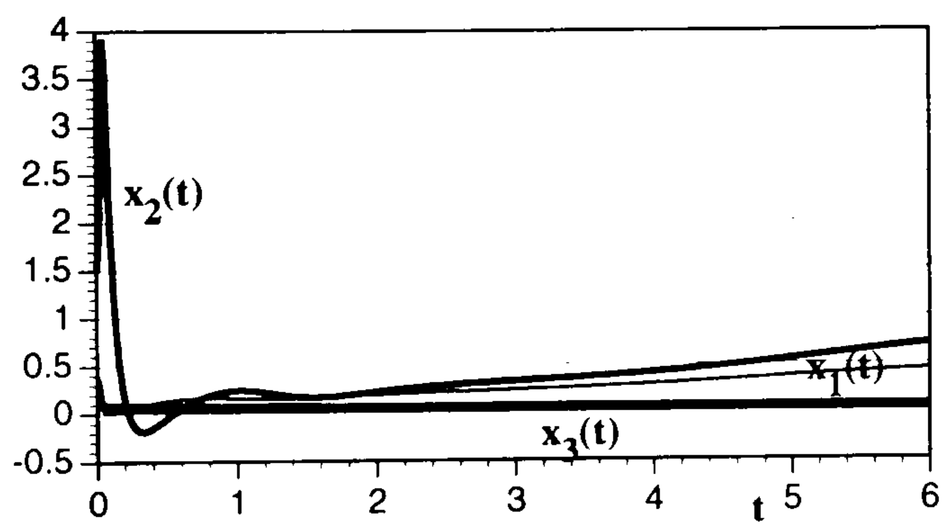

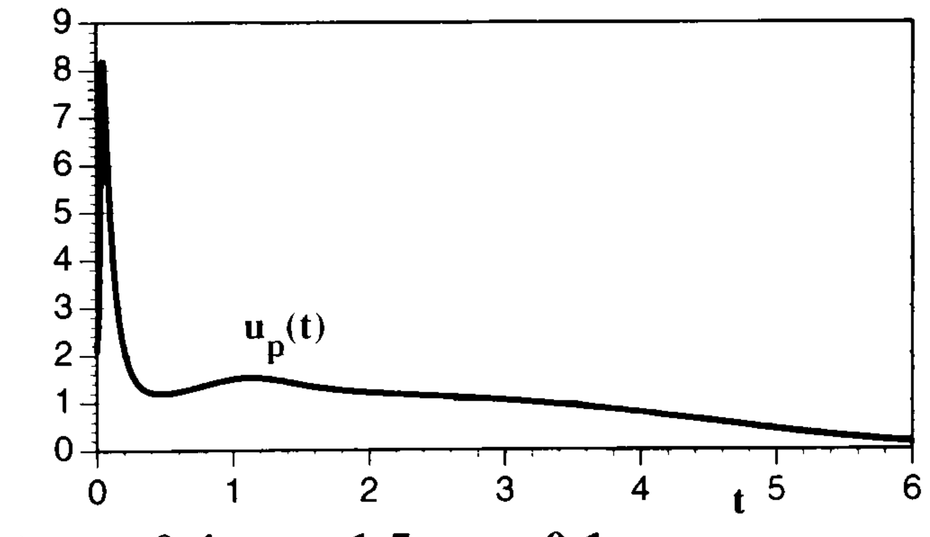

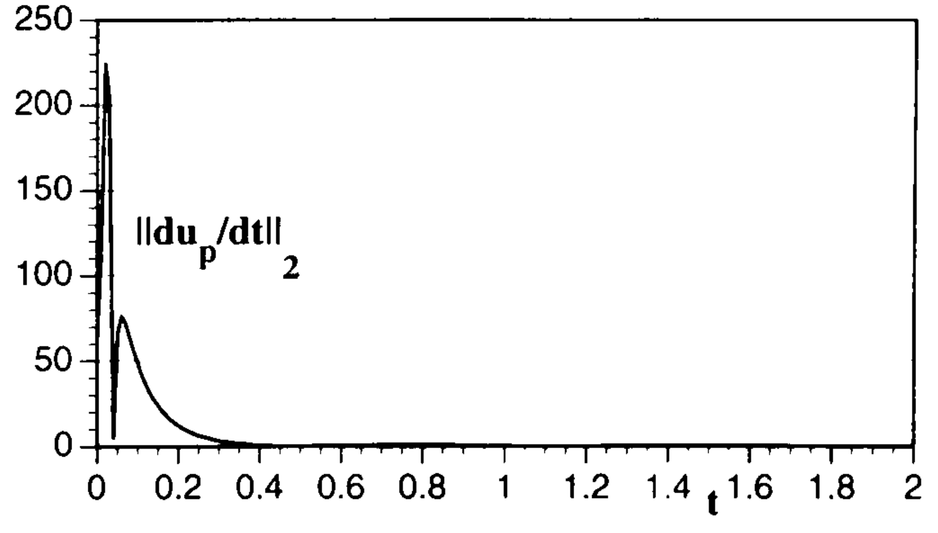

c) x_{1o}=0.4, x_{2o}=1.5, x_{3o}=0.1

Closed-loop time responses for PMMA reactor with first-order control.

FIGURE A.VII.1

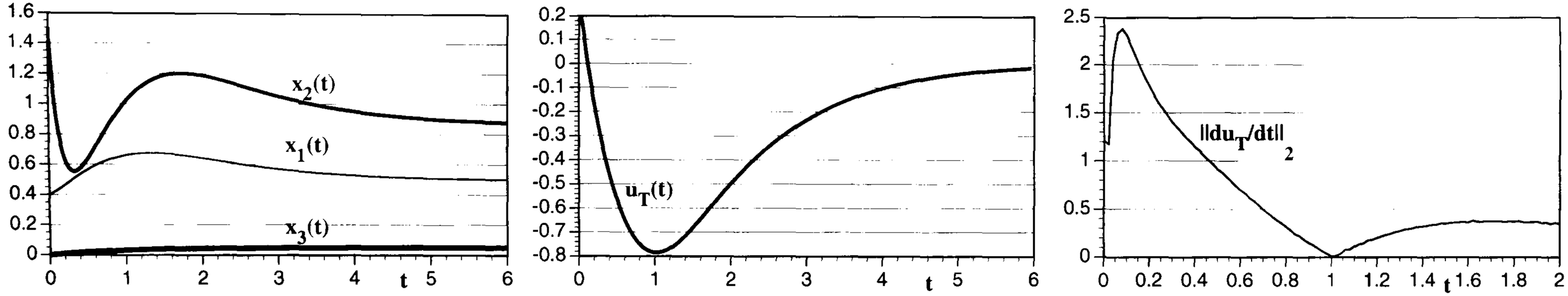

a) $x_{1o}=0.4,\ x_{2o}=1.5,\ x_{3o}=0.001$

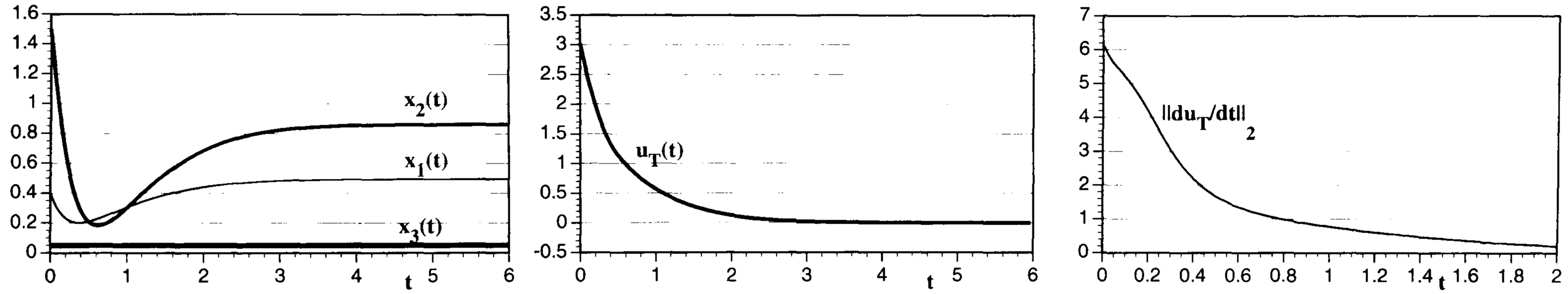

b) $x_{1o}=0.4,\ x_{2o}=1.5,\ x_{3o}=0.05$

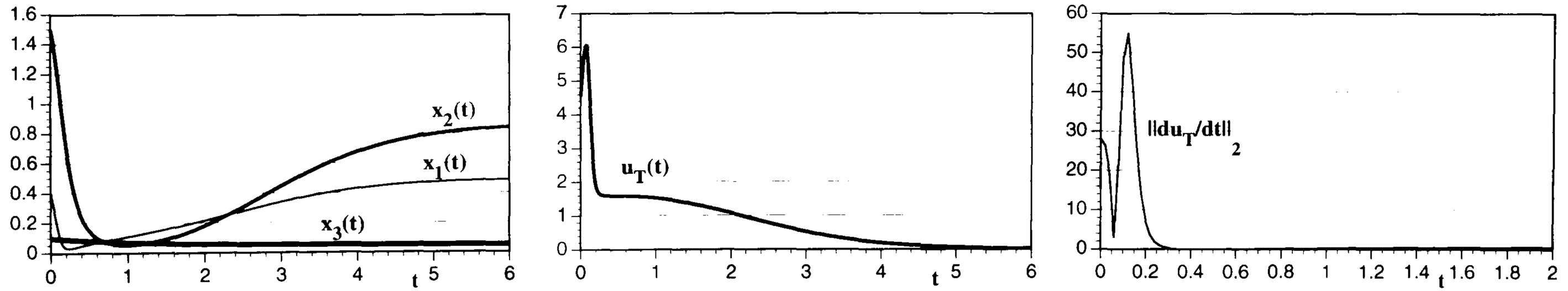

c) $x_{1o}=0.4,\ x_{2o}=1.5,\ x_{3o}=0.1$

Closed-loop time responses for PMMA reactor with temperature input/output linearization control.

FIGURE A.VII.2

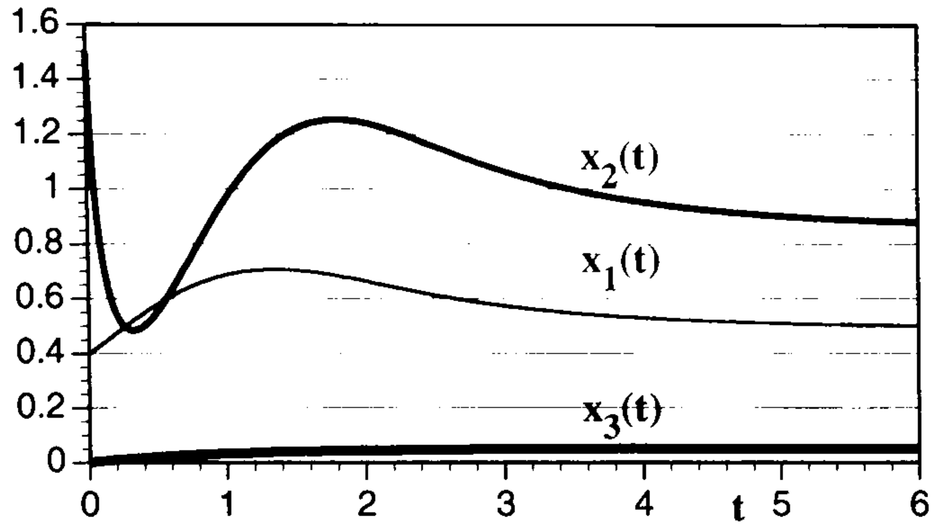

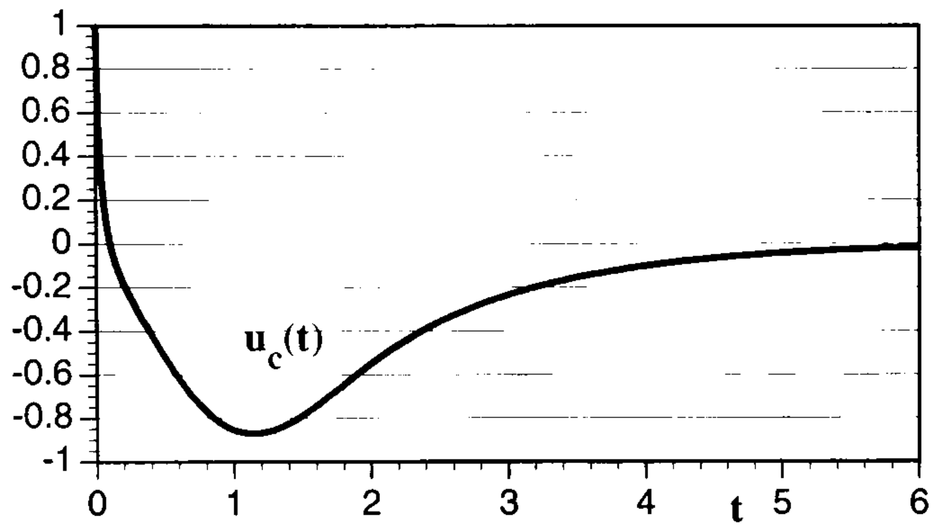

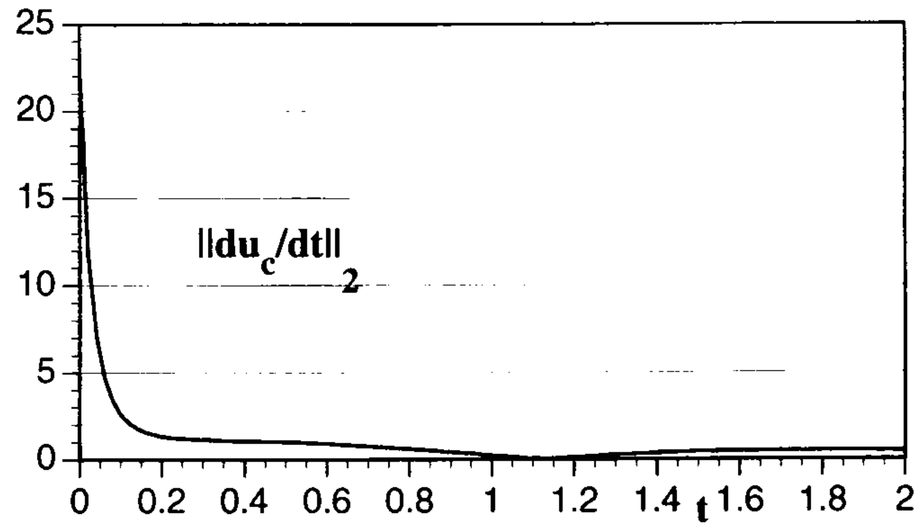

a) $x_{1o}=0.4,\ x_{2o}=1.5,\ x_{3o}=0.001$

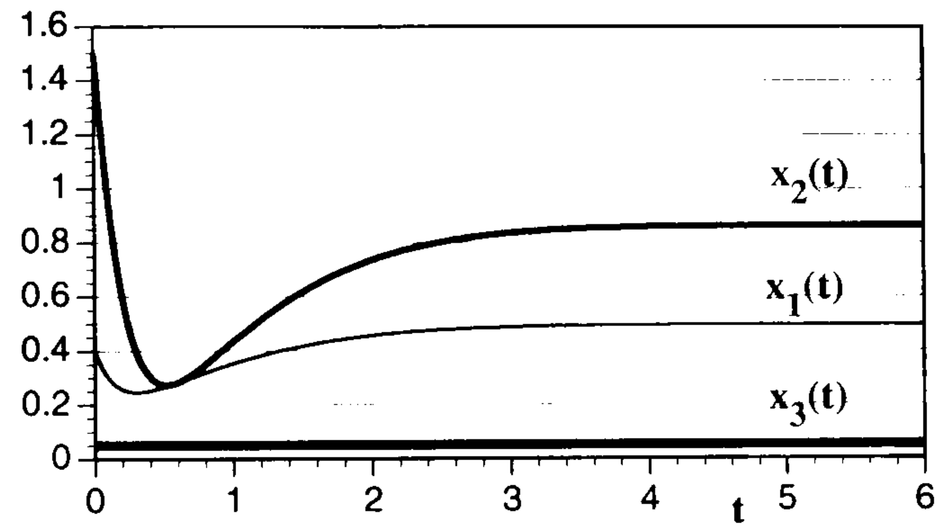

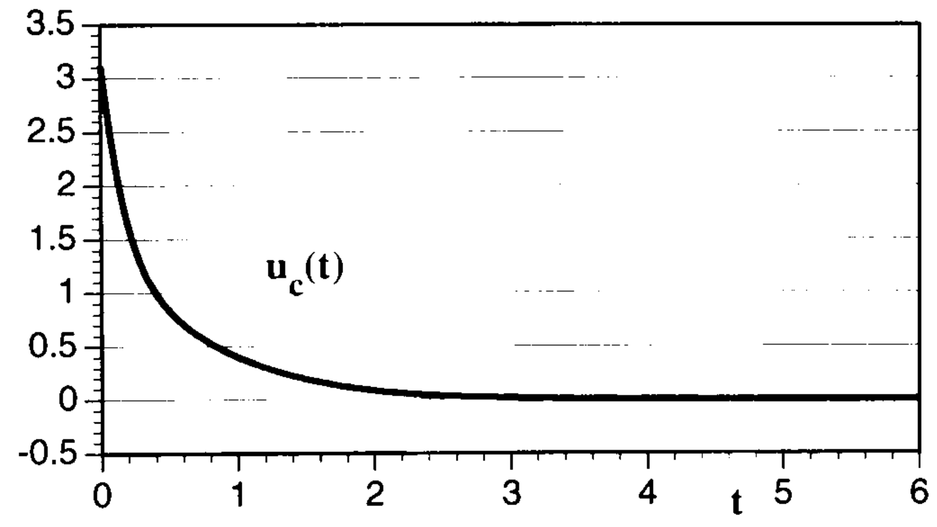

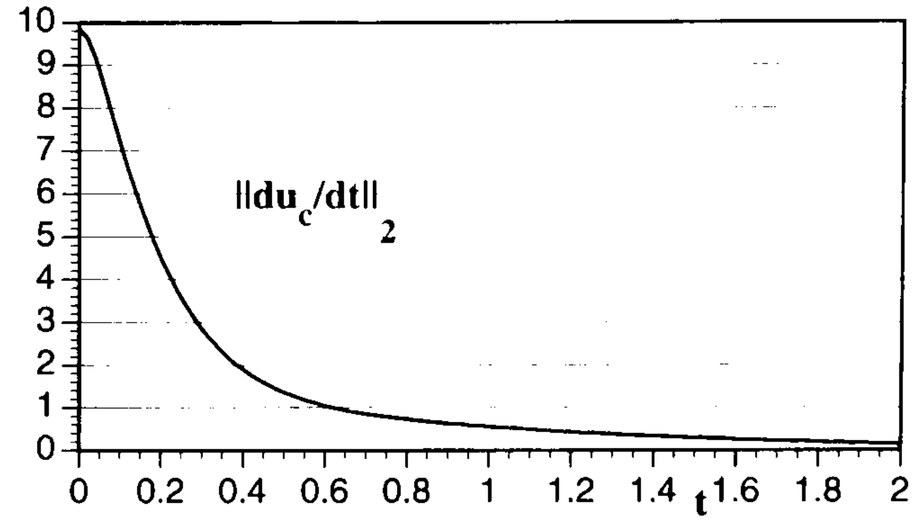

b) $x_{1o}=0.4,\ x_{2o}=1.5,\ x_{3o}=0.05$

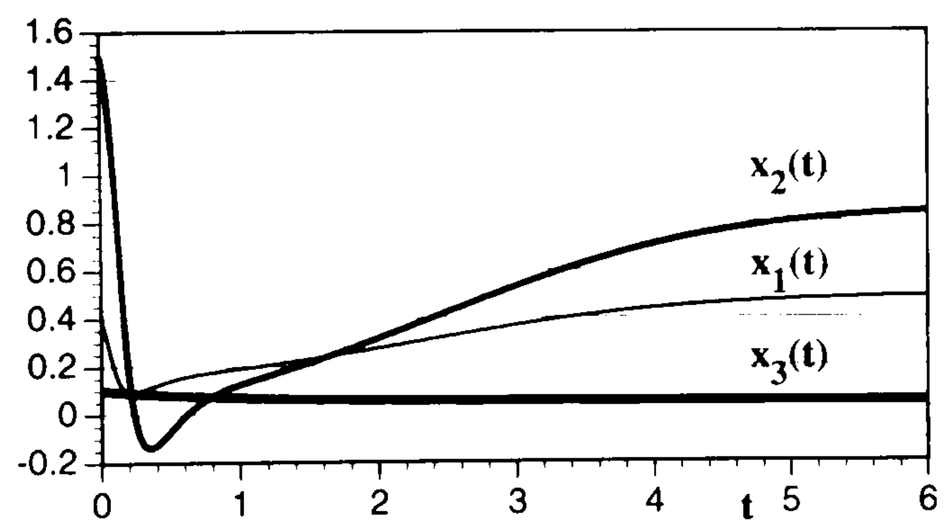

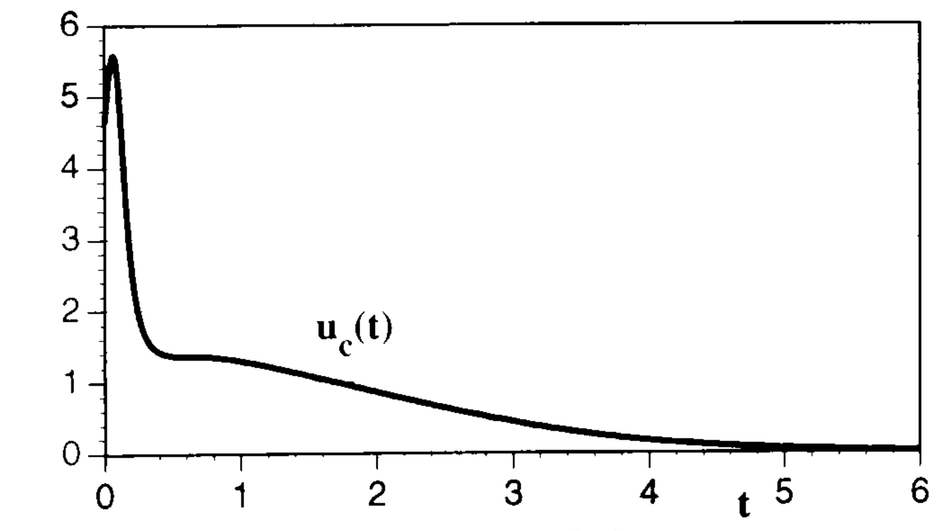

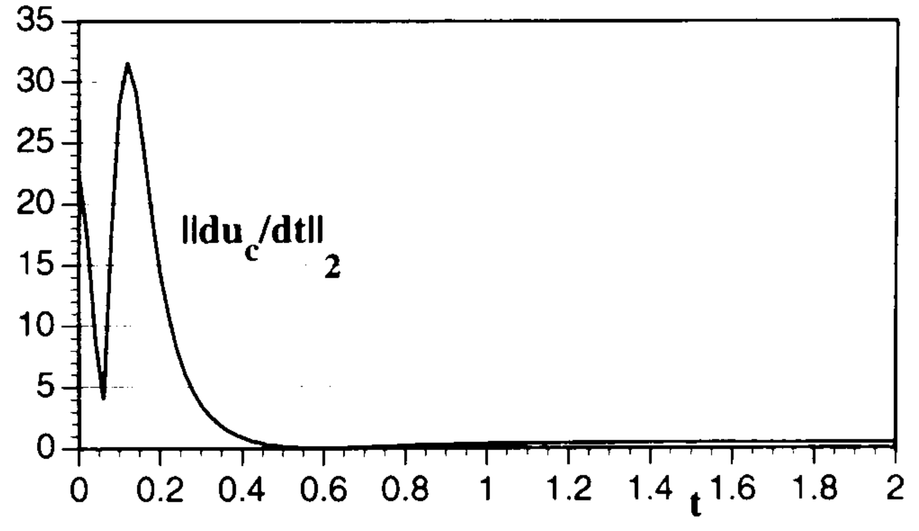

c) $x_{1o}=0.4,\ x_{2o}=1.5,\ x_{3o}=0.1$

Closed-loop time responses for PMMA reactor with cubic control.

FIGURE A.VII.3

REFERENCES

Andreini, A., Baccotti, A. and Stefani, G. (1988). "Global stabilizability of homogeneous vector fields of odd degree," *Systems & Control Letters*, **10**, 251-256.

Aris, R. and Amundson, N. R. (1958). "An analysis of chemical reactor stability and control - I, II, III," *Chem. Engng. Sci.*, **7**, 121-155.

Baillieul, J. (1980). "The geometry of homogeneous polynomial dynamical systems," *Nonlinear Analysis, Theory, Methods & Applications*, **4**-2, 879-900.

Baillieul, J. (1981). "Controllability and observability of polynomial dynamical systems," *Nonlinear Analysis, Theory, Methods & Applications*, **5**-5, 543-552.

Bequette, B. W. (1991). "Nonlinear control of chemical processes: A Review", *Ind. Eng. Chem. Res.*, **30**, 1391-1413.

Bruns, D. D. and Bailey, J. E. (1975). "Process operation near an unstable steady state using nonlinear feedback control," *Chem. Engng. Sci.*, **30**, 755-762.

Chen, H., Kremling, A. and Algöwer, F. (1995). "Nonlinear predictive control of a benchmark CSTR," *Proc. 3rd European Control Conference ECC'95*, Rome/Italy, 3247-3252.

Coleman, C. (1963). "Systems of differential equations without linear terms," *International Symposium no Nonlinear Differential Equations and Nonlinear Mechanics,* 445-453, New York: Academic Press.

Coleman, C. (1970). "Growth and decay estimates near non-elementary stationary points," *Canadian Journal of Mathematics*, **XXII**-6, 1156-1167.

Coleman, C. (1984). "Boundedness and unboundedness in polynomial differential systems," *Nonlinear Analysis, Theory, Methods & Applications*, **8-**11, 1287-1294.

Date, T. (1979). "Classification and analysis of two-dimensional real homogeneous quadratic differential systems," *Journal of Differential Equations*, **32**, 311-334.

Dancsó, A. and Farkas, H. (1989). "On the 'simplest' oscillating chemical system," *Periodica Polytechnica*, published by the Technical University Budapest (Hungary), 275-285.

Davis, H. T. (1962). *Introduction to Nonlinear Differential and Integral Equations.* New York: Dover.

Dayawansa, W. P., Martin, C. F. and Knowles, G. (1990). "Asymptotic stabilization of a class of smooth two-dimensional systems," *SIAM J. Control and Optimization,* **28**-6, 1321-1349.

Dayawansa, W. P. (1992). "Recent advances in the stabilization problem for low dimensional systems," *Proceedings* of IFAC-NOLCOS 1992 (Bordeaux, France), *Ed*. M. Fliess, p. 1-8.

Engell, S. and K.-U. Klatt (1993). "Nonlinear control of a non-minimum-phase CSTR," American Control Conference Proceedings, San Francisco 1993, 2941-2945.

Frommer, M. (1939). "Über das Aufreten von Wirbeln und Strudeln (geschlossener und spiraliger Integralkurven) in der Umgebung rationaler Unbestimmtheitsstellen," Math. Annalen, **109**, 395-424.

Gray, B. F. (1990). "Analysis of chemical kinetic systems over the entire paramenter space. III. A wet combustion system," *Proc. R. Soc. Lond.* A, **429**, 449-458.

Gray, P. and Scott, S. K. (1994). *Chemical Oscillations and Instabilities - Non-linear Chemical Kinetics*, Clarendon Press - Oxford.

Guckenheimer, J. and Holmes, P. (1983). *Nonlinear Oscillations, Dynamical Systems, and Bifurcations of Vector Fields*, Berlin, Heidelberg, New York: Springer-Verlag.

Hodgkin, A. J. and Huxley, A. F. (1952a.). Current carried by sodium and potassium ions through the membrane of the giant axon of Loligo, *J. Physiol.*, **116**, 449-472.

Hodgkin, A. J. and Huxley, A. F. (1952b.). A quantitative description of membrane current and its applications to conduction and excitation in nerve, *J. Physiol.*, **117**, 500-544.

Isidori, A. (1989). *Nonlinear Control Systems*, Springer-Verlag, New York.

Jaisinghani, R. and Ray, W. H. (1977). "On the dynamic behavior of a class of homogeneous continuous stirred tank polymerization reactors," *Chem. Eng. Sci.*, **32**, 811-825.

Kaplan, J. L. and Yorke, J. A. (1979). "Nonassociative, real algebras and quadratic differential equations," *Nonlinear Analysis*, **3**, 49-51.

Kravaris, C. and Kantor, J. C. (1990). "Geometric Methods for Nonlinear Process Control. 1. Background / 2. Control Synthesis", *Ind. Eng. Chem. Res.*, **29**, 2295-2310/ 2310-2323.

Liaghina, L. S. (1951). "The integral curves of the equations $y'=(ax^2+bxy+cy^2)/(dx^2+exy+fy^2)$," *Uspeki Matem. Nauk*, **6**-2(42), 171-183.

Markus, L. (1960). "Quadratic differential equations and non-associative algebras," *Contributions to the Theory of Non-linear Oscillations*, **5**, 185-213, Princeton, NJ: Princeton University Press.

Newton, T. A. (1978). "Two-dimensional homogeneous quadratic differential systems," *SIAM Review*, **20**-1, 120-138.

Nicolis, G. and Prigogine, I. (1977). *Self-Organization in Nonequilibrium Systems*, John Wiley & Sons, New York.

Oka, M. (1980). "Classification of two-dimensional homogeneous cubic differential equation systems I," *TRU Mathematics*, **16**-2, 19-62.

Oka, M. (1981). "Classification of two-dimensional homogeneous cubic differential equation systems II," *TRU Mathematics*, **17**-1, 65-88.

Röhrl, H. (1977). "A theorem on non-associative algebras and its application to differential equations," *Manuscripta Mathematica*, **21**, 181-187.

Samardzija, N. (1983). "Stability properties of autonomous homogeneous polynomial differential systems," *Journal of Differential Equations*, **48**-1, 60-70.

Samardzija, N. (1984). "Controllability, pole placement, and stabilizability for homogeneous polynomial systems," *IEEE Transactions on Automatic Control*, **AC-29**-11, 1042-1045.

Samardzija, N. (1985). "Morphal properties of purely complex homogeneous polynomial spectra," *Proc. of the American Control Conference*, Vol.**2** of **3**, 956-960: IEEE Catalog Number; 85CH2119-6.

Samardzija, N. and Greller, L.D. (1988). "Explosive route to chaos through a fractal torus in a generalized Lotka-Volterra model," *Bulletin of Mathematical Biology*, 50, 465-491.

Samardzija, N., Greller, L.D., and Wasserman, E. (1989). "Nonlinear chemical kinetic schemes derived from mechanical and electrical dynamical systems," *J. Chem. Phys.*, **90**, 2296-2304.

Samardzija, N. and Greller, L.D. (1992). "Nested tori in a 3-variable mass action model," *Proc. R. Soc. Lond.* A, **439**, 637-647.

Samardzija, N. and Waterland, R. L. (1991). "A neural network for computing eigenvectors and eigenvalues," *Biological Cybernetics*, **63**, 81-89.

Samardzija, N. (1993). "Applications of information storage matrix neural networks," *Neural Networks*, 6, 1159-1167.

Samardzija, N. (1994). "Homogeneous spectra and nonlinear controllability," *Proc. of the 33-rd IEEE Conference on Decision and Control*, Vol.**2** of **4**, 1256-1257: IEEE Catalog Number 94CH3460-3.

Samardzija, N. (1995). "Low dimensional worm-holes," *Physica D*, **80**, 21-25.

Scott, S. K. (1994). *Chemical Chaos* , Clarendon Press - Oxford.

Smale, S. (1976). "On the differential equations of species in competition," *J. Math. Biol.*, **3**, 5-7..

Tyson, J. J. and Light, J. C. (1973). "Properties of two-component bimolecular and trimolecular chemical reaction system," *J. Chem. Phys.*, **59**, 4164.

Vulpe, N. and Sibirskii, K. (1977). "Geometric classification of quadratic differential systems," *Differential'nye Uravnenija*, **13**, 548-556.

Uppal, A., Ray, W. H. and Poore, A. B. (1974). "On the dynamic behavior of continuous stirred tank reactors," *Chem. Engng. Sci.*, **29**, 967-985.